

UHI Research Database pdf download summary

Improving understanding of fish farm organic waste dispersal in higher energy environments

Fox, Clive; Hicks, Natalie; Webb, C.; Grant, J.; Brain, Stevie; Fraser, Stephen; Abell, Richard

Publication date:
2022

The re-use license for this item is:
Unspecified

[Link to author version on UHI Research Database](#)

Citation for published version (APA):

Fox, C., Hicks, N., Webb, C., Grant, J., Brain, S., Fraser, S., & Abell, R. (2022). *Improving understanding of fish farm organic waste dispersal in higher energy environments*. (SAMS Internal reports; No. 313). Scottish Association for Marine Science.

General rights

Copyright and moral rights for the publications made accessible in the UHI Research Database are retained by the authors and/or other copyright owners and it is a condition of accessing publications that users recognise and abide by the legal requirements associated with these rights:

- 1) Users may download and print one copy of any publication from the UHI Research Database for the purpose of private study or research.
- 2) You may not further distribute the material or use it for any profit-making activity or commercial gain
- 3) You may freely distribute the URL identifying the publication in the UHI Research Database

Take down policy

If you believe that this document breaches copyright please contact us at RO@uhi.ac.uk providing details; we will remove access to the work immediately and investigate your claim.

INCREASE and NAMAQI Project Report

Improving understanding of fish farm organic waste dispersal in higher energy environments

Fox, C.J. *, Hicks, N. **, Webb, C. *, Grant, J. ****, Brain, S. *, Fraser, S. *, Abell, R. ***

*Scottish Association for Marine Science, Dunstaffnage, Oban, PA37 1QS, UK

**School of Life Sciences, University of Essex, Wivernhoe Park, Colchester, CO4 3SQ, UK

***Cooke Aquaculture, Orkney Islands, Crowness Rd, Kirkwall, KW15 1RG, UK

**** Dalhousie University, Department of Oceanography, 1355 Oxford Street, Halifax, Nova Scotia B3H 4J1, Canada



This report describes work undertaken under the projects INCREASE and NAMAQI which were funded by the Scottish Aquaculture Innovation Centre (now called the Sustainable Aquaculture Innovation Centre).

The recommended citation is:

Fox, et al. (2022) INCREASE and NAMAQI project report: Improving understanding of fish farm organic waste dispersal in higher energy environments. Scottish Association for Marine Science, Oban. U.K., SAMS Report, No 313, 199 pp.

Contents

Improving understanding of fish farm organic waste dispersal in higher energy environments	1
Executive summary.....	6
1. Introduction and literature review	10
1.1. The importance of salmon aquaculture in Scotland	10
1.2. Nutrient release from open-cage aquaculture	10
1.3. The benthic impact of particulate organic waste from fish farms	11
1.4. Relationship between the INCREASE research project and environmental regulation in Scotland	19
1.5. The use of numerical models in predicting organic waste dispersal from a farm site.....	23
1.6. The processes included in computer models of fish farm waste dispersal	23
1.7. The link between organic carbon deposition and changes to the benthic biota.....	32
1.8. The problem of organic waste resuspension.....	37
1.8.1. Studies where critical shear stress and erodibility of fish farm waste have been measured.....	38
1.8.2. Field studies on organic waste resuspension and erosion.....	40
1.8.3. Calculation of erosion rates in DEPOMOD and NewDEPOMOD	41
1.8.4. Studies where different approaches to resuspension have been compared	42
1.9. Studies where model predictions have been compared with direct measurements of carbon deposition rates around fish farms.	44
1.10. Overall aims of the INCREASE project.....	46
2. Introduction to diagenesis and the NAMAQI project.....	47
2.1. Visual assessment of organic enrichment in marine sediments.....	51
2.2. Electrochemical measurements of organic enrichment in marine sediments	52
2.3. Non-electrode methods for the analysis of free sulphides.....	53
2.4. The use of sulphide measurements in assessing fish farm benthic impacts	55
2.5. Overall aims of the NAMAQI project.....	60
3. Materials and methods.....	61
3.1. Study sites.....	62
3.1.1. Bay of Vady site description.....	62
3.1.2. Quanterness site description	70
3.1.3. Bay of Meil site description.....	78
3.2. Common methods.....	85
3.2.1. Deployment and recovery of sediment boxes to measure organic carbon flux.....	85
3.2.2. Collection of syringe cores for sediment particle size, particulate organic carbon and sulphide analyses	88

3.2.3. Collection of benthic grabs for sediment, macrofaunal and sulphides	88
3.2.4. Sediment analysis from benthic grab samples	90
3.2.5. Infaunal analysis of benthic grab samples	90
3.2.6. Laboratory measurement of particle size from syringe cores.....	91
3.2.7. Laboratory measurement of particulate organic carbon from syringe cores	91
3.2.8. On-site measurement of sulphides in benthic sediment samples.....	91
3.2.9. Sediment samples for eDNA	93
3.2.10.Laboratory measurement of particulate organic carbon (POC) in the sediment boxes	93
3.2.11.Modelling of organic particulate waste dispersal and settlement using NewDEPOMOD	95
3.2.12.Comparison of sediment sulphide measurements with infaunal indices for selected Canadian fish farms	96
4. Results	98
4.1. Bay of Vady field study results	98
4.1.1. Sediment particle size from syringe cores	98
4.1.2. Sediment POC from syringe cores	98
4.1.3. Sediment eDNA.....	99
4.1.4. Benthic grabs collected at Bay of Vady	99
4.1.5. Macrofaunal analyses from benthic grabs at Bay of Vady.....	100
4.1.6. Carbon flux from sediment boxes deployed at Bay of Vady.....	100
4.1.7. Comparison between measured variables at Bay of Vady	101
4.1.8. Modelling organic waste dispersal at Bay of Vady using NewDEPOMOD	101
4.2. Quanerness field study results	104
4.2.1. Sediment particle size from syringe cores collected at Quanerness.....	104
4.2.2. Sediment POC from syringe cores collected at Quanerness	104
4.2.3. Sulphides from syringe cores collected at Quanerness	105
4.2.4. Sediment eDNA from syringe cores collected at Quanerness.....	106
4.2.5. Benthic grabs collected at Quanerness	106
4.2.6. Sulphides from benthic grabs collected at Quanerness	107
4.2.7. Faunal analyses from benthic grabs collected at Quanerness.....	110
4.2.8. Carbon flux from sediment boxes deployed at Quanerness	114
4.2.9. Comparison between measured variables at Quanerness	114
4.2.10.Modelling organic waste dispersal at Quanerness using NewDEPOMOD	117
4.3. Bay of Meil field study results.....	118
4.3.1. Sediment particle size from syringe cores	119
4.3.2. Sediment POC from syringe cores collected at Bay of Meil.....	119

4.3.3. Sulphides from syringe cores collected at Bay of Meil.....	120
4.3.4. Sediment eDNA from syringe cores collected at Bay of Meil	120
4.3.5. Benthic grabs collected at Bay of Meil.....	120
4.3.6. Sulphides from benthic grabs collected at Bay of Meil.....	121
4.3.7. Faunal analyses from benthic grabs collected at Bay of Meil.....	122
4.3.8. Carbon flux from sediment boxes deployed at Bay of Meil.....	126
4.3.9. Comparison between measured variables at Bay of Meil	126
4.3.10. Modelling organic waste dispersal at Bay of Meil using NewDEPOMOD	128
4.3.11. Comparison of sulphide data from Quanterness and Bay of Meil against the infaunal indices, ITI and IQI.....	131
4.3.12. Comparison of sediment sulphides from Shelburne Bay and Port Mouton, Nova Scotia with IQI.....	132
5. Discussion of the INCREASE project results	135
5.1. Main conclusions from the INCREASE project.....	135
5.2. Background data from the fieldwork sites.....	136
5.2.1. Water currents.....	136
5.2.2. Sediment particle size	136
5.2.3. Sediment particulate organic carbon	137
5.2.4. Use of sediment boxes to estimate organic carbon deposition	139
5.2.5. Comparing modelled carbon deposition using NewDEPOMOD against estimated carbon deposition from the sediment boxes	142
6. Discussion of the NAMAQI project results	143
6.1. Main conclusions from the NAMAQI Project.....	143
6.2. Discussion on the practicalities of making sulphide measurements at Scottish fish farms	146
6.3. Discussion on including a diagenetic module in NewDEPOMOD.....	148
7. Recommendations	153
7.1. Recommendations for future work from the INCREASE project.....	153
7.2. Recommendations for future work from the NAMAQI Project.....	153
8. Acknowledgements	155

Executive summary

Organic waste from open cage fish farms can negatively impact the benthos if the quantities of settling material exceed the natural assimilative capacity of the seabed. The amounts of total organic material which are allowed to be released are thus regulated in most countries where open-cage fish farming takes place. In Scotland, limits on settling organic waste are one of the main factors determining the maximum fish biomass permitted at a farm site. Computer models of the dispersal of total organic waste to the seabed have become an important tool in both initial site licencing, but also continued site monitoring. The main organic waste dispersal model used in Scotland is DEPOMOD. Originally developed in the late 1990s this model has gone through several upgrades, the latest version being NewDEPOMOD. The original model was developed and calibrated for relatively sheltered, low dispersal sea-loch sites with muddy seabed, where the model's predictive capability has proven to be generally high. However, many newer fish farms have been developed in more dispersive sites. Despite NewDEPOMOD incorporating a relatively sophisticated waste resuspension sub-model, problems have been encountered with accurately predicting the benthic footprint of fish farm organic waste at these more dispersive sites. The main aim of the INCREASE project was to try and improve our understanding of why these predictive problems are occurring and to suggest future work to address any issues identified.

The problem of predicting safe organic loading to the seabed can be broken down into four broad process steps (i) the amount of feed used and its assimilation efficiency by the fish (ii) the settlement of waste material from the cages through the water column to reach the seabed (iii) the potential for resuspension and movement of waste material from its initial settlement site (iv) the biologically facilitated breakdown of the accumulated organic waste material on the seabed.

The studies undertaken in the INCREASE project are concerned with process (iii). Some additional research was conducted on sulphides measurement (in relation to process iv) as a potential tool for assessing benthic impacts, under a separately funded project, NAMAQI. However, both projects conducted research at the same farms, so the results are presented as a combined report, avoiding the need to repeat large parts of the introduction, materials and methods etc.

The research comprised:-

1. Conducting a comprehensive literature review on
 - 1.1. modelling waste dispersal from cage finfish farms, especially in higher energy sites.
 - 1.2. marine sediment diagenesis and sediment chemistry in relation to sulphide production under and adjacent to fish farms.
2. Undertaking field studies at three sites located over sandy, as opposed to soft mud, sediments to
 - 2.1. attempt to quantify organic waste deposition rates to the seabed directly.
 - 2.2. model the waste deposition using NewDEPOMOD.
 - 2.3. compare the modelled and observed organic carbon deposition rates to investigate problems encountered when using NewDEPOMOD for more dispersive sites.
3. Additional work was undertaken at two farm sites to evaluate whether quantifying sulphides in the sediment may be a useful tool for rapid monitoring of benthic impacts by comparison with the Infaunal Quality Index (IQI). This component of the program also drew on experience from Canada where sulphide measurements are used as part of the routine regulatory process.

4. Production of recommendations for future studies and potential changes to NewDEPOMOD which might improve modelling of total organic waste dispersal at more dispersive locations.
5. Production of recommendations on whether sediment sulphide measurements could be a practical and useful tool for monitoring fish farm benthic impacts in Scotland.

The main conclusions from the literature review under INCREASE were that problems with modelling waste dispersal at higher energy sites have been noted in several other published studies. In addition, a limited number of flume experiments have been conducted which suggest that the critical erosion threshold for organic waste is strongly related to the coarseness of the sediments as well as the level of organic loading.

The main conclusions from the literature review under NAMAQI were that there is relatively good understanding of the diagenetic processes and the relationships between sediment oxic state, organic carbon loading, free sulphide production by microbial action and subsequent impacts on benthic macrofauna. Several diagenetic process models are available, but these have been developed as research tools rather than for operational use by regulators and fish farm managers. Published data, mainly from Canada but also some from Scotland, suggests that while the extremes of macrofauna-benthic state may be predictable from free sulphide concentrations, intermediate levels of sulphides result in a wide range of benthic community responses.

Fieldwork was undertaken at three Cooke Aquaculture farms located in the Orkney Islands, namely Bay of Vady, Qaunterness and Bay of Meil. At each site extensive sampling was undertaken to characterise the sites including particulate size analysis (PSA), sediment particulate organic carbon (POC), sediment sulphides (Qaunterness and Bay of Meil only) and infaunal analyses (ITI and IQI). In addition, a novel design of sediment traps was deployed along four transects at each site during spring and neap tides to estimate the deposition of organic carbon whilst allowing resuspension of settled organic material. The estimated deposition rates were then compared with the site characteristics, IQI patterns and NewDEPOMOD model results.

The main conclusions were that patterns and quantities of estimated carbon deposition were generally consistent with expectations and with the infaunal impacts (IQI), suggesting that the novel sediment traps can capture realistic patterns of organic waste deposition around fish farms. Modelling using the NewDEPOMOD default parameter settings led to nearly all simulated particles being moved out of the model domain, meaning that no benthic footprint could be captured. To generate a benthic footprint at these sites it was necessary to increase critical shear stress in the model to levels at which resuspension was almost completely turned off. However, particularly at times of spring tide this then led to waste deposition estimates which declined too rapidly with distance from the fish cages i.e., waste resuspension and re-dispersal was then being underestimated in the model. These results, taken with other published results on fish farm waste resuspension reviewed in part 1 of this report, suggest that NewDEPOMOD is not fully capturing the resuspension and redistribution processes occurring in the field. This behaviour most likely arises from the use of a spatially invariant critical shear stress in the model (although other issues cannot be ruled out). It seems likely that organic waste is more easily eroded from heavily enriched areas but becomes harder to resuspend when dispersed onto less enriched areas and that this behaviour is more significant over coarser sediments, including sands and gravels, compared to mud.

Patterns in sediment sulphides also largely agreed with infaunal impact patterns although benthic samples with mid-range sulphide concentration (~200 – 1500 μM) showed a wide range of ecological states. Taken along with previously published results from Scotland and additional information from Canada, sulphide measurements do appear to be a rapid and reliable indicator of whether a sample is in ‘High’ IQI status but cannot discriminate between ‘Moderate’ and ‘Poor’ IQI status based on sulphide concentration alone. Samples with sulphides above 1500 μM are likely to have a ‘Bad’ IQI status, but this conclusion is based on a limited number of highly impacted samples. Recent analytical advances might alter this perception somewhat by giving more accurate sulphide measurements, although the overall patterns with biological community response are likely to remain.

The main recommendations from the projects are:-

- a) Particle resuspension as encoded in NewDEPOMOD remains problematic. The present configuration requires *ad hoc* fixes to be applied to reduce levels of particle dispersion at higher energy sites. The most likely cause of the problems may be the use of a single value for bed shear-stress across the model domain. This leads to a recommendation that NewDEPOMOD code should be reviewed to evaluate the feasibility of allowing critical bed shear stress to be related to the degree of organic enrichment and sediment type. The modified model will then need to be re-evaluated to assess if this change improves its predictive capability in more dispersive environments.
- b) The use of sediment boxes placed flush with the seabed to directly measure net (considering resuspension) organic carbon deposition appeared successful. The technique could be applied at additional farm sites to generate more measurements across a wider range of site conditions for direct comparison with predictions from NewDEPOMOD (or other particle dispersal modelling tools). However, the technique does have limitations, especially regarding maximum deployment depth by divers. Furthermore, in any future studies, additional traditional design sediment traps (which do not allow resuspension) should also be deployed for comparison, and one or two reference sites included to confirm the background organic flux.
- c) Sulphide measurements may be useful to farm managers as a quick indication of stations which are likely to have less than ‘Moderate’ ecological status but is unlikely to provide a complete replacement for infaunal analyses as required by SEPA because it does not appear to allow discrimination between ‘Moderate’, ‘Poor’ and ‘Bad’ IQI status samples.
- e) Whilst measurement of sulphides on farm sites was demonstrated to be achievable using the ion-specific electrode (ISE) approach, the method is not without problems. Achieving accurate results requires careful maintenance and calibration of the probes and a recent study claims the method is less accurate than direct quantification of sulphides by UV-absorption, although ISE remains one of the standard fish farm benthic monitoring tools in Canada. We cannot therefore recommend the ISE approach at this time as an “easy, rapid, and reliable method for evaluating benthic community status” on Scottish fish farms in-line with SEPA requirements.
- f) Further field work at Scottish fish farms should explore the application of the recently published spectrophotometric methods described by Cranford et al. (Cranford *et al.*, 2017, 2020 #11968). These methods may improve the accuracy of sulphide measurements compared with the ion-selective electrode (ISE) approach but would require additional equipment (UV-spectrophotometer) to be available at fish farm sites if analyses were to be performed on-site. Alternatively, samples may be preserved with zinc acetate and subsequently analysed using the methylene blue method, although this technique is not as sensitive as measuring UV-absorption

on fresh samples. These approaches could potentially improve analytical precision and thus might improve discrimination between IQI status levels of benthic grab samples based on sulphide measurements. However, it must be cautioned that evidence to date suggests that biological responses to sediment sulphides appear to be quite variable and site specific, especially when sulphides levels are in the intermediate range (200 – 1500 μM). The method would thus require extensive further calibration against IQI for use within the Scottish regulatory framework.

g) Further work on sulphides could be piggybacked on existing SEPA compliance monitoring to reduce costs but the equidistant sampling designs used are not ideal as they tend to lead to an unbalanced number of samples at each IQI state. Additional sampling for sulphides (and using sediment traps if deployed) would therefore probably be required to fully investigate the relationships between sulphide concentrations, IQI, sediment type and other site-specific factors. Log-distance sampling designs may be preferable to account for the usual exponential decline in organic waste deposition with distance from the cage edge.

h) Incorporation of a diagenesis sulphide module into NewDEPOMOD would be achievable but would require a dedicated software development project. We suggest that it may be more useful to address recommendation (f) initially, because we cannot yet say how useful sulphide measurements around fish farms would be in the context of the Scottish regulatory framework.

1. Introduction and literature review

1.1. The importance of salmon aquaculture in Scotland

Since its inception at Loch Ailort in Inverness-shire in 1965, farming of Atlantic salmon (*Salmo salar*) in Scotland has increased substantially with production reaching nearly 204,000 tonnes in 2019 (Figure 1). The sector is also a major source of employment providing 1,651 direct production jobs (Scottish Government, 2020) and many secondary jobs supplying hardware, engineering, vessel support, and in the wider supply chain (Biggar Economics, 2020).

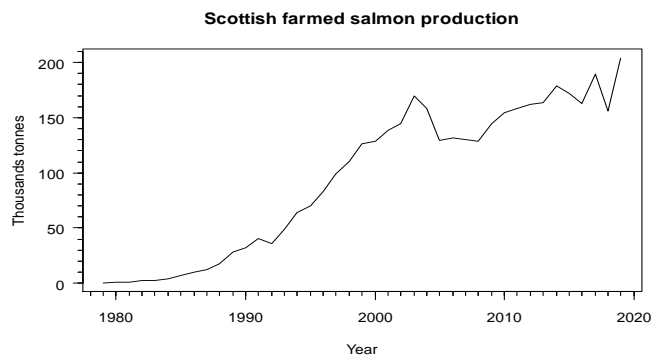


Figure 1: Annual Scottish farmed salmon production (Scottish Government, 2020).

At present, most Scottish salmon production takes place in seawater cages located along the Scottish west coast, and around the Orkney and Shetland Islands (Figure 2).

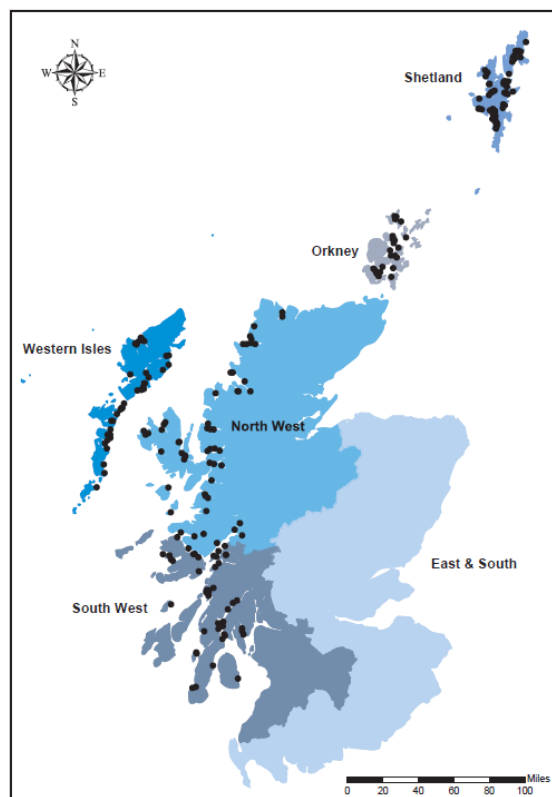


Figure 2: The locations of active salmon production sites in 2019 (Scottish Government, 2020).

1.2. Nutrient release from open-cage aquaculture

In Scotland, Atlantic salmon are on-grown using formula pellets. Because feed is one of the major costs in fish farming, farmers wish to maximise feed conversion and minimise feed waste. The composition of salmon pellets has thus been optimised over time, not only in terms of the nutrient content, but also their sinking rates, palatability, and digestibility. The type of pellet used is also varied over the growing cycle e.g., changing pellet size to match fish size or to increase lipid content towards the harvesting period.

Open-cage fish farming relies on exchange with the sea to remove waste products and maintain water quality in the cages. Waste products can be divided into dissolved substances which originate mainly as excretory products from the fish e.g. ammonia and urea, and organic matter comprised mainly of faeces and residual uneaten food (Price *et al.*, 2015).

Dissolved nutrients from fish farms have been of concern as their elevation has the potential to trigger algal blooms. However, a review by Karakassis *et al.* (2005) found few published studies which had recorded significant increases in dissolved nutrients close to fish farms. In addition, instances of eutrophication (defined as excessive algal growth due to the increased availability of one or more limiting nutrients) have only been linked to fish farms on a limited number of occasions. Most excess nutrients in the coastal zone derive from terrestrial sources, such as agriculture and urban wastewater and those few studies which did report problems linked to aquaculture were often from sites with minimal flushing (Price *et al.*, 2015).

The fate and impacts of dissolved substances released from fish farms have been simulated using a variety of dilution models (SEPA, 2019a), but these are not suitable for modelling the fate of particulate wastes, which is the focus of the projects reported on here.

1.3. The benthic impact of particulate organic waste from fish farms

The major transport pathways for salmon farm feed-derived waste are shown in Figure 3. The waste material is relatively high in organic carbon and thus has the potential to lead to negative benthic impacts, both immediately below the cages but also over a wider area due to dispersion of the waste particles by local water currents.

Much of the earlier work examining the impacts of organic enrichment on marine benthic communities was associated with disposal of sewage and paper pulp processing waste (Pearson and Rosenberg, 1976). Mesocosm studies cited in Cromey (1998) suggested that organic loading rates of less than $36 \text{ g C m}^{-2} \text{ y}^{-1}$ had little effect, rates between $36 - 365 \text{ g C m}^{-2} \text{ y}^{-1}$ enriched the benthic community but loadings over $548 \text{ g C m}^{-2} \text{ y}^{-1}$ led to degraded conditions. In a field study, experimental addition of sewage sludge to a sea-loch at a rate of $767 \text{ g C m}^{-2} \text{ y}^{-1}$ led to an increase in faunal biomass, but addition of $1,498 \text{ g C m}^{-2} \text{ y}^{-1}$ resulted in degraded conditions. Such studies formed the basis for understanding the benthic impacts of organic wastes and led to models of how the epi- and infaunal biological communities would respond to different organic loadings. With the development of open cage salmon aquaculture, similar concerns arose about the impact of organic waste on the benthic communities beneath and adjacent to fish-farms.

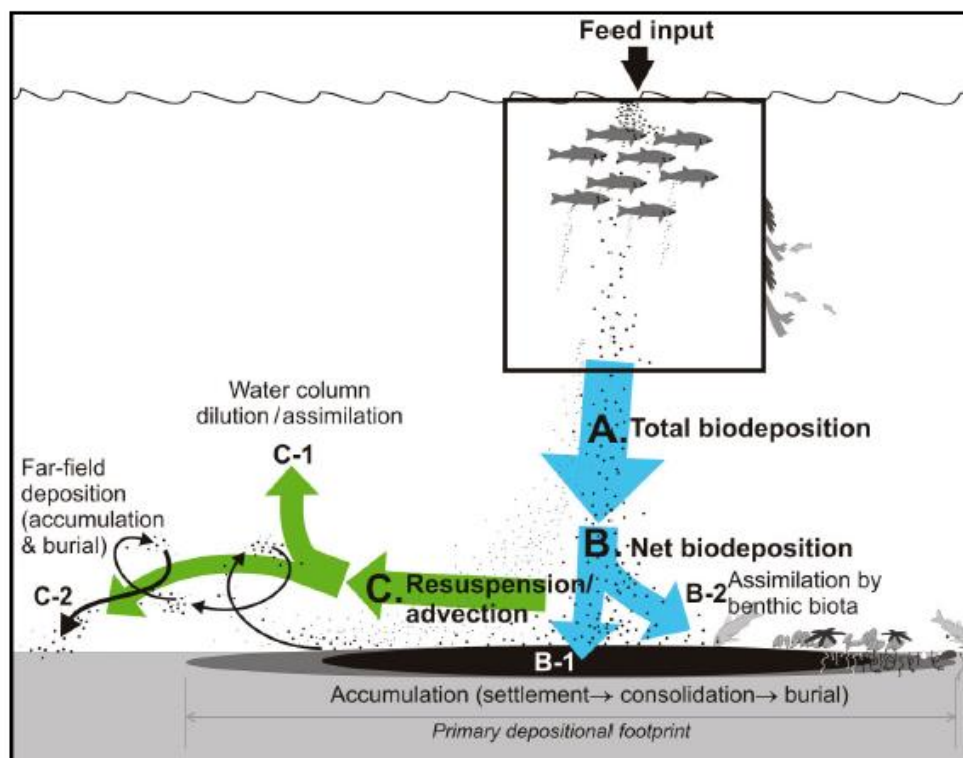


Figure 3: Major pathways of salmon feed-derived waste deposition. Note that the waste particles shown comprise a mix of faeces and uneaten feed pellets. Most waste is assumed to fall through the bottom of the cage although a small amount may be transported through the cage sides (Keeley *et al.*, 2013b).

Organic matter from farm cages settles to the seabed where it can accumulate or be broken down. Although some breakdown may occur whilst it is settling through the water column, the time taken for material to reach the seabed is usually relatively short e.g., using the widely accepted mean settling velocity for salmon faeces of 3 cm s^{-1} , the material would take about 27 mins to settle through 50 m (Cromeey *et al.*, 2002a).

Because feed represents a major cost in salmon farming considerable efforts have been made to reduce pellet wastage through adjusting size, composition and buoyancy, and the introduction of video monitoring to control feeding rates. Although the major component of the organic waste will be faecal material, a proportion of the waste will be comprised of uneaten feed pellets but there does not appear to be recent published scientific assessments of pellet wastage rates. It is possible that average pellet waste rates have changed from those reported in earlier studies due to the recent technical advances in fish feeding and husbandry.

There is evidence that uneaten pellets are eaten by fish and crustacea outside the cages and that this food source may attract wild fish to salmon farms although dietary preference for waste feed pellets appears to vary with species and location (Mente *et al.*, 2008; Sardenne *et al.*, 2020). Ghanawi and McAdam (2020) found feed pellets in around 10% of mackerel (*Scomber scombrus*) and 30% of whiting (*Merlangius merlangus*) stomachs in fish sampled close to several Scottish salmon farms. Whiting most likely feed on pellets which have settled to the seabed whilst mackerel probably consume pellets as they settle through the water column. Fish and shellfish can certainly feed at fish farms for extended periods of time as changes have been observed in the muscle fatty acid profiles of specimens caught close to fish farms. Typical

profile changes include elevated levels of terrestrial plant-derived fatty acids originating from material included in salmon feeds. Several studies have thus questioned whether such changes in fatty acid profiles might affect the health or reproductive success of the wild organisms although there is little published scientific evidence to address this question (Ghanawi and McAdam, 2020; Uglem *et al.*, 2020).

Although the total settling time for uneaten pellets and faecal pellets is usually quite short, horizontal movement of the water will disperse the material to some extent. The material will therefore be spread over an area whose footprint will largely be determined by the strength and direction of the currents and the water depth beneath the cages. Since tidal currents usually form an ellipse, then the fish farm benthic footprint will also usually be elliptical, although this can be modified by bottom topography. The magnitude of the flux of organic material to the seabed will also usually be highest close to the cages and decline rapidly with distance.

Water movements induced by the ebb and flood of the tides are particularly pronounced at inshore locations. Since at present most Scottish fish farms are located inshore (Figure 2), the strength and direction of the water flow near the seabed is constantly varying at these sites. At very shallow sites, wind-driven water movements may also be a significant factor generating additional unpredictable increases in near-bed currents (Mayor *et al.*, 2010). When the tidal flow near the bed exceeds a critical threshold, previously settled organic material may become re-suspended and transported further but re-settling once the flow drops. This process of re-suspension and re-sedimentation can extend the benthic footprint over a larger area than that generated by the initial settlement of the waste (Figure 3).

The degree to which organic material reaching the seafloor can be degraded will depend upon the rate of supply of material to the seabed, the composition of the organic material (Westrich and Berner, 1984), the local physical conditions (Burdige, 2007), and the composition of benthic communities at the site (Heilskov and Holmer, 2001). A major influence on the condition of the surface sediment is the availability of oxygen, that is whether the sediment is in an oxic, hypoxic or anoxic state (Burdige, 2007).

In sediments in productive coastal waters, the oxygen penetration depth may be only a few millimetres (Cathalot *et al.*, 2012). However, the presence of bioturbating macrofauna creates a complex three-dimensional mosaic which can increase the surface area over which oxygen can diffuse (Burdige, 2007), and hence bioturbation serves to increase the effective average oxic depth (Kristensen, 2000). The presence of macrofaunal bioturbators also enhances mixing of newly settled organic material deeper into the sediment whilst returning partially degraded material from depth to the oxic zone (Duplisea, 1998; Heilskov and Holmer, 2001; Deng *et al.*, 2020).

Moderate increases in organic matter often stimulate macrofauna production and increase species diversity (Hargrave, 2003; Macleod *et al.*, 2007; Keeley *et al.*, 2013b). Thus, providing the site is not over-loaded or suffering from some other form of stressor, most of the additional organic material will be quite rapidly reduced by denitrification or consumed by benthic invertebrates living in and on the sediment. However, beyond a certain level increasing organic matter supply will have a deleterious effect and changes in community composition may be observed within a few weeks (Ritz *et al.*, 1989).

Observations have demonstrated that the sediment oxygen demand is proportionate to the rate of carbon deposition with a typical molar ratio of 1:0.7 (Findlay and Watling, 1994; Findlay and Watling, 1997). At water speeds of less than 10 cm s^{-1} , the flow will be smooth-turbulent resulting in a viscous sublayer at the sediment-water interface. In the absence of biogenic transport, movement of oxygen into the sediment will then be limited to diffusion. The rate at

which oxygen will diffuse into the sediment is dependent on the oxygen concentration in the overlying water (which is in turn related to the water temperature¹), and the thickness of the boundary layer. This allows a calculation of the maximum oxygen supply to the sediment and hence the maximum organic carbon flux that will not deplete the sediments of free oxygen (Figure 4). However, at times of high flow this relationship may break down due to turbulent disruption of the boundary layer and more oxygen will be supplied to the sediment.

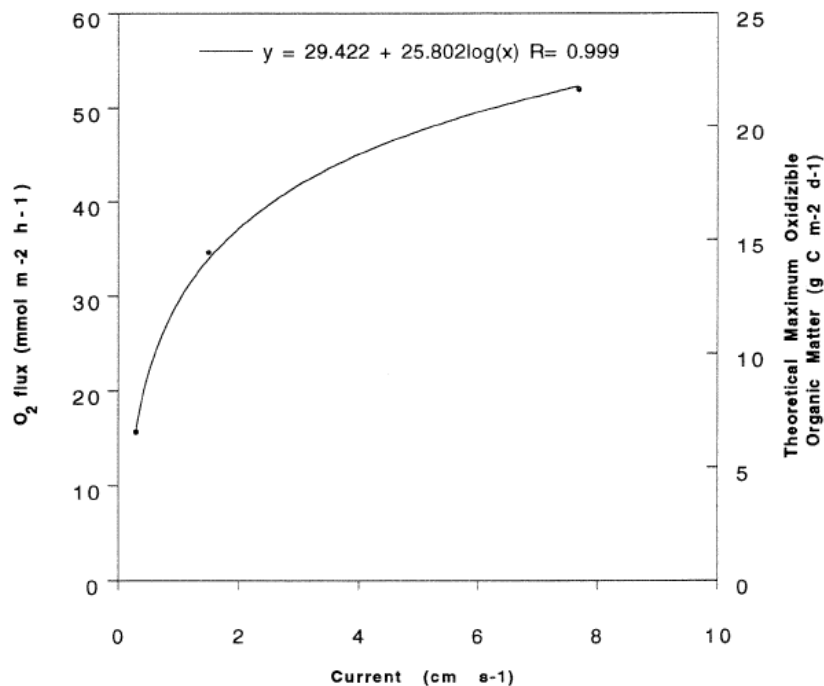


Figure 4: The theoretical rate of delivery of oxygen to sediments as a function of current speed and at 20°C. Axis Y₂ shows the resulting theoretical maximum rate of aerobic oxidation of organic matter calculated from relationships presented in Findlay *et al.* (1994) and (1997).

The degree of oxygenation in the surficial sediment at a site will often fluctuate due to tidally driven flushing (Cromey *et al.*, 2002b; Burdige, 2007) but also changes seasonally with temperature and biological activity (Cathalot *et al.*, 2012). At shallow sites, wind-driven increases in near-bed water flow can also alter the degree of sediment oxygenation (Panchang *et al.*, 1997; Dudley *et al.*, 2000).

Although many benthic marine organisms can tolerate short periods of hypoxia, they will begin to suffer under prolonged low oxygen conditions (Hargrave *et al.*, 2008). Macrobenthic organisms, especially filter feeders, may also become physically smothered by accumulating organic waste (Weston, 1990). The depletion of macrobenthic bioturbators leads to a further reduction in the aeration of the sediment through irrigation (Cathalot *et al.*, 2012), and will thus contribute to its transition to a hypoxic state (Kristensen, 2000; Heilskov and Holmer, 2001).

The combination of deteriorating physical and physiological conditions can lead to the replacement of the macro-fauna with one dominated by small opportunistic species, such as *Capitella* sp, *Mediomastus fragilis* and *Malacocerus fuliginosus*, species which are able to tolerate hypoxic conditions (Pereira *et al.*, 2004; Tomassetti and Porrello, 2005; Bannister *et*

¹ Although temperature is the main determinant of the level of dissolved oxygen in seawater, oxygen levels can also become depleted through the breakdown of organic material in the water column. Such material can itself come from fish farms, decaying algal blooms or other sources of organic waste, such as sewage outfalls.

al., 2014; Keeley *et al.*, 2019). Under appropriate conditions such opportunistic organisms may flourish in huge numbers and their abundance is thus often used as an indicator of organic enrichment (Hargrave *et al.*, 2008; SEPA, 2019a).

Under even more intense organic enrichment the surficial sediment itself can become anoxic (Brown *et al.*, 1987). The sediment biota then become dominated by micro-organisms, including sulphate reducing bacteria (Westrich and Berner, 1984; Chamberlain, 2002; Wilding *et al.*, 2012). The actions of the microbial community are discussed in more detail in Section 2 of this report. Under extreme conditions (low turbulence and high organic input), the overlying water may itself become anoxic (Brown *et al.*, 1987; Hargrave *et al.*, 1993).

Where anoxic conditions reach the sediment-water interface, mats of distinctive white sulphide oxidising bacteria (*Beggiatoa* sp.) may develop on the sediment surface (Hamoutene, 2014). Whilst the full negative impacts of organic enrichment beneath a fish farm may take some time to develop, the abundance of opportunistic species can increase rapidly (Tomassetti and Porrello, 2005). Based on observations at farms in Maine, Sowles (1994) suggested that the full suite of negative impacts (azoic conditions or outgassing adjacent to or directly beneath the pens, *Beggiatoa* sp. mats, feed, and faeces build-up extending more than 5 m away from pen footprint) would take about two years to become apparent (Figure 5).

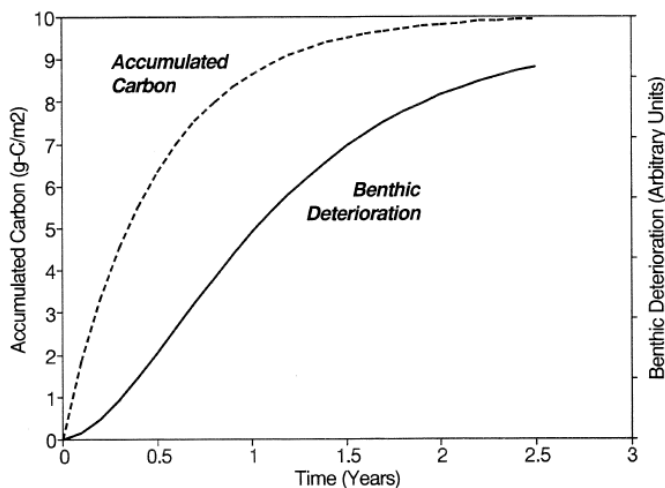


*Figure 5: Theoretical comparison between the dynamics of accumulated carbon (AC) and benthic deterioration (BD) and accumulated carbon, based on observations of benthic condition beneath farm sites in Maine, USA (Sowles *et al.*, 1994).*

Such changes in the surficial sediment and associated benthic communities with increasing organic loading were described in the classic conceptual community succession model of Pearson and Rosenberg (Figure 6).

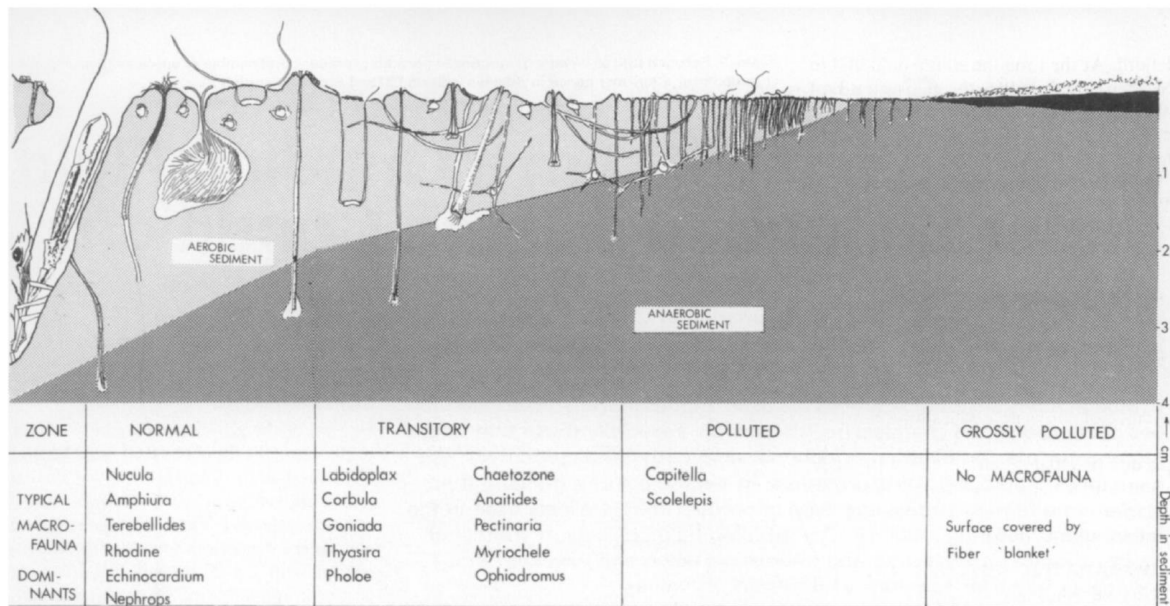


Figure 6: Diagrammatic representation of faunal and sedimentary changes under increasing organic loading. From right to left is seen a "fiber blanket", burrows of polychaetes, bivalves, brittle stars, a sea-urchin and finally a Norway lobster (*Nephrops*). Illustration from (Pearson and Rosenberg, 1976).

The nature of sedimented organic carbon also changes over time as labile² carbon is broken down more rapidly compared to the less labile components (Burdige, 2007). Therefore, the ratio of labile to less-labile carbon changes over time and eventually the material becomes dominated by the less-labile material, which is resistant to further breakdown. This material will naturally become gradually buried and consolidated, but this process occurs over relatively long timescales (Beulig *et al.*, 2018).

In the deep ocean, deeper parts of the shelf seas and in some of the deeper basins of the sea-lochs, currents are sufficiently low that buried carbon remains undisturbed and therefore contributes to the sequestering of carbon via build-up of the long-term 'blue' carbon pool (Burdige, 2007). Because this process is tightly linked with whether a site is depositional or erosional, both the natural sedimentation rate and the organic carbon content are highest for marine muds and lowest for sands and gravels (Burrows *et al.*, 2014).

The amount of organic waste originating from fish farms which becomes buried can also be quite high. Hall (1990) constructed a multi-seasonal mass balance for a marine trout farm in Norway which suggested that about 3% of the organic carbon reaching the seabed would be respired and released back into the water, with the remaining 97% becoming buried. Sediment immediately under the cages was described as severely impacted being black, loose and highly reducing³ so these burial estimates likely only reflect heavily impacted conditions. This compares with burial rates rates of between 1 to 60% and net sediment accumulation rates of only 0.0001 – 1 g cm² y⁻¹ in natural marine sediments (Burdige, 2007).

Keeley *et al.* (2019) studied the fate of settled material across the production cycle and at various distances from a Norwegian farm located in an area of sand and coarse sediment. The results suggested that about 50% of the settled carbon became buried with the remainder

² Labile organic carbon refers to carbon which is oxidizable, mainly by micro-organisms. The non-labile fraction is resistant to breakdown and is also sometimes referred to as the refractory component.

³ A reducing environment is one where oxidation is prevented by low levels of the absence of free oxygen.

contributing to somatic growth of benthic biota or was respired by the macrofauna and microbes.

If the supply of organic material from a fish farm ceases, sedimented and buried organic material will gradually be re-worked by bed erosion and recolonization by macrofauna (Keeley *et al.*, 2019). However, the rate at which this occurs will be related to both the strength of the near bottom water currents and the level to which the sediment has been impacted.

Tomassetti *et al.* (2005) reported recovery of the benthic community beneath a sea bass (*Dicentrarchus labrax*) and shi drum (*Argirosomus regiumbut*) farm within two months, but the total biomass being reared was only 180 tonnes, which is small by today's standards. Fallowing periods of three months are not uncommon in commercial fish farming. Based on a study in Tasmania, Macleod *et al.* (2006) found that there were improvements in the benthic community during this time, but conditions had not returned to those of adjacent reference sites. There were also differences in the degree of recovery related to exposure with the community at a sheltered site likely being more resilient to organic enrichment (Macleod *et al.*, 2007), and thus recovering faster when compared to a more exposed site. Brooks *et al.* (2003) reported that biogeochemical and biological recovery around salmon farms in British Columbia (with peak biomass of around 2,000 tonnes) was almost complete after six months of fallowing. Studying a salmon farm at a dispersive site in Norway, Keeley *et al.* (2019) found that macro and microbial respiration rates returned to near baseline conditions within seven months. However, they did note that macrofaunal diversity and species richness were still suppressed at the end of the fallow period, echoing the earlier findings of Macleod *et al.* (2006). Other researchers have reported longer recovery times, but conclusions can vary depending on how 'recovery' is defined (Lumb, 1989; Johannessen *et al.*, 1994; McGhie *et al.*, 2000; Pohle *et al.*, 2001; Pereira *et al.*, 2004).

Once established, conditions at either end of the Pearson and Rosenberg cline (Figure 6) are usually relatively easy to identify (from physicochemical measurements and from the fauna associated with aerobic versus fully anaerobic conditions). However, the relationship between organic enrichment and changes to the benthic community is often not as straightforward as the model may suggest (Brown *et al.*, 1987; Weston, 1990; Hargrave *et al.*, 1993; Sowles *et al.*, 1994; Cromey *et al.*, 1998; Chamberlain, 2002; Wilding *et al.*, 2012; Keeley *et al.*, 2013b). Based on sampling at a redundant farm site in Loch Creran, Pereira *et al.*, (2004) reported that the percentage of organic carbon in the sediment was not a good indicator of temporal changes in the recovering macrobenthic community. The authors suggested that this might be in part due to changes in the fraction of labile carbon in the total pool of organic carbon. In an unimpacted medium to fine sand sediment, Grant and Hargrave (1987) estimated that only around 10% of the particulate organic carbon pool would be labile. Oxidising labile organic carbon at a hypoxic or anoxic site enriched with fish farm waste to this low level could thus take a considerable time (Pereira *et al.*, 2004). Karakassis *et al.* (1999) reported an interesting case in the Mediterranean where following the removal of fish cages, phosphate enrichment from farm waste appeared to trigger a secondary benthic macroalgal bloom which then inhibited the recovery of the benthic community for up to 23 months. The authors concluded that the classic Pearson and Rosenberg succession is not necessarily reversible, at least in terms of short-term macrofaunal responses to declining enrichment.

The important site-specific factors affecting the benthic community response to enrichment by fish farm waste thus include the species being reared (Cromey *et al.*, 2009; Weise *et al.*, 2009), the feeding routine (Cromey *et al.*, 2002a), water temperature (Hargrave *et al.*, 1993), the current regime (Findlay and Watling, 1994; Cromey *et al.*, 2002a; Keeley *et al.*, 2013b), the

seabed's physical (Kalantzi and Karakassis, 2006) and biological characteristics (Keeley *et al.*, 2013b) and seasonality (Brown *et al.*, 1987; Keeley *et al.*, 2013b).

The importance of water circulation in facilitating higher sediment assimilative capacity is clearly demonstrated in Loch Ailort (Scotland). The fjordic nature of this loch results in periods of stagnation of the bottom water and hypoxic conditions. The sediments tend to be rich in organic matter and have benthic communities typical of those found under hypoxic conditions. Although biological communities in depositional environments may be better adapted to cope with some additional organic loading (Macleod *et al.*, 2007), Gillibrand *et al.* (1996) suggested that hypoxic sites like Loch Ailort might be more sensitive to additional organic waste because of their naturally reduced assimilative capacity.

Because assimilative capacity is affected by so many factors, predicting the level of additional organic carbon a site can safely assimilate has proven challenging. Theory and observations (Findlay and Watling, 1994) suggests that sediments should be able to assimilate quite high organic fluxes ($5 - 20 \text{ g C m}^{-2} \text{ d}^{-1}$), even when the water flow is relatively slow ($1 - 8 \text{ cm s}^{-1}$). However, other studies have indicated that signs of negative impacts become apparent at lower carbon deposition rates.

According to the Pearson and Rosenberg model, the faunal composition of benthic communities will gradually change as carbon sedimentation rates increase. Crustaceans and filter (suspension) feeding molluscs tend to be sensitive to organic loading and may disappear as major components of the macrofauna when sedimentation rates exceed $5 \text{ g C m}^{-2} \text{ day}^{-1}$ (Hargrave *et al.*, 2008). This can occur in response to hypoxia, transient anoxia or simply physical smothering, that is before fully anoxic conditions develop.

Anoxic conditions can however develop at even lower sedimentation rates. Based on data collected at 23 sites, Hargrave (1994b) proposed that most sites would start to show signs of anoxia when sedimentation exceeded $1 \text{ g C m}^{-2} \text{ d}^{-1}$. Based on an arbitrary impact index, Sowles (1994) suggested that negative impacts started to become apparent at sites where sedimentation exceeded about $2 \text{ g C m}^{-2} \text{ d}^{-1}$, but there was a large degree of scatter in the data. Chamberlain and Stucchi (2007), studying a site in British Columbia, used both modelling and field measurements and concluded that the transition between an oxic and anoxic benthic status occurred at organic carbon fluxes of between ~ 1 and $5 \text{ g C m}^{-2} \text{ d}^{-1}$. Keeley *et al.* (2013a) reported that at non-dispersive sites, moderate benthic enrichment was associated with a flux of around $0.3 \text{ g C m}^{-2} \text{ d}^{-1}$ but that $5 \text{ g C m}^{-2} \text{ d}^{-1}$ resulted in more severe impacts. At dispersive sites, moderate impacts were associated with a flux of $0.8 \text{ g m}^{-2} \text{ d}^{-1}$ and more severe impacts with a flux of $11.2 \text{ g C m}^{-2} \text{ d}^{-1}$. Based on Canadian experience, Bravo and Grant (2018) suggested that the safe assimilative capacity would vary over quite a large range (0.6 to $22.1 \text{ g organic C m}^{-2} \text{ d}^{-1}$) in poorly flushed environments whilst at sites exposed to mean tidal currents greater than 9.5 cm s^{-1} there might be no upper limit as the organic material was expected to be widely dispersed (in that study safe assimilation capacity was defined as avoiding sulphide concentrations of $>1500 \mu\text{M}$ in the upper 2 cm of the sediment in accordance with Canadian environmental regulations).

At many sites the nature of the seabed also varies at small spatial scales. At higher energy sites in particular, the seabed can be comprised of patches of sand interspersed with areas of coarser sediment or exposed rock (Carvajalino-Fernández *et al.*, 2020b). This will give rise to fine spatial variability in processes such as sediment oxygen penetration (Hargrave, 2010), assimilation capacity and waste matter settlement and resuspension (see Section 1.8).

Because of the complexity of the waste dispersal and settlement process, computer models have been developed which aim to provide environmental managers with tools to assess the

benthic impact from fish farms (Table 1). These tools aim to identify the biomass level which can be stocked whilst keeping the amount of waste reaching the seabed within acceptable levels, in accordance with local environmental regulations. However, it is important to realise that even if the fine-scale variability in seabed characteristics (sediment type, porosity etc.) around a farm site has been mapped, computer models such as NewDEPOMOD cannot at present utilise such fine-scale information (Carvajalino-Fernández *et al.*, 2020b). This limitation needs to be born in mind when using these tools, and when evaluating the results of benthic monitoring programs, particularly at more dispersive sites (SEPA, 2019a).

1.4. Relationship between the INCREASE research project and environmental regulation in Scotland

Fish farmers clearly want to maximise the biomass they can rear at a site whilst minimising seabed impacts, since these can have negative impacts on the fish. There is also strong public interest in protecting the marine environment and concerns remain around the benthic impacts of open cage fish farming (Whitmarsh and Wattage, 2006; SEPA, 2019b).

In response, public regulators usually specify environmental quality standards to which fish farms must conform. In Scotland, the Scottish Environmental Protection Agency (SEPA) have recently issued a revised framework for controlling discharges from marine fish cages (SEPA, 2019b). A new framework was required because the average size of farms has increased, locations have shifted away from very sheltered, non-dispersive sites and scientific understanding of the fate of organic discharges in the sea has improved in recent years.

Consideration of the spread of fish farms from sheltered low energy to more dispersive locations requires an understanding of the water flows in these two environments. For semi-enclosed Scottish sea lochs, mean current speeds away from narrows may be of the order of 5 or 6 cm s⁻¹ (Cromey *et al.*, 2002a). In contrast, more open sites may have mean current speeds of 15 cm s⁻¹ or higher (this study).

Studies in sheltered locations have generally found that the benthic impacts from fish farms are confined close to the cages (generally < 100 m), the so-called near-field impact (Brooks and Mahnken, 2003), but in more energetic locations waste material can be transported further. This material may be dispersed to below detectable levels, although it may still cause biological changes (Keeley *et al.*, 2013b), but it can also accumulate to give more serious far-field impacts (Pohle *et al.*, 2001; Hargrave, 2003; Bannister *et al.*, 2016; Law *et al.*, 2016; Broch *et al.*, 2017; SEPA, 2019b).

Recently advances in the analysis of free sulphides, fatty acids, and eDNA in sediments have detected changes linked to fish farm waste at distances exceeding 100 m from the cages (Kutti *et al.*, 2007; White *et al.*, 2017; Keeley *et al.*, 2019; Cranford *et al.*, 2020). In some cases, even traditional infauna quantification has shown community level changes at distances of up to 200 m from fish farm cages (Brooks and Mahnken, 2003). Tracing of fish farm derived waste material at even greater distances has been reported in some studies. Studying a Norwegian farm located in an area of coarse sand, Keeley *et al.* (2019) recorded elevated deposition of organic material and associated ecological changes up to 600 m from the cages. However, they noted that there were few visible impacts and that the opportunistic macrofaunal and microbial activities returned to near background levels within seven months of the fish being harvested. Kutti *et al.* (2007) deployed sediment traps around another Norwegian fish farm located in deep water. Although most of the farm waste settled close to the farm, some was detected up to 1 km

away. However, the study concluded that the far-field deposition rates were not sufficient to cause ecological problems.

Despite some evidence of resilience to organic enrichment in sediment infaunal communities in dispersive environments (Macleod *et al.*, 2007; Keeley *et al.*, 2013b), far-field dispersion and impacts must be considered by regulators (Stigebrandt, 2011; Keeley *et al.*, 2019; Carvajalino-Fernández *et al.*, 2020b; Chary *et al.*, 2021). In addition, the habitats in dispersive areas can be patchy and include areas of exposed rock, rocky reef (Keeley *et al.*, 2019) and biogenic reef (Hall-Spencer *et al.*, 2006) and the organisms associated with such areas may be more sensitive to smothering, compared to infaunal organisms (Airoldi, 2003; Hall-Spencer and Bamber, 2007).

In terms of benthic impacts, the SEPA framework in Scotland uses the concept of a “mixing zone”. This brings the approach taken with fish farms into line with how SEPA regulates other discharges into the Scottish marine environment (Figure 7).

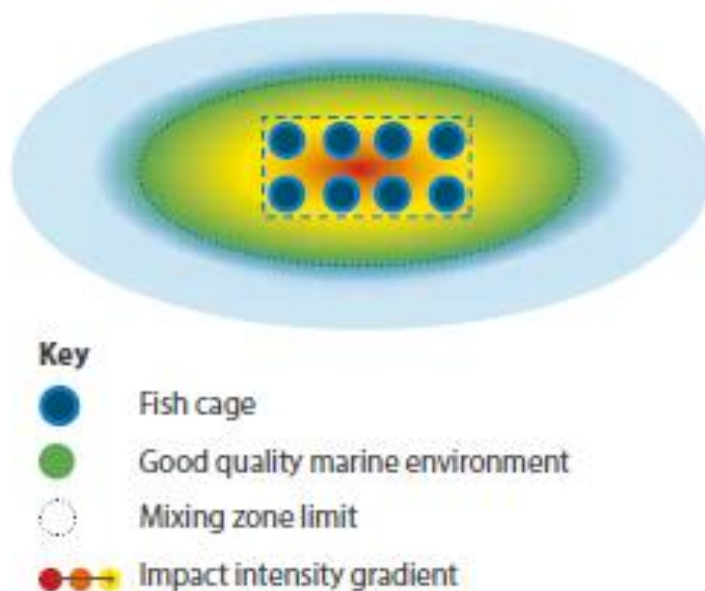


Figure 7: Spatial limit on mixing zones under revised fish farm discharge framework (SEPA, 2019b).

Box 1: Text from the revised framework Protection of the marine environment: Discharges from marine pen fish farms: A strengthened regulatory framework (SEPA, 2019b).

“On the sea bed immediately around fish farm pens, there is a zone in which wastes are not fully mixed and dispersed in the surrounding sea. Under the regulatory framework, we will limit the maximum scale of this mixing zone (Figure 7). The limit will be equivalent to the 100 meters based limit we apply to all other discharges to the marine environment, including industrial discharges and discharges of sewage effluent via long-sea outfalls. Fish farm operators will have to manage their sites so that there is no significant adverse impact on the biodiversity of sea life beyond the edge of the mixing zone. The mixing zone is defined as an area equivalent to that lying within 100 metres of the pens in all directions. However, the shape of the zone does not have to be symmetrical. It can extend more than 100 metres from the pens in some directions provided its total area does not exceed that of the equivalent symmetrical area.”

“An additional requirement is that at pen edges, biological processes must be functioning to break down and assimilate waste. This pen-edge limit on the intensity of impact ensures that the wastes do not accumulate within the mixing zone to levels that would compromise the biological process needed to breakdown and assimilate them.”

“The revised framework also acknowledges that waste from fish farms can accumulate at distance due to dispersal by water currents. Fish farm operators are required to demonstrate, and then manage their sites so that, where waste accumulation does occur, the degree of that accumulation is sufficiently limited to prevent it having a significant adverse impact on the biodiversity of sea life.”

“In sheltered waters with weak tides, the pen edge requirements will normally be the dominant factor controlling the quantities of waste that can be discharged and, hence, the sizes of farms that can operate with open-net pens. At locations that are moderately dispersive, larger farms can be supported and the mixing zone size limit will start to be the dominant control on farm scale. At the most dispersive sites, little waste is deposited for long in mixing zones and avoiding any cumulative risks to the wider marine environment will become the primary factor governing the farm sizes that can be accommodated.”

Scottish fish farms have always had to undertake a certain level of benthic monitoring to ensure they were compliant with their permitted discharges. However, under the revised SEPA framework this monitoring requirement has been strengthened (Enhanced Benthic Monitoring) meaning that an increased number of samples must be collected and analysed close to peak fish biomass. The aim is also to demonstrate that the spatial shape of the mixing zone footprint is being captured (Figure 8).

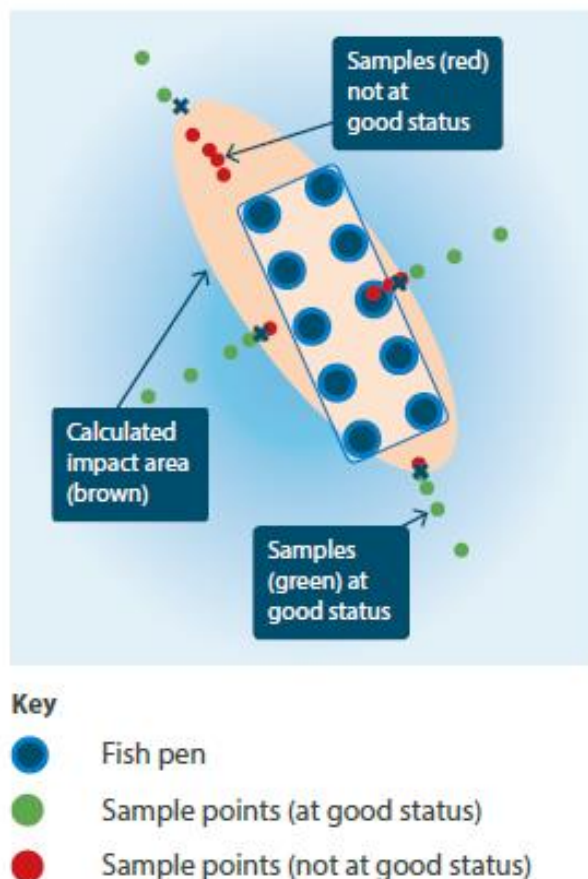


Figure 8: Monitoring transect design at a typical farm following the revised SEPA framework (SEPA, 2019b).

Whether a sample is at a ‘Good’ or less than ‘Good’ status is determined using an Infaunal Quality Index (IQI) – see Section 1.7.

The main control on the amount of waste released from a farm is the setting of site-specific biomass limits as part of a farm’s Controlled Activities Regulations 20054 (CAR) licence. The use of feed input limits was considered but for now biomass limits are the main licence condition. However, setting a biomass limit requires understanding how large a biomass can be reared at a site without breaching the permitted mixing zone area or cage edge standards. This in turn implies a need to model waste dispersal and settlement on a site-by-site basis, as well as understanding the relationship between organic waste deposition and biological impact (SEPA, 2019a).

⁴ The Water Environment (Controlled Activities) (Scotland) Regulations (2011) originates from the Water Framework Directive (2000/60/EC) which established a framework for Community action in the field of water policy. Article 11 of that Directive required Member States to establish a programme of measures for each river basin district to prevent deterioration of water body status, to protect, enhance and restore water bodies with the aim of achieving good status by 2015, and to progressively reduce pollution of water bodies from priority substances and to cease or phase out emissions, discharges and losses of priority hazardous substances. The Directive was transposed into Scottish law via the Water Environment and Water Services (Scotland) Act of 2003 which set the relevant authority (SEPA) for implementing the Controlled Activities Regulations or CAR.

1.5. The use of numerical models in predicting organic waste dispersal from a farm site

Early efforts to estimate the dispersal of organic waste from fish farms relied on statistical approximations of the footprint dependent on averaged water currents (Silvert, 1994). Such models were quick to run and provided at least a first approximation of the benthic footprint from fish farms. However, Gowen et al. (1994) noted that at that time there were no models that were suitable for use as management tools.

In the late 1990s, the availability of more computing power allowed the approach to shift to one where large numbers of simulated waste particles were tracked within the model (Table 1). This approach has the advantage of allowing more processes to be explicitly included in the model, but because large numbers of particles must be tracked to simulate the overall likely footprint, it places considerable demands on computing power.

Since then, computer models of waste dispersal have evolved in sophistication and are now accessible to commercial fish farm operators, although newer models may still require a powerful non-standard PC to run at useable speeds.

A further development has been the shift from basing particle dispersal on an averaged water current flow field (usually derived from observations from a single current meter) to allowing spatially varying water currents. These are normally derived from a separate physical oceanographic model. This allows modelling of waste dispersal in more topographically complex areas, such as the fjordic environments of Scotland, Norway and Chile where many salmon farms are located. However, the use of spatially varying current flow fields by the industry is still limited because of the additional strains it places on computing power and the need to have access to the outputs from a high-resolution physical ocean model of the area.

Although now used routinely as environmental management tools in countries including Scotland, Canada and New Zealand, it must be noted that the availability of particle tracking models to industry is a relatively recent phenomenon (Table 1). The available models are thus really in the ‘continuous improvement’, rather than the ‘fully mature’, phase of applications development.

SEPA have written a comprehensive overview of the use of computer models in relation to fish farm discharges to which the reader is directed for a more in-depth discussion (SEPA, 2019a).

1.6. The processes included in computer models of fish farm waste dispersal

Computer models have been developed for application to both shellfish and finfish aquaculture. Rearing of shellfish generally relies on natural phytoplankton production whilst finfish aquaculture usually involves the addition of natural or artificial feeds. This difference affects the processes which need to be included especially when dealing with the initial production of organic waste from the food source (Silvert, 2005).

However, once the simulated waste particles are released, these models have many features in common e.g., both groups of models rely on principles from physical oceanography to predict how the simulated particles will be dispersed in the water column (Figure 9).

Once the simulated particles have reached the seabed, the underlying mechanisms will be similar because in real life the seabed under and around both shellfish and finfish farms will be responding to additional organic loading. The computer models will however need to be parameterised for the composition of the appropriate shellfish or fish waste (and uneaten feed)

as differences in the composition of the waste will affect the rates of sinking, resuspension and the diagenetic processes occurring in the sediments.

The common mechanistic underpinning between shellfish and finfish waste dispersal models can be seen in Weise *et al.* (2009) who simulated the benthic footprint of a blue mussel (*Mytilus edulis*) farm using a modified version of the DEPOMOD salmon model (Figure 9).

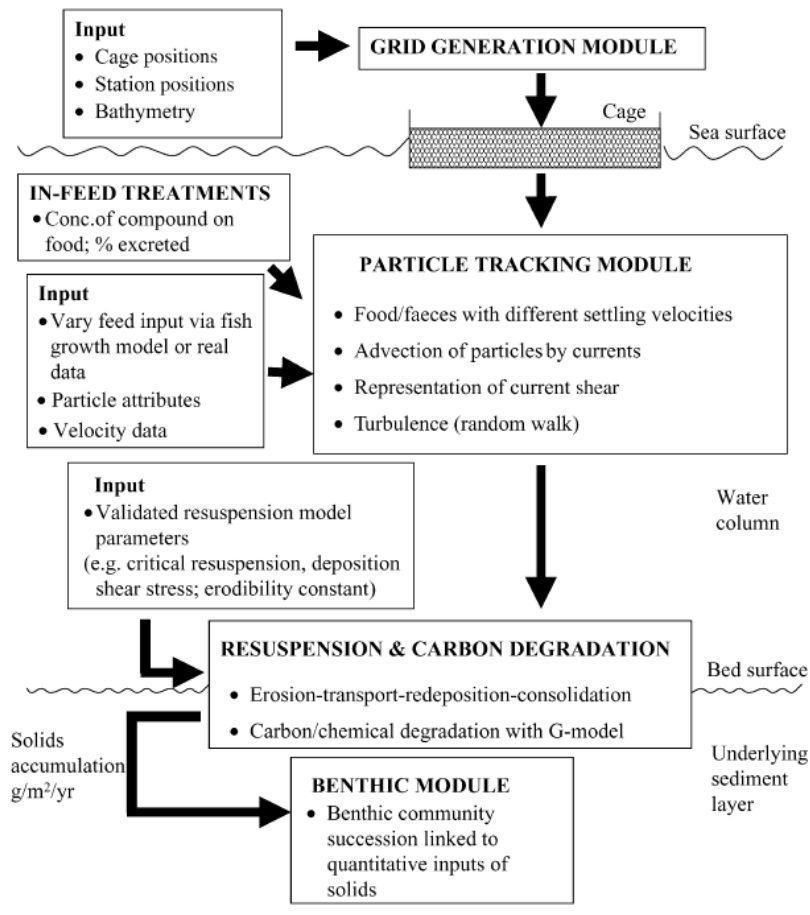


Figure 9: Flow diagram representing the basic DEPOMOD model inputs, modules and processes (Cromey *et al.*, 2002a).

Table 1: A selection of computer models for predicting waste dispersal from aquaculture operations demonstrating their evolution and common ancestry.

Model	Model parameterised for waste source	Current model ⁵	Mechanistically modelled e.g. by particle tracking	Indirectly modelled i.e., based on empirical relationships	Comments	Reference
Gowen <i>et al.</i>			No	Benthic footprint		(Gowen <i>et al.</i> , 1989)
Various	<i>Salmo salar</i> (Atlantic salmon)	2D	No	Initial waste dispersal and settlement	Describes several models available at the time	(Gowen <i>et al.</i> , 1994)
Hevia <i>et al.</i>						(Hevia <i>et al.</i> , 1996)
Gillibrand and Turrell	<i>Salmo salar</i> (Atlantic salmon)	2D	Based on particle tracking Initial waste dispersal and settlement		Included random walk to simulate diffusion	(Gillibrand and Turrell, 1997)
Panchang <i>et al.</i>	<i>Salmo salar</i> (Atlantic salmon)	2D	Feed to waste Waste dispersal and settlement	Exponential decay of settled waste Resuspension of settled particles		(Panchang <i>et al.</i> , 1997)
AWATS	<i>Salmo salar</i> (Atlantic salmon)	2D	Feed to waste Waste dispersal and settlement	Improved parameterisation of waste resuspension in Panchang model		(Dudley <i>et al.</i> , 2000)
DEPOMOD	<i>Salmo salar</i> (Atlantic salmon)	2D	Feed to waste Initial waste dispersal and settlement Waste resuspension	Infaunal taxonomic indices	- Aimed to parameterise a model suitable for operational use	(Cromey <i>et al.</i> , 2002a)
DEPOMOD	<i>Mytilus edulis</i> (Blue mussel)	2D	Initial waste dispersal and settlement Waste resuspension	Benthic community impacts	Re-parameterised DEPOMOD for mussel farm waste	(Chamberlain, 2002)

⁵ The dimensionality of the ocean current model can be confusing. By 1D we mean a model representing processes at a single point in horizontal space; by 2D we mean models which use either observations collected at a single point or a mathematical relationship of the change in current speed with depth through the water column but extrapolated across a two-dimensional horizontal frame; by 3D we mean models which use either observations of current speed and direction collected at multiple locations and depths, or where the outputs from a fully three-dimensional oceanographic model are used as the basis for particle tracking.

Table 1: A selection of computer models for predicting waste dispersal from aquaculture operations demonstrating their evolution and common ancestry.

Model	Model parameterised for waste source	Current model5	Mechanistically modelled e.g. by particle tracking	Indirectly modelled i.e., based on empirical relationships	Comments	Reference
Doglioli <i>et al.</i>	Gilthead Sea Bream (<i>Sparus aurata</i>) and Sea Bass (<i>Dicentrarchus labrax</i>)	2D	Initial waste dispersal and settlement		Based on 2D version of Princeton Ocean model Mediterranean has low bottom currents, so authors considered modelling resuspension was not necessary	(Doglioli <i>et al.</i> , 2004)
Stucchi <i>et al.</i>	<i>Salmo salar</i> (Atlantic salmon)	2D	Feed to waste	Initial waste dispersal and settlement	Analytical current model to speed up run-times	(Stucchi <i>et al.</i> , 2005)
Harstein and Stevens	<i>Perna canaliculus</i>	3D	Initial waste dispersal and settlement		No resuspension model but observations at high energy site suggested wide dispersal of waste	(Hartstein and Stevens, 2005)
Giles <i>et al.</i>	<i>Perna canaliculus</i> (Green shell mussel)	2D	Initial waste dispersal and settlement Waste resuspension		Compared model results with and without resuspension and compared with observed benthic footprint	(Giles <i>et al.</i> , 2009)
Shellfish-DEPOMOD	<i>Mytilus edulis</i> (Blue mussel)	2D	Initial waste dispersal and settlement Waste resuspension	Benthic community impacts	Re-parameterised DEPOMOD for mussel farm waste	(Weise <i>et al.</i> , 2009)
Ali <i>et al.</i>	<i>Salmo salar</i> (Atlantic salmon)	3D	Initial waste dispersal and settlement		Dispersal based on Bergen Ocean Model	(Ali <i>et al.</i> , 2011)
Stigebrandt	<i>Salmo salar</i> (Atlantic salmon)	2D		Dispersion and resuspension based on statistical relations with current variability		(Stigebrandt, 2011)
Bannister <i>et al.</i>	<i>Salmo salar</i> (Atlantic salmon)	3D	Initial waste dispersal and settlement		Dispersal based on Regional Ocean Model System (ROMS)	(Bannister <i>et al.</i> , 2016)

Table 1: A selection of computer models for predicting waste dispersal from aquaculture operations demonstrating their evolution and common ancestry.

Model	Model parameterised for waste source	Current model5	Mechanistically modelled e.g. by particle tracking	Indirectly modelled i.e., based on empirical relationships	Comments	Reference
Bravo and Grant	<i>Salmo salar</i> (Atlantic salmon)	1D	Initial waste dispersal and settlement Waste resuspension Diagenetics		On-going development work implementing a 3D version	(Bravo and Grant, 2018)
NewDEPOMOD	<i>Salmo salar</i> (Atlantic salmon)	2D or 3D	Feed to waste Initial waste dispersal and settlement Waste resuspension	Infaunal taxonomic indices	Dispersal can be based on measured current profiles or take input from oceanographic models including unstructured models such as FVCOM.	(SRSL, 2021)

The problem of simulating the impact of organic waste from a fish farm can be broken down into five steps:–

- (i) Modelling the amount of feed used, its assimilation efficiency by the fish and therefore the amount of waste (faeces and uneaten pellets) produced.
- (ii) Modelling the settlement of the waste material from the cages through the water column to reach the seabed.
- (iii) Modelling the resuspension and movement of waste material from its initial settlement site.
- (iv) Modelling the diagenetic breakdown of the accumulated organic waste material on the seabed.
- (v) Relating changes in the sediment condition, caused by the accumulation of organic matter, to changes in the benthic biological community.

Step (i) The main driver for the quantity of waste material settling to the seabed will clearly be the level of input. The amount of feed being supplied will be related to the biomass of fish in the cage at any time and hence the point within the overall production cycle. The amount of waste produced will thus be determined by the composition of the feed, the amount of feed being provided to the fish in the cage, how much of the feed is directly consumed by the fish (and how much is uneaten) and the feed conversion efficiency. Regulators may require an assessment of the maximum impact (taking a precautionary approach) which will then require running the model for a period of time equivalent to maximum biomass in the cages.

Step (ii) - Once released from the cage, waste faeces and any uneaten feed pellets will settle towards the seabed but also be dispersed by the local water currents. The strength and direction of the water currents during the initial settlement and dispersal phase will be related to the state of the tide and whether feeding is timed to coincide with a certain tidal state. Uneaten pellets and faecal material are also known to settle at different rates, and these have been measured experimentally for several fish species. However, both Reid (2009) and Bannister *et al.* (2016) caution that common assumptions about faecal settling rates used in models are often based on limited experimental data, and that simulation results can be sensitive to departures from these assumptions.

Bannister *et al.* (2016) measured the settling velocities of faeces collected from three sizes of fish at a Norwegian salmon farm. These data suggested that the material contains a spectrum of different sizes which results in different settling velocities. These data were used to parameterise a particle tracking model which was coupled to a three-dimensional current model (ROMS) of the Uggalsfjord. The fjord is deep (up to 150 m) relative to most present Scottish sites and with moderate dispersion (water currents up to 10 cm s⁻¹). Particles were considered settled when they reached 150 m depth and resuspension was not modelled. If particles were simulated using a constant mean settling velocity, then most settled within 1.5 km of the release site. In contrast, when mass fraction settling velocities were used (that is a range of settling velocities better representing those measured from the faecal samples), about 75% settled within 500 m of release site but 1-3% were transported more than 2 km. The authors concluded that predictions of far-field dispersal were sensitive to the approach to settling velocity with use of a

mean with normal distribution (as in DEPOMOD) potentially not capturing far-field dispersal. A similar conclusion was reached by Magill *et al.* (2006) after conducting experiments on settling velocity of faeces produced by gilthead sea bream (*Sparus aurata*) and sea bass (*Dicentrarchus labrax*).

Cromey *et al.* (2002a) also conducted faecal settling experiments but only reported a mean and variance for their measured settling velocities and did not show the particle-size settling velocity distribution.

In addition to robust estimates of settling velocities of waste material, modelling the initial settlement and dispersal of simulated particles requires information on how the local water currents change in strength and direction over time. Most of the available waste dispersal models either make use of currents measured at the site, or derive the currents from a separate physical oceanographic model.

In simple models which use current meter data to advect particles (e.g., Hevia *et al.* (1996) horizontal diffusion is an inherent property, but in models such as DEPOMOD which separate the particle motion into advection and diffusion components, it must be explicitly included (Gillibrand and Turrell, 1997).

Accurately measuring diffusion by commonly used tracers, such as the rhodamine dye, does not adequately mimic the dispersal of non-neutrally buoyant particles, such as fish waste. Nevertheless, the commonly assumed dispersion coefficients are largely based on dye tracer experiments (Okubo, 1971; Talbot and Talbot, 1974). It is important to realise that dispersion coefficients are also scale dependent, so the value chosen must be appropriate to the temporal and spatial scales of interest. According to Riera (2015), dispersion coefficients relevant to modelling fish waste dispersal at Mediterranean sites vary from $< 0.01 \text{ m}^2 \text{ s}^{-1}$ to $> 0.4 \text{ m}^2 \text{ s}^{-1}$. In Scotland, it is recommended to apply a horizontal dispersion coefficient of $0.1 \text{ m}^2 \text{ s}^{-1}$ in the DEPOMOD model, unless site-specific data are available to support a different value (SEPA, 2019a).

Cromey *et al.* (2002a) also applied a vertical dispersion coefficient of $0.001 \text{ m}^2 \text{ s}^{-1}$ to the simulated particle random-walk, although Gillibrand and Turrell (1997) suggested that vertical diffusion makes little difference to the rate of descent of waste particles during the initial settling phase. This is because the sinking velocity of the particles dominates the turbulent component of their vertical motion. According to SRSL (2021) this value for vertical diffusion is retained in NewDEPOMOD because it helps overcome bathymetry artefacts in the resuspension module.

The seabed is also not generally flat and changes in topography will affect the local water flow. Some of the more sophisticated fish farm waste dispersal models allow bottom topography to be included. Although computer simulations have shown that even moderate topographic variations can affect where material should accumulate on the seabed (Jusup *et al.*, 2007), experience has shown that the impacts on predictions of including variable seabed topography usually have to be explored on a case-by-case basis.

In relation to the issue of how sheltered a farm site is, the role of wind-forcing and periodic extreme events such as storms in further dispersing waste has not been widely studied. The impact of wind-driven flows on waste dispersal was considered by Panchang (1997) and Dudley *et al.* (2000) using a two-dimensional

oceanographic model. The importance of including wind forcing when simulating waste dispersal was apparent at one of the sites examined (Cutler Harbour).

Step (iii) – Settled organic material will begin to be broken down by macrofauna and microbes (Section 11). However, as previously discussed if the rate of settlement exceeds the local assimilation capacity, the organic material will begin to accumulate and consolidate, but can also become resuspended and dispersed further afield (Keeley *et al.*, 2019). These processes have proven important to include in waste dispersal models (Giles *et al.*, 2009) but have also proven particularly challenging to parameterise (Panchang *et al.*, 1997; Dudley *et al.*, 2000; Chamberlain, 2002; Cromey *et al.*, 2002a; Hartstein and Stevens, 2005; Silvert, 2005; Black *et al.*, 2016). Issues associated with this process as implemented in NewDEPOMOD are the focus of the work reported here.

Step (iv) – Fish farm waste dispersal models may, or may not, explicitly model the diagenetic processes (Table 1). In some models, including NewDEPOMOD, diagenesis is represented using simple estimates of the rate of organic carbon degradation, but a few models include explicit biogeochemical processes occurring in the sediment (Table 1). There are pros and cons to either approach. Including a full diagenetic model will significantly increase the computer model runtimes which may make undertaking multiple runs problematic, especially when the model is expanded into three dimensions. A full diagenetic model will also need many flux variables (Bravo and Grant, 2018), potentially making the predictions sensitive to parametrisation error. On the other hand, the lack of diagenetic modelling means that the model cannot produce mechanistically based predictions of factors such as sulphide production and sediment oxic state which may be of interest to regulators and farm managers.

Some additional research was therefore conducted in relation to sulphides production which is related to the diagenetic⁶ processes occurring once organic waste has settled to the seafloor. This additional work is described in the report section for the SAIC funded project, NAMAQI.

Step (v) - The final step of relating the physical and chemical changes at a site to changes in the benthic biological community is also challenging. Although the Pearson and Rosenburg model appears conceptually straightforward, it can be difficult to apply in practice because rather than abrupt shifts from one community to another the model describes a gradual change. Furthermore, as mentioned previously, different sites have differing capacities for assimilating additional organic loading dependent on local conditions.

The approaches to evaluating the biological impact of fish farm waste using dispersal models have usually been either to attempt to relate modelled organic carbon deposition rates to observed changes in the biota (for example from macrobenthos samples collected at various distances from the fish cages using sediment grabs), or to adopt a critical level which is thought to be deleterious e.g. the threshold of 1500 μM of sulphides in the upper 2 cm of the sediment adopted under Canadian fish farm regulations.

⁶ Diagenetic processes are those occurring within the sediments, these typically refer to sediment chemistry but also include biological processes such as bioturbation.

Given an adequate computer model for a site, multiple runs can be made gradually increasing the fish (or shellfish) stocking biomass to estimate the level at which the farm's benthic footprint becomes unacceptable according to the relevant environmental regulations.

The most widely used predictive benthic impacts model for fish farms in Scotland is DEPOMOD. This was originally developed by Cromey *et al.* (2002a) for predicting waste dispersal and benthic impacts from salmon farms⁷. Each version of the DEPOMOD software has gone through several updates which have been written in response to advances in computing power and operating systems, the changing needs of the industry, and to accommodate regulatory changes (Table 2). The use of NewDEPOMOD for simulating fish farm waste dispersal is described in detail in SEPA (2019a) and SRSL (2021).

⁷ The DEPOMOD models can also simulate dispersal of in-feed chemotherapeutics, such as teflubenzuron and emamectin benzoate because of their association with total waste. However, testing the simulated dispersal of chemotherapeutics was outside the scope of the present project.

Table 2: The evolution of the DEPOMOD software family.

Software	Main features	Operating system	Comments	Reference
BenOSS 2	Initial waste dispersal and settlement Waste resuspension Benthic community impacts	DOS	Model for organic totals from sewage discharges into the marine environment	(Cromeley <i>et al.</i> , 1998)
DEPOMOD	Initial waste dispersal and settlement Waste resuspension Benthic community impacts	DOS	Evolution of BenOSS2 applied to salmon farms	(Cromeley <i>et al.</i> , 2002a)
CODMOD	as DEPOMOD	DOS	Re-parameterisation of DEPOMOD for cod farm	(Cromeley <i>et al.</i> , 2009)
MERAMOD	as DEPOMOD	DOS	Re-paramaterised for gilthead sea-bream (<i>Sparus aurata</i>), sea-bass (<i>Dicentrarchus labrax</i>)	(Cromeley <i>et al.</i> , 2012)
Auto-DEPOMOD	More user-friendly version of DEPOMOD Used from 2005 by SEPA for modelling discharges from Scottish salmon farms Only used single current flow Only flat seabed Limited in spatial extent (1 km ²)	Windows '98 to NT	Almost all dialog input centralised in one .ini file Automatic iteration towards solutions Checked against SEPA method with Depomod Used commercial package Surfer© for plotting results	
MACAROMOD	Re-paramaterised for gilthead sea-bream (<i>Sparus aurata</i>), sea-bass (<i>Dicentrarchus labrax</i>) and meagre (<i>Argyrosomus regius</i>)	Windows '98 to NT	Essentially MERAMOD reparameterised for Macaronesian fish farms but also allowing a larger spatial grid	(Riera <i>et al.</i> , 2017)
New-DEPOMOD	- Rewritten AutoDEPOMOD - Allows larger model domain for simulating far-field deposition - Ability to use variable 3D current model output - Ability to include variable seabed topography	Java for Windows 2000 or later or Unix	NewDEPOMOD includes more functionality but also allows plugins and easier future upgrading Removed commercial package Surfer© for plotting results	(Black <i>et al.</i> , 2016; SRSL, 2021)

1.7. The link between organic carbon deposition and changes to the benthic biota

The aim of the biomass limit in the CAR is thus to avoid unacceptable impacts outside of the permitted mixing zone. However, defining “unacceptable impacts” is more complex than it may at first appear.

The areas which are most intensely impacted by the deposition of waste solids are normally underneath the cages. SEPA requires that although these areas are likely to experience significant ecological change, they must be able to sustain an appreciable population of enrichment species which can maintain the aeration of sediments and the turnover of carbon (Table 4).

Outside of the cage boundary lies the mixing zone where some ecological change due to waste deposition is still permissible (Figure 8).

Among the many faunal indices proposed in the 1970s for assessing changes in benthic communities, the Infaunal Trophic Index (ITI) was rapidly adopted in many countries for assessing the impacts of water pollution. The ITI assumes that a change in the abundance of organisms feeding on suspended materials to those that feed on deposited materials provides evidence for increases in the amount of sedimented total organic material (Word, 1979). ITI was used for several years by SEPA to evaluate benthic impacts of fish farms in Scotland.

For the calculation of ITI (Equation 1), organisms are enumerated and grouped into: N1 Suspension feeders; N2 Surface detritus feeders; N3 Surface deposit feeders; and N4 Surface deposit feeders.

$$ITI = 100 - [33.3 \{(N2 + 2N3 + 3N4) / (N1 + N2 + N3 + N4)\}] \quad \text{Equation 1}$$

Increases in nutrient input tend to result in a reduction in the proportion of filter feeders and an increase in the proportion of deposit feeders which is reflected in the ITI value. The ITI score gives a rough indication of the pollution status of the benthic community with the following boundaries: 60 – 100 Normal; 30 – 60 Perturbed; <30 Degraded.

With the transposition of the European Union Water Framework Directive (2000/60/EC) into UK law, an alternative harmonised approach for monitoring impacts in coastal and transitional waters called IQI (Infaunal Quality Index) was developed (Phillips *et al.*, 2014). IQI was intended to be applicable to a wider range of stressors than just organic enrichment (e.g. heavy metals), and to deliver a quantitative index with defined boundaries in terms of ‘Good Ecological Status’ (Table 3). An expanded normative definition of the different Ecological Quality Status levels is given in Appendix 1.

IQI is based on the general premise that a multi-metric index based on macroinvertebrate diversity and abundance will be more powerful in detecting disturbance. The selected metrics included were taxa number, the AZTI Marine Biotic Index (AMBI, a measure of sensitivity to disturbance which was selected in preference to ITI as the functional metric) and Simpson’s evenness (a measure of the distribution of individuals across the different taxa)⁸.

⁸ It is worth noting that IQI only applies to soft sediments and, as SEPA acknowledge, environmental standards have not yet been developed for all seabed habitats e.g. rocky seabed. Such habitats may become more likely to be impacted as fish farms move into more exposed locations.

Table 3: Normative definitions (as outlined in WFD Annex V section 1.2) for the classification of the benthic invertebrate quality element into five ecological status classes.

IQI boundary	quantitative	Ecological status	Normative definition
>0.75		High	The level of diversity and abundance of invertebrate taxa is within the range normally associated with undisturbed conditions. All the disturbance-sensitive taxa associated with undisturbed conditions are present.
>0.64		Good	The level of diversity and abundance of invertebrate taxa is slightly outside the range associated with the type-specific conditions. Most of the sensitive taxa of the type-specific communities are present.
>0.44		Moderate	The level of diversity and abundance of invertebrate taxa is moderately outside the range associated with the type-specific conditions. Taxa indicative of pollution are present. Many of the sensitive taxa of the type-specific communities are absent.
>0.24		Poor	Major alterations to the values of the biological quality elements for the surface water body type. Relevant biological communities deviate substantially from those normally associated with the surface water body type under undisturbed conditions.
<0.24		Bad	Severe alterations to the values of the biological quality elements for the surface water body type. Large portions of the relevant biological communities normally associated with the surface water body type under undisturbed conditions are absent.

In the context of the ecological changes in the mixing zone (Figure 7), SEPA has adopted IQI such that at the limit of the mixing zone, the seabed ecological status must be ‘Good’ or ‘High’ (Table 3). Because IQI is a numerical index (with range 0–1), the acceptable benthic status is then expressed in quantitative terms (Table 4).

As explained previously, the basic relationship between organic enrichment and changes to benthic communities is described in the Pearson and Rosenberg (1976) model. This suggests that as the level of organic enrichment increases, there will be a gradual transition from a well-aerated sediment containing macro-fauna to an increasingly anoxic one dominated by microbes. However, the relationship between the benthic community and the level of organic loading at a specific site is complicated by other factors including the periodicity of organic enrichment, the composition of the organic enrichment, the sediment type, local differences in benthic community composition and the level of re-oxygenation by water flushing.

It is also important to note that most studies on impacts from organic enrichment have been conducted on muddy cohesive sediments with relatively few studies on permeable (or mixed sandy-silt) sediments. Assumptions derived from studies in low-energy sites may not hold for higher energy sites on coarser sediments. As fish farms are developed in more dispersive environments, this is a gap in our understanding of organic enrichment impacts on the benthos.

It has therefore been difficult to derive consistent relationships between organic waste deposition rates and biological impact which might apply across all mixing zones and across all sites. NewDEPOMOD does not therefore include an explicit modelling of the relationship between organic waste deposition and IQI⁹.

To deal with the problem of there being no defined relationship between IQI and waste flux across the whole IQI range, SEPA defined a critical level equivalent to the moderate to good status boundary. This was based on empirical relationships between organic waste deposition and ecological state.

The information on ecological state (IQI) came from analysis of benthic samples collected around several existing fish farms which was fitted against estimated waste deposition rates derived from DEPOMOD models which had been tuned to a number of specific sites (SEPA, 2019a). As far as we are aware these relationships have not been published by SEPA but have been used to set the critical loading indicated in Table 4.

Table 4: Environmental standard and equivalent modelled waste deposition at the cage edge and in the mixing zone (SEPA, 2019a; SRSL, 2021).

Standard	Type	Definition	Model requirement
Cage edge	Intensity	>1 species of enrichment polychaete at densities >1000 m ⁻² at cage edge locations.	Mean deposited mass within the 250 g m ⁻² impact area should not exceed 1000 g m ⁻² (over 90 days at peak biomass).
Mixing zone	Extent	Total area (m ²) impacted to worse than 0.64 IQI should not exceed the 100 m composite mixing zone area (m ²).	Mean deposited mass within the 250 g m ⁻² impact area should not exceed 1000 g m ⁻² (over 90 days at peak biomass).

SEPA are continually revising guidance as experience with NewDEPOMOD develops and the latest draft guidance was issued as (SEPA, 2021).

Although providing a practical solution to the requirement to define critical levels of organic waste deposition resulting in unacceptable benthic impacts, this approach is not a direct validation of the organic waste deposition results in the DEPOMOD models.

Furthermore, SEPA now states that areas subject to wave exposures of 2.8 or greater have been shown to be able to support higher biomasses. Wave impacts are not included in NewDEPOMOD so SEPA have now adjusted the modelling standards in Table 4 with additional criteria for sites subject to wave exposure (Table 5).

⁹ It should be noted that NewDEPOMOD still includes a prediction of ITI based on an empirical relationship with waste deposition rate described in Cromey et al. (2002a) but, as explained above, ITI is no longer used for regulatory purposes in Scotland and ITI cannot be converted to IQI (SEPA, 2021).

Table 5: Draft NewDEPOMOD guidance issued on 25 June 2021 (SEPA, 2021). Changes from the standard shown in Table 4 are underlined.

Standard	Type	Definition	Model requirement
Pen edge	Intensity	>1 species of enrichment polychaete at densities >1000 m ⁻² at pen edge locations.	Mean deposited mass within the 250 g m ⁻² impact area should not exceed 2000 g m ⁻² <u>where wave exposure¹⁰ is less than 2.8, or 4000 g m⁻² where wave exposure is 2.8 or greater</u> (averaged over 90 days at peak biomass in accordance with Table 6).
Mixing zone	Extent	Total area (m ²) impacted to worse than 0.64 IQI should not exceed the 100 m composite mixing zone area (m ²).	Total area (m ²) with a mean deposited mass in excess of 250 g m ⁻² should not exceed the 100 m mixing zone area (m ²) where wave exposure is less than 2.8, <u>or 120% of the mixing zone area (m²) where wave exposure is 2.8 or greater</u> (averaged over 90 days at peak biomass in accordance with Table 6).

For licencing purposes, the modelled impacts are still considered precautionary by SEPA because the default model settings are for a run at peak biomass for 365 days with settings shown in Table 6.

Table 6: NewDEPOMOD model setup for solids (SEPA, 2021).

Setup option	Requirement
Run duration	365 days
Biomass	Peak
Feed rate	7 kg t ⁻¹ d ⁻¹
Waste rate	3%
Feed water content	9%
Feed digestibility	85%
Feed carbon content	49%
Faeces carbon content	30%
Output period	Last 90 days
Output resolution	3 hourly or greater

The latest SEPA guidance (SEPA, 2021) suggests calibrating NewDEPOMOD by adjusting the vertical dispersion until the size of the 250 g m⁻² contour matches the monitored 0.64 IQI footprint.

The vertical dispersion coefficient for the resuspension phase should be set as function of the mean flow speed at the bed (u , in m/s) as follows (Equation 2):

$$\sigma_{z,r} = 0.0003 u^{-0.762} \quad \text{Equation 2}$$

¹⁰ Wave exposure is based on the fetch and wind energy at a site and for the Scottish coast is available from the National Marine Planning Interactive (NMPi) portal <https://marinescotland.atkinsgeospatial.com/nmpi/default.aspx?layers=780>.

Note that this parameterization represents a method for accommodating the numerical structure and associated emergent behaviour of the model. It is not considered to reflect true differences in the physical processes between sites of differing flow characteristics (SEPA, 2021).

However, calibrating the NewDEPOMOD model to measured IQI can only apply to existing sites where extensive infaunal monitoring has already taken place and the IQI footprint is well established. It leaves a significant problem for modelling new farm sites.

1.8. The problem of organic waste resuspension

Locating fish farms in areas of higher current flow has often been recommended because it increases water exchange in the cages and should disperse both dissolved and total organic waste over a wider area, potentially reducing benthic impacts (Hartstein and Stevens, 2005; Belle and Nash, 2008).

Locating fish farms in areas of deeper water will also tend to lead to a larger benthic footprint because the waste particles will take more time to settle to the seabed (Kutti *et al.*, 2007).

However, even with wider dispersal, waste particles can still accumulate in localised patches at larger distances from fish farm cages (Hargrave, 2003). Whether or not this happens will be largely determined by the patterns of local water flow (Bannister *et al.*, 2016).

There is thus a trade-off between greater contamination of a smaller area (as occurs at shallow, low-flow sites) versus lower contamination of a larger area (as occurs at deeper and higher-flow sites) (Carvajalino-Fernández *et al.*, 2020b).

As shear at the sediment water interface increases above a critical level, sediment particles begin to be lifted back into the water column. The resuspended particles will be transported horizontally until a drop in the near-bottom flow combined with their vertical descent rate allows them to resettle.

In NewDEPOMOD, the seabed shear stress is calculated from the density of seawater and the square of the bottom friction velocity. The bottom friction velocity is estimated either from a “Clauser plot” or using “the law of the wall” (SRSL, 2021).

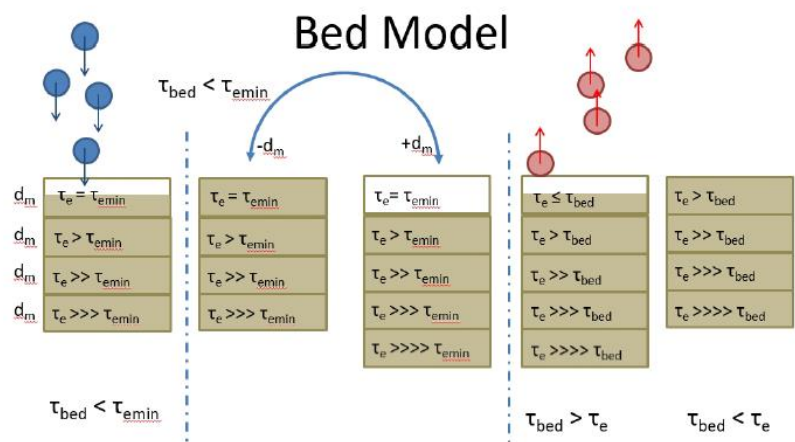


Figure 10: Depiction of particle movement in the NewDEPOMOD bed sub-model from pure deposition (left), to consolidation (centre) and erosion (right). (SRSL, 2021).

1.8.1. Studies where critical shear stress and erodibility of fish farm waste have been measured

Unfortunately, it has proven challenging to constrain the critical shear stress in sediment transport models because it varies with the sediment type, bedform and characteristics of the settled material (Law *et al.*, 2016). Furthermore, estimates have been made under a variety of conditions and with a range of methods, such as tracers (Cromey *et al.*, 2002b), laboratory flumes (Law *et al.*, 2016; Carvajalino-Fernández *et al.*, 2020a) and benthic flumes (Dudley *et al.*, 2000; Adams *et al.*, 2020). Carvajalino-Fernández (2020a) mention that some studies have failed to report important aspects, such as the height above the bed at which the current speeds were measured.

There has thus been considerable debate regarding critical thresholds for resuspension of organic waste. Early studies mostly concerned resuspension of natural sediments or sewage. These studies suggested that freshly deposited organic material in sewage appeared to be quite easily resuspended but yielded a wide range of near bed critical water speeds ranging from 7 cm s^{-1} to more than 50 cm s^{-1} (Cromey *et al.*, 2002b). To validate resuspension parameter settings in the BenOss model, Cromey *et al.* (1998) conducted a tracer experiment using fluorescent particles added to a sewage sludge plug. The model was able to reasonably reproduce the observations using a critical water speed of 9 cm s^{-1} but Cromey *et al.* expressed some concerns as to whether the tracer fully mimicked the dispersal of the organic material.

Sewage sludge and fish farm waste have different physical characteristics so it cannot be assumed that the resuspension values applied in the BenOss model will necessarily apply to fish farm waste. Cromey *et al.* (2002b) conducted an additional tracer study to validate resuspension parameters for the DEPOMOD model. Again, fluorescent particles pre-selected to have similar physical properties to salmon faecal material were released near the seabed and their dispersion tracked over 30 days using benthic grabs. The farm was in the Firth of Lorn, an area of sandy mud sediment with mean and maximum current speeds of 4.9 and 23 cm s^{-1} respectively. Based on the results, the critical shear stress for resuspension of the particles was estimated at 0.0179 N m^{-2} (equivalent to about 9.5 cm s^{-1} near-bed current speed). It should be noted that when estimating the critical shear stress from tracer results, the estimate is also sensitive to the critical deposition shear stress and M , the erodibility constant (Cromey *et al.*, 2002a).

Several other studies have used laboratory flumes to directly measure the relationship between near-bed current speed and resuspension of fish farm waste. These devices apply an increasing shear to the sediment and generally use optical sensors to assess the critical shear stress, that is the point at which the shear becomes sufficient to remobilise the sediment into the water and thus affect its optical properties.

Law *et al.* (2016) experimented with salmon faecal waste and uneaten pellets which they settled onto different sediment types in a laboratory Gust Microcosm Erosion Chamber flume. This device is designed to apply controlled shear stress to the sediment-water interface. The stress was gradually increased in a stepwise manner up to 0.6 N m^{-2} . Eroded particles were measured by monitoring turbidity and by filtration and gravimetry. The results showed that some faecal particles began to become resuspended at a stress of 0.01 N m^{-2} but the large increase in resuspension occurred at 0.08 N m^{-2} , for all substrate types. The authors noted that this value for the critical shear stress is quite close to the 0.018 N m^{-2} suggested by (Cromey *et al.*, 2002b).

The experiments by Law *et al.* (2016) also showed that much less faecal material was eroded when the underlying substrate was coarser. On cobble, less than 25% of the organic material was eroded whereas nearly complete resuspension of the faecal particles occurred when the

substrate was mud (Figure 11). Erodibility for salmon waste on mud was estimated at 1.3×10^{-6} $\text{kg m}^{-2} \text{s}^{-1}$, for sand 3.5×10^{-7} $\text{kg m}^{-2} \text{s}^{-1}$, for sand gravel 6.0×10^{-7} $\text{kg m}^{-2} \text{s}^{-1}$ and for sand cobble 5.8×10^{-7} $\text{kg m}^{-2} \text{s}^{-1}$.

The authors explained the results in terms of the capacity of the bed to provide spatial refuges. Cobble clearly has the largest potential, and it was suggested that most of the organic material was driven into the crevices at low stress, resulting in only the most easily eroded flocculated material becoming resuspended. In contrast, consolidated mud provides little scope for spatial refuge while sandy substrates provide an intermediate level allowing about 50% of the organic material to be retained.

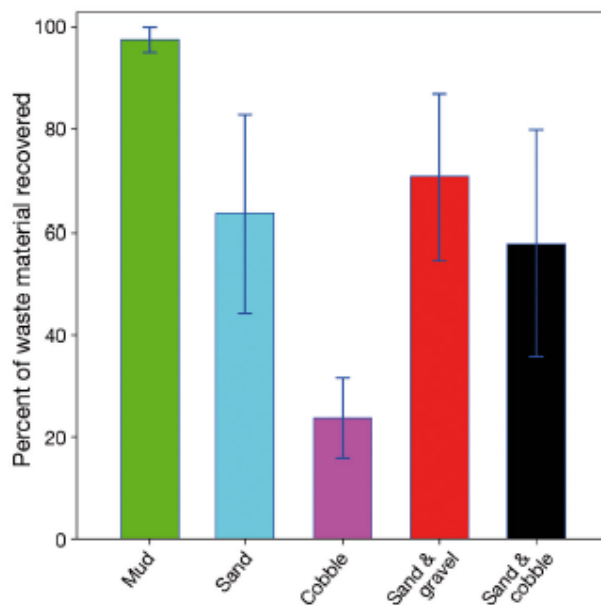


Figure 11: Percent of salmon waste material recovered from laboratory erosion experiment when the underlying substrate was varied ($n=6$ per treatment) (Law *et al.*, 2016).

Carvajalino-Fernández *et al.* (2020a)¹¹ used a horizontal flume to study the resuspension of intact salmon faecal pellets obtained from a Norwegian farm. Several substrate types were tested placing individual faecal pellets on the surface. Pellets were allowed to age for up to 6 days before being exposed to increasing water speeds up to 30 cm s^{-1} . The response of the pellets was monitored by video. Pellets began to bounce (saltation) at around 5.4 cm s^{-1} and became resuspended from about $5 - 20 \text{ cm s}^{-1}$. Substrate type appeared to affect resuspension, but not saltation of fresh pellets with resuspension occurring at lower water speeds when they were on smooth surfaces, including mud and slate. The effect of pellet ageing on resuspension was inconsistent between the substrate treatments. Across the four aged groups, mean values for critical near bed shear stress for pellet resuspension of 0.06 on slate, 0.07 on mud, 0.12 on sand and 0.32 N m^{-2} on fractured rock, were suggested.

Although these experiments again demonstrated the need to develop substrate appropriate parameterisation, the authors cautioned that the results are unlikely to apply to broken down and flocculent material, for which lower critical shear stresses are expected (Carvajalino-Fernández *et al.*, 2020a). Field studies may thus be more appropriate to measure the critical

¹¹ These authors report critical shear stress in terms of the SI unit for pressure (Pascal), but 1 Pa is equivalent to 1 N m^{-2} .

shear stress and erodibility of fish farm waste under more natural conditions but there have been relatively few such studies, probably because of the cost and logistical difficulty of deploying benthic flumes. Benthic flumes are also unsuitable for use on very coarse sediments as a good seal may not form between the flume skirt and sediment surface (Adams *et al.*, 2020).

Although uneaten feed pellets usually comprise a small fraction of the overall waste, modelling their transport is also of interest. In flume experiments conducted on cobble, feed pellets became wedged in crevices and so did not move (Law *et al.*, 2016). On mud, pellets began to bounce (saltation) at 0.08 N m^{-2} but on sand this did not occur until the shear stress reached 0.16 N m^{-2} . Once moving there was little difference in the overall horizontal distance travelled on mud or sand ($2 - 3 \text{ cm s}^{-1}$ at $0.16 - 0.24 \text{ N m}^{-2}$). At stress levels above 0.16 N m^{-2} exposed pellets began to break up while buried pellets would be excavated at shear stresses above 0.48 N m^{-2} . These results were in broad agreement with conclusions in Kutti *et al.* (2007).

1.8.2. Field studies on organic waste resuspension and erosion

Dudley *et al.* (2000) described a study using an annular flume at a farm in Eastport, Maine, USA where measurements were made out to around 100 m from the cages. Critical water speeds (at 100 cm above the bed) were estimated at between 33 and 55 cm s^{-1} . It is of interest that the study also reported seasonal differences which the authors ascribed to an effect on critical speed of varying amounts of organic matter on the seabed. However, Cromey *et al.* (2002b) noted that these critical speeds seemed high and that applying these levels to Scottish fish farms would result in virtually zero resuspension events, which was considered unrealistic.

Adams *et al.* (2020) describe a series of experiments on the Scottish west coast which used two designs of benthic flume. The smaller flume could be deployed close to the cage edges to measure near-field whilst the larger flume could only be deployed at distances of $100 - 500 \text{ m}$ from the cages. Although there was a lot of variation between different sites, the results suggested an average critical shear stress of 0.02 N m^{-2} (range $0.01 - 0.04 \text{ N m}^{-2}$) for heavily organically enriched sediments (e.g., close to the cage edge). This value was in close agreement with the result from Cromey *et al.* (2002b) who suggested 0.018 N m^{-2} based on fluorescent tracer dispersal. However, away from the cage edge, the flume study suggested higher critical shear stresses (mean 0.19 N m^{-2}), and with more variability (range $0.12 - 0.55$).

The authors suggested that heavily enriched sediment, typically found under the cages, would be relatively easily abraded and remobilised. However, away from the cage edge the covering of waste material becomes discontinuous and more mixed into the underlying sediments. The authors hypothesised that local bed roughness might then serve to entrap organic particles, thus requiring higher shear stress to remobilize it. Diving at several farms located in high-flow regimes in the Shetland and Orkney Islands, Hall-Spencer *et al.* (2006) observed that waste particles settled in seabed depressions and became trapped within the complex interlocking matrix of maerl thalli during periods of slow water flow. Those researchers suggested that resuspension dynamics for waste particulates would be strongly influenced by bed complexity. This is similar to the conclusions reached by Law *et al.* (2016) and Carvajalino-Fernández *et al.* (2020a) who used laboratory flumes to test resuspension of farm waste and intact faecal pellets on different substrates.

Most studies define a critical shear level as a threshold, that is below the critical stress resuspension does not occur and above the critical stress it does. However, resuspension will also be affected by particle size and different fractions of the material will have slightly different critical shear stresses (Carvajalino-Fernández *et al.*, 2020a). This is especially relevant to mixed material which will comprise a spectrum of intact and broken faecal pellets

and uneaten pellets in different states of breakdown. Biofilms produced by microbes may also alter the physical properties of the particles and can either strengthen or weaken the material cohesion. Droppo *et al.* (2007) suggested that in general, bio-stabilized sediments impacted by farm waste tend to have slightly lower critical stress thresholds relative to other natural sediments. This is due to their high organic and water content, non-consolidated structure, and diffuse microbial biofilm which provides limited cohesion. These aspects are not explicitly dealt with by NewDEPOMOD, although faecal material and uneaten pellets are tracked separately and the new feature of bed hardening partially addresses this aspect.

1.8.3. Calculation of erosion rates in DEPOMOD and NewDEPOMOD

In earlier versions of DEPOMOD the sediment was treated as a single layer of variable thickness (Cromey *et al.*, 2002a). When the near-bed shear exceeds the critical stress, particles are resuspended according to the erosion rate (Equation 3).

$$M_{e1} = M_1 \left(\left(\frac{\tau_0}{\tau_{crit}} \right) - 1 \right) \quad \text{Equation 3}$$

The default setting for the critical shear stress was suggested to be 0.018 N m⁻² and the erodibility constant (M₁) was suggested to be 7.0 x 10⁻⁷ kg m⁻² s⁻¹ (Cromey *et al.*, 2002b).

In contrast, in NewDEPOMOD particles can become consolidated into a sub-surface layer (Figure 10). Once consolidated, the layer's critical erosion threshold is increased over time so that the older the material, the harder it becomes to erode. New material is deposited into the surface layer with a minimum critical shear stress for which the default setting is 0.02 N m⁻², equivalent to a flow speed of about 8.5 cm s⁻¹ at 3 m above the bed (SEPA, 2019a).

In NewDEPOMOD, particles in the surface layer can become resuspended at a rate determined by the excess shear stress and an erodibility parameter, when the near-bed shear stress exceeds the critical level (SRSL, 2021).

$$M_{e2} = M_2 (\tau_0 - \tau_{crit})^n \quad \text{Equation 4}$$

The default settings are to set the exponent to 1 and the erodibility parameter (M₂ in Equation 2) to 0.031, this value is derived from the benthic flume studies described in Adams *et al.* (2020) as shown in *Figure 12*. This suggests typical erosion rates of up to 0.025 kg m⁻² s⁻¹ with excess shear stress of 0.08 N m⁻². However, the linear model appears to underestimate the observed erosion rates when the excess bed shear stress is less than 0.02 N m⁻². The data may be better fitted using a curvilinear model but this has not been adopted in the default settings for NewDEPOMOD (SRSL, 2021).

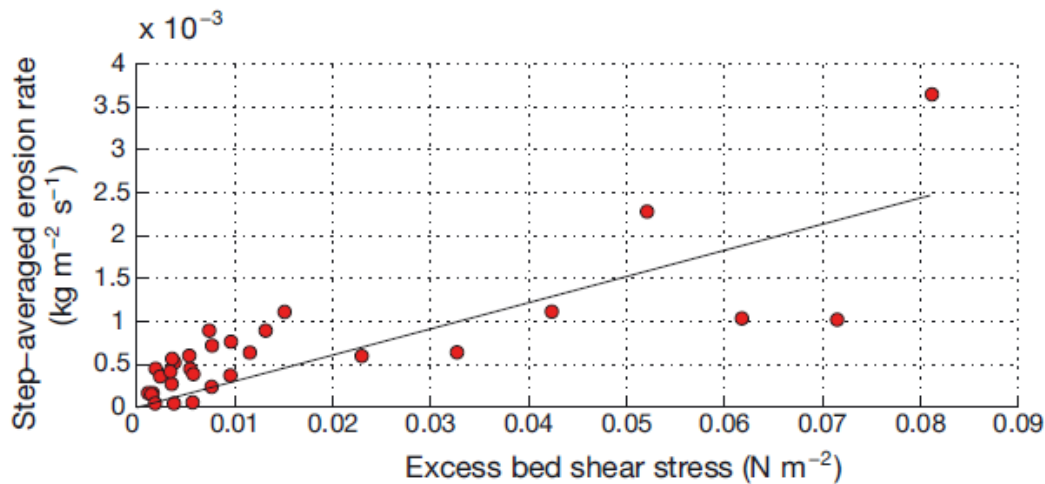


Figure 12: Erosion rate versus the excess bed stress ($\tau_0 - \tau_{0,crit}$) from the benthic flume deployments described in Adams *et al.* (2020). Note the y-axis scaling in $\times 10^{-3}$ i.e. equivalent to $\text{g m}^{-2} \text{s}^{-1}$.

Applying the substrate-specific erodibility estimates from Law *et al.* (2016) does give slightly different erosion rates over mud and sand, but results are very similar to the DEPOMOD default for the coarser substrates:- sand and gravel, or sand and cobble¹² (Table 7).

However, the default erosion rate calculation in NewDEPOMOD, which is based on the benthic flume results reported in Adams *et al.* (2020), appears to give higher erosion rates than were previously produced by DEPOMOD (Table 7).

Table 7: Erosion rates calculated using the DEPOMOD and NewDEPOMOD equations and the DEPOMOD equations with erosion coefficients estimated by Law *et al.* (2016). All calculations assumed $\tau_{0,crit} = 0.018 \text{ N m}^{-2}$.

Near bed shear stress (τ_0) (N m^{-2})	Using Eqn 1, DEPOMOD default $M_1 = 7.0 \times 10^{-7}$ Cromey <i>et al.</i> (2002b) ($\text{g m}^{-2} \text{s}^{-1}$)	Using Eqn 1, $M_1 = \text{mud} = 1.3 \times 10^{-6}$ (Law <i>et al.</i> , 2016) ($\text{g m}^{-2} \text{s}^{-1}$)	Using Eqn 1, $M_1 = \text{sand} = 3.5 \times 10^{-7}$ (Law <i>et al.</i> , 2016) ($\text{g m}^{-2} \text{s}^{-1}$)	Using Eqn 1, $M_1 = \text{sand and gravel} = 6 \times 10^{-7}$ (Law <i>et al.</i> , 2016) ($\text{g m}^{-2} \text{s}^{-1}$)	Using Eqn 2, NewDEPOMOD default $M_2 = 0.031$ (SRSL, 2021) ($\text{g m}^{-2} \text{s}^{-1}$)
0.02	0	0	0	0	0
0.04	0.0009	0.0016	0.0004	0.0007	0.68
0.06	0.0016	0.0030	0.0008	0.0014	1.32
0.08	0.0024	0.0045	0.0012	0.0021	1.92
0.10	0.0032	0.0059	0.0016	0.0027	2.54

1.8.4. Studies where different approaches to resuspension have been compared

Chamberlain and Stucchi (2005) and (2007) tested DEPOMOD using data from a salmon farm in British Columbia. They found that in simulations where resuspension was enabled that 98% of the wastes were exported from the model domain, a result they felt was unrealistic as

¹² The erosion coefficient for sand and cobble is given as $5.8 \times 10^{-7} \text{ kg m}^{-2} \text{s}^{-1}$ which is almost the same as for sand and gravel given the margins of error quoted in Law *et al.* (2016).

observed benthic impacts suggested that organic waste deposition was occurring at the site. The authors speculated that either critical shear thresholds were not applicable to their site, that uneaten feed pellets were a significant contributor but were not re-suspended and transported in the same manner as faecal material, or that the modelled resuspension was correct but highly labile carbon deposited for short periods of time on the seabed was still leading to ecological benthic impacts.

Keeley *et al.* (2013a) used DEPOMOD to simulate the footprint of 5 salmon farms in New Zealand. The model was run with the resuspension mode turned on and off and the results compared with observed benthic impacts (which are presented more fully in (Keeley *et al.*, 2013b). For non-dispersive (mean current velocities at 20 m depth of less than 9 cm s^{-1}) linear-log regressions with r^2 exceeding 0.89 were obtained between a multivariate index of enrichment and predicted organic waste flux. At these sites turning on particle resuspension had a noticeable but minor impact. In contrast at the dispersive sites (mean current velocities more than 15 cm s^{-1}), turning on particle resuspension resulted in zero benthic carbon flux, even though ecological impacts (but not substantial accumulation of organic matter) had been observed. At the dispersive sites, the best fits were again obtained by turning off the resuspension module. Comparing the spatial predicted footprints without particle resuspension appeared to give reasonable agreement with the observed impact footprint, although impacts directly below the cages were less intense than predicted at the dispersive sites. Taken overall the results suggested that for the dispersive sites, turning off resuspension led to a small under-dispersal of simulated particles but turning on the resuspension sub-model led to complete loss of material from the observed impact domain. Keeley *et al.* (2013a) discussed at some length why turning on resuspension seemed to lead to unrealistic impact predictions. Potential ideas included incorrect understanding of critical shear stresses or incorrect understanding of how benthic ecology is impacted by organic loading under high-glow, high oxygen conditions. The authors favoured this latter explanation based on the appearance of opportunistic taxa at the dispersive sites even though there appeared to be little accumulation of organic matter (Keeley *et al.*, 2013b). This hypothesis seems to suggest that the ecology in erosional sediments is more sensitive to low to moderate levels of organic enrichment compared with depositional sediments. This is not an illogical conclusion given that the background organic flux to depositional sediments might be expected to be higher, and hence the assimilation capacity of the biota in depositional sediments could be more adapted to deal with naturally higher organic loads.

Chang *et al.* (2012) and (2014) used DEPOMOD (version 2) to simulate waste dispersal from six salmon farms in Bay of Fundy, Canada. Predictions were compared with observations on sediment sulphides. The model predictions correlated with elevated sulphides at only three sites, and also only when resuspension was turned off. Again, when resuspension was turned on it had the effect of moving most particles out of the model domain. The authors suggested a range of additional factors which might affect the relationship between carbon deposition and sediment sulphides including fine-scale heterogeneity in bathymetry and water circulation (the analyses using DEPOMOD were based on observations of water flow from single current meters at each site), waves (especially in shallow water or exposed sites), large resuspension events such as storms, and fish husbandry practices. They also noted that in other areas, such as Nova Scotia, non-tidal water currents and waves are likely to have a greater impact. In Chang *et al.* (2014), the authors further considered the possible reasons for the over-dispersion predicted by the model but they were unable to provide more support for any of the particular hypotheses proposed in Keeley *et al.* (2013a).

Chary *et al.* (2021) used NewDEPOMOD to simulate waste dispersal from hypothetical red drum (*Sciaenops ocellatus*) farms in a lagoon in Mayotte (Indian Ocean) for marine spatial planning of future expansion. In this exercise, the authors effectively turned off the resuspension module (by setting critical shear stress to 2 N m^{-2}) to optimize model performance. As might be expected, there were clear negative (linear) relationships between mean barotropic current intensity and the maximum flux of solids to the seabed, and positive (linear) relationships between mean barotropic current intensity and the total area over which farm waste settled. The authors suggested that siting farms in areas with mean currents of about $25 - 30 \text{ cm s}^{-1}$ would avoid detectable benthic impacts, regardless of farm size. They did however caution that the impacts of organic enrichment on the benthos are much less well understood for tropical compared with temperate waters.

In Scotland, SEPA have recognised these problems in modelling more dispersive sites and suggest adjusting the vertical dispersion coefficient (SEPA, 2019a). However, SEPA acknowledge that this does not reflect the true vertical dispersion but is used as an *ad hoc* tuning. As such, this is a somewhat unsatisfactory approach because the fundamental issues behind the problem remain unresolved.

In conclusion, several published reports, and experience of using DEPOMOD suggests that particle dispersal must be tuned down to the extent that it is effectively switched off when modelling more dispersive sites. However, many of the studies have had to infer organic deposition from secondary indices such as changes in taxa abundance, appearance of opportunistic species and increased sediment sulphides (Department of Fisheries and Oceans, 2012; Chang *et al.*, 2014). This is potentially problematic because the relationship between secondary indicators and actual carbon flux is not well understood for more dispersive environments (Keeley *et al.*, 2013a). There remain rather few studies which have attempted to measure organic flux from fish farms directly to test DEPOMOD model predictions.

1.9. Studies where model predictions have been compared with direct measurements of carbon deposition rates around fish farms.

The standard approach for directly validating fish farm waste dispersal models has been to use sediment traps to collect depositing organic matter at different distances from the cages. Sediment traps are a standard oceanographic tool, but the results can be significantly affected by trap design, especially in higher flow environments (Baker *et al.*, 1988; White, 1990). Bloesch and Burns (1980) provide a detailed review of the theoretical and practical issues of using sediment traps to measure benthic fluxes.

Findley *et al.* (1994) and (1995) deployed cylindrical sediment traps throughout the year at the cage boundary of a farm in Swans Island, Maine and compared the observations with carbon fluxes estimated from a simple mass balance model. Observed fluxes were between around $1 - 5 \text{ g C m}^{-2} \text{ d}^{-1}$ which was somewhat lower than the model estimate. Despite relatively low flow rates at the of the sites (average $> 2 \text{ cm s}^{-1}$ and maximum $> 17 \text{ cm s}^{-1}$), the authors observed that resuspension was an important process and that resuspension of material at the cage edge might explain the discrepancy between observed and modelled carbon fluxes.

Stucchi *et al.* (Stucchi *et al.*, 2005) employed cylindrical traps at a salmon farm in Knight Inlet, British Columbia, a site with weak tidal flows. Four traps were placed up to 500 m from the cages. Observed organic matter flux declined with distance from the cages except for a trap at 580 m distance. This far-field flux was not well predicted by the dispersal model which also considerably over-estimated the flux close to the cages. Stucchi *et al.* (Stucchi *et al.*, 2005) suggested that resuspension and topographic concentration may have occurred but that the

model was also sensitive to the assumed feed wastage rate. The study was also hampered by the low number of sediment traps deployed. Finally, the authors commented that the cylindrical design of traps was not ideal for measuring organic fluxes in shallow depths of water.

Cromey *et al.* (2002a) deployed sediment traps at two Scottish farms, site (A) was classed as dispersive (mean current speed $\sim 6.6 \text{ cm s}^{-1}$, maximum current speed $\sim 32 \text{ cm s}^{-1}$) and site (B) as depositional (mean current speed $\sim 5 \text{ cm s}^{-1}$, maximum current speed $\sim 24.5 \text{ cm s}^{-1}$). Two sets of triplicate cylindrical traps were deployed at 0, 4 and 8 m from the corner cage-edge at each site and settling material collected over 24 h. The quantity of material settled in the traps over 24 h was compared with that predicted using DEPOMOD. The results showed good overall agreement between the model predictions and observations although it was noted that the model underpredicted deposition at the further distances at site A but tended to slightly overpredict deposition at site B. The authors identified several potential contributing factors including local natural patchiness or movement of the cages. Despite site A being classed as dispersive, both sites were in relatively sheltered locations. It was concluded that DEPOMOD performed adequately at predicting the flux of organic material at sites located within sheltered sea lochs.

As shown in Table 2, DEPOMOD has been adopted for several species other than salmon. Riera *et al.* (2017) re-parameterised the model for sea bream, sea bass and meagre and tested it at eight sites (seven farms in the Canary Islands and one in Madeira). Near-bed current speeds exceeded 20 cm s^{-1} and the benthos comprised unvegetated sand. Cylindrical benthic sediment traps were placed at 0, 20, 40 and 60 m in a longitudinal and 0, 20 and 40 m in perpendicular transects. Three control samples were collected at more than 500 m from the farm. Correlations between observed and predicted fluxes were extremely high ($R^2 > 0.85$) at four sites and a little lower ($R^2 = 0.58$) at a fifth site.

An interesting insight into the resuspension problem is given by Carvajalino-Fernández *et al.* (2020a). They studied waste dispersal from salmon farms in the Altafjorden (a sheltered location) and the Frøya Archipelago (an exposed location) in Norway. Water circulation fields were generated using the ROMS model and particle dispersal tracked using the standard advection-diffusion approach. A custom resuspension sub-model was added, and three scenarios compared. In the first, there was no particle resuspension. In the second, a fixed critical shear stress of 0.018 N m^{-2} was used (as in DEPOMOD) whilst in the third, sediment specific critical shear stresses based on Carvajalino-Fernández *et al.* (2020a) were implemented. The resulting benthic footprints were quite strongly affected by the resuspension mode used. With scenario two, deposition close to the farms was reduced and the footprint either much extended or shifted in location. Results from scenario three were generally closer to scenario one, that is more material tended to be retained close to the farm. The model results were compared with sediment trap data. Scenario two showed poorer agreement to the observations suggesting that resuspension without accounting for sediment specific critical shear stresses over dispersed the waste particles. The authors put these large differences down to the generally coarse sediments in their locations where the shear stress needed to be $0.1 - 0.3 \text{ N m}^{-2}$ to move material.

The available observational data generally support the conclusion that the DEPOMOD models seem to capture the initial settlement and deposition stages reasonably accurately (Cromey *et al.*, 2002a) but struggle with resuspension and redistribution of particles. Direct measurements of far-field deposition ($> 100 \text{ m}$ away from the cage edge) have also been much more limited than observations collected closer to cages making it difficult to evaluate particle dispersion in higher energy locations (Keeley *et al.*, 2019).

1.10. Overall aims of the INCREASE project

Given recent laboratory, field and modelling results (Law *et al.*, 2016; Keeley *et al.*, 2019; Carvajalino-Fernández *et al.*, 2020a) it seems likely that further work on particle resuspension is needed in order that NewDEPOMOD can be applied with confidence to more dispersive sites.

Following from the above, the main aim of the INCREASE project was to improve our understanding of how to model moderate to high flow sites in Scotland using NewDEPOMOD by:–

- (i) developing a method for directly measuring organic carbon deposition rates around fish farms but which allows for local resuspension.
- (ii) deploying the method at three, moderate to high flow farm sites.
- (iii) comparing the observed organic carbon deposition rates with NewDEPOMOD model predictions using both default and tuned¹³ settings.

¹³ The difference between the use of default and tuned parameter settings in NewDEPOMOD is explained in SEPA (2019a).

2. Introduction to diagenesis and the NAMAQI project

In geology, the term diagenesis refers to all the physical and chemical changes occurring in sediments. In terms of the breakdown of organic waste from marine cage fish farms, the term has been used to cover the relatively short-term, at least in geological timescales, processes which have occurred within the few decades such commercial fish farms have been operating.

The following description of the diagenetic processes is based largely on a review by Kristensen (2000), unless indicated otherwise.

Organic matter in the marine environment is degraded mainly by an array of aerobic and anaerobic processes mainly due to microbial activity. In oxic sediments in good condition, macrofauna will also contribute some breakdown, but overall, the microbial processes tend to dominate.

The purpose to a living organism of breaking down organic matter is to release and capture a fraction of the energy contained in the material. Energy is captured and utilised via a series of electron transfer reactions but for each an appropriate electron acceptor is required. Under aerobic conditions, oxygen acts as a highly efficient electron acceptor and so organisms utilising aerobic respiration tend to dominate. However, under anoxic conditions alternative electron acceptors must be used¹⁴.

Sulphate (SO_4^{2-}) is relatively abundant in seawater at about 28 mM, and so is also abundant in sediment pore water. The marine sulphur cycle is therefore of major importance in oxygen deprived waters and sediments (Figure 13).

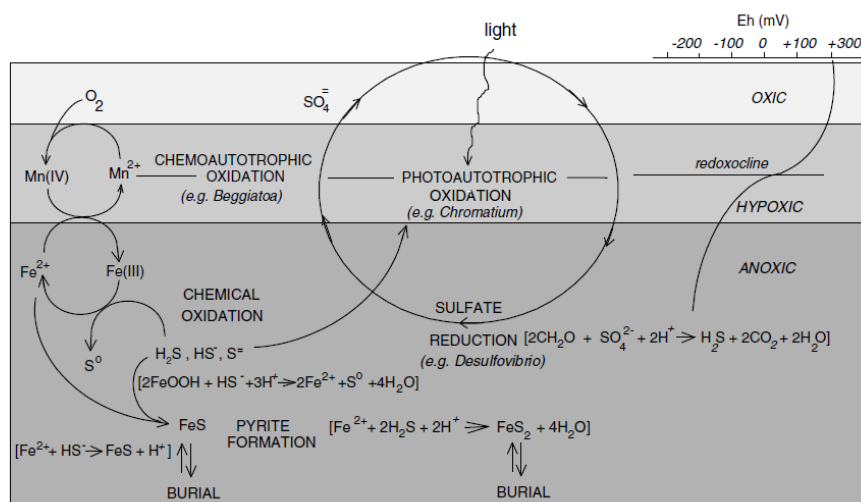


Figure 13: The main geochemical reactions in the sulphur cycle and an illustrative redox profile in the oxic (light grey), hypoxic (medium grey) and anoxic (dark grey) zones. Hypoxic sediments have dissolved oxygen in range $0.5 - 2 \text{ ml l}^{-1}$. From Hargrave et al. (2008).

¹⁴ The transition from an oxidizing to reducing environment in sediments is often expressed in terms of the redox potential (Eh) profile. A high redox potential is associated with higher levels of free oxygen and redox reduces with increasing shifts towards an anoxic reducing environment. However, there can be high variability in redox measurements and Eh is therefore probably best regarded as an indicative index of sediment state.

The total contributions of aerobic versus anaerobic respiration to the breakdown of organic material in marine sediments are difficult to quantify but in coastal sediments are probably of about equal importance. However, in organically enriched sediments, anaerobic sulphate reduction may contribute 70 – 100% of overall respiration.

Coastal marine sediments are typically characterised by several layers each dominated by differing processes of breakdown of organic material (Figure 14). The actual rates of decay, and which microbial community dominates, depend primarily on oxygen availability, organic matter quality (the content of protein, cellulose, lignin etc.), age (decomposition stage) and temperature (season)(Westrich and Berner, 1984).

It should be appreciated that the zonations shown in Figures 13 and 14 are idealized and will be complicated by inhomogeneities in the sediment and presence of bioturbators (Heilskov and Holmer, 2001). Areas of discrete organic enrichment in natural systems can result from dropout of phytoplankton and jellyfish blooms (Sweetman and Chapman, 2015) and animal carcasses (Alfaro-Lucas *et al.*, 2018). At fish farms, uneaten feed pellets can also create local anaerobic conditions, even within a generally oxic environment.

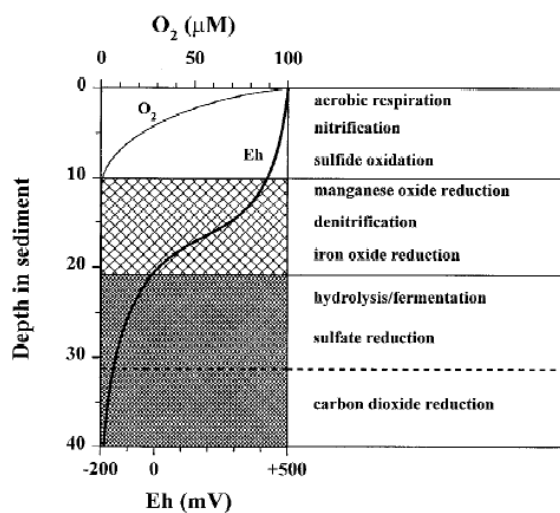


Figure 14: The idealized vertical distribution of diagenetic processes in marine sediments. The oxic zone is illustrated by an oxygen profile (white zone), the suboxic zone is shown as the layer where the redox discontinuity is evident (light cross-hatched), the reduced zone is shown as the layer where the redox potential (Eh) is below zero (dark cross-hatched). The depth scale is arbitrary (Kristensen, 2000).

Aerobic degradation of organic carbon can be performed by a variety of bacteria, fungi and micro- and macrofauna which have the enzymatic capacity to perform a total mineralization of the organic matter. The result of these reactions is water, carbon dioxide and inorganic nutrients. These reactions can only occur in an oxic environment because oxygen is required as an electron acceptor (Table 8, Equation [1])

Because the oxic zone in coastal sediments is limited to a thin layer (of the order of a few millimetres depth for mud and a few centimetres for coarser sediments although the depth of the oxic layer can be substantially altered by bioturbation), a fraction of the organic matter escapes aerobic breakdown and becomes incorporated into the lower hypoxic and anoxic layers. Under these low or zero oxygen conditions, aerobic processes are replaced by anaerobic decomposition, which is accomplished by mutualistic consortia of bacteria and archaea (Glud, 2008).

Organic enrichment at the sediment surface tends to increase oxygen demand and, under limiting oxygen renewal, the oxygen penetration depth into the sediment will be reduced

(Cathalot *et al.*, 2012). Under heavy organic enrichment, the oxic zone may be completely absent and the anoxic zone reach the sediment-water interface, or even extend into the overlying water.

Anaerobic decomposition takes place in a stepwise manner (Glud, 2008; Jørgensen *et al.*, 2019). The first step is to split complex insoluble polymeric organic molecules into water soluble monomers (amino acids, monosaccharides, and fatty acids) by hydrolysis and fermentation to yield propionic acid and acetate (Table 8, Equation [2]). The resulting small organic molecules are then oxidized by other micro-organisms using a variety of electron acceptors (recalling that oxygen is not available as an electron acceptor under anoxic conditions). The sequence of receptors used is related to their decreasing willingness to receive electrons, the sequence being Mn^{4+} , NO_3^- , Fe^{3+} , SO_4^{2-} and CO_2 .

Respiration in the suboxic zone tends to favour Mn^{4+} , NO_3^- , Fe^{3+} as electron receptors because of their availability in this zone. When nitrate is used the process is termed denitrification (Table 8, Equation [3]).

Sulphate respiration (Table 8, Equation [5]) is the main organic degradation reaction occurring in the fully anoxic zone. Although sulphate (SO_4^{2-}) is less willing to act as an electron receptor than Mn^{4+} , NO_3^- or Fe^{3+} , sulphate is found in seawater at high levels (equivalent to the concentration of O_2) and so is also abundant in sediment pore water (Black and Nickell, 2014).

Sulphate reduction results in the release of hydrogen sulphide (H_2S) which is responsible for the rotten egg smell often noted in enriched anoxic sediments and is moderately soluble in seawater. Hydrogen sulphide (H_2S) in aqueous solution dissociates into the hydrosulphide anion (HS^-) and the bisulfide anion (S^{2-}), the proportions varying with pH. At near neutral pH sulphide will be present in approximately equal amounts H_2S to the HS^- (Figure 15).

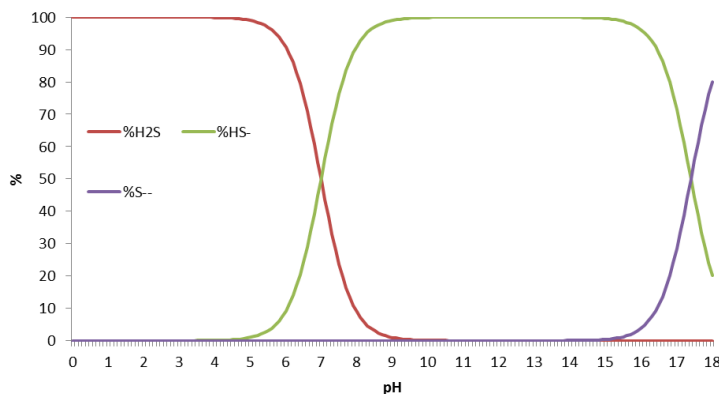


Figure 15: pH dependence of sulphide speciation (reproduced from (Black and Nickell, 2014)).

Within sediments, H_2S is itself involved in a complex set of chemical and micro-organism mediated reactions with iron and other metals (Figure 13). Sulphide may precipitate with iron to produce FeS , or FeS_2 , with precipitates either being permanently sequestered within sediments (Bravo and Grant, 2018), or re-oxidized if oxygen becomes available. The presence of metal sulphide precipitates gives a black colouration to the sediment.

H_2S will also diffuse upwards and be re-oxidized at the oxic/anoxic boundary. Although some re-oxidation occurs purely chemically, most is mediated by micro-organisms. Sulphide re-

oxidation may account for around half of sediment oxygen uptake. The degree and depth at which sulphide re-oxidisation occurs will also vary temporally and spatially depending on the degree of oxygen renewal (Panchang *et al.*, 1997; Dudley *et al.*, 2000; Cathalot *et al.*, 2012).

At very heavily impacted sites it is possible for the pool of reactive metals to be depleted and H₂S to reach the sediment surface. This may then support the growth of chemoautotrophs such as *Beggiatoa* spp. (Hamoutene, 2014). Some strains of these bacteria can oxidise sulphide by both aerobic and anaerobic reactions and thus are well adapted to life under low oxygen conditions.

Methane producing archaea can respire acetic acid directly (Table 8, Eqn. [6]) to produce methane and carbon dioxide, but other longer chain organic compounds must be first broken down by fermentation (acidogenesis) and acetogenesis. The use of CO₂ as an electron acceptor is the least energetically favoured of the available options (Table 8, Eqn. [7]), but can be used by some methanogens (Ferry and Lessner, 2008).

In turn, some of the methane produced can itself be anaerobically oxidised, again involving sulphate reduction (Table 8, Eqn. [8]). Out-gassing of methane can also occur from marine sediments.

The efficiency of degradation of organic matter also tends to decline with depth in the sediment but this appears to be more related to the organic material becoming increasingly dominated by more refractory components, rather than shifts in the use of electron receptors.

Table 8: The main aerobic and anaerobic respiration reactions in marine sediments.

Eqn	Starting compounds	Products
1	(CH ₂ O) _x (NH ₃) _y (H ₃ PO ₄) _z + xO ₂	xCO ₂ + xH ₂ O + yNH ₃ + zH ₃ PO ₄
2	8(CH ₂ O) _x (NH ₃) _y (H ₃ PO ₄) _z	xCH ₃ CH ₂ COOH + xCH ₃ COOH + 3xCO ₂ + 3xH ₂ + yNH ₃ + zH ₃ PO ₄
3	CH ₃ COOH + 1.6NO ₃ ⁻ + 1.6H ⁺	0.7N ₂ + 2CO ₂ + 2.8H ₂ O
4	CH ₃ COOH + 4FeOOH + 8H ⁺	4Fe ²⁺ + CO ₂ + 7H ₂ O
5	CH ₃ COOH + SO ₄ ²⁻ + 2H ⁺	H ₂ S + 2CO ₂ + 2H ₂ O
6	CH ₃ COOH	CH ₄ + CO ₂
7	CO ₂ + 4H ₂	CH ₄ + 2 H ₂ O
8	CH ₄ + SO ₄ ²⁻	HCO ₃ ⁻ + HS ⁻ + H ₂ O

Recent research is uncovering increasing complexity in the marine sulphur cycle pathways and the range of micro-organisms involved (Glud, 2008; Jørgensen *et al.*, 2019).

As shown in Figure 6, the Pearson-Rosenberg model provides a general framework for how benthic communities respond to increasing organic enrichment. However, the precise impact at a specific location and time will be more complex and variable as the biology is responding to multiple interacting variables including oxygen availability, water temperature, prey availability etc., which themselves fluctuate on varying timescales.

While FeS is biologically inert, elevated total S²⁻ in sediment pore water can create toxic conditions. Hydrogen sulphide (H₂S) can cross cell membranes and act as an inhibitor to a range of important metabolic enzymes whilst HS⁻ binds with the ferric (Fe³⁺) ion of cytochrome preventing oxygen release by oxyhaemoglobin (Grieshaber and Völkel, 1998; Hargrave *et al.*, 2008). In marine sediments, sensitive species may begin to show declines in abundance at sulphide levels above 10 µM (Brooks *et al.*, 2003). However, the toxic effects of sulphide can be difficult to separate from those of hypoxia as organisms are likely responding to a combination of both factors (Bagarinao, 1992; Nilsson and Rosenberg, 2000; Hargrave *et al.*, 2008).

Although persistent high levels of sediment sulphide will prove toxic to many organisms, they may be able to tolerate short periods of transient exposure. The tolerance of organisms to sulphides is also related to their normal exposure. For example, the asteroid *Ctenodiscus crispatus* which lives on muddy seabeds can survive combined hypoxia and sulphide exposure for much longer than *Asterias vulgaris*, which normally lives in the rocky intertidal (Bagarinao, 1992). The opportunistic polychaete, *Capitella capitata* is often found in high abundance under fish farm cages and is therefore used as an indicator species for organic pollution, but *Capitella* includes many sibling sub-species with varying tolerances to hypoxia and sulphide with some able to tolerate the extreme conditions around hydrothermal vents. However, even this organism becomes absent when free sulphide levels exceed 7200 μM (Hargrave *et al.*, 2008).

Some organisms have become specialised to live within sulphidic sediments through detoxification using enzymes such as sulphide:quinone oxidoreductase to convert sulphide to sulphate (Black and Nickell, 2014).

Using a simulation model, Duplisea *et al.* (2001) found that sensitivity of the bioturbating macrofauna to toxic sulphides was a key factor affecting carbon pathways in marine sediments. However, relating sulphide levels to biological impacts, as captured in measures like the IQI, is complex (Brooks and Mahnken, 2003), although Germano *et al.* (2011) suggest the general relationships shown in Table 9.

*Table 9: Benthic organic enrichment zonation based on oxygen gradients determined from relationships between oxidation-reduction (Eh) potentials (mV), total sulphide concentrations (μM), dominant benthic metabolic processes and taxonomic groups. From (Germano *et al.*, 2011).*

	Oxic A [III]	Oxic B [II]	Hypoxic [I]	Anoxic [0]
Eh (NHE mV)	>+100	+100 to 0	0 to -100	< -100
Total sulphides (μM)	<300	300 to 1300	1300 to 6000	>6000
Dominant process	Aerobic metabolism O_2 and CO_2	Sulphate reduction SO_4^- reduced to H_2S and S^-		Anaerobic chemosynthesis CO_2 reduced to carbohydrates by oxidation of H_2 , H_2S , Fe^{++} , NO_2^-
Dominant fauna/flora	benthic Megafauna Macrofauna Meiofauna Aerobic algae/bacteria	Meiofauna Nematodes Facultative anaerobic bacteria	Protozoa Ciliates Facultative anaerobic bacteria	Anaerobic bacteria and archaea

2.1. Visual assessment of organic enrichment in marine sediments

Because elevated levels of hydrogen sulphide can react with metal ions to form black precipitates, Sediment Profiling Imaging (SPI) can be used to visually assess the levels of organic enrichment in marine sediments (Nilsson and Rosenberg, 2000; Wildish *et al.*, 2003; Germano *et al.*, 2011). In this technique, a wedge-shaped housing containing a camera and glass plate is driven into the sediment and an image of the sediment vertical profile recorded. The depth of the redox layer can then be estimated by eye. A further development was proposed by Bull and Williamson (2001) who used image analysis to semi-quantitatively measure the colour related to the concentration of sulphide precipitates, a technique which has since been applied to mussel farms (Wilson and Vopel, 2015). Another development has been combining SPI with planar optodes to directly image the oxygen state of the sediment profile (Cathalot *et*

al., 2012). During the NAMAQI project we attempted to deploy a SPI camera at the Quanterness site, but without success. This technique typically works best in soft, muddy sediments because it can be difficult to get the camera to penetrate coarser sediments. Because dispersive sites in Orkney are characterised by coarse sediments, we did not attempt to deploy the SPI camera at additional locations.

2.2. Electrochemical measurements of organic enrichment in marine sediments

Redox is often recorded using electrode probes during benthic sediment monitoring (although this measure is no longer required in Scotland by SEPA) and has been suggested as a useful measure of organic enrichment impacts. Hargrave (1994a) proposed a benthic enrichment index as the product of organic carbon concentration and redox potential. However, several researchers have noted that redox can be highly variable, even within a single sampling station (Black and Nickell, 2014; Cranford *et al.*, 2017). Redox probes are also prone to contamination and results can be substantially affected by how the probe is inserted into the sediment (Wildish *et al.*, 2004). The current view is that redox is not especially useful for evaluating benthic enrichment impacts from fish farms and is best regarded as a semi-quantitative internal validation of total sulphide when sediments are anoxic or hypoxic.

Measurement of total free sulphides (S^{2-}) can also be undertaken using an ion selective probe. It is possible to produce sediment profiles of dissolved sulphides using microelectrodes (Cathalot *et al.*, 2012), but these probes are very delicate and so more suited to research than routine monitoring use. Generally, a larger and more robust probes such as those marketed under the Thermo Scientific Orion™ brand are preferred. Again, the method requires careful maintenance and calibration of the probes but with care can provide useful data for benthic monitoring (Wildish *et al.*, 2004). According to Schaanning *et al.* (2005) the method is less accurate for sulphide quantification than iodometric titration or spectrophotometry and the term pS ($=-\log[\Sigma H_2S]$) was preferred to denote sulphide concentrations calculated from such electrode measurements. In a laboratory inter-calibration, Wildish *et al.* (2004) reported a CV of 38% for samples taken from farms. Brown *et al.* (2011) reported that the reproducibility of total free sulphide measurements in aqueous standards ($SE \pm 12\%$) tended to be markedly better than measurements made using natural marine sediments containing high sulphide levels ($SE \pm 55\%$).

An additional complication is that the sulphide antioxidant alkaline buffer used (20.0 g sodium hydroxide, 17.9 g EDTA and 8.75 g L-ascorbic acid per litre distilled water) can lead to dissolution of precipitated sulphides under high pH (usually around 14) potentially leading to erroneously high concentrations of measured free sulphides (Brown *et al.*, 2011). In that study, measurements on pore water gave higher sulphide concentrations compared with a sediment slurry. Furthermore, manipulating the pH of the test solution to above pH 10 showed increased sulphide concentrations and SEM-EDS X-ray mapping of elemental distribution in sediment grains suggested sulphide was being liberated into solution.

This issue was discussed at length in Black and Nickell (2014) including correspondence with Barry Hargrave whose reply suggested that precipitate dissolution likely has a minor impact on the relationship between measured sulphide and biological response.

“Sediments with $<700 \mu M S$ could have extremely low free S but even if all of the measured S is due to solubilized metal-S complexes, concentrations below this threshold are still considered to be characteristic of oxic conditions. This is consistent with the macrofauna species richness data. On the other hand, if brief exposure of hypoxic sediments (1300 to $3000 \mu M S$) to SAOB increases free S concentrations by solubilizing metal-S complexes which

are then measured along with true free S, we still know that species richness decreases dramatically, and opportunistic species become dominant in this concentration range. At higher concentrations (>4500 μM and especially >6000 μM S) measured with SAOB treatment, we know that macrofauna biodiversity is highly impacted even though at these high levels perhaps even more S of the total measured is derived from the solubilized fraction.”

Brown et al. (2011) recommended two courses of action which could make the method more reliable (1) obviating the use of SAOB by conducting measurements of sediment-free sulphide at natural pH, using paired measurement of S^{2-} and pH (2) isolation of porewater from the collected sediments, followed by immediate analysis with the current Ministry of Environment (British Columbia, Canada) protocol or preservation with zinc acetate for later analysis using spectrophotometry by methylene blue.

Black and Nickell (2014) concluded that changing the analytical methodology would require considerable field validation, and given the existing large datasets from Canada, would not be justified. That project also attempted some time-course experiments as an approach to estimating the degree of metal precipitate stripping, but the results were inconclusive. Hargrave et al. (2008) suggested that keeping extraction times to less than 5 mins after adding the SAOB would minimise any dissolution of sulphide precipitates.

In the context of Scottish practice where sulphide measurements are not routine, changes to the procedures might be considered. The easier option for modifying the method would probably be to separate pore water from sediment particles (including sulphide precipitates) before addition of the high pH buffer. From a practical point of view, pore water can be extracted from marine sediments by several techniques. If the core is intact, it can be sliced, and pore water simply squeezed out by pressure. Unfortunately, this does not work in cores of sandy or coarser material which cannot be sliced easily and accurately. An alternative, which will work with unconsolidated core samples, is high-speed centrifugation (Schaanning and Hansen, 2005; Brown *et al.*, 2011) but the equipment needed is unlikely to be available on most fish farms. Alternatively, pore water can be extracted from cores using Rhizons (Seeberg-Elverfeldt *et al.*, 2005). These are hydrophilic porous polymer tubes, with a typical pore diameter of 0.1 μm and an outer diameter of around 2.4 mm. Under gentle negative pressure using a syringe, peristaltic pump, or vacuum tube the sampled fluid flows into the space between the porous tube and a support. A ceramic version (RhizoCera tubes) may be preferable as their more rigid structure reduces ingress of atmospheric oxygen (Cranford *et al.*, 2017).

2.3. Non-electrode methods for the analysis of free sulphides

Recently a revised analytical approach has been suggested based on spectrophotometric analysis. In addition to quantifying S^{2-} , Cranford et al. (2017) measured dissolved oxygen using a micro-sensor, although oxygen data were not included in a subsequent paper describing the field application of the method (Cranford *et al.*, 2020). The spectrophotometric method for sulphides is claimed to be suitable for muddy and sandy sediments, aims to overcome the concerns about dissolution of metal-sulphide precipitates under high pH SAOB conditions and can be used in the field.

Under this method, sediments were collected using a specialized coring device, the “mini slo-corer” which yields an undisturbed sediment-water interface although in a subsequent study the analytical method was applied to van Veen grab samples (Cranford *et al.*, 2020). On recovery to the vessel, the core tubes were drilled to allow insertion of RhizoCera tubes which allowed sampling of the pore water at various depths below the sediment-water interface. The pH of the samples was then buffered to 8 – 9 using ammonium hydroxide (0.44 M) and the

concentration of S^{2-} directly quantified by ultraviolet absorbance at 230, 240 or 250 nm using a UV-spectrophotometer. Calibration of the instrument was against sodium sulphide nonahydrate standards checked using potentiometric titration with an Ag^+/S^{2-} ion-selective electrode (ISE) probe. Calibration can also be against high purity $Na_2S \cdot 9H_2O$, providing these have been stored under nitrogen. Based on the spectrophotometer used in the study, the lower limit of quantitation was $3.7 \mu M$.

Cranford et al. (2020) suggested that the ISE approach used as standard monitoring in Canada can both under- and over-estimate free sulphides. Underestimation may occur by oxidation and/or volatilization during sampling, storage or transport of sediment samples to the laboratory, even when the analysis is conducted on the same day as sample collection. The standard sampling protocol mixes sediments from 0 to 2 cm depth, allowing O_2 in the surface sediments to mix with any free S^{2-} accumulated below this layer. Over-estimation may arise from dissolution of metal-sulphide precipitates in high pH buffer as proposed by Brown et al. (2011).

When performed on the same field samples a comparison of UV-spectrophotometer S^{2-} against ISE probe measurements suggested that for permeable sediments, total free sulphides were reduced by a factor of 10x – 100x while for muddy sediment samples there was general agreement between the two methods down to concentrations of around $500 \mu M$, but at lower sulphide concentrations the UV method gave higher readings (Figure 16). This latter difference is quite hard to explain but may be due to rapid oxidation of free sulphide by surficial oxygen when the sediment samples are mixed to a slurry with the SAOB as required by the ISE protocol. This would have a larger relative impact at lower sulphide concentrations.

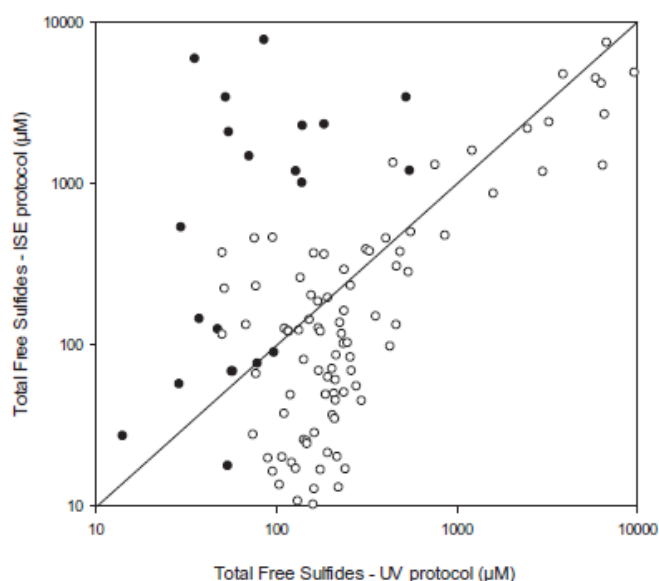


Figure 16: Comparison of total free sulphide concentrations measured using the standard ion selective electrode protocol (analysis of sediment/water slurries from 0 to 2 cm depth) and the direct UV spectrophotometric method based on porewater analysis (average for 1 and 2 cm depth). Samples were obtained between September 15 and October 16, 2016 and between April 2 and May 25, 2017 adjacent to salmon aquaculture pens at farms overlying permeable (sand; closed circles) and cohesive (mud; open circles) substrates. The unity line (1:1 relationship) is shown. From Cranford et al. (2020).

Alternatively, samples can be preserved using zinc acetate and free sulphides subsequently analysed using the methylene blue method. Preserved sulphide samples are reacted with a 2:1 (by volume) mixture of 20 mM N,N-dimethyl-p-phenylenediamine dihydrochloride and 30

mM iron (III) chloride hexahydrate. Absorbance is then read at 660 nm using a microplate reader. Calibration of the instrument is against sodium sulphide nonahydrate standards checked against potentiometric titration with an $\text{Ag}^+/\text{S}^{2-}$ ISE probe. Calibration can also be against high purity $\text{Na}_2\text{S}\cdot 9\text{H}_2\text{O}$, providing these have been stored under nitrogen. The method is not quite as sensitive as direct UV-absorption on fresh pore water (Cranford *et al.*, 2017), having a lower limit of quantitation of around $200\ \mu\text{M}$. A comparison of free sulphide concentrations measured on pore water extracted from the same field samples showed good correspondence between direct UV-absorbance and methylene blue results, although there was increasing variance at lower sulphide concentrations (Cranford *et al.*, 2020).

2.4. The use of sulphide measurements in assessing fish farm benthic impacts

Although it is known that sediment sulphide is an indicator of organic enrichment from fish farms (Cathalot *et al.*, 2012), and that changes to the biota are associated with increasing free sulphide concentrations, a strong coupling between sulphide concentrations and biological community structure is required if ecological condition is to be predicted from sediment sulphide concentrations.

In Norway, measurement of Eh, pH and S in the upper 2 cm of sediments has been used to define acceptable, transition and unacceptable benthic conditions beneath and surrounding fish farms since the late 1990s (Ervik *et al.*, 1997).

Wildish *et al.* (2003) measured sulphide and redox in sediment cores collected under farms in Bay of Fundy, Canada and Tasmania. Redox ranged from -183 to 25 and sulphide from 5200 to $230,000\ \mu\text{M}$. These values compared with 23 to 350 and 0.01 to $5000\ \mu\text{M}$ respectively at reference sites suggesting that these electrochemical measurements could distinguish impacted samples from reference material.

Brooks *et al.* (2003) summarised data from seven farms in British Columbia. Highly elevated sulphides ($> 6000\ \mu\text{M}$) were recorded within 30 m of the cages during times of peak biomass. High levels (up to $1300\ \mu\text{M}$) were generally restricted to within 100 m of the cages, but at two sites, high sulphide levels were found up to 185 m distant. At two farms, subtle chemical changes, and alterations to the macrobenthos were also observed up to 225 m from the cages. Timeseries from four farms showed rapid declines in sediment sulphides after fish were harvested, even at the cage edges. Equally there was a rapid increase in sediment sulphides when the cages were restocked. It was concluded that sediment sulphides can provide a sensitive and rapidly responding measure of organic enrichment.

Schaanning and Hansen (2005) examined benthic chemistry data collected from around 31 farm sites in Norway. Although not all the data were collected in a standardised manner, directly below cages Eh tended to be lower than -161 mV compared with 82 mV at reference stations. Lowered pH (< 7) was observed to correlate with visible gas bubble production. Consideration of the dissociation constants for sulphide and carbonic acids implied that the reduced pH was the result of combined sulphate reduction and methanogenesis. Although stations directly below cages could be distinguished from those further away using pH, pE (redox determined using electrode on untreated sediment) and pS (sulphides determined using electrode on untreated sediment) results, abandoned sites, transition zone (5 – 100 m from cages) and reference sites (> 100 m from cages) could not be distinguished from each other.

In North America, (Holmer *et al.*, 2005) and Canada measurement of sediment sulphide is used for monitoring farm impacts and levels of more than $1500\ \mu\text{M}$ are considered unacceptable.

Hargrave et al. (2008) presented data on sediment S^{2-} and the total number of macrofaunal taxa and their abundance from farms in British Columbia (Figure 17). These data suggest there is a general relationship between sediment sulphide concentration and infaunal community composition. However, there is a large scatter in the data suggesting a substantial influence of additional, likely site specific, factors on the benthic community response (Brooks and Mahnken, 2003).

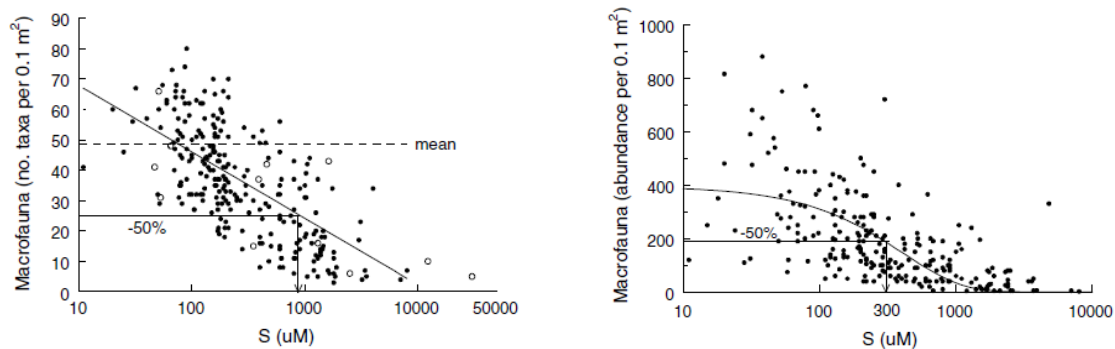


Figure 17: Relations between S^{2-} and total number of macrofauna taxa and abundance in surface sediments observed at various distances up to 1 km away from salmon farms in the Broughton Archipelago (BC). Solid points represent data from BC and open circles from southwestern Bay of Fundy. From Hargrave et al. (2008).

Based on considering data from a range of studies, Hargrave et al. (2008) produced a nomogram which related benthic biological impacts to redox, pH, total free sulphides and DEPOMOD modelled carbon sedimentation (Figure 18). The nomogram categorised samples into four groups, 'Normal', 'Transitory', 'Polluted' and 'Grossly polluted'. However, these categories do not map directly to the ecological status categories used in Scotland.

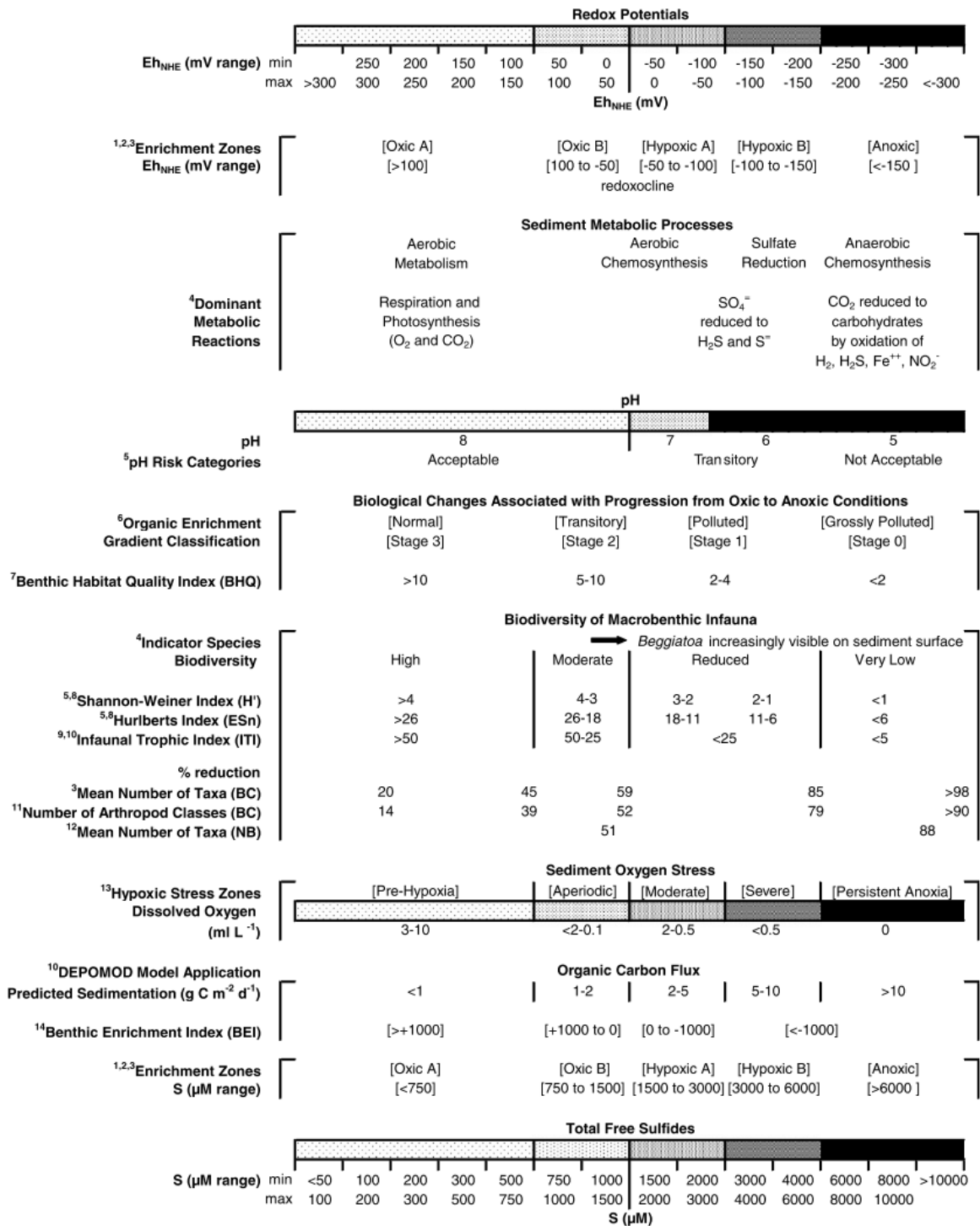


Figure 18: Nomogram for benthic organic enrichment zonation (Hargrave et al., 2008).

Keeley (2013b) collected redox and sulphide measurements over three years at six New Zealand salmon farms which were in variable flow environments. Low flow sites (near-bed flow 3.2 – 8.1 cm s⁻¹) had higher mud content (55 – 84% based on averages at each site) whilst higher flow sites (15.4 – 19.0 cm s⁻¹) had lower mud (28 – 32%). As expected, organic content was lower at high flow reference sites and macrofaunal communities were more diverse and abundant. Below the cages at the low flow sites the benthic community was impoverished whilst at high flow sites higher taxa diversity was maintained. Low flow sites were characterised by a severely impacted but spatially constrained benthic footprint, whilst for high

flow sites impacts could be detected further from the cages but were less severe. Comparing infaunal data with redox and sulphides for low flow sites gave relationships in broad agreement with those presented in Hargrave et al. (2008) and Hargrave (2010). At the high flow sites however, taxa richness remained largely unaffected until sulphide concentrations approached 2000 μM . Multidimensional scaling also suggested different trajectories in biological community responses in relation to organic enrichment between low and high flow sites. The flow regime at a fish farm site will have multiple impacts including on the sediment type and its oxygenation, on the dispersal extent of fish farm waste but also on the natural biological community composition and its ability to assimilate additional organic carbon (Macleod *et al.*, 2007). However, for both flow regimes, taxa richness showed a steep decline when sulphides exceeded 1500 μM suggesting that this critical level, as used in Canadian monitoring, may be relatively robust to flow regime.

Bannister et al (2014) measured sulphides and a variety of other parameters in sediments collected adjacent to a Norwegian salmon farm located in deep water (180 m) and which had been in production for 7 years. Maximum water currents exceeded 30 cm s^{-1} and the sediment consisted of coarse and medium sands. Surficial pore water SO_4^{2-} and TH_2S were both low and concentrations were not noticeably different from samples collected at a nearby reference site. Despite this, some differences in dominant species were apparent with *Capitella capitata*, *Abram nitida* and nematodes being elevated in farm sediment samples. These results showed that water depth can be a critical factor. Secondary production in deeper benthic habitats is generally more food limited compared with shallower sites, resulting in lower natural standing biomass. Moderate organic enrichment may then have a strongly stimulating effect at such sites, as long as the enrichment is not excessive enough to cause the deleterious effects associated with anoxia.

To develop the sulphide approach for Scottish farms, Black and Nickell (2014) collected both redox and sulphide measurements (using the selective ion electrode method) at ten Scottish salmon farms in 2012 and compared the findings with the infaunal trophic index (ITI). The redox data did not appear informative as nearly all the measurements were positive and failed to show a relationship with mean sulphide, which was ascribed to a failure of the probe. However, further measurements were taken at other sites with a new probe, but little relationship was found between Eh and sulphide concentrations. However, there was a general relation between the infaunal trophic index (ITI) and sulphide concentrations (Figure 19).

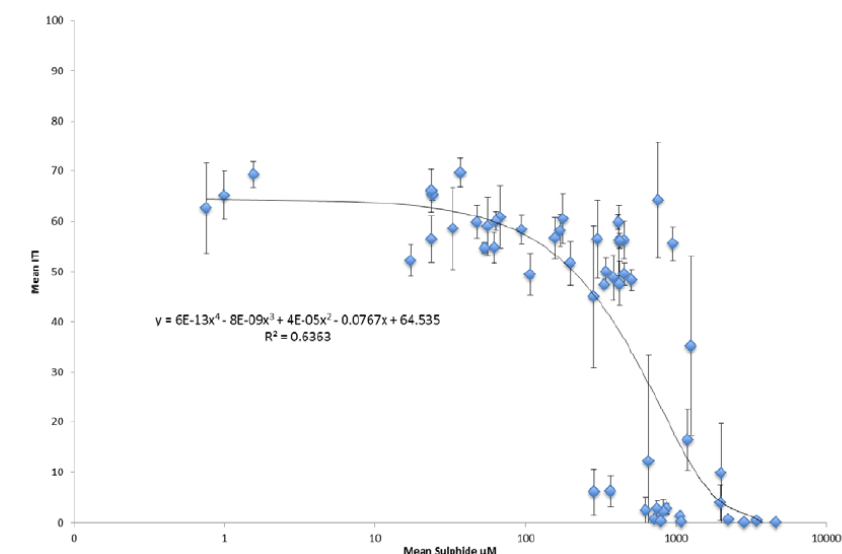


Figure 19:
Relationship between the mean infaunal trophic index (ITI) and mean sulphide concentrations in sediments at ten Scottish salmon farms, from Black and Nickell (2014).

The range of sulphide concentrations and their general relationship with the infaunal index (Figure 19) were like the previous published findings shown in Figure 17. Again, the range of ITI associated with sulphides in the intermediate concentration range (~500 – 1000 μM) was considerable. Black and Nickell (2014) also showed similar relationships with other community measures (number of taxa, Margalef's, Pielou's and Shannon-Weiner index).

There is one final caveat considering the published data described above and that is that doubts have been raised about the accuracy of the ISE analytical method used in most of the studies (Brown *et al.*, 2011). It is likely that the broad conclusions will still be correct because of the known toxicity of free sulphides to most marine organisms but the relationships between biological response and sulphides at intermediate concentrations, and some of the variability in reported finding, may be due to this methodological issue.

Recently Cranford *et al.* (2020) proposed a revised sediment classification system based on total dissolved sulphides measured by UV-spectrophotometry (see Section 2.2 for a discussion of the methodology). The approach was trialled in five coastal aquaculture regions in Canada plus one in New Zealand. Sediments ranged from very fine sand to silt and were sampled with Slo-corers, diver deployed coring tubes, or van Veen grabs. Although the quality of sampling, in terms of protection from oxygen exposure and accuracy of sampling depth in the sediment, will be greater with the 'Slo-core' approach, direct sampling of pore water from van Veen grabs using RhizoCera tubes also appeared to produce acceptable results.

Empirical relationships between free sulphide concentrations and indices of community richness (S), heterogeneity (H' , $1/D$), and species sensitivity/tolerance to free sulphides (GrV, BPOFA, AMBI and M-AMBI) were plotted. Although there was a large scatter in the data at lower sulphide concentrations, macrofauna species richness declined strongly when total free sulphide exceeded 500 μM (Figure 20). The relationship of sulphide with total organism abundance was less obvious but clearly declined to low densities when sulphides exceeded 1000 μM .

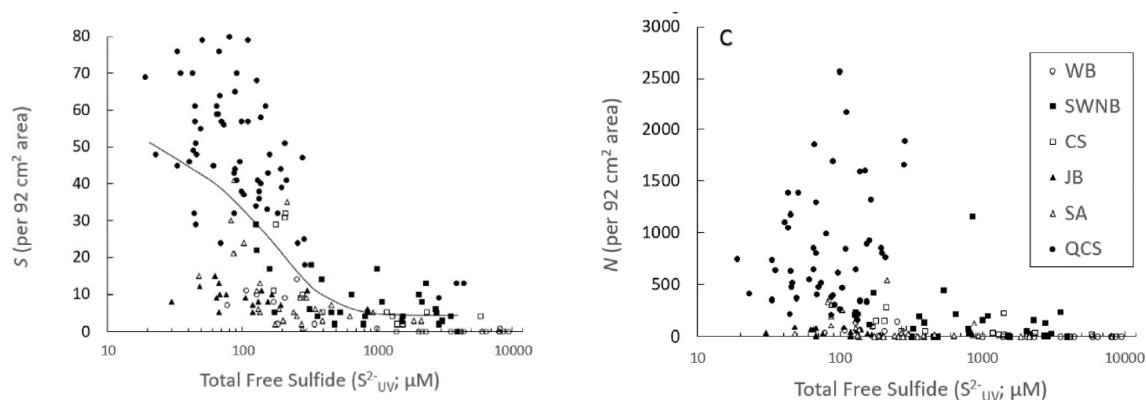


Figure 20: Relationship between total free sulfide (S^{2-}) concentration in surficial sediments measured using the UV-absorbance method and benthic macrofauna species richness (S) and total organism abundance (N). From Cranford *et al.* (2020).

Although there was still quite large variability in the relationship between species richness and sulphide, the data were even more scattered when sulphides were analysed using the selective ion electrode (ISE) approach.

To conclude, application of the revised methodology for analysing sulphides may tighten the relationship between sulphide concentration and biological metrics but is unlikely to change the underlying form of the relationships with measures such as taxa richness and abundance. The relationship between organic enrichment, sulphides and ecological response will be moderated by local water speeds, sediment type and natural background biological community. However, available published data suggests that above 1500 μM , deleterious impacts are highly likely as few taxa can tolerate such levels of free sulphide.

2.5. Overall aims of the NAMAQI project

Although there have been several changes over the years in how SEPA require benthic impacts to be monitored (see Section 1.7), all the approaches require macrofauna samples to be collected and analysed. This requires sediment samples to be sorted and organisms identified and enumerated, a process which must be undertaken by analysts with the relevant taxonomic expertise. Most fish farming companies therefore send samples to external consultants, although a few of the largest companies may maintain a benthic sample sorting in-house team. The main problem with this is the expertise and time required to work up the samples. As well as being costly (Hargrave *et al.*, 2008), this can lead to lags of several months between samples being collected and the data becoming available. Furthermore, in Scotland the regulator (SEPA) now requires enhanced benthic monitoring which requires many more samples to be analysed from each farm than previously. This has led to a shortage of appropriately trained taxonomic analysts and further backlogs in sample processing. There is thus considerable industry interest in developing potentially more rapid techniques, including the analysis of sulphides and eDNA.

Given that sulphide measurements are used for regulatory purposes in Canada, the aim of the NAMAQI project was to evaluate whether measuring sediment sulphides could provide a more rapid indicator of benthic sample ecological quality at more dispersive sites by:–

- (i) conducting sulphide measurements at two Orkney farms to evaluate the practicality of the approach for coarse sediment sites.
- (ii) comparing the sulphide measurements with IQI for the two farms (Note that previous work by Black *et al.*, (Black and Nickell) compared sulphide data to ITI for Scottish farms and those results are discussed further later in this report).
- (iii) comparing the results from Orkney with available Canadian data.

3. Materials and methods

Studies were undertaken at three farms in the Orkney Islands owned by Cooke Aquaculture, namely Bay of Vady, Quanterness (2021) and Bay of Meil (2021). There were some differences in the approach taken at each site as our methods evolved during the project (Table 10). Results from the Bay of Vady site are treated as developing the techniques whilst the results from Quanterness and Bay of Meil are more complete, allowing comparisons between the all the physical and biological data (carbon flux, macrofaunal index, particle size and organic carbon content and sulphides) and modelled results using NewDEPOMOD.

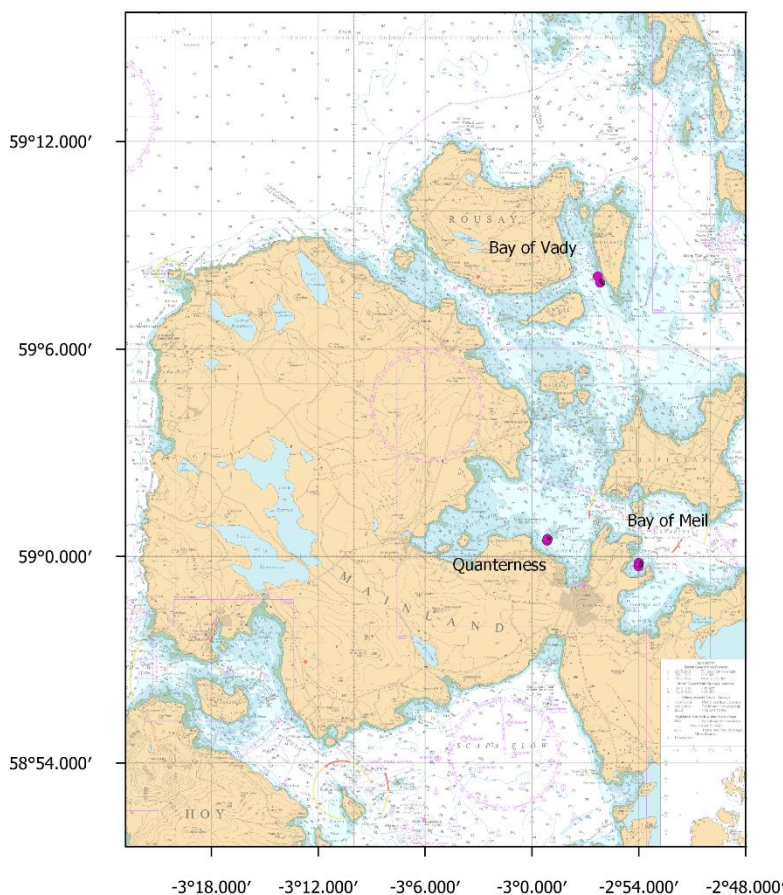


Figure 21: Location of the three farm study sites within the Orkney Islands, the location of each farm is indicated by the solid purple polygon. © British Crown and OceanWise, 2021. All rights reserved. Licence No. EK001-20180802. Not to be used for Navigation.

Table 10: Samples collected at each study site.

Site	Sediment boxes	Box layout	Particle size	Organic carbon	Sulphides	Macro fauna	eDNA	NewDEPOMOD modelling
Bay of Vady	Yes	Bow tie	Yes	Yes	No	Limited	No	Yes
Quanterness	Yes	Cruciform	Yes	Yes	Yes	Yes	Yes	Yes
Bay of Meil	Yes	Cruciform	Yes	Yes	Yes	Yes	No	Yes

3.1. Study sites

Note that near seabed residual currents were recalculated from available ADCP data using the tidal prediction method to ensure consistency between datasets. This has resulted in slight differences to the residual currents reported in the site licencing survey reports prepared by Xodus AURORA (Aurora, 2009b; Aurora, 2009a; Aurora, 2010).

3.1.1. Bay of Vady site description

The farm (SEPA licence CAR/L/1003063/V4) lies at the southern end of the Sound of Rousay with the island of Rousay to the west and Egilsay to the east (Figure 22). The shore is rocky but shelves quickly to a seabed of around 16 – 18 m charted depth. The site is moderately deep with cages in around 20 m water depth. There are 12 circular cages arranged in a northwest to southeast orientation, approximately parallel to the shore of the island of Egilsay (Figure 23) and the maximum licenced biomass is 1,000 tonnes.

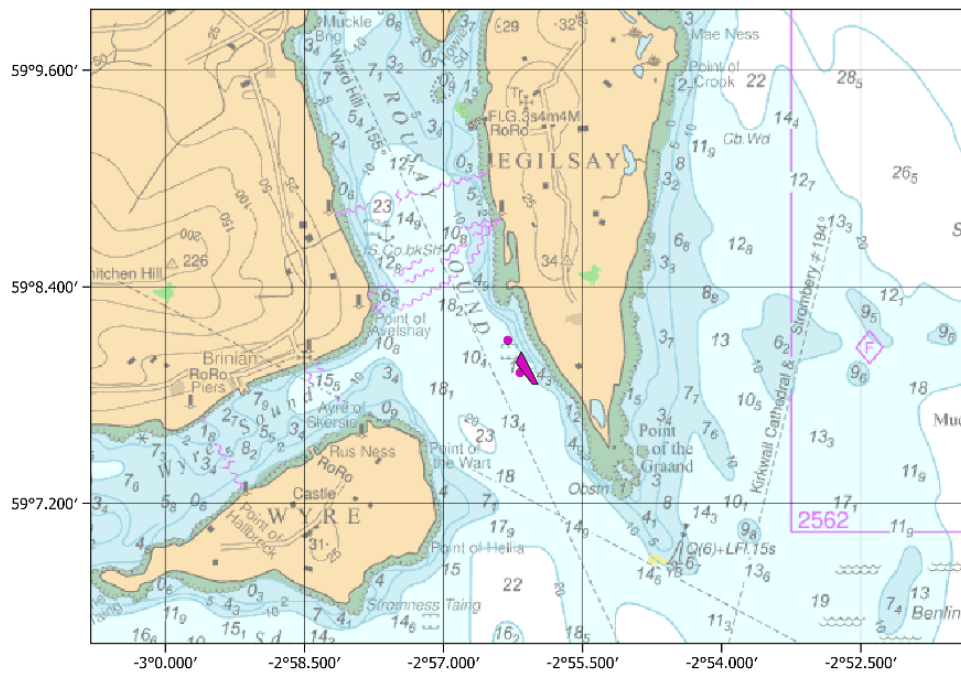
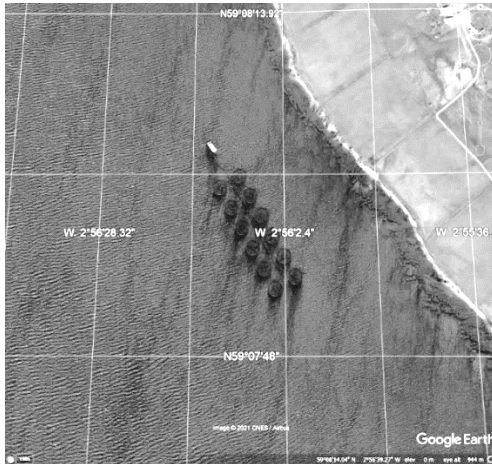


Figure 22: Bay of Vady farm site, the location of the farm is indicated by the solid purple polygon and the current meter locations as purple circles. © British Crown and OceanWise, 2021. All rights reserved. Licence No. EK001-20180802. Not to be used for Navigation.

Figure 23: Google Earth image of the Bay of Vady salmon farm.



The original bathymetry survey for licencing purposes at the Bay of Vady site is reported in Aurora (2009a). Charted data for this area were considered by Aurora to be insufficient for modelling waste dispersal from the proposed farm because: the data obtained from the Admiralty maps were not of sufficient resolution for modelling purposes; the methods for collecting this data were deemed not to be accurate (lead line by the British Government Surveys between 1839 and 1848); and spot depth measurements obtained at the site did not match the chart data. The consultants therefore took twenty-two additional soundings within the area of proposed cage deployment and then contoured the resulting dataset (Figure 24). These data were also re-gridded using kriging (Surfer 11, Golden Software) as different grid production methods can produce varying results.

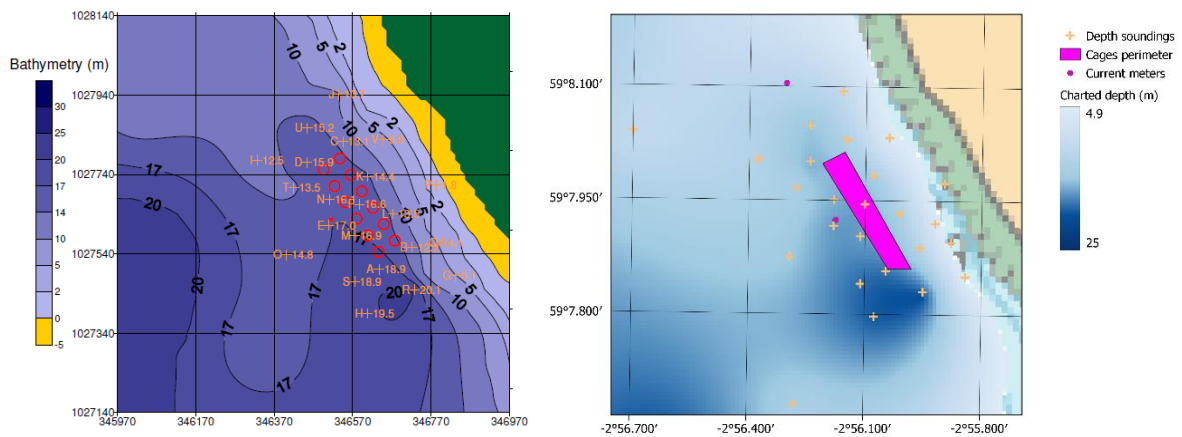


Figure 24: Original consultants bathymetry (shown as depths below chart datum) for the Bay of Vady farm site (left panel) compared with re-gridded data (right panel). The locations of the soundings data are shown as orange crosses. Note the two images are scaled identically but metric easting and northing (OSGB36) are shown in the original plot and geographic co-ordinates are shown on the re-gridded image. The cage locations in the left panel are those proposed at the site licence application stage, the cage perimeter in the right panel is based on observed corner cage locations during the INCREASE study.

The comparison in Figure 24 shows very similar patterns with an area of deeper water to the south of the cages. Deeper water is also indicated to the southwest corner of the mapped area, but the kriging analysis suggested that the shallower projection (shown as the 17 m contour on the original mapping) might continue to the southern boundary of the mapped area. This

demonstrates how the use of different gridding methods can lead to differences, even when the same original sounding data are used.

The Admiralty chart (Figure 22) indicates strong tidal currents on the eastern side of Egilsay (tidal diamond F) where the European Marine Energy Tidal Test Site is located. However, currents through the Rousay Sound are somewhat weaker due to the narrows at the northern end of the Sound.

Two sets of current meter data were available for the Bay of Vady site.

The first set is that used in the licencing of the site and was collected between 1st July to 17th July 2009 using a meter deployed just off the southwest edge of the cage array at 59° 7.924' N 002° 56.176' W (Figure 22).

As expected, water speeds close to the bed tended to be slightly lower than in mid-water or nearer to the surface (Figure 25). Mean flows were 12.4, 14.6 and 15.1 cm s⁻¹ at 2.1, 8.6 and 12.5 m above the seabed respectively. Near seabed peak flows ranged from just over 10 to 26.8 cm s⁻¹.

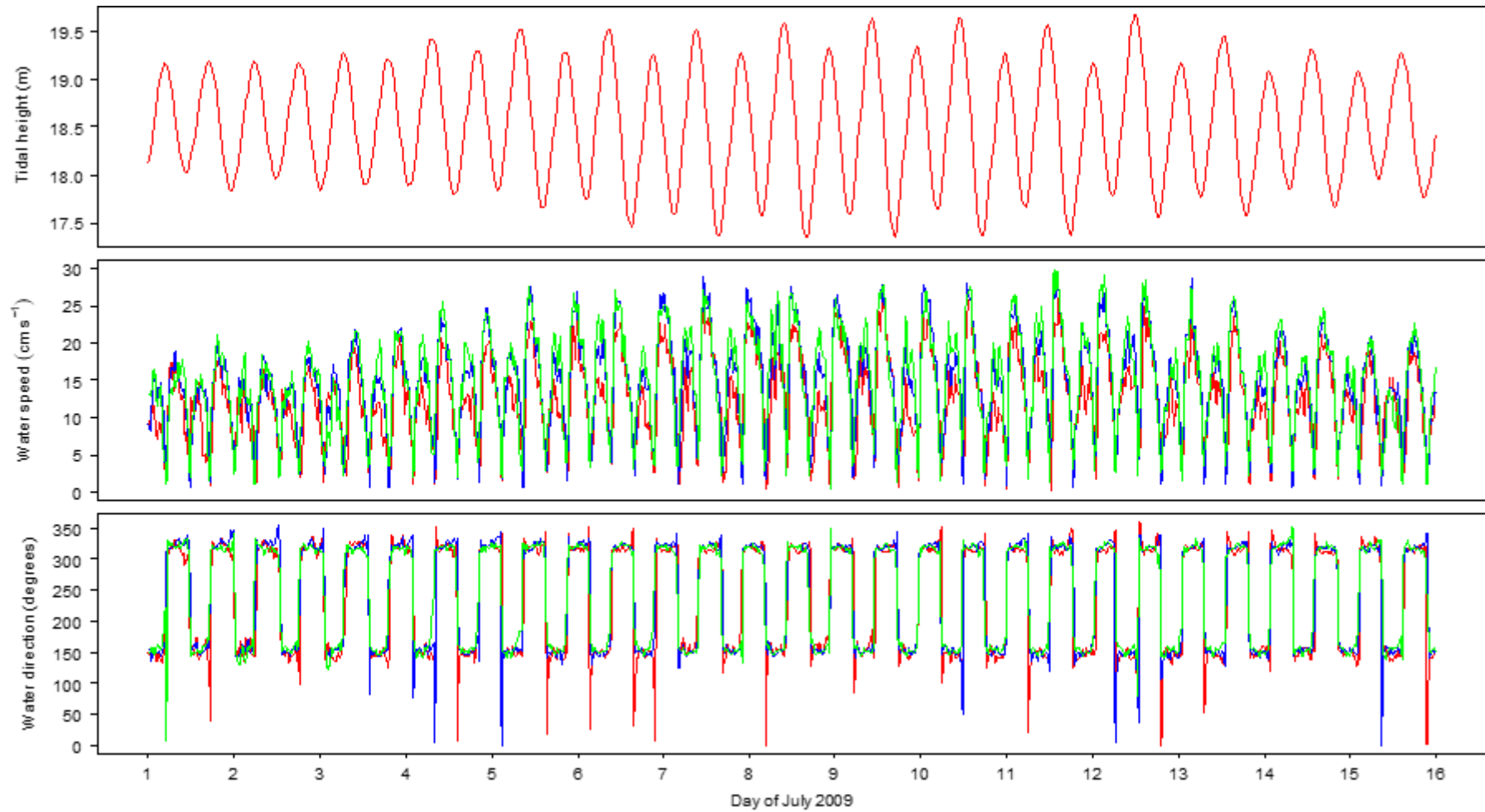


Figure 25: Tidal height, current speeds and directions from current meter data collected at Bay of Vady site in 2009. Red lines are the near bed depth (2.1 m above seabed); blue lines are cage-bottom depth (8.6 m above seabed) and green lines are sub-surface depth (12.5 m above seabed).

An additional deployment was undertaken in 2018 using an Aanderaa SeaGuardII Acoustic Doppler Current Profiler deployed between the May 8th to 13th anchored at 59° 08.104' N, 002° 56.306' W, just to the northwest of the feed barge (Figure 22).

The 2018 current meter timeseries only covered part of the tidal cycle and the data were noisy in places (Figure 26). The 2018 data should therefore only be used with caution. Average current speeds were slightly lower than in the 2009 data, perhaps reflecting the neap tidal phase. Mean flows were 11.1, 11.6 and 11.7 cm s⁻¹ at 2.1, 8.6 and 12.5 m above the seabed respectively. Despite this being a period of neap tides, near seabed peak flows still reached nearly 30 cm s⁻¹.

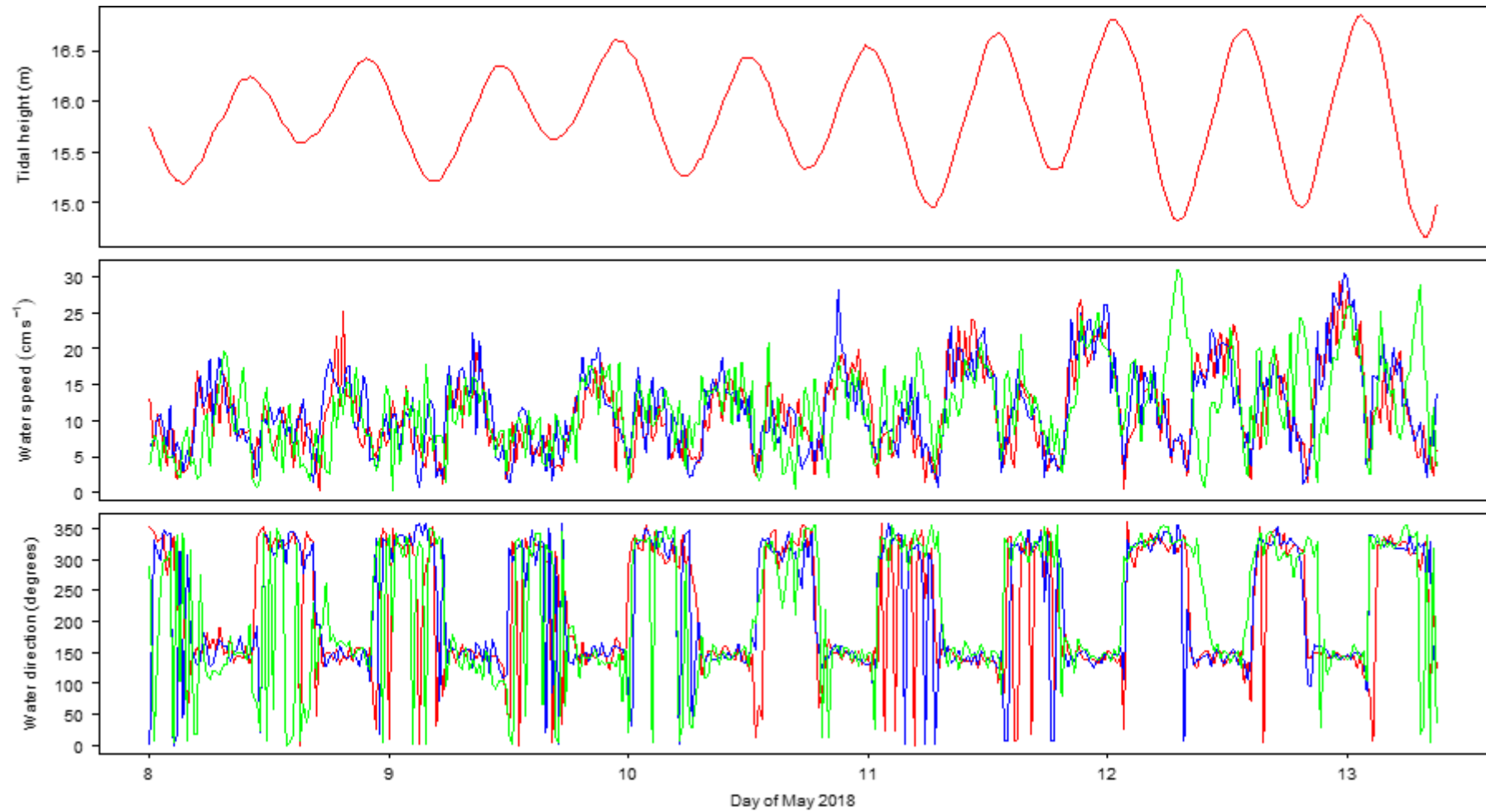


Figure 26: Tidal height, current speeds and directions from current meter data collected at Bay of Vady site in 2018. Red lines are the near bed depth (2.1 m above seabed); blue lines are cage-bottom depth (8.6 m above seabed) and green lines are sub-surface depth (12.5 m above seabed).

Based on the 2009 data (Figure 27), the strongest flows were towards the northwest (mean speed 14.7 cm s^{-1} , mean direction 318°) with slightly weaker flows towards the southeast (mean speed 10.0 cm s^{-1} , mean direction 143°). There were only minor differences between the three depths.

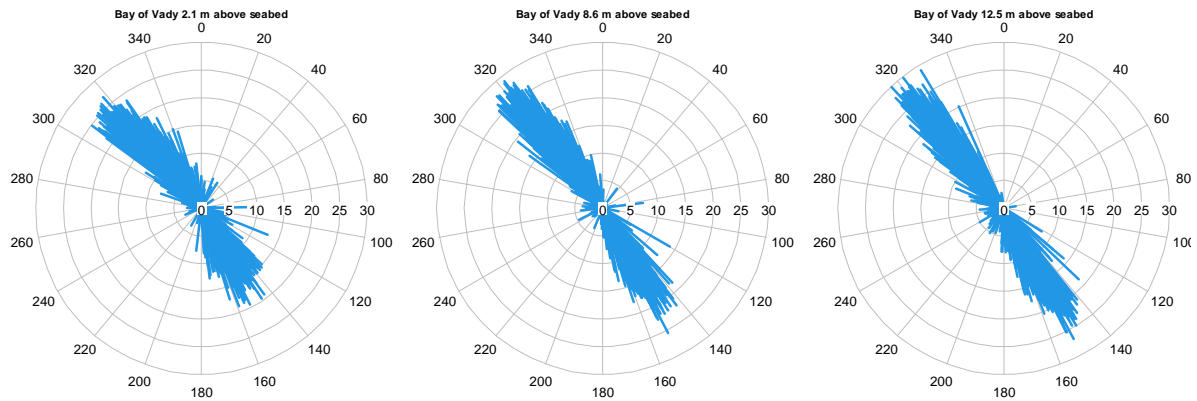


Figure 27: Polar plots of current speed (cm s^{-1}) and direction (degrees relative to grid north) at three depths for Bay of Vady current meter data collected in 2009.

At 2.1 m above the seabed the residual current from the Bay of Vady 2009 data was estimated to be 4.3 cm s^{-1} at a direction of 292° (Figure 28).

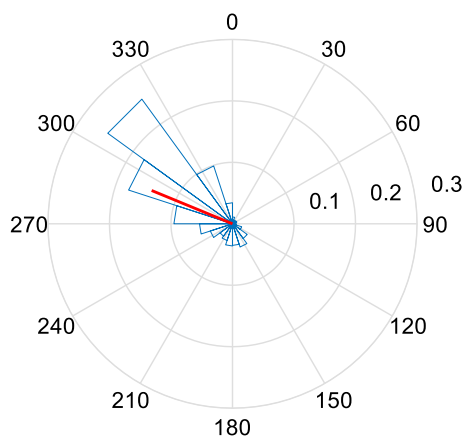


Figure 28: Polar histogram of residual currents at 2.1 m above the seabed for Bay of Vady current meter data collected in 2009 (the red line indicates the averaged residual flows).

Parts of the 2018 current direction timeseries appear unusually erratic and may represent erroneous readings (Figure 26). The 2018 timeseries indicate similar near seabed current directions as recorded in 2009 but with more variability at the near surface depth (Figure 29). Because the 2018 timeseries only covered part of the full tidal cycle, the residual current speed and direction were not calculated.

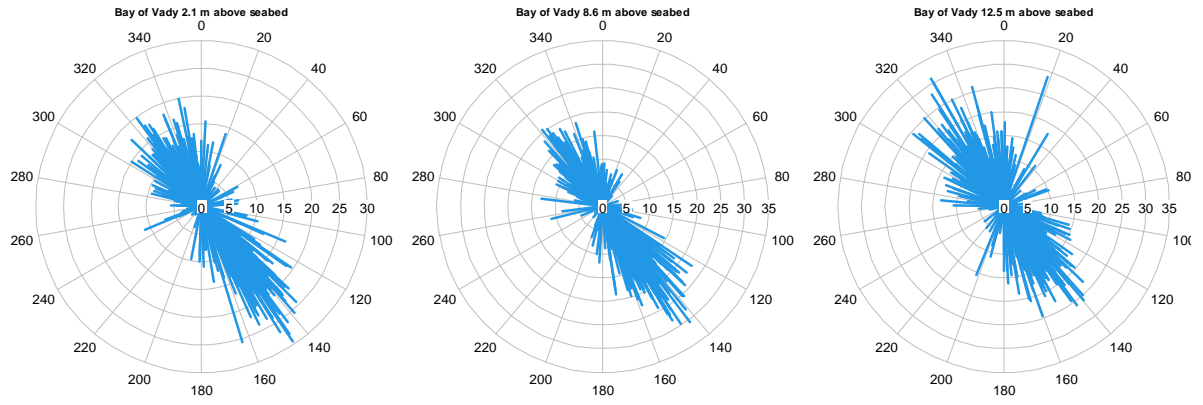


Figure 29: Polar plots of current speed (cm s^{-1}) and direction (degrees relative to grid north) at three depths for Bay of Vady current meter data collected in 2018.

3.1.2. Quanterness site description

The farm (SEPA licence CAR/L/1001931/V1) lies to the northwest of the town of Kirkwall (Figure 30). The shore is rocky but shelves quickly to a seabed of around 10 m charted depth. The cages are thus sited in relatively shallow water. There are eight, 90 m circumference circular cages arranged in an approximately north to south orientation (Figure 31) and the maximum licenced biomass is 600 tonnes.

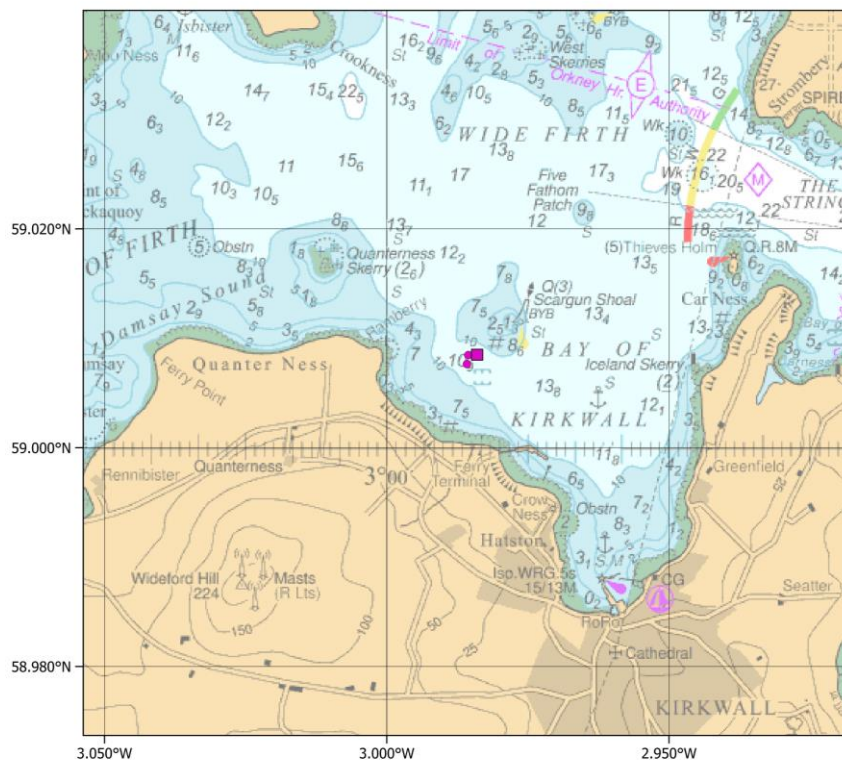


Figure 30: Quanterness farm site, the location of the farm is indicated by the solid purple polygon and the current meter locations as purple circles. © British Crown and OceanWise, 2021. All rights reserved. Licence No. EK001-20180802. Not to be used for Navigation.

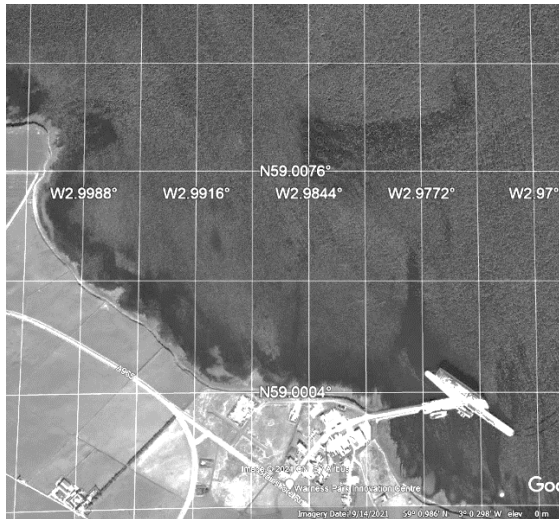


Figure 31: Google Earth image of the Quanterness salmon farm.

The original bathymetry survey for licencing purposes at the Quanterness site is reported in Aurora (2009b). The consultants took thirteen additional soundings within the area of proposed cage deployment, incorporated charted soundings from the surrounding area and then contoured the resulting dataset (Figure 32). These data were also re-gridded using kriging (Surfer 11, Golden Software) as different grid production methods can produce varying results.

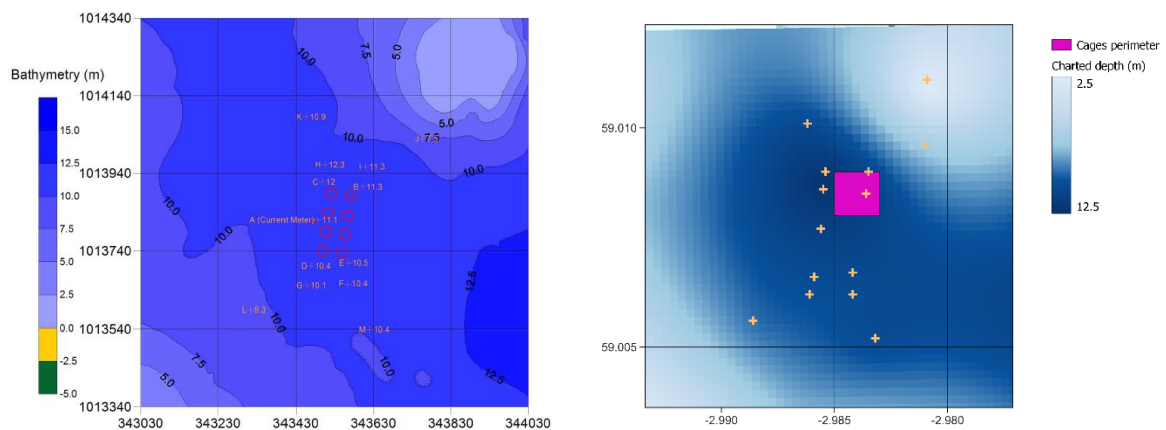


Figure 32: Original consultants bathymetry (shown as depths below chart datum) for Quanterness farm site (left panel) compared with re-gridded data (right panel). The locations of the soundings data are shown as orange crosses. Note the two images are scaled identically but metric easting and northing (OSGB36) are shown in the original plot and geographic co-ordinates are shown on the re-gridded image. The cage locations in the left panel are those proposed at the site licence application stage, the cage perimeter in the right panel is based on observed corner cage locations during the INCREASE study.

The comparison in Figure 32 shows very similar patterns with areas of shallower water to the northeast and west of the cages. There are some minor differences between the bathymetries with the northeast extension of the 10 m contour (343230, 1013740) shown in the original report less obvious in the replotting. The seabed towards the northwest of the cages also shallows in the replotting slightly more than indicated by the contours in the Aurora report (2009b). This demonstrates how the use of different gridding methods can lead to differences, even when the same original sounding data are used.

The Admiralty chart (Figure 30) indicates near surface tidal currents up to 5.1 knots (260 cm s^{-1}) to the north in the Wide Firth (tidal diamond M). However, currents in the Bay of Kirkwall are weaker due to the semi-enclosed nature of the bay.

Two sets of current meter data were available for the Quanterness site.

The first data are that used in the licencing of the site and were collected in 2009 between June 16th to July 1st using an RDI 600 kHz Workhorse Acoustic Doppler Current Meter (ADCP) meter anchored at $59^{\circ} 00.459' \text{ N } 02^{\circ} 59.148' \text{ W}$, slightly to the west of the cage group (Figure 30).

Water speeds close to the bed and at pen net depth were slightly slower than nearer to the surface (Figure 33). Mean flows were 11.3 , 13.1 and 15.4 cm s^{-1} at 2.1 m (taken as near bed for licencing purposes), 4.6 m (net depth) and 6.1 m above the seabed (taken as sea surface for licencing purposes) respectively. Near seabed peak flows were up to 11.3 cm s^{-1} .

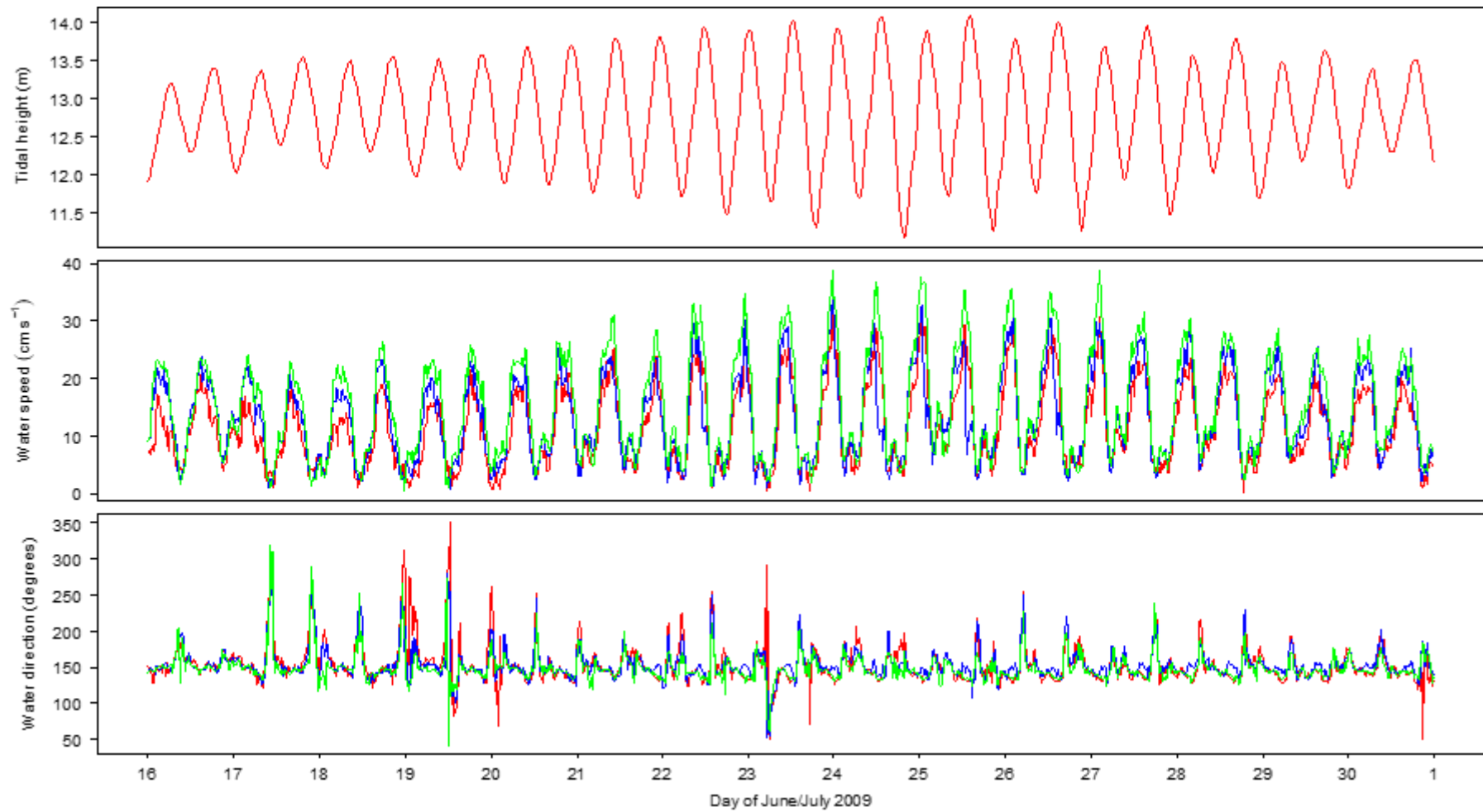


Figure 33: Tidal height, current speeds and directions from current meter data collected at *Quanterness* site in 2009. Red lines are the near bed depth (2.1 m above seabed); blue lines are cage-bottom depth (4.6 m above seabed) and green lines are sub-surface depth (6.6 m above seabed).

An additional deployment was undertaken in 2019 using an Aanderaa SeaGuardII Acoustic Doppler Current Profiler deployed between the May 29th May to June 17th anchored at 59° 00.508' N, 002° 59.134' W, towards the northwest edge of the farm (Figure 30).

Water speeds close to the bed were slower than in mid-water or nearer to the surface (Figure 34). Mean flows were 13.9, 16.0 and 45.7 cm s⁻¹ at 2.1 (taken as near bed for licencing purposes), 4.6 m (net depth) and 6.1 m above the seabed (taken as sea surface for licencing purposes) respectively. Near seabed peak flows were up to 46.4 cm s⁻¹.

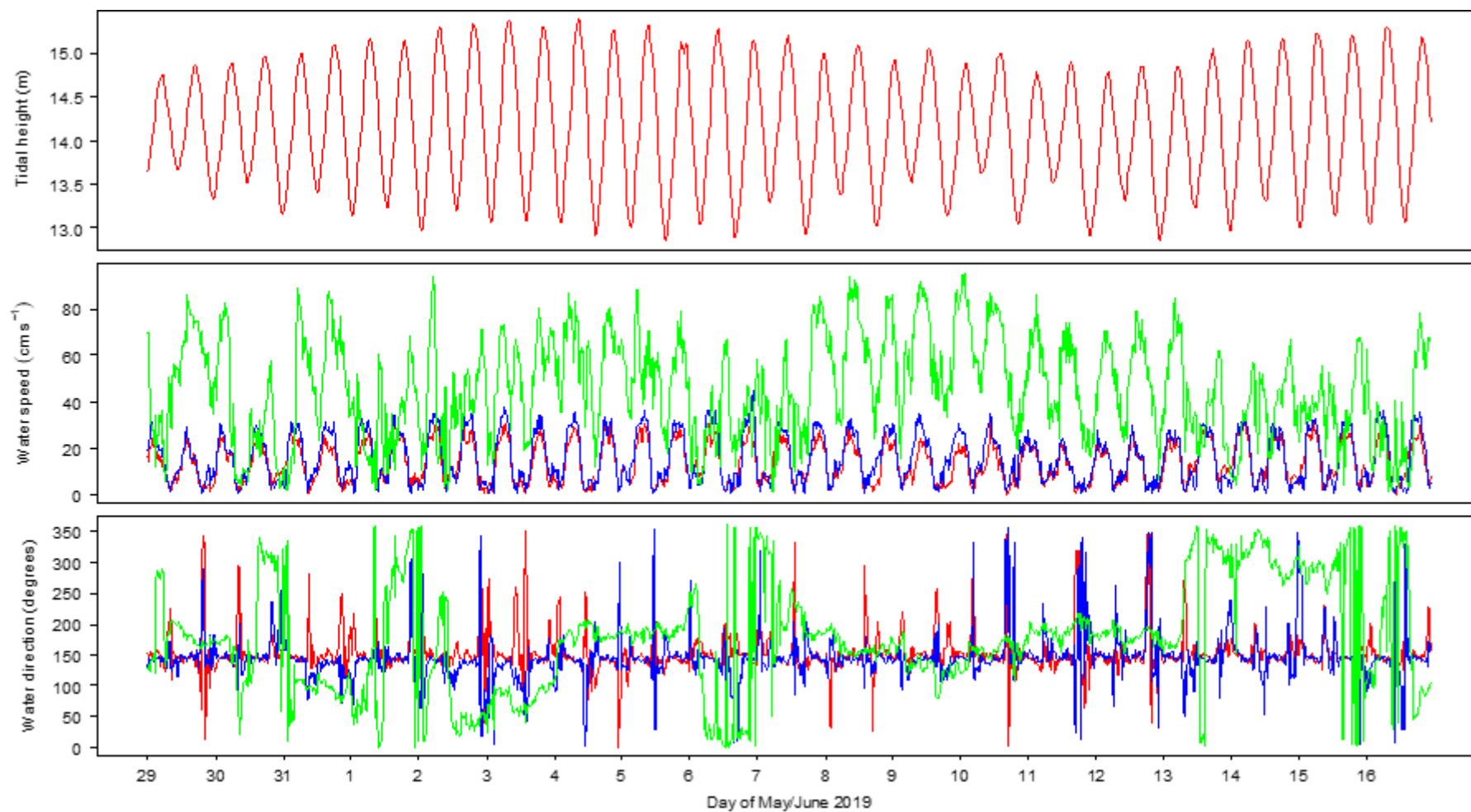


Figure 34: Tidal height, current speeds and directions from current meter data collected at *Quanerness* site in 2019. Red lines are the near bed depth (2.1 m above seabed); blue lines are cage-bottom depth (4.6 m above seabed) and green lines are sub-surface depth (6.6 m above seabed).

Based on the 2009 data (Figure 35), the near seabed current was strongest when flowing towards the southeast (mean speed 11.8 cm s^{-1} , mean direction 148°) with weak flows towards the west (mean speed 3.4 cm s^{-1} , mean direction 238°). There were only minor differences in current directionality between the three water depths.

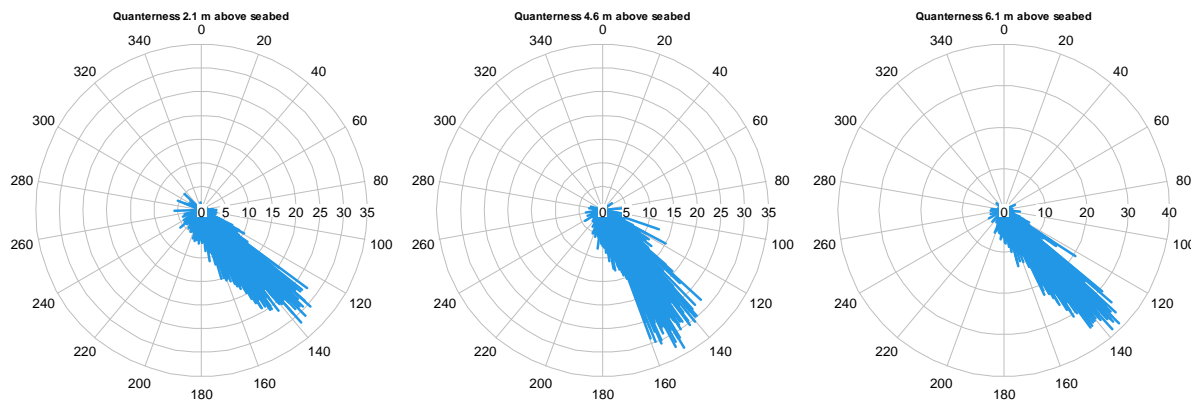


Figure 35: Polar plots of current speed (cm s^{-1}) and direction (degrees relative to grid north) at three depths for Quanterness current meter data collected in 2009.

At 2.1 m above the seabed the residual current from the Quanterness 2009 data was estimated to be 13.3 cm s^{-1} at a direction of 147° (Figure 36).

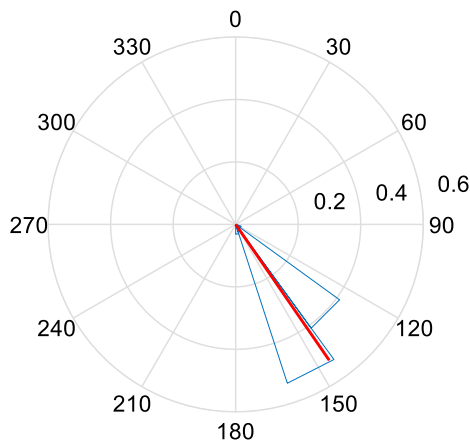


Figure 36: Polar histogram of residual currents at 2.1 m above the seabed for Quanterness current meter data collected in 2009 (the red line indicates the averaged residual flows).

Based on the 2019 data (Figure 37), the pattern of near seabed currents was almost identical to the 2009 timeseries being strongest when flowing towards the southeast (mean speed 14.3 cm s^{-1} , mean direction 148°) with weaker flows towards the west (mean speed 3.3 cm s^{-1} , mean direction 271°). There were only minor differences in current directionality between the two lower water depths but directionality at the near surface was much more variable.

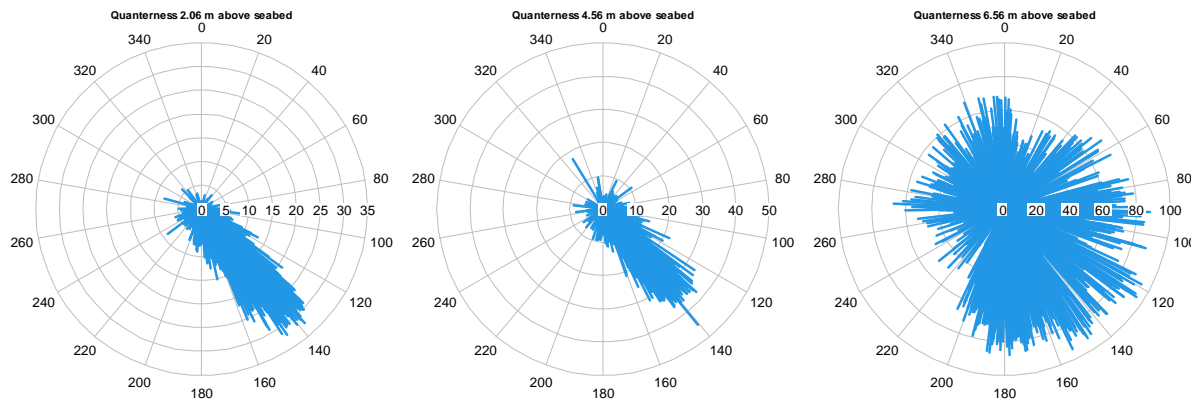


Figure 37: Polar plots of current speed (cm s^{-1}) and direction (degrees relative to grid north) at three depths for Quanterness current meter data collected in 2019.

At 2.1 m above the seabed the residual current from the Quanterness 2019 data was estimated to be 13.3 cm s^{-1} at a direction of 147° (identical to the result from the analysis of the 2009 timeseries).

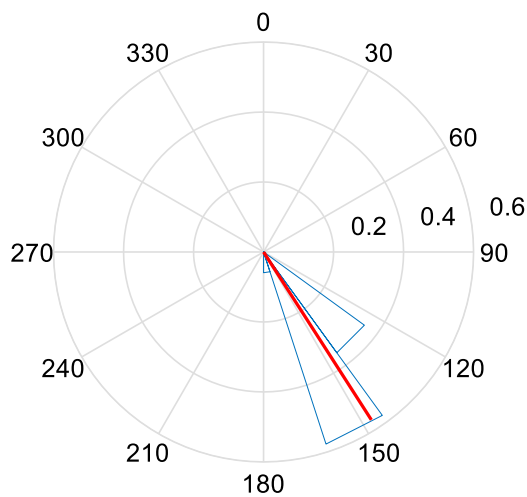


Figure 38: Polar histogram of residual currents at 2.1 m above the seabed for Quanterness current meter data collected in 2019 (the red line indicates the averaged residual flows).

3.1.3. Bay of Meil site description

The farm (SEPA licence CAR/L/1003888/V4) lies in a small bay to the east of Kirkwall (Figure 39). The shore is rocky but shelves gradually to a seabed of 10 – 17 m charted depth in the bay itself. Further out, Shapinsay Sound has charted depths of around 23 m. The site is reasonably shallow with cages in around 10 m water depth. There are 10 circular cages arranged in a northeast to southwest orientation (Figure 40) and the maximum licenced biomass is 884 tonnes.

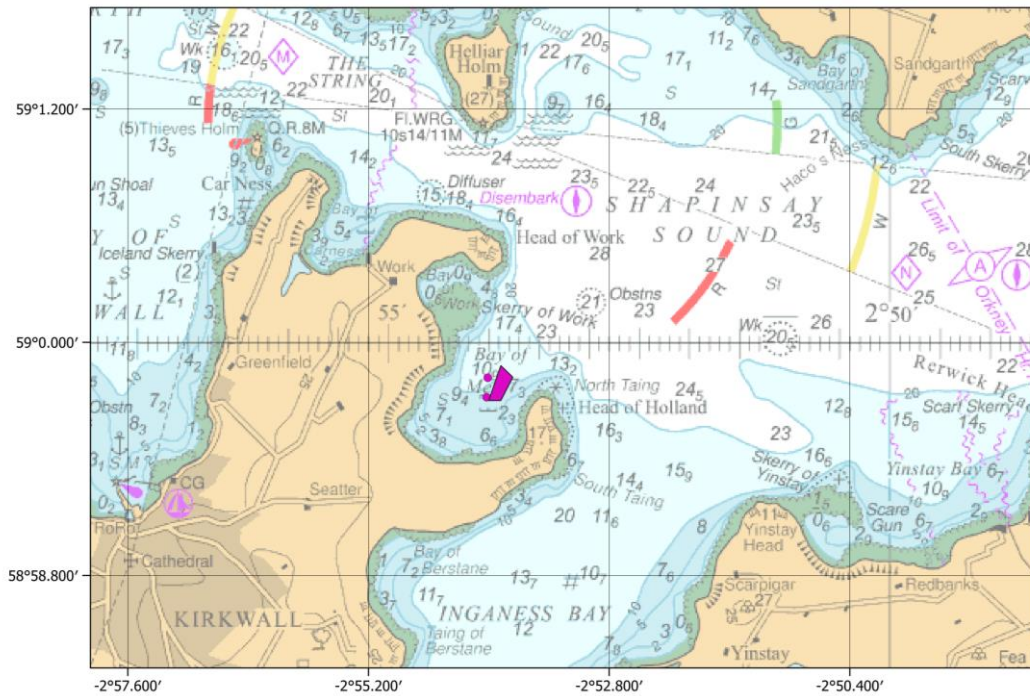


Figure 39: Bay of Meil farm site, the approximate location of the farm is indicated by the solid purple polygon and the current meter locations as purple circles. © British Crown and OceanWise, 2021. All rights reserved. Licence No. EK001-20180802. Not to be used for Navigation.

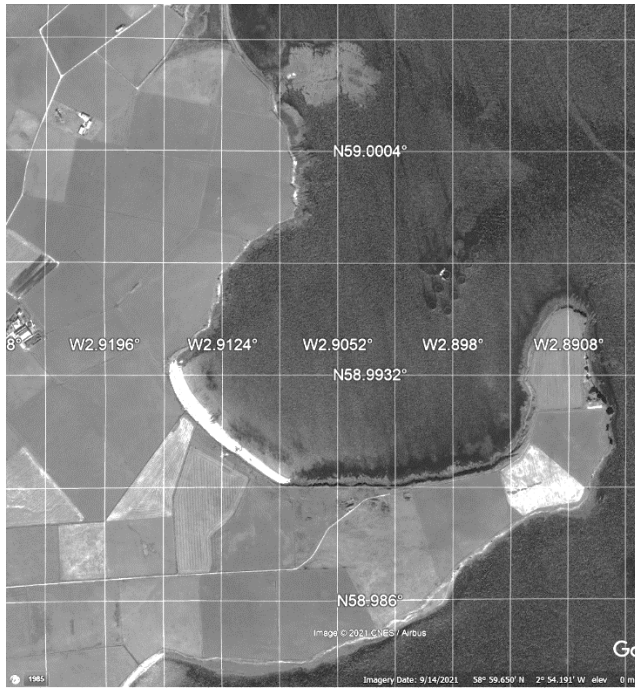


Figure 40: Google Earth image of the Bay of Meil salmon farm.

The original bathymetry survey for licencing purposes at the Bay of Meil site is reported in Aurora (2010). The consultants took ten additional soundings within the area of proposed cage deployment, incorporated charted soundings from the surrounding area and then contoured the resulting dataset. An additional 28 soundings were recorded in 2018 as part of efforts to improve the modelling of dispersal at this site. The combined data were re-gridded using kriging (Surfer 11, Golden Software) and compared with the original site licence bathymetry (Figure 41).

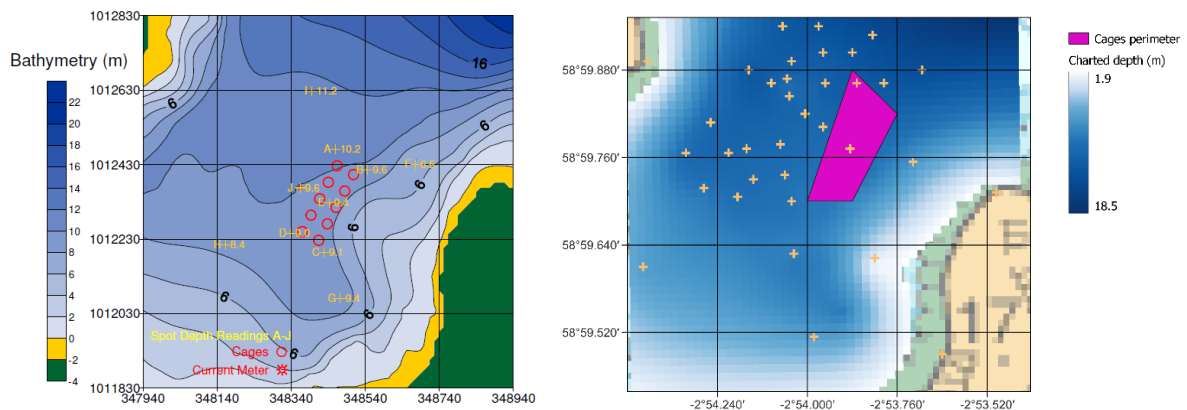


Figure 41: Original consultants bathymetry (shown as depths below chart datum) for Bay of Meil farm site (left panel) compared with re-gridded data (right panel). The locations of the soundings data are shown as orange crosses. Note the two images are scaled identically but metric easting and northing (OSGB36) are shown in the original plot and geographic co-ordinates are shown on the re-gridded image. The cage locations in the left panel are those proposed at the site licence application stage, the cage perimeter in the right panel is based on observed corner cage locations during the INCREASE study.

The comparison in Figure 41 shows very similar patterns although the actual cage locations are slightly north of those shown in the original report (Aurora, 2010).

The Admiralty chart (Figure 39) indicates near surface tidal currents up to 2.8 knots (140 cm s^{-1}) in the Sound of Shapinsay (tidal diamond N). However, currents in the Bay of Meil are much weaker due to the semi-enclosed nature of the bay.

Two sets of current meter data were available for the Bay of Meil site.

The first data are that used in the licencing of the site and were collected between the 6th to 21st November 2009 using a RDI 600 kHz Workhorse Acoustic Doppler Current Meter (ADCP) meter located at $58^{\circ} 59.717' \text{ N } 002^{\circ} 54.022' \text{ W}$, 90 m south-west of the cage group centre (Figure 39).

Water speeds close to the bed were not very different from mid-water or nearer to the surface (Figure 42). Mean flows were 3.4 , 3.3 and 3.2 cm s^{-1} at 2.06 (taken as near bed for licencing purposes), 4.06 m (net depth) and 5.56 m above the seabed (taken as sea surface for licencing purposes) respectively. Near seabed peak flows were up to 9.7 cm s^{-1} .

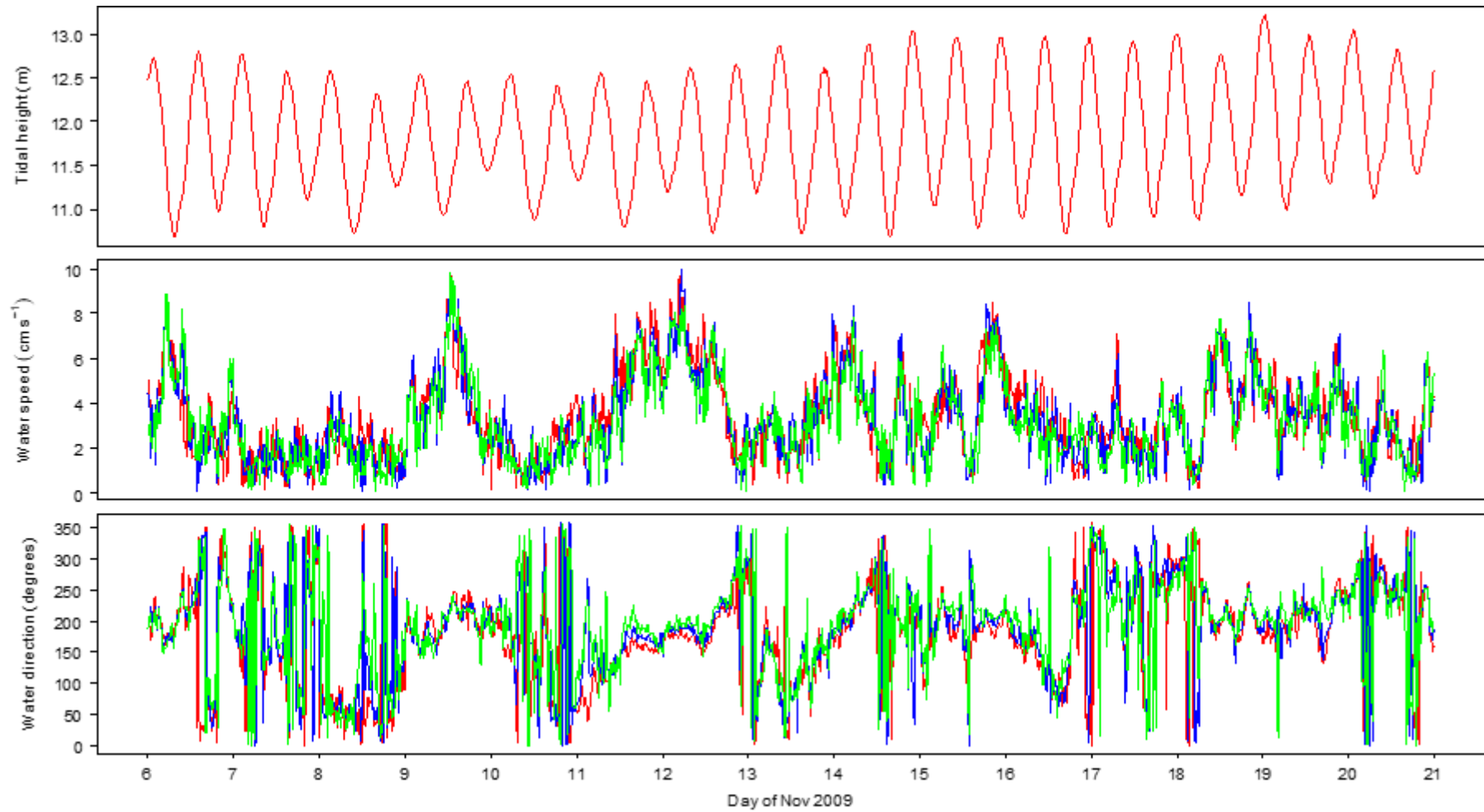


Figure 42: Tidal height, current speeds and directions from current meter data collected at Bay of Meil site in 2009. Red lines are the near bed depth (2.1 m above seabed); blue lines are cage-bottom depth (4.06 m above seabed) and green lines are sub-surface depth (5.56 m above seabed).

The second set of current data were collected between 28th March and 23rd April 2018 using a Seaguard II ADCP located at 58° 59.817' N 002° 54.010' W to the north-west of the farm (Figure 39).

At this location there were large differences between the water speeds close to the bed and in the water column (Figure 42). Mean flows were 3.7, 9.1 and 33.5 cm s⁻¹ at 2.1, 4.2 m and 5.7 m above the seabed respectively. The maximum near seabed peak flow was 13.2 cm s⁻¹.

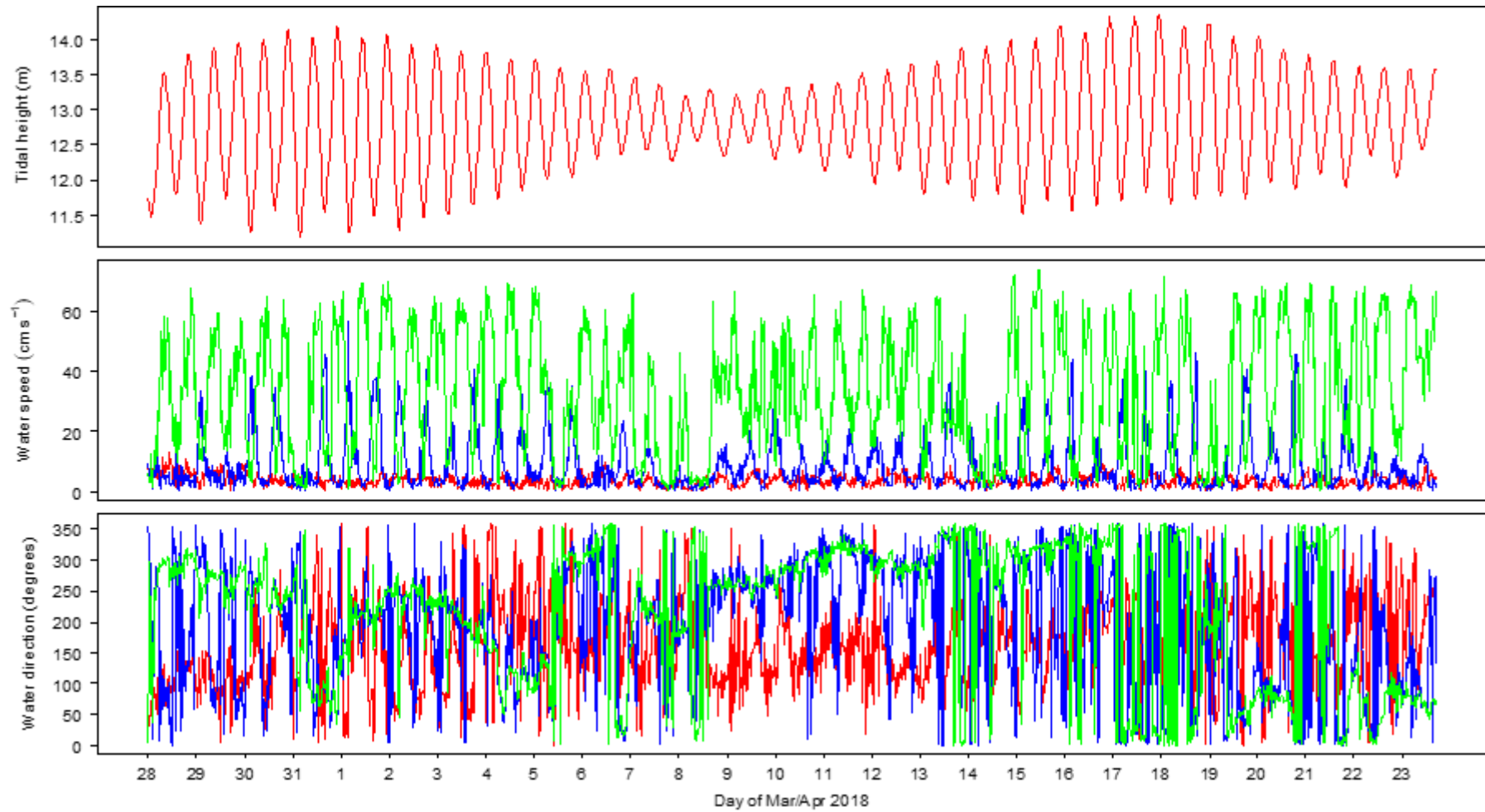


Figure 43: Tidal height, current speeds and directions from current meter data collected at Bay of Meil site in 2018. Red lines are the near bed depth (2.1 m above seabed); blue lines are cage-bottom depth (4.2 m above seabed) and green lines are sub-surface depth (5.7 m above seabed).

There was little clear tidal directionality in the 2009 current data (Figure 44) although flows were slightly stronger in a southerly (2.1 m above seabed) or southwesterly direction (other depths).

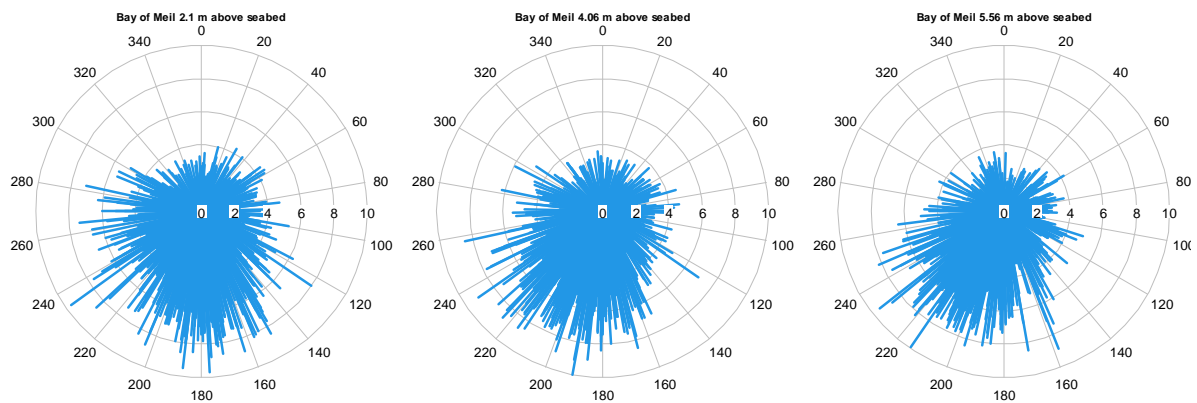


Figure 44: Polar plots of current speed (cm s^{-1}) and direction (degrees relative to grid north) at three depths for Bay of Meil current meter data collected in 2009.

At 2.1 m above the seabed the residual current from the Bay of Meil 2009 data was estimated to be 3.1 cm s^{-1} at a direction of 188° (Figure 45).

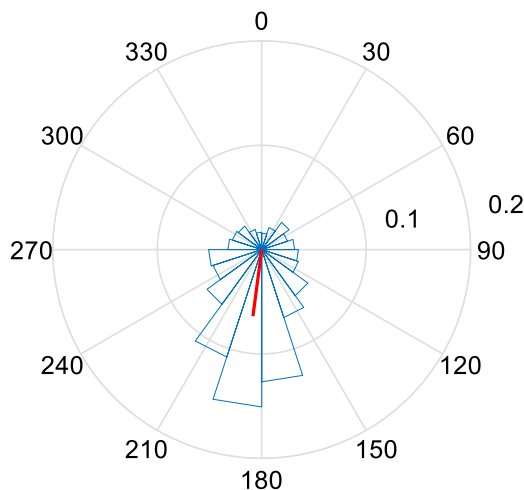


Figure 45: Polar histogram of residual currents at 2.1 m above the seabed for Bay of Meil current meter data collected in 2009 (the red line indicates the averaged residual flows).

From the 2018 data, which were collected at the slightly more northerly position (Figure 39), near-bed flows tended to be slightly stronger in an easterly direction (mean speed 3.6 cm s^{-1} , mean direction 119°), with slightly weaker flows to the southwest (mean speed 3.6 cm s^{-1} , mean direction 236°) (Figure 46). Flows at the other depths did not show strong tidally related directionality.

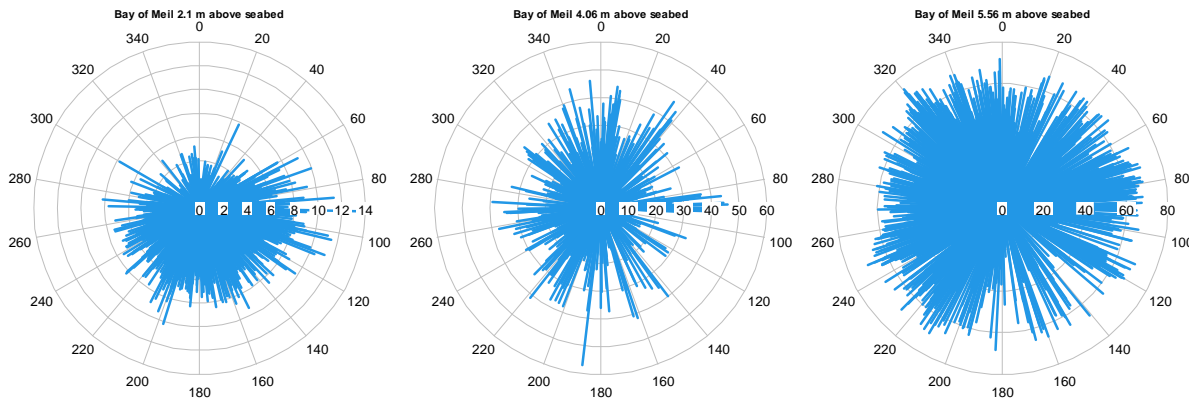


Figure 46: Polar plots of current speed (cm s^{-1}) and direction (degrees relative to grid north) at three depths for Bay of Meil current meter data collected in 2018.

At 2.1 m above the seabed the residual current from the Bay of Meil 2018 data was estimated to be 3.3 cm s^{-1} at a direction of 143° .

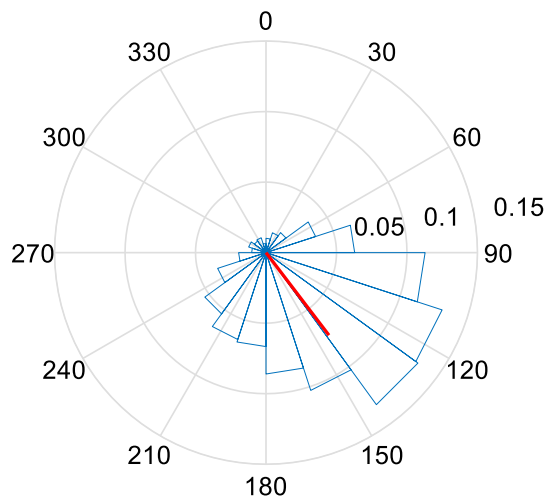


Figure 47: Polar histogram of residual currents at 2.1 m above the seabed for Bay of Meil current meter data collected in 2018 (the red line indicates the averaged residual flows).

3.2. Common methods

This section describes the methods used across all three sites.

3.2.1. Deployment and recovery of sediment boxes to measure organic carbon flux

The study used an approach described in Grant (1985) where clean beach sediment was deployed in metal trays at a Nova Scotian beach to measure organic carbon deposition during flood and resuspension during ebb tides. In the present study, transect lines were first laid by divers from the edge of the cages out to temporary moorings placed 120 to 180 m distance (depending on site). The transect ropes were pre-marked at set distances to enable placement of the sediment boxes (Appendix 2).

Plastic trays (Sistema® KLIP IT™ bakery boxes, capacity 3.5 l, 85 x 238 x 264 mm) were filled with clean, medium-fine grade kiln dried marine sand (Specialist Aggregates, Rugeley, UK). This material had grain sizes between 300 – 600 μm . Because of the volumes required it was not feasible to use sediment taken from the study sites as in the original method described

in Grant (1985) but the sediment used was considered a reasonable proxy for the natural sediment at the study sites. At each site the trays were gently filled with seawater and the plastic lids clipped into place. The boxes were lowered to the seabed from the fish farm service vessel, distributed along the transect lines by diver and then buried so that the lips were as flush with the seabed as possible. The lids were then carefully removed, and the trays left in place for 7 days. An example of the transect line and a deployed sediment box is shown in Figure 55.

In the initial study at Bay of Vady, based on the likely pattern of organic waste deposition from initial site modelling (using AutoDEPOMOD), a bow-tie design was trialled with boxes spaced 20 m apart along the transect lines (Figure 48). The aim was to try and capture the shape of the expected waste sediment footprint to the north-west of the farm.

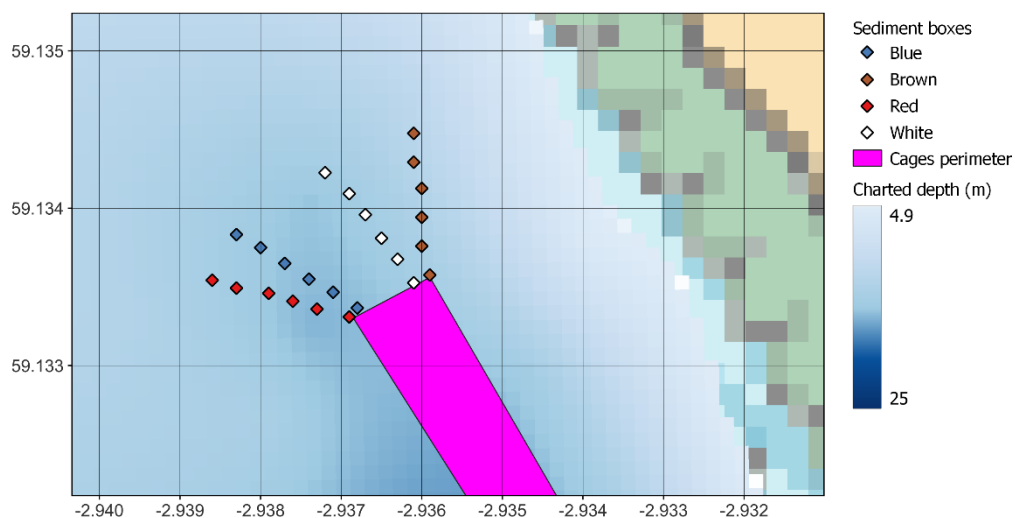


Figure 48: Sediment box locations for Bay of Vady carbon flux measurements.

For the two subsequent studies, the layout of the sediment boxes was changed to align with the revised benthic sampling requirements from SEPA for site quality monitoring. This requires a cruciform sampling design along the expected maximum and minimum axes of the likely depositional footprint (as determined from prior waste dispersal modelling and any previous benthic sampling undertaken at the site).

This change in approach would allow comparison of carbon flux estimates from the sediment boxes with other parameters, such as the IQI benthic quality index determined under the statutory SEPA monitoring program for Quanterness and Bay of Vady.

The sediment box layout for Quanterness is shown in Figure 49. More boxes were placed along the expected extended axes of the footprint. The cages perimeter vertices recorded at the surface will be affected by the tide which likely explains the approximately 10 m offset with where the seabed transect lines originate, as the surface locations were recorded at a different time to the transect laying.

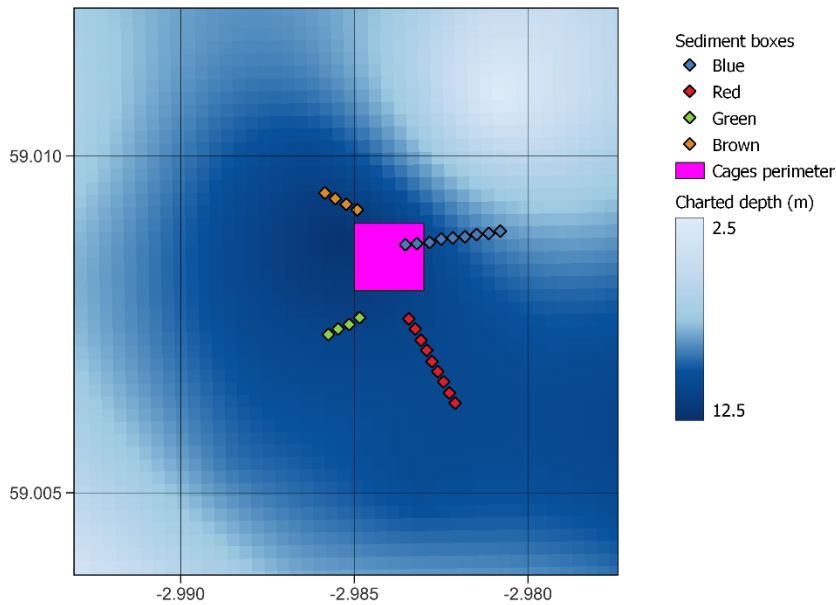


Figure 49: Sediment box locations for *Quanterness* carbon flux measurements. Note the slight offsets between cages perimeter at surface and the start of transect lines on the seabed.

The sediment box layout for Bay of Meil is shown in Figure 50. The expected footprint was expected to be less elliptical than at the more energetic *Quanterness* location so an equal number of boxes and spacings were used along each sampling axis. The cages perimeter vertices recorded at the surface will be affected by the tide explaining the offset with where the seabed transect lines originate, as the surface locations were recorded at a different time to the transect laying.

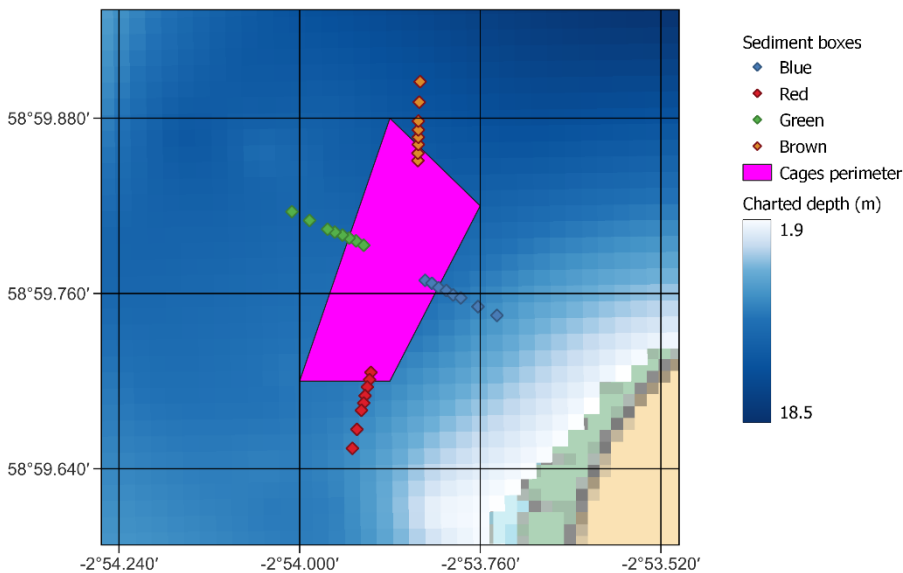


Figure 50: Sediment box locations for *Bay of Meil* carbon flux measurements.

After 7 days, the boxes were recovered by divers who replaced the clip lids before recovering the boxes to the fish farm support vessel. Once ashore, the boxes were frozen at -20°C and then transported in insulated containers to the SAMS laboratory, Oban for further processing (see Section 3.2.10).

3.2.2. Collection of syringe cores for sediment particle size, particulate organic carbon and sulphide analyses

Three sediment cores were collected adjacent to each sediment box by the divers using 50 ml plastic syringes (Terumo Corp., Leuven, Belgium) with the tubes cut flush at the nozzle ends. Each syringe was pushed into the sediment keeping the angle as vertical as possible while steadily withdrawing the plunger. Once filled to the 50 ml mark, the syringe was withdrawn from the sediment and the open end sealed underwater with a second plunger. The samples were recovered to the fish farm support vessel and, once ashore, were frozen at -20°C before being transported in insulated containers to the SAMS laboratory, Oban for further processing. The original intention had been to section at least some of the sediment core samples but the coarse nature of the sediment resulted in many of the syringes being inserted at an angle and some mixing of material during sampling. The syringe cores therefore needed to be treated as samples of surficial sediment mixed down to a maximum depth of 7 cm. Because of this mixing, the POC results do not necessarily reflect the carbon concentration on the seabed surface but an average down to a maximum depth of 7 cm.

3.2.3. Collection of benthic grabs for sediment, macrofaunal and sulphides

Benthic grab sampling at Bay of Vady was undertaken in compliance with SEPA requirements at the time. Benthic sampling was due to be undertaken in 2020 but Covid-19 restrictions prevented this so the latest available data for this site come from 2019 (Biotikos Ltd., 2019). Three replicate grabs were collected at each sampling location on 5th September 2019 (Appendix 3, Figure 51).

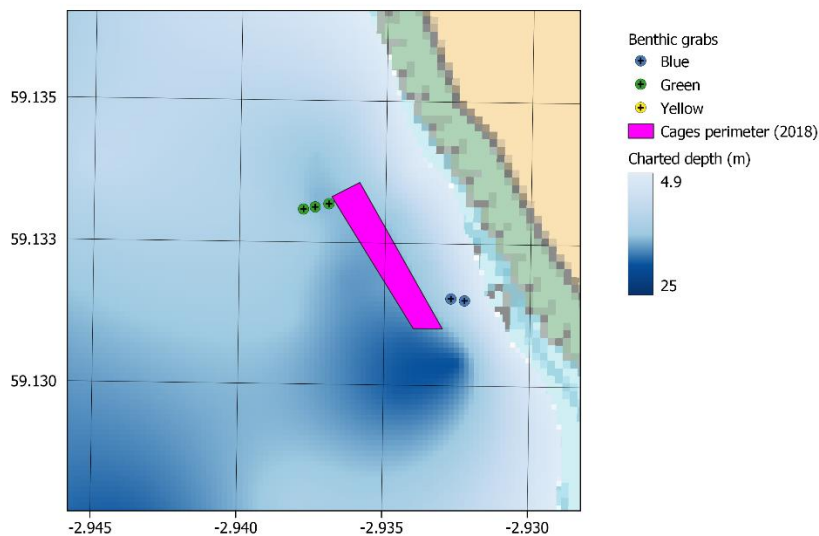
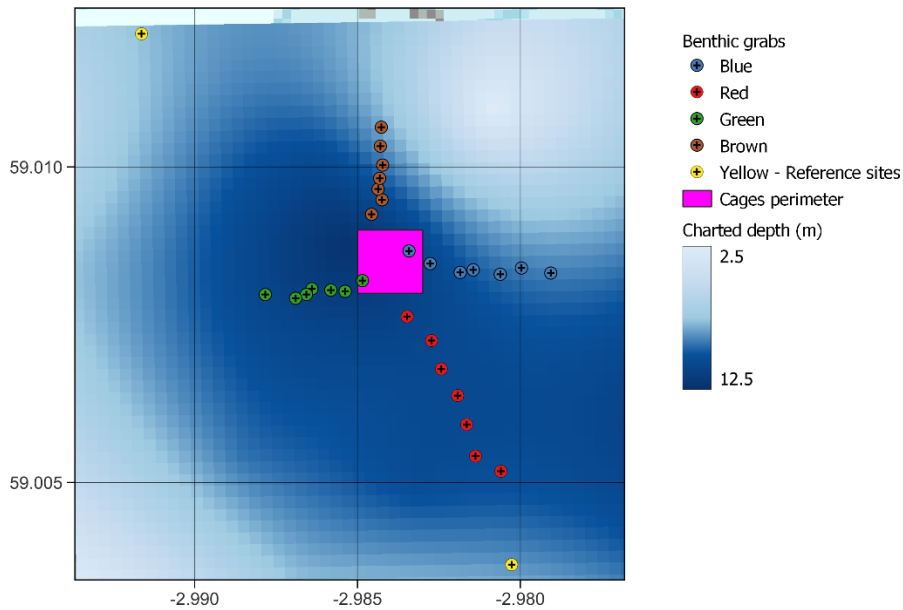


Figure 51: Locations of benthic grabs collected at Bay of Vady. Note cages perimeter was based on positions recorded in 2018 during sediment box deployments.

Benthic grab sampling at Quanterness and Bay of Meil was more comprehensive than at Bay of Vady due to changes in SEPA monitoring requirements.

The Quanterness site was sampled using duplicate benthic grabs at each location between the 3rd and 5th July 2019 (Appendix 4, Figure 52).



*Figure 52:
Locations of
benthic grabs
collected at
Quanterness.*

The Bay of Meil site was sampled using triplicate benthic grabs at each location on 31st Aug and 1st Sep 2021 (Appendix 5, Figure 53).

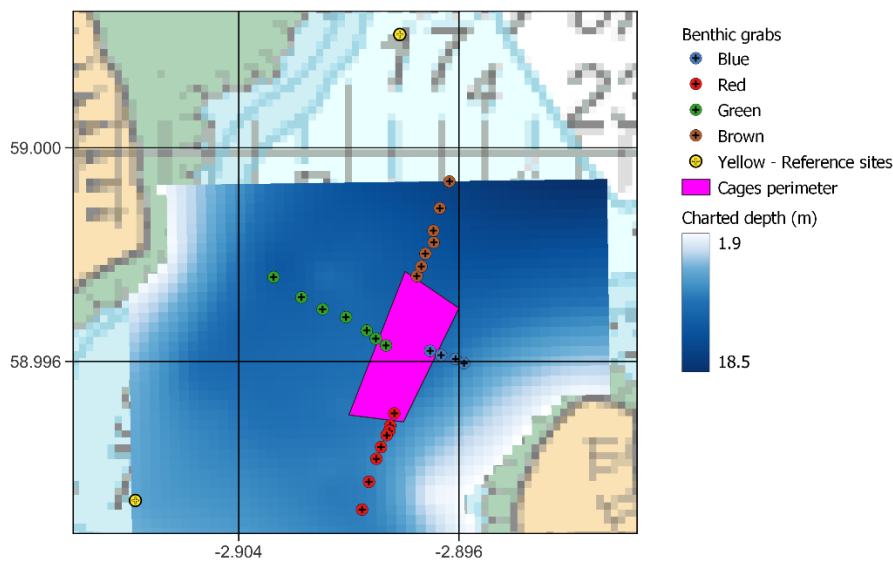


*Figure 53:
Locations of
benthic grabs
collected at Bay
of Meil.*

Samples were collected using a 0.045 m² Van-Veen grab deployed from the fish farm support vessel. Grab positions were recorded from the vessel’s GPS plotter and the survey designs followed a cruciform pattern where the axes of sampling corresponded to the expected major and minor axes of the organic waste footprints based on previous dispersal modelling and knowledge of the sites.

On recovery of the grab to the vessel, an estimate of the volume of sediment in the grab, any obvious smell of hydrogen sulphide and the surficial appearance (colour, texture, presence of bacterial mats, feed pellets or visible faeces) was recorded. Samples were then taken from the

surface material in the grabs using 5 cm³ plastic syringes with rubber piston seals. Prior to sampling, the Luer-slip connection end was carefully removed by cutting the syringe flush to the graduation marker. The sediment was sampled at a 45° angle from the top 2 cm of the sediment surface to limit depth influences and care was taken not to entrain air bubbles (Black and Nickell, 2014). The sample was removed and sealed with an additional rubber seal before placing in a cool box to be analysed on shore. Black and Nickell (2014) cautioned that only benthic grabs which retained surface water should be sampled for sulphides, this precaution being to prevent exposure of the sediment to oxygen. However, with samples collected using a grab from coarse sediment, water is likely to drain from the grab during recovery. Samples for sulphide analyses were therefore collected as rapidly as possible after recovery of the grab to the vessel. The grab samples were then sieved using a 1 mm sieve and macrofauna preserved for subsequent analysis in accordance with SEPA guidelines (see Section 3.2.4).

3.2.4. *Sediment analysis from benthic grab samples*

A visual assessment of the sediment was recorded. Colour and texture were noted, along with the presence or absence of feed pellets, *Beggiatoa* mats and any indication of outgassing or the presence of hydrogen sulphide.

A 150 – 200 ml sub-sample of sediment was collected from the surface (0 – 2 cm) of the grab sample and frozen for later analysis. Particle size analysis (PSA) was undertaken by dry sieving using a stack of 10 sieves ranging from 2 mm to 38 µm.

An additional 100 ml sub-sample of sediment was collected from the surface (0 – 2 cm) of a separate single grab at each station. Loss on ignition (LOI) was subsequently determined by weight difference after heating dried sediment to 450°C (Fish Vet Group, 2019; Pharmaq Analytiq, 2021). Sediment classification was based on the Phi value calculated in Gradistat (v8).

3.2.5. *Infaunal analysis of benthic grab samples*

Based on the faunal analyses of the benthic grab samples, a range of univariate and multivariate statistics were calculated from the pooled duplicate grab samples and so correspond to a sampling area of 0.09 m² (Fish Vet Group, 2019) for Quanterness and 0.135 m² for Bay of Meil (Pharmaq Analytiq, 2021).

- Number of species or taxa (S) – Low numbers may be an indication of a polluted environment.
- Abundance (N) – Enrichment may lead to elevated abundances of opportunistic species.
- Margalef's richness index (d) – An index of species presence for a given number of individuals. The index value tends to be higher where there is less environmental stress.
- Pielou's evenness Index (J) – The evenness of distribution of individuals for each species (taxa). The value is lower where only a few species dominate which may be indicative of a polluted environment.
- Shannon Wiener Diversity Index (H'Log2) – An index which combines species richness and evenness. The index is higher when species (taxa) diversity is high and the abundance of each species is relatively even, a low index may be indicative of a polluted environment.
- Infaunal Trophic Index (ITI) – An index based on enumerating organisms to feeding types.
- Infaunal Quality Index (IQI) – A weighted average of taxa richness (with taxa identified to the lowest practical level); AMBI (a weighted sensitivity score of all individuals in

a sample) and Simpson's evenness index (a measure of the distribution of individuals across different taxa groups in the sample).

Sample details and the faunal data were entered into an Excel macro workbook supplied by SEPA which then performs the relevant calculations based on Phillips et al. (2014).

3.2.6. Laboratory measurement of particle size from syringe cores

Syringe cores were freeze dried under vacuum for up to 5 days. Dried samples were sieved through a 1.18 mm screen and duplicate samples of 1 g of sediment were placed in 50 ml centrifuge tubes, then 5 ml of Calgon dispersant was added and topped up with water to 25 ml volume. The samples were then vortex mixed for 1 minute. Suspended sediment was then introduced into an LS230 Beckman Coulter laser diffraction particle size analyser following the standard operating procedure (SAMS Enterprise SOP 707). Particle size control used standard 500 µm glass bead matrix (Coulter Control GB500/1) run at the beginning and end of each batch of sample analyses. Data were analysed using Gradistat (version 6) software (Blott, 2008). The grain size categories corresponding to sediment descriptive terms are shown in Table 11.

Table 11: Gradistat size scale (Wentworth, 1922).

Lower bound size (mm)	Group	Name	Lower bound size (µm)	Group	Name
1024	Boulders	Very large	1000	Sands	Very coarse
512		Large	500		Coarse
256		Medium	250		Medium
128		Small	125		Fine
64		Very small	63		Very fine
32	Gravels	Very coarse	31	Silts	Very coarse
16		Coarse	16		Coarse
8		Medium	8		Medium
4		Fine	4		Fine
2		Very fine	2		Very fine
			< 2		

3.2.7. Laboratory measurement of particulate organic carbon from syringe cores

Syringe cores were freeze dried under vacuum for up to 5 days. Dried samples were sieved through a 1.18 mm screen and the sub 1.18 mm fraction was ground and homogenised at 350 rpm for 3 mins in a ball mill grinder. Sediment sub-samples of 15 – 35 mg were weighed into 2 ml glass ampoules and 1 ml of sulphurous acid added to each to remove any inorganic carbon in the sample (Verardo *et al.*, 1990). Vials were left to degas for 8 hrs then stored under vacuum in a dessicator for at least 4 h. The vials were then frozen followed by freeze drying for a further 24 h. The contents of each vial, along with acetanilide standards, were then transferred into tin capsules and combusted in a Model 4010 EAS Elemental Combustion System Total Carbon and Nitrogen analyser (Costech Analytical Technologies, Valencia, USA). Quality control included calibration using acetanilide and running of blanks (SAMS Enterprise, SOP 706).

3.2.8. On-site measurement of sulphides in benthic sediment samples

Sulphides were only chemically measured at Quanterness and Bay of Meil. Two approaches were trialled. Firstly, sulphides were measured in the syringe core samples collected by divers

(see Section 3.2.2). Secondly, a sample of sediment was taken from the benthic grabs collected as part of the statutory SEPA monitoring program (see Section 3.2.3).

Prior to measuring the sulphide levels, the syringe cores were visually assessed in terms of the proportion of the syringe containing water. Results from samples with more than 20% of the overlying volume as seawater were considered separately for the purposes of sulphide quantification. Note that this is less of a problem for the determination of PSA and POC because those variables are more chemically stable, and analyses conducted on dried sediment. Examples of the syringe core appearances are shown in Figure 54.



Figure 54: Examples of syringe cores used for on-site sulphide quantification. Photos are for cores collected at *Quanerness* during *Deployment a*. (left panel) Red transect at 80 m from cage edge; (middle panel) Green transect 0 m from cage edge; (right panel) Blue transect 160 m from cage edge (right panel).

Sulphide was measured using an Thermo Scientific Orion™ silver/sulphide electrode (9616BNWP) coupled with an Orion Star A324 (#1215001) portable electrode meter following the protocol set out in Hargrave *et al.* (2008) and Black and Nickell (2014). Calibration curves were produced at the start of each analytical session by the analysis of 7 dilutions (from 100 to 10,000 μM) of a Na_2S standard. The standards were prepared quantitatively using analytical grade Na_2S (>99.99% Sigma Aldrich) dissolved in deionised and deoxygenated 18.2 M Ω water. Prior to analysis, standards and samples were diluted 1:1 in a pre-prepared sulphide antioxidant buffer (Thermo Scientific) containing ethylenediaminetetraacetic acid disodium salt dehydrate and NaOH. The buffer was activated prior to use with addition of L-ascorbic acid. On addition of the activated buffer, samples were agitated in a vortex for 30 seconds to thoroughly mix sample and buffer. Ion-selective probe measurements were then recorded after 2 minutes. This cut off allowed the reading to stabilise but without leading to significant loss through volatilisation, or conversely, sulphur introduction from possible dissolution of metal-sulphide precipitates (Hargrave *et al.*, 2008). Absolute concentrations were confirmed via titration of the stock Na_2S solution against a 0.1M lead calibration standard (Thermo Scientific). A straight line between the log (10) of the standard concentration and the voltage recorded from the probe was used to interpolate the unknown sample concentrations. Once activated, the buffer solution was used within 3 hours. The CV (reproducibility) of results from the standards was typically less than 10% over the course of an analytical session of several

hours. All samples were measured within 48 hours of collection in duplicate or triplicate (dependent on the analytical time available).

3.2.9. *Sediment samples for eDNA*

There is currently great interest in use of eDNA as a potential alternate method for monitoring benthic community impacts and as a potentially cheaper and faster replacement, or supplement, to macrofaunal taxonomic analyses. Because of this, SAIC has supported several eDNA projects including a PhD (Shraveena Venkatesh) and supervised by Dr Tom Wilding (SAMS). One syringe core from each triplicate was sent to Shraveena for use in her research.

3.2.10. *Laboratory measurement of particulate organic carbon (POC) in the sediment boxes*

Normally, organic carbon deposited into sediment traps can be measured directly because it is concentrated into a clean tube and thus easily removed and quantified. However, because we aimed to quantify deposition and resuspension using a more natural settlement medium (coarse sand), a more complex analytical process was required. Based on previous DEPOMOD models, the amount of organic carbon deposited into the sediment boxes close to the cages over the 7-day deployments was expected to be up to 25 g, giving a concentration of up to 5 mg POC g⁻¹ of coarse sand (because each box contained around 5000 g of sediment). The quantity of organic carbon was to be determined using a Primacs^{MCS} analyser (Skalar Ltd.) owned by the University of Essex. This instrument has a manufacturer recommended detection range of 0.5 mg to 40 mg carbon in up to 3 g of sample weight (although calibrations performed at the University of Essex suggest the instrument has a linear response down to 0.01 mg carbon). Sediment boxes containing high levels of POC could thus be directly quantified but most of the sediment boxes were expected to have much lower POC, so an indirect approach was developed to increase detectability at lower POC levels. Particulate organic carbon was extracted from larger than 3 g sub-samples of the coarse sand sediment and the POC extracted for analysis using a filtration approach.

Once returned to the laboratory the frozen sediment traps were freeze dried under vacuum. Two drying cycles were used, the first of 5–7 days, followed by a further 2–3 days. Once dried, any visible macrofauna or macroalgae on the sediment surface were removed and discarded. Salt was present on the surface of the freeze-dried sediment (based on the volume of seawater likely to be in a box, salt would be possibly up to ~ 50 g per box). A salt correction was not made as the error contribution to the total sediment weight would be less than 1%. The sediment was then sieved and gently mixed in a clean bucket and the total weight of sediment recorded.

Triplicate sub-samples of between 20 – 60 g were then weighed out from each sediment box. To avoid over-loading the filters and carbon detection instrument, it was necessary to take smaller sub-samples from sediment boxes with heavier organic carbon loading i.e. generally those nearer to the fish farm cages. Sediment boxes likely to have a heavy loading could also often be detected by odour and the slightly darker coloration of the mixed sediment. Each weighed sub-sample was placed into a 2.5 l plastic mixing bottle and 500 ml of de-ionised water added and the sediment and water mixed using a kitchen hand blender (Bosch) on a maximum speed setting for 20 seconds. The supernatant was then gently poured into a vacuum filtration funnel set-up with a pre-ashed 47 mm diameter GF/F filter. The mixing and filtration steps were then repeated with another 500 ml of de-ionised water so that about 1000 ml of supernatant were filtered in the first wash. Both mixing and filtration steps were then repeated, but this time pouring the supernatants into a second clean GF/F filter cup. Vacuum suction was then applied for up to several hours. Once filtration was complete, the GF/F filter papers were removed and placed overnight on a perforated tray in a desiccator over a small amount of 37%

HCl to remove any inorganic carbon which might be present. The following day the acidified filters were placed in a warm oven and dried at 50°C overnight. Blank extractions were also performed using the clean sediment used to fill the sediment trays. Dried filters were then individually wrapped in foil and shipped to the University of Essex for analysis of the quantity of organic carbon retained on each filter paper. The quantity of organic carbon on each GF/F filter was determined using a Primacs^{MCS} analyser (Skalar Ltd.). Calibrations were made at low, medium, and high detection ranges before each sample run using desiccated acetanilide.

The estimated filter capture efficiency of the particulate organic carbon in each sediment subsample was calculated as:-

$$E = 1 - (T_2/T_1) \quad \text{Equation 5}$$

where E is the capture efficiency at each filtration step, T₁ and T₂ are the quantities of POC (mg) measured on the first and second wash filters respectively.

The estimated particulate organic carbon (mg) in each sediment subsample was then calculated as:-

$$T = T_1 + T_2 + (T_2 * (1 - E)/E) \quad \text{Equation 6}$$

The last bracketed term in the equation corrects for the fraction of organic carbon not retained on the second wash GF/F filter. Any samples where the capture efficiency was estimated to be less than 0.5 were repeated.

The particulate organic carbon in each sediment sub-sample was then corrected for any trace organic carbon in the clean sediment used to fill the boxes.

$$T_{\text{corrected}} = T - B1 * \text{Sub} \quad \text{Equation 7}$$

where B1 is the mean organic carbon (mg g⁻¹ in clean sand from the blank measurements) and Sub is the sediment sub-sample weight (g).

Based on each sediment sub-sample, the particulate organic carbon (mg) deposited into each sediment box was then estimated as:-

$$T_{\text{box}} = T_{\text{corrected}} * S / \text{Sub} \quad \text{Equation 8}$$

The surface area of each sediment box was 0.0504 m² so the estimate of the organic carbon deposited as g m⁻² over the sediment box deployment period is given by:-

$$\text{Deposition} = T_{\text{box}} / (50.4) \quad \text{Equation 9}$$

For each sediment box the triplicate estimates of deposition were compared. The filtration and analysis of any samples where there was large disagreement between the replicates was repeated. The final estimates of the organic carbon deposited into each sediment box were taken as the mean of the accepted triplicate analysis results from each box.

Note that the estimated organic carbon deposition rates are expressed as g m⁻² over the 7-day periods that the sediment boxes were in place (not as a daily rate).

3.2.11. Modelling of organic particulate waste dispersal and settlement using NewDEPOMOD

Organic waste dispersal was modelled for each field site using NewDEPOMOD (v1.4.0-rc02-WORLD edition) run for 7-day periods to correspond with the length of time sediment boxes were deployed. Water currents were taken from the longer of the available current meter records at each site and the period extracted corresponding to the tidal state during sediment box deployments. Modelled bathymetry was based on the data described in Sections 3.1.1, 3.1.2 and 3.1.3 augmented with data from Admiralty surveys (datahub.admiralty.co.uk/portal/). Where modelled domains included coastline this was taken from data.gov.uk. Feed input files were based on feed and biomass data supplied by Cooke Aquaculture covering the times sediment boxes were deployed at each site.

Firstly, models were run using recommended SEPA defaults except for the adjustments shown in Table 12 (SEPA, 2019a). The full list of baseline model parameter values is given in Appendix 18.

Table 12: Parameter adjustments from SEPA recommended default settings for baseline model runs.

Parameter	SEPA default	Value used	Reason
Bathymetry.bufferZoneWidth	100	250	Allows particles to move further in a timestep – model crashes with low value when resuspension is very active.
Bathymetry.minimumSurfaceDX/DY	25	10	Sample boxes are closer than 25 m – a smaller resolution was required to allow sediment box locations to be in separate cells.
Bathymetry.surfaceDX/DY	25	10	
Transports.BedModel.surfaceDX/DY	25	10	
Transports.BedModel.contractionT50	Infinity	900	To allow tuning of the bed model.
Transports.BedModel.expansionT50	1	14400	
Transports.BedModel.releaseParticles.particlesPerArea	0.0016	0.01	Maintains the setting of 1 resuspension particle per bathymetry cell.

The results for modelled carbon deposition were compared with the estimated depositions from the sediment boxes deployed along the sampling transects using root-mean-squared-error (RMSE). Potential ranges for five parameters typically adjusted when tuning DEPOMOD were scoped as shown in Table 13. To explore which parameter values would most improve model fit, each of the parameters shown in Table 13 were then adjusted in turn to the values shown, whilst keeping the remaining parameters set to the mid-value and RMSE recalculated for each model run.

Table 13: Baseline modelling parameter scoping. Parameter name in NewDEPOMOD given in parentheses: Resup height (*Transports.BedModel.releaseHeight.height*); Hydraulic rough (*Transports.bottomRoughnessLength.smooth*); Crit stress (*Transports.BedModel.tauECritMin*); Layer mass (*Transports.BedModel.dLayerMass*); Horizontal bed dispersion (*Transports.suspension.walker.dispersionCoefficient X and Y*).

Parameter	Default	Low	Mid	High
Resup height	0.12	0	0.0144	0.0555
Hydraulic rough	0.001273	0.000001	0.00001	0.0001
Crit stress	0.02	0.00002	0.0002	0.002
Layer mass	3375	5	15	45
Dispersion	0.1	0.1	0.2	0.5

A multiple linear regression in R was carried out for each model to rank the sensitivity of each parameter. The RMSE value for the model fit was used as the dependent variable, with the five parameters that were altered used as the independent variables. The p-value was used to assess which parameters held the most significance. If a parameter showed no significance ($p > 0.05$), then the SEPA default was used in further model runs. For parameters that showed high significance ($p < 0.05$), further runs were carried out using values near those that showed the best RMSE values in initial runs.

For Quanterness, models were run both including, and removing the tidal residual flow as recommended by SEPA for modelling highly dispersive sites (SEPA, 2019a). For the less dispersive Bay of Meil site, model runs included the tidal residual flow only.

Results were presented as comparisons using the regression approach and contoured waste deposition footprints compared with field observations from the sediment boxes. Contour plots were presented using a logarithmic scaling to better visualise changes across the large range of depositional values, especially close to the cages' perimeter.

3.2.12. Comparison of sediment sulphide measurements with infaunal indices for selected Canadian fish farms

Fish farming in Nova Scotia occurs in a variety of locations but is somewhat concentrated in the South Shore region, corresponding to southwest Nova Scotia. Over the past dozen years, research efforts have been concentrated in Port Mouton, Liverpool Bay, and Shelburne Bay. Among these sites, data sets which include both macrofauna and sediment geochemistry are available for Port Mouton and Shelburne. At both sites, fish farms are in ~15 m depth over fine sediments. Sediment sulphide data are available for numerous aquaculture sites in eastern Canada, but associated macrofauna data are relatively rare as biodiversity measurements are not part of the standard benthic monitoring undertaken in Canada.

Data on sulphides, redox, POM, and porosity are available for Port Mouton and Shelburne Bay¹⁵. Some data records go back to 2009 and are reported annually. All data have longitude and latitude so that the distance of the sample from the cages can be estimated. Where the farm is fallowed, samples are also collected from directly below the former cage locations. All faunal samples were identified by Dr. Lin Lu (Vancouver BC), a long-time taxonomic expert.

Port Mouton – This is a smaller and more protected site than Shelburne and contained a steelhead trout farm until several years ago. There are various published studies for Port Mouton, some of them controversial due to public opposition to cage fish farming (for example, <https://www.friendsofportmoutonbay.ca/>). The most recent study models nutrient release from

¹⁵ <https://data.novascotia.ca/Fishing-and-Aquaculture/Environmental-Monitoring-Program-Data/i2vy-qyt6>

the farm and potential effects on eelgrass (Filgueira *et al.*, 2021). Benthic faunal sampling was conducted from 2009 – 2011, with up to 40 stations covering the whole bay. Sulphide samples were collected simultaneously but there were problems with the analysis. However, the Nova Scotia Environmental Monitoring Program also contains sulphide data from this period and site.

Shelburne Bay – This site is a large coastal bay with three fish farms, two of which are in the inner bay/harbour (Burke *et al.*, 2021). Sulphide data has been collected at the three farm sites and surrounding reference sites for two years across multiple seasons. The inner bay includes Sandy Point where macrofauna data were collected in 2011, 2012, and 2013. Fish were harvested in 2011 and this site fallowed so that the 2011 macrofauna samples constitute the benthic response to maximal organic input from the farm. However, different sampling equipment was used in 2013 (Ponar grab) compared with 2011 and 2012 (Ekman grab) and faunal identification was not undertaken by Dr. Lu. These data were inconsistent with results from 2011 and 2012 (Milewski, 2014), and so were excluded from the analysis.

The infaunal index IQI is not used in Canada but AMBI and diversity have been computed for these sites. These data were converted to IQI using the relationships given in Phillips *et al.* (2014).

4. Results

4.1. Bay of Vady field study results

4.1.1. Sediment particle size from syringe cores

The results from particle size analyses of sediment samples collected using syringe cores at Bay of Vady are given in Appendix 6. There was little variability in the seabed sediment along the sampling transects although an increased percentage of finer grades tended to be found closer to the cages. Overall, the sediment was dominated by fine sands ($50.5\% \pm 6.4\%$, mean \pm std dev., $n = 24$) and very fine sands ($19.0\% \pm 2.7\%$, mean \pm std dev., $n = 24$). The percentage of total silt averaged 10.6% with the maximum value of 22% along the white transect 20 m from the cage edge. There was also a slight elevation of the clay fraction close to the cages along the Blue and Brown transects but the maximum proportion of clay size particles was only 2%.

Visual inspection confirmed that the seabed around the farm is comprised of rippled sands with some loose macroalgae as seen in this image captured while the dive team were deploying the sediment trap boxes (Figure 55). Active bioturbation also appears to be occurring as evidenced by the worm casts visible on the sediment surface.



Figure 55: Image of the seabed at Bay of Vady captured while divers were deploying sediment trap boxes – see section 3.2.1 above. The rope marks one of the transects along which the sediment trap boxes were deployed.

4.1.2. Sediment POC from syringe cores

Results for the analysis of particulate organic carbon in the sediment core samples collected at Bay of Vady are given in Appendix 7. There was no evidence of high levels of organic enrichment in the sediments at the Bay of Vady site. The maximum values were seen close to the cages (Figure 56) but were still less than 2% by dry weight. There were slight increases in POC at 80 and 100 m from the cages along the white and brown transects perhaps suggesting that some wider dispersal of organic waste may occur at this site.

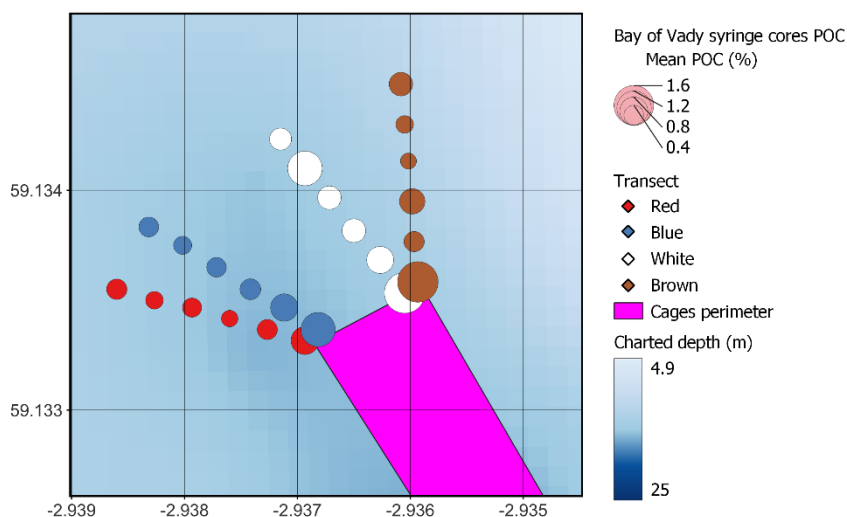


Figure 56: Sediment particulate organic carbon (POC) at Bay of Vady. The surface area of the circles is proportional to the mean POC as a dry weight percentage based on analysis of duplicate syringe cores collected adjacent to each sediment sampling box.

4.1.3. Sediment eDNA

Samples were not analysed for eDNA from the Bay of Vady as the eDNA PhD project commenced after fieldwork was completed at this site.

4.1.4. Benthic grabs collected at Bay of Vady

Sediment grab samples collected at Bay of Vady were (Biotikos Ltd., 2019). Sediment composition from the grabs was mainly fine sand with a mid-brown appearance. A smell of hydrogen sulphide was only noted for sample WSW0 and none of the grabs had surficial gas bubbling, bacterial mat, intact feed pellets or faeces present. The sediment composition (Table 14) was in close agreement with that derived from the syringe cores (see Section 4.1.1). Loss on ignition (LOI) values from benthic grab samples were low, indicative of low organic carbon content.

Table 14: Particle size analysis of benthic grab samples from Bay of Vady.

Grab	>2 mm (%)	<63µm (%)	Geo Mean (µm)	Std Dev (µm)	Phi (φ)	Class Description	LOI (%)
WSW0	0.01	0.82	145.43	1.33	2.78	Slightly/Very fine gravelly fine sand	2.14
WSW25	7.18	1.35	183.87	3.20	2.44	Coarse gravelly fine sand	1.71
WSW50	0.23	1.46	158.79	1.65	2.65	Slightly/Very fine gravelly fine sand	1.71
ENE25	13.19	2.83	313.23	3.63	1.67	Very fine gravelly fine sand	2.07
ENE50	8.31	3.49	346.06	3.20	1.53	Very fine gravelly fine sand	2.93
REF 1	3.46	1.35	191.57	1.97	2.38	Slightly medium gravelly fine sand	1.71
REF 2	7.64	1.25	338.72	2.797	1.562	Medium gravelly medium sand	2.25

4.1.5. Macrofaunal analyses from benthic grabs at Bay of Vady

Fauna collected in the benthic grabs from Bay of Vady in 2019 was analysed for univariate indices and ITI only. This was in accordance with SEPA monitoring guidelines in place at the time. A summary of the results taken from Biotikos Ltd. (Biotikos Ltd.) is given in Table 15.

The heaviest impacts were noted at the cage edge on the westerly (Green) transect located at the northern edge of the farm. The cage edge samples were characterised by high numbers of enrichment polychaetes (*Capitella* spp.). There was little evidence of benthic enrichment impacts for the ENE samples, located at the southern end of the farm.

Table 15: Summary of infaunal analyses N = number of taxa, H' = Shannon-Weiner index, PD = polychaete density, EPD = enrichment polychaete density, ITI = Infaunal trophic index.

Grab	N	(H')	PD	EPD	ITI	Comments
WSW0	14	0.42	77067	76978	0.2	Very high PD which may be indicative of instability but good species richness for a cage edge suggests disturbance is not as severe as it may seem.
WSW2 5	70	4.04	3763	2237	35.1	Marked reduction in PD – comparable to remaining stations and controls. Increase in species number, diversity and ITI, although the latter is still somewhat compromised by group 4 taxa which account for just under half of total individuals present.
WSW5 0	81	4.56	4437	800	61.9	Further increases in species richness, and diversity and marked improvement in ITI which now classifies as “normal.”
ENE25	124	5.37	4474	400	66.3	Communities vary in faunal make-up but species richness and diversity are high or very high, communities are surface feeding with “normal” ITI scores.
ENE50	95	4.86	3704	911	60.3	
REF1	70	4.21	2111	96	73.0	Communities in the wider locale are quite distinct but are species rich, highly diverse with surface feeding trophic profiles.
REF2	87	5.42	1496	289	64.8	

4.1.6. Carbon flux from sediment boxes deployed at Bay of Vady

The results from the estimates of organic carbon deposited into the sediment boxes deployed at Bay of Vady are given in Appendix 8. Several of the Bay of Vady sediment boxes were either not recovered or were damaged in transit resulting in loss of sediment and so were excluded from further analysis (from deployment ‘a’: Blue 80 m, White 40 m; from deployment ‘b’: Red 60 m, Blue 60 m, White 0 m, white 80 m, Brown 40 m, Brown 60 m). The relatively high rate of failures compared with the later studies at Quanterness and Bay of Meil may be partly down to this being the first time the method had been used by the dive team.

The maximum carbon depositions over the 7-day neap tides deployment occurred close to the cages on the blue and white transects (Figure 57). However, there was still an apparent elevated deposition as far as 100 m out along the red transect and a slight elevation at distance along the brown transect. During the spring tides deployment, deposition locations appeared to be generally shifted further away from the cages apart from the red transect where the previous elevated deposition at 100 m distance was absent.

The elevated depositions noted at 100 m along the Red and Blue transects during neap and spring tides respectively suggest that the transects were not long enough to fully capture the extent of waste particle transport from the cages at this relatively energetic site. The scale of

deposition (up to around 300 g m^{-2} over a 7-day period) was in-line with expectations based on previous modelling of the site. The results were therefore encouraging enough to suggest that this method may allow direct measurements of organic carbon deposition from a salmon farm, even in relatively energetic sites. However, the elevated deposition at 100 m out along the blue transect was unexpected and would need confirming with additional sampling. As this was the first time this technique had been used by the dive team there is the possibility that boxes on this transect could have become mixed up.

Deployment a – Neap tides

Deployment b – Spring tides

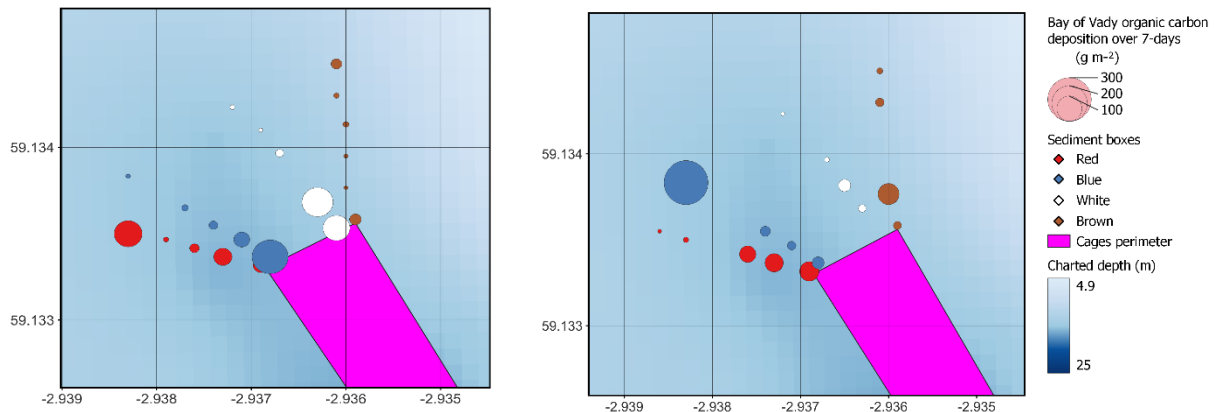


Figure 57: Mean deposition of organic carbon at Bay of Vady as estimated from seven-day deployments of sediment boxes. The surface area of the circles is proportional to the mean POC deposited based on triplicate analyses from the sediment boxes.

4.1.7. Comparison between measured variables at Bay of Vady

Because the positions of the sediment boxes and benthic grabs were not coincident it is not possible to compare the estimated carbon deposition rate with indices of benthic impact for Bay of Vady. For subsequent work at Quanterness and Bay of Meil, the sampling design was changed to allow such intercomparisons to be made.

4.1.8. Modelling organic waste dispersal at Bay of Vady using NewDEPOMOD

Using the SEPA defaults, no RMSE could be computed because all the waste particles were moved completely out of the model domain during both 7-day periods corresponding to sediment box deployments. These issues with more dispersive sites are known and possible approaches discussed in SEPA (2019a) and SRSL (2021).

To produce a depositional footprint, critical shear stress (τ_{ECrit}) had to be set to 20. Further adjustments of remaining parameters listed in Table 16 only led to marginal improvements in model fit as measured by the RMSE. The following combinations of parameter values yielded four models with the lowest RMSE.

Table 16: Parameter values for four best fit NewDEPOMOD models at Quanterness using the full current meter data (that is without the tidal residual current removed). Parameter names in NewDEPOMOD: Resusp height (Transports.BedModel.releaseHeight.height); Hydraulic rough (Transports.bottomRoughnessLength.smooth); Crit stress (Transports.BedModel.tauECritMin); Layer mass (Transports.BedModel.dLayerMass); Horizontal bed dispersion (Transports.suspension.walker.dispersionCoefficient X and Y).

	Model			
	4	3	2	1
RMSE	58.9072	58.3129	58.0517	57.6057
Resusp height	0	0	0.12	0.12
Hydraulic rough	1	1	1	1
Crit stress	20	20	20	20
Layer mass	5	5	5	20
Dispersion	0.1	0.1	0.1	0.1

Because there were only marginal differences between the fits of the four models, results from just the best-fit (model 1) are shown (Figure 58).

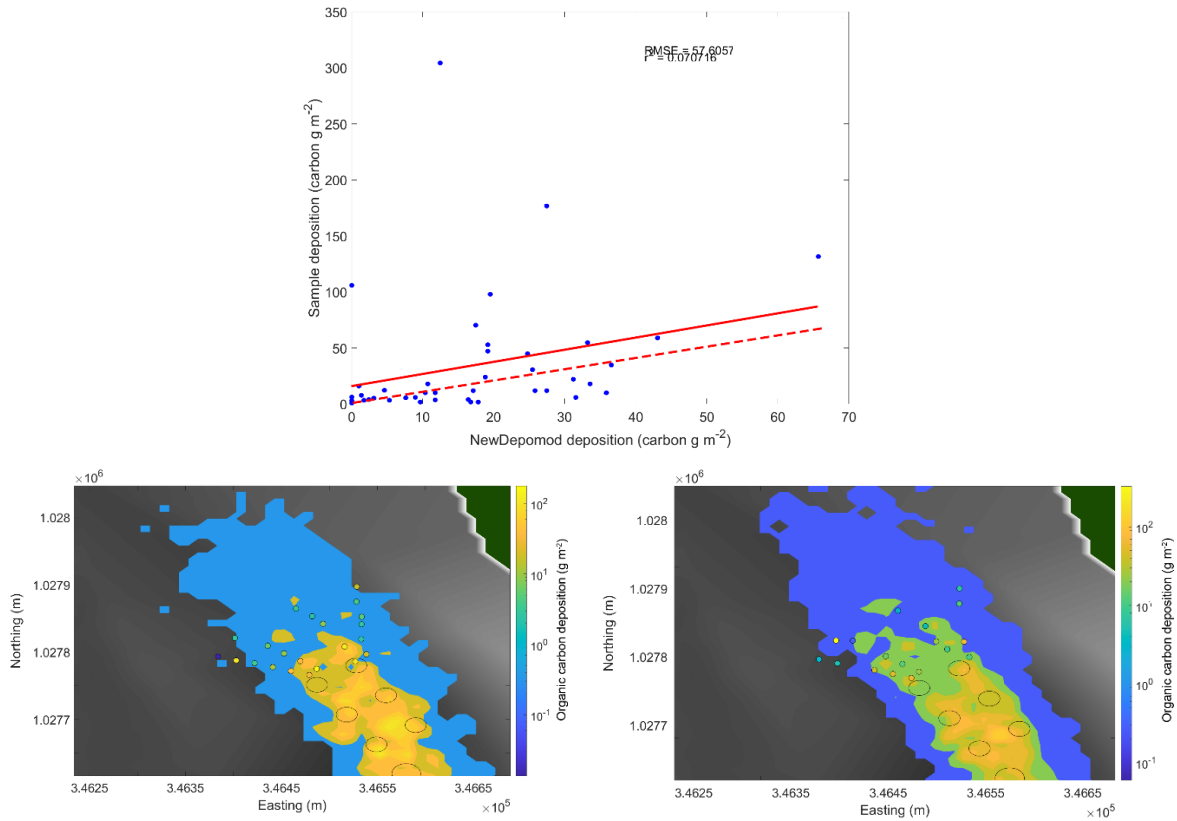


Figure 58: Best fit model results for Bay of Vady. Top panel: Scatterplot of model predictions matched against estimated organic carbon deposition in the sediment boxes across both tidal state deployments. Dashed red line is a 1:1 relationship, solid red line is the RMSE fit. Lower panels: NewDEPOMOD predicted footprint (model 1) as contours; Filled circles show the estimated carbon deposition in the sediment boxes plotted on the same colour scale. Lower left: Deployment 'a' (neap tide) Lower right: Deployment 'b' (spring tide). The organic carbon deposition scale is logarithmic to cover the 'exponential' decline in organic carbon deposition values with distance from the cages.

The contour plots show that adjusting critical shear stress (τ_{ECrit}) has constrained the particles to be under and close to the fish farm cages. The model footprint does now extend somewhat further to the north and there is a little more dispersion in under spring versus neap tides, as expected from consideration of the water current patterns. However, the extension of organic carbon deposition declines too rapidly with distance in the model predictions, particularly along the furthest west transect, suggesting that the resuspension and redistribution processes have not been fully captured in the model.

4.2. *Quanterness field study results*

4.2.1. *Sediment particle size from syringe cores collected at Quanterness*

The results from particle size analyses of sediment samples collected using syringe cores at Quanterness are given in Appendix 9. Overall, the sediments were dominated by fine sands ($45.5\% \pm 17.7\%$, mean \pm std dev., $n = 26$) and very fine sands ($17.7\% \pm 4.1\%$, mean \pm std dev., $n = 26$). The percentage of coarse sand was a little higher along the green (westerly) and brown (northerly) transects (averaging 7.9 – 9.0% respectively cf less than 4.6% in the blue and red transect samples). The percentage of silt was also a little higher in green transect samples (24.5% cf less than 13.5% along the other transects). The maximum percentage of clay size particles was only 3.3% and occurred 40 m out from the cages in the south-west direction (green transect).

Visual inspection confirmed that the seabed surrounding the farm is comprised of mainly sand with occasional whole shells and shell fragments (*Figure 59*). Patches of attached and loose macroalgae were also observed on the video. The seabed appears relatively flat without evidence of significant rippling.

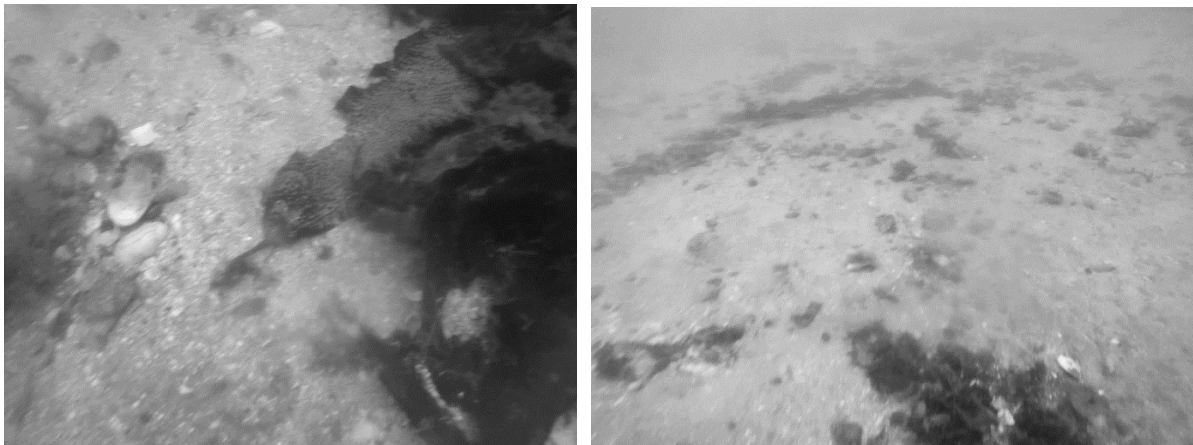


Figure 59: Images of the seabed at Quanterness from video captured by diver on 14th Dec 2021, approximately 30 to 50 m southwest of the cages.

4.2.2. *Sediment POC from syringe cores collected at Quanterness*

Results for the analysis of particulate organic carbon in the sediment core samples collected at Quanterness are given in Appendix 10. There was no evidence of high levels of organic enrichment in the sediments at the Quanterness site. The maximum value ($1.3 \pm 0.04\%$, mean \pm SD) was observed along the Green transect although there was slight enrichment in cores taken nearer to the cages along the blue and red transects (*Figure 60*).

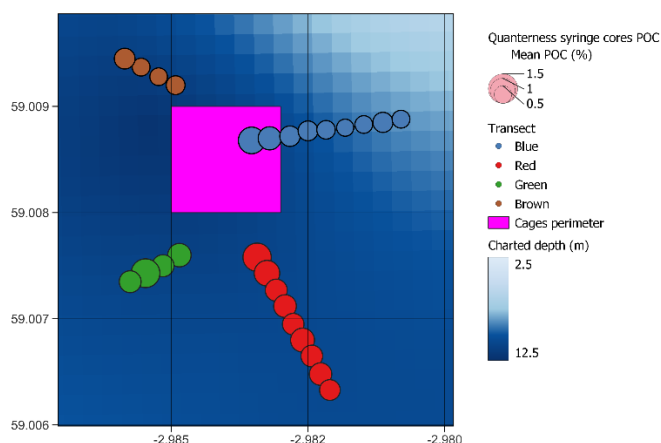


Figure 60: Sediment particulate organic carbon (POC) at Quanterness. The surface area of the circles is proportional to the mean POC as a dry weight percentage based on analysis of duplicate syringe cores collected adjacent to each sediment sampling box.

4.2.3. Sulphides from syringe cores collected at Quanterness

Results for the analysis of sulphide in syringe cores collected at Quanterness are given in Appendix 11. Twenty-seven out of 52 syringe cores contained more than 20% overlying seawater and results from those samples should be treated with caution. The coefficients of variance of most of the sample means were less than 20% (Figure 61).

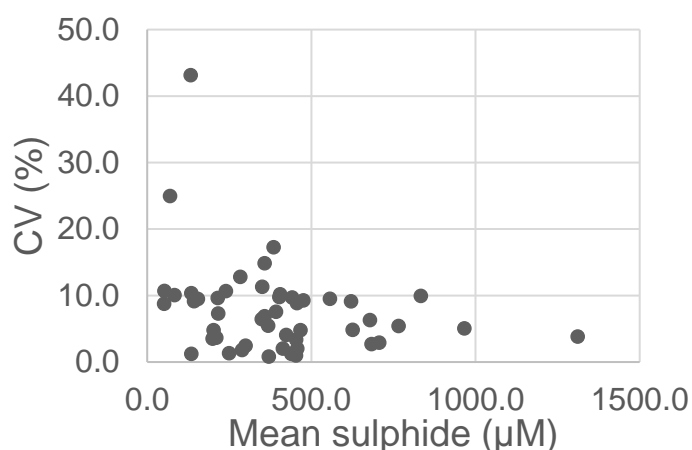


Figure 61: Relation between coefficient of variance (CV) and mean sulphide for replicated measurements on syringe cores collected at Quanterness.

Considering all the samples, the highest level of sulphide was 1,311 μM detected in the core taken from the Blue transect, deployment 'a' during neap tides (Note, this sample had a high percentage of overlying seawater). Sulphide levels during the spring tide deployment were slightly lower with a maximum of 834 μM at 20 m from the cage edge along the Red transect. Considering all the samples (including those with large amounts of overlying seawater in the syringe core), there was a trend for the highest levels of sulphide to occur in the syringe core samples collected close to the cages during neap tides but for the maxima to be shifted further away from the cages during the spring tides. Despite the presence of overlying seawater in many of the cores, the data do appear to make sense in terms of the likely pattern of organic waste deposition at this site.

Sulphides were also subsequently measured in benthic grabs collected at this site for SEPA monitoring, providing additional estimates of sediment sulphide concentrations.

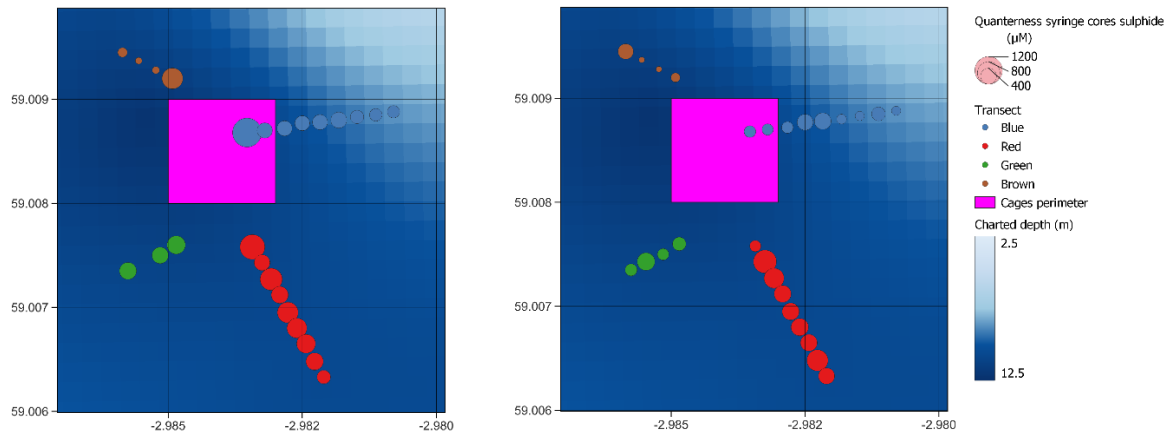


Figure 62: Sulphide levels measured in syringe cores collected at Quanterness. The surface area of the circles is proportional to the mean sulphide (μM) based on triplicate analyses of each syringe core (one core per location). Note that all syringe core data have been presented, including measurements derived from cores with more than 20% over overlying seawater.

4.2.4. Sediment eDNA from syringe cores collected at Quanterness

The eDNA results are the subject of a separate PhD thesis and are not commented on further here.

4.2.5. Benthic grabs collected at Quanterness

The results from the visual assessment of the benthic grab samples are shown in Table 17.

Table 17: Visual appearance of surficial sediments collected at Quanterness by benthic grab

Grab	Transect	Distance from cage edge	Grab content	Consistency	Colour	H ₂ S	Beggiatoa	Faeces	Pellets
		(m)	(%)						
T3EE01	Blue	0	80	Fine sand	Mid-brown	N	N	N	N
T3EE02		44	80	Fine sand	Mid-brown	N	N	N	N
T3EE03		98	80	Fine sand	Mid-brown	N	N	N	N
T3EE04		118	80	Fine sand	Mid-brown	N	N	N	N
T3EE05		167	80	Fine sand	Mid-brown	N	N	N	N
T3EE06		200	80	Fine sand	Mid-brown	N	N	N	N
T3EE07		253	80	Fine sand	Mid-brown	N	N	N	N
T2SE01	Red	0	80	Fine sand	Mid-brown	N	N	N	N
T2SE02		60	80	Fine sand	Mid-brown	Y	N	N	N
T2SE03		111	80	Fine sand	Mid-brown	Y	N	N	N
T2SE04		165	80	Fine sand	Mid-brown	N	N	N	N
T2SE05		217	80	Fine sand	Mid-brown	N	N	N	N
T2SE06		275	80	Fine sand	Mid-brown	N	N	N	N
T2SE07		319	80	Fine sand	Mid-brown	N	N	N	N
T4W01	Green	0	60	Coarse sand, broken shell	Mid-brown	N	N	N	N
T4W02		36	60	Coarse sand, broken shell	Mid-brown	N	N	N	N
T4W03		58	60	Coarse sand, broken shell	Mid-brown	N	N	N	N
T4W04		90	60	Coarse sand, broken shell	Mid-brown	N	N	N	N
T4W05		102	60	Coarse silty sand, bits shell	Mid-brown	N	N	N	N
T4W06		122	60	Coarse sand, bits shell	Mid-brown	N	N	N	N
T4W07		173	60	Coarse sand, bits shell	Mid-brown	N	N	N	N
T1NN01	Brown	0	80	Coarse sand	Mid-brown	N	N	N	N
T1NN02		33	60	Coarse sand	Mid-brown	N	N	N	N
T1NN03		48	80	Coarse sand	Mid-brown	N	N	N	N
T1NN04		66	60	Coarse sand	Mid-brown	N	N	N	N
T1NN05		92	60	Coarse sand	Mid-brown	N	N	N	N
T1NN06		123	80	Coarse sand	Mid-brown	N	N	N	N
T1NN07		155	80	Coarse sand	Mid-brown	N	N	N	N

The visual assessments of sediment consistency are consistent with results from the particle size analyses (Section 4.2.1), being mainly fine and very fine sands but with an increased percentage of coarser grades moving to the southwest and north from the cages (Green and Brown transects). This clearly affected the grab sampling as grab contents were often lower in green and brown transect samples. There was no variability in visual colour between the samples. An odour of hydrogen sulphide was only noted in two samples from the red transect.

Carbon loss on ignition (LOI) was extremely low at all stations being between 1.30 – 3.94% on a dry weight basis.

4.2.6. Sulphides from benthic grabs collected at Quanterness

The results of the sulphide measurements from the Quanterness benthic grabs are reported in Appendix 12. Coefficients of variance were generally better than 60% but were poorer for low sulphide samples (Figure 63). This is not unexpected as the lowest levels were below the lower calibration point (100 µM). Because of time constraints the sulphide means were only based on duplicate, as opposed to triplicate analyses. Increasing the number of replicate analyses on each sample would likely reduce the CVs but the mean results were considered to be of acceptable quality because of the large range in the data.

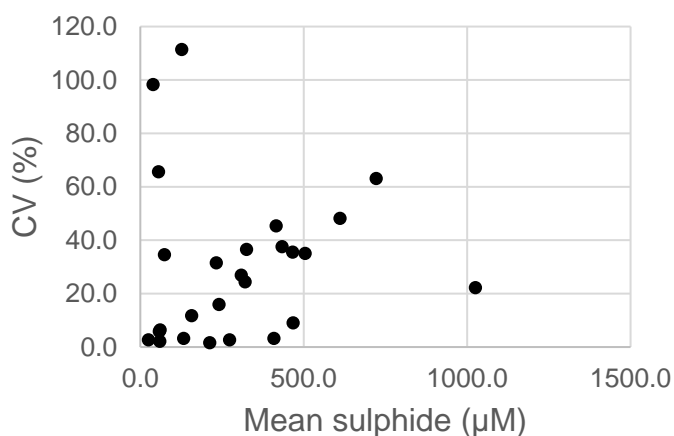


Figure 63: Relation between coefficient of variance (CV) and mean sulphide for replicated measurements on benthic grab samples collected at *Quanterness*.

At the reference sites (509 and 503 m from the nearest cage edge), mean sulphide levels were 68.8 ± 18.5 (mean \pm std dev) and 141.9 ± 14.4 μM .

The mean sulphide data around the farm are mapped in Figure 64. The highest levels of 1,025 and 722 μM were recorded close to the cages on the Red and Blue transects respectively. Levels of sulphide generally declined moving away from the cages reaching levels of less than 150 μM in the furthest distant grabs, apart from along the green transect where levels were above 240 μM .

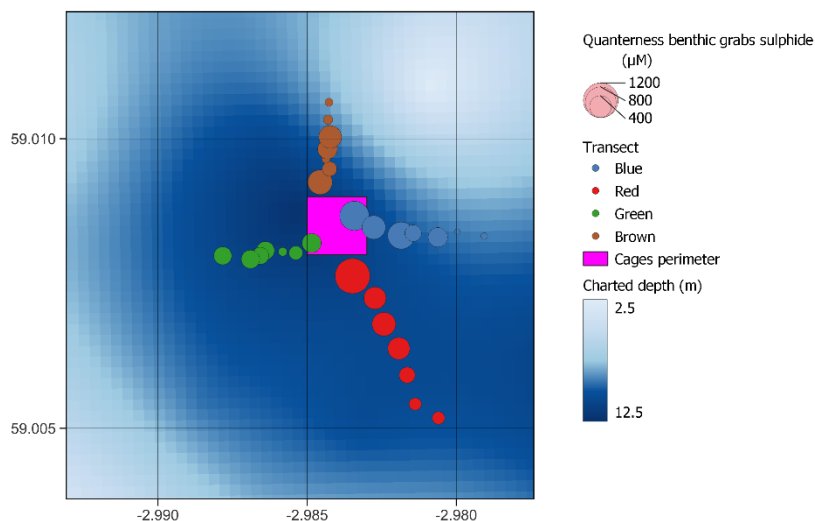
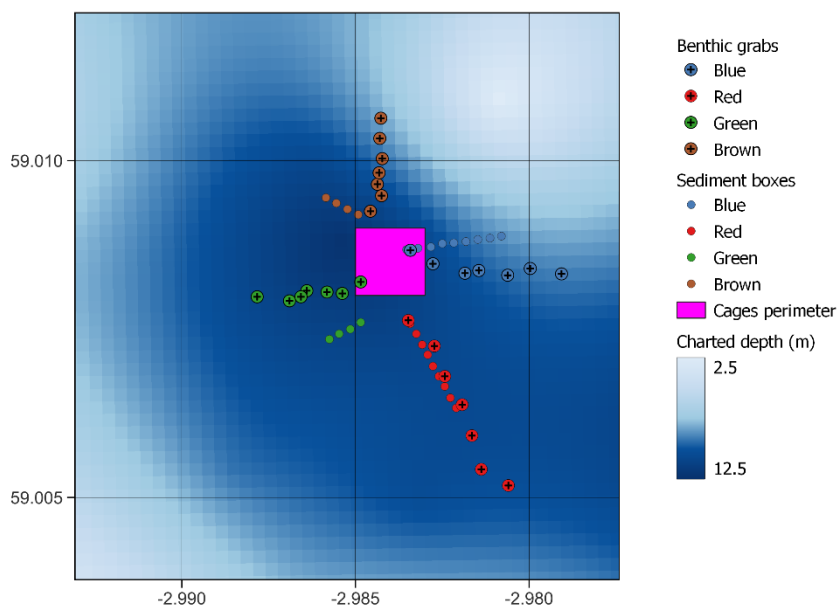


Figure 64: Mean sulphide levels as measured in benthic grabs collected at *Quanterness*. Reference site results not shown to allow zooming into the immediate farm results.

The locations of the sediment boxes and benthic grabs were approximately coincident, so it seems reasonable to compare measurements made along the four transects (Figure 65).



*Figure 65:
Comparison of the
locations of the
sediment boxes and
benthic grab samples
at Quanterness.*

Comparing the sulphide measurements based on syringe cores and benthic grabs (Figure 66) showed reasonable agreement, despite the concerns about the amount of overlying seawater in many of the syringe cores. For the transects with higher sulphide maxima (Blue and Red), sulphide levels close to the cages were in good agreement when measured in cores collected during neap tides (deployment a) and from benthic grabs (during spring tides). However, sulphide levels close to the cages were lower in cores collected during spring tides (deployment b). These differences could be due to rapid changes in anaerobic activity related to differences in the near-bed water speeds during spring, compared with neap tides (Figures 33 & 34) as near-bed water speed will affect the degree of benthic oxygenation, and thus levels of anaerobic microbial activity. On the other hand, some of the sulphide measurements from the syringe cores may have been affected by the high volumes of overlying water in many of the samples.

Despite these issues with sampling, a general pattern of periods of elevated sulphides close to the cages, particularly on the Blue and Red transects, with a decline with distance from the cages is apparent. When compared with the levels measured at the Reference sites ($< 150 \mu\text{M}$), the sulphides data also suggest some degree of elevation up to 200 m from the cages' perimeter.

A hydrogen sulphide smell was only noted at two of the Red transect benthic grabs during SEPA-monitoring sampling. In contrast, analytical measurement showed elevated sulphide concentrations on both Blue and Red transects.

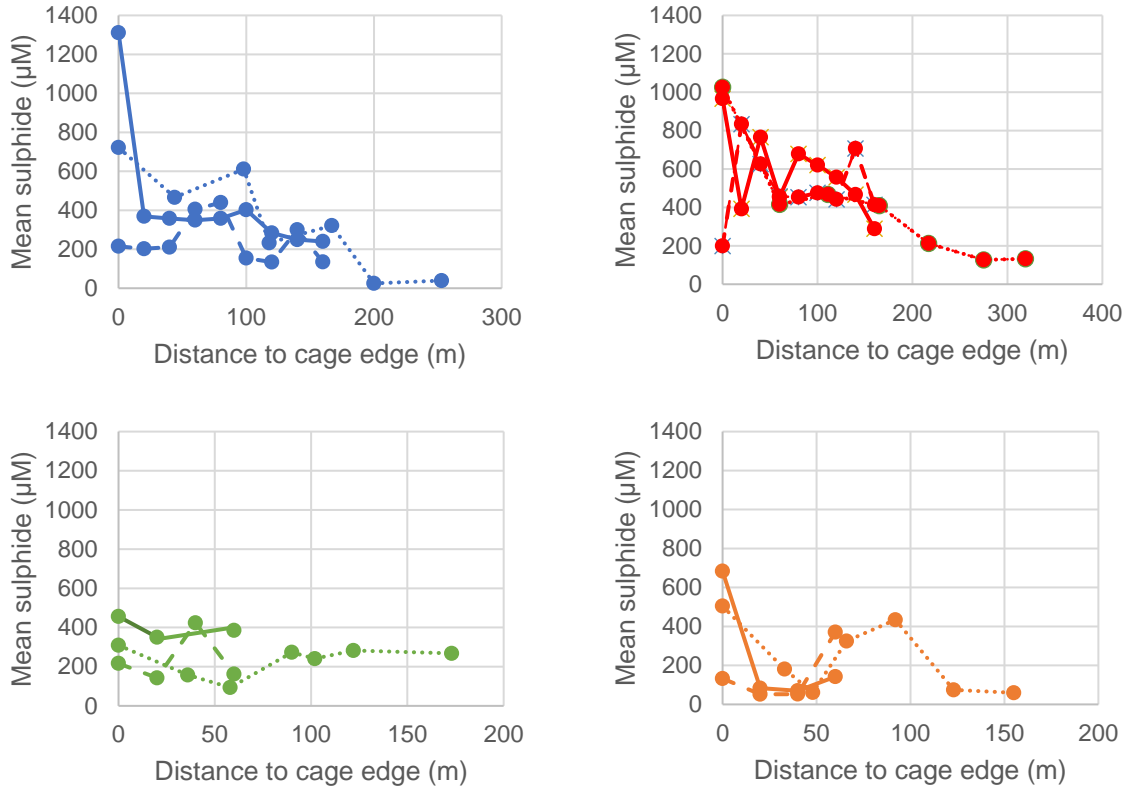


Figure 66: Comparisons of the mean sulphide levels measured along the sampling transects at Quanterness. Solid line is measurements from deployment 'a' neap-tide syringe cores, dashed line is measurements from deployment 'b' spring tide syringe cores, dotted line is measurements from benthic grabs.

4.2.7. Faunal analyses from benthic grabs collected at Quanterness

A more complete discussion of the macrofaunal analyses, including more detail on the species recorded, can be found in the report prepared by FishVet Gp. and submitted to SEPA by Cooke Aquaculture. A summary of the infaunal results is shown in Table 18.

Results from the Blue (easterly) transect showed evidence of enrichment at the cage edge apparent as lower taxa richness and elevated densities of enrichment polychaetes. Univariate indices all indicated poorer conditions out to EE03 (98 m) but improved conditions further away from the cages. IQI scores classed EE01 (cage edge) and EE02 (44 m from cage edge) as 'Poor', EE03 (98 m from cage edge) as 'Moderate' and further out as 'Good' or 'High'.

Faunal results from the Red (south-easterly) transect showed evidence of enrichment at the cage edge with a low number of taxa but at high abundance. Impact was also evident at 60 m where the enrichment tolerant *Capitella* sp., dominated. At SE03 (111 m) and SE04 (165 m), species numbers and community indices showed some recovery whilst further out taxa richness and community indices were higher. Based on IQI, the first two grabs along the transect were classified as 'Bad' or 'Poor' with the next immediate grab out (111 m) having a 'Moderate' status.

Results from the Green (westerly) transect generally had higher taxa with moderate abundance. Excluding WW04, indices were indicative of good conditions with Margalef's richness index above 11, Pielou's evenness index above 0.7 and the Shannon-Wiener index above 5. In

contrast, WW04 (90 m from the cage edge) had lower indices and a high proportion of *Capitella* sp. indicative of enrichment. Based on IQI, status was 'Moderate' at the cage edge but 'Poor' status at 90 m out.

Results from the Brown (northerly) transect were quite variable with little obvious pattern with distance. At NN04 (66 m from cage edge) an elevated abundance of *Capitella* sp., was noted, but more in one than the other replicate grab samples. This variability could reflect the slightly coarser sediment composition resulting in more patchiness. All grabs along the Brown (northerly) transect were ranked as 'Good' or 'High' condition according to IQI apart from station NN04 which was 'Moderate'.

Overall, apart from a few anomalous results from mid-transect points on the Green (westerly) and Brown (northerly) transects, the faunal results suggest that the depositional footprint at Quanterness is heavily skewed towards the east and particularly the southeast.

Table 18: Results of enhanced benthic monitoring at Quanterness, sampled on 3rd July 2019. *S* = Number of taxa, *N* = Abundance, *d* = Margalef's richness index, *J'* = Pielou's evenness index, *H' log2* = Shannon-Wiener index, *EP* = Number of enrichment polychaete species (ITI taxa list); *EP density* = density of enrichment polychaete species (ITI taxa list); *ITI* = Infaunal Trophic Index; *IQI* = Infaunal Quality Index (ver 4); *EP spp(IQI)* = Number of enrichment polychaete species (IQI taxa list); *EP density (IQI)* = Density of enrichment polychaete species (IQI taxa list); Sulphide = Mean sulphide results from SAMS on-site analysis of benthic grab samples.

Station	Transect	Distance from cage edge (m)	S	N	d	J'	H' log2	EP spp (ITI)	EP density (ITI) (m ⁻²)	ITI	IQI	Eco Status	Sulphide (µM)
EE01	Blue	0	22	628	3.26	0.12	0.52	2	6610	2.98	0.276	Poor	721.9
EE02	Blue	44	24	1027	3.32	0.09	0.42	2	10943	2.44	0.269	Poor	466.3
EE03	Blue	98	29	182	5.38	0.54	2.61	2	1767	20.68	0.449	Mod	611.4
EE04	Blue	118	44	178	8.30	0.80	4.35	1	367	52.28	0.695	Good	232.8
EE05	Blue	167	80	619	12.29	0.74	4.69	3	333	67.86	0.741	Good	321.2
EE06	Blue	200	50	182	9.42	0.86	4.83	1	11	72.01	0.728	Good	24.9
EE07	Blue	253	65	230	11.77	0.85	5.14	1	11	73.01	0.788	High	39.1
SE01	Red	0	19	4181	2.16	0.06	0.27	2	45229	0.31	0.240	Bad	1025.6
SE02	Red	60	13	223	2.22	0.28	1.05	1	2111	7.52	0.263	Poor	415.9
SE03	Red	111	20	37	5.26	0.86	3.70	1	11	50.93	0.639	Mod	467.9
SE04	Red	165	31	96	6.57	0.69	3.41	1	44	57.81	0.714	Good	409.2
SE05	Red	217	72	368	12.02	0.80	4.95	3	67	63.32	0.719	Good	212.8
SE06	Red	275	71	391	11.73	0.78	4.79	2	89	64.08	0.729	Good	127.0
SE07	Red	319	41	186	7.65	0.83	4.42	2	44	63.79	0.657	Good	132.8
WW01	Green	0	83	304	14.34	0.78	4.94	1	422	42.82	0.633	Mod	309.2
WW02	Green	36	69	320	11.79	0.80	4.88	4	67	68.56	0.720	Good	157.3
WW03	Green	58	102	527	16.12	0.80	5.36	2	267	69.56	0.788	High	61.0
WW04	Green	90	40	689	5.97	0.21	1.11	4	6777	9.13	0.326	Poor	273.1
WW05	Green	102	79	527	12.45	0.78	4.91	3	744	61.57	0.718	Good	240.8
WW06	Green	122	60	215	10.99	0.84	4.97	0	0	71.39	0.777	High	282.5
WW07	Green	173	98	396	16.22	0.82	5.46	2	189	69.68	0.797	High	267.7

Table 18: Results of enhanced benthic monitoring at Quanterness, sampled on 3rd July 2019. *S* = Number of taxa, *N* = Abundance, *d* = Margalef's richness index, *J'* = Pielou's evenness index, *H' log2* = Shannon-Wiener index, *EP* = Number of enrichment polychaete species (ITI taxa list); *EP density* = density of enrichment polychaete species (ITI taxa list); *ITI* = Infaunal Trophic Index; *IQI* = Infaunal Quality Index (ver 4); *EP spp(IQI)* = Number of enrichment polychaete species (IQI taxa list); *EP density (IQI)* = Density of enrichment polychaete species (IQI taxa list); *Sulphide* = Mean sulphide results from SAMS on-site analysis of benthic grab samples.

Station	Transect	Distance from cage edge (m)	S	N	d	J'	H' log2	EP spp (ITI)	EP density (ITI) (m ⁻²)	ITI	IQI	Eco Status	Sulphide (µM)
NN01	Brown	0	59	256	10.46	0.81	4.79	4	111	61.05	0.675	Good	504.3
NN02	Brown	33	45	144	8.85	0.87	4.80	1	11	73.01	0.707	Good	180.9
NN03	Brown	48	103	346	17.45	0.85	5.67	1	11	76.62	0.877	High	58.5
NN04	Brown	66	48	421	7.78	0.57	3.16	1	2166	33.18	0.539	Mod	325.1
NN05	Brown	92	69	277	12.09	0.78	4.74	1	67	67.4	0.663	Good	434.0
NN06	Brown	123	71	438	11.51	0.72	4.43	1	89	71.52	0.671	Good	74.2
NN07	Brown	155	79	464	12.70	0.79	4.98	1	33	77.23	0.740	Good	55.9

4.2.8. Carbon flux from sediment boxes deployed at Quanterness

The results from the estimates of organic carbon deposited into the sediment boxes deployed at Quanterness are given in Appendix 13. Overall, there were fewer failures in recovery of sediment boxes compared with the Bay of Vady deployments although one box during the neap tide deployment, and four boxes during the spring tide deployment were not found. In addition, sediment boxes from the red transect at 160 m from the cage edge were recovered, but in both deployments were largely empty of sediment which seems to have been washed out at this location. The red transect was aligned with the strongest near-bed water current direction at this site (Figure 37) and this, combined with the proximity to the adjacent shallower depths might explain why most of the sediment added to these boxes seemed to have been washed away.

Compared with Bay of Vady, the maximum estimated organic carbon deposition was lower at Quanterness at 55 g m^{-2} deposited over 7-days (Figure 67). Under neap tides the highest deposition was estimated to be occurring within 20 m of the cage edge along the blue and red transects but there was evidence of slightly elevated deposition at around 40 m along the brown and green transects. During deployment 'b' (spring tides) material appeared to be moved further afield, especially along the blue and red transect directions although the maximum rate of deposition still occurred at the start of the blue transect (38.6 g m^{-2}).

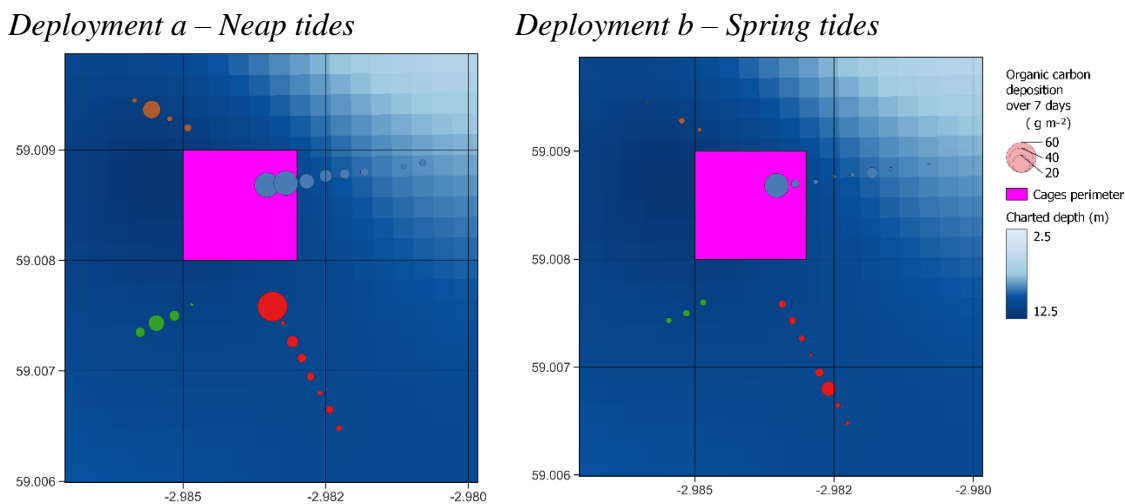


Figure 67: Mean deposition of organic carbon at Quanterness as estimated from seven-day deployments of sediment boxes. The surface area of the circles is proportional to the mean POC deposited based on triplicate analyses from the sediment boxes.

4.2.9. Comparison between measured variables at Quanterness

Relationships between the measured variables were compared along each transect with the IQI as determined from the benthic grabs (Figures 68 & 69). Note that the IQI colour band transitions are shown at the distance that a different IQI status occurred, because it is not known where the transition point would have been located between sampling points. The transition between states could thus occur closer to, but not further from the cage edge than indicated. It must also be born in mind that the location of the measurements made on sediment cores, boxes and from benthic grabs were not completely aligned (Figure 65). Therefore, some of the differences between the patterns within and between the variables could be due to fine-scale

spatial heterogeneity. Where results were determined from samples collected during neap and spring tides (sediment boxes and syringe cores), the results from each deployment were also averaged on the basis that this will likely represent the parameter over a whole tidal cycle.

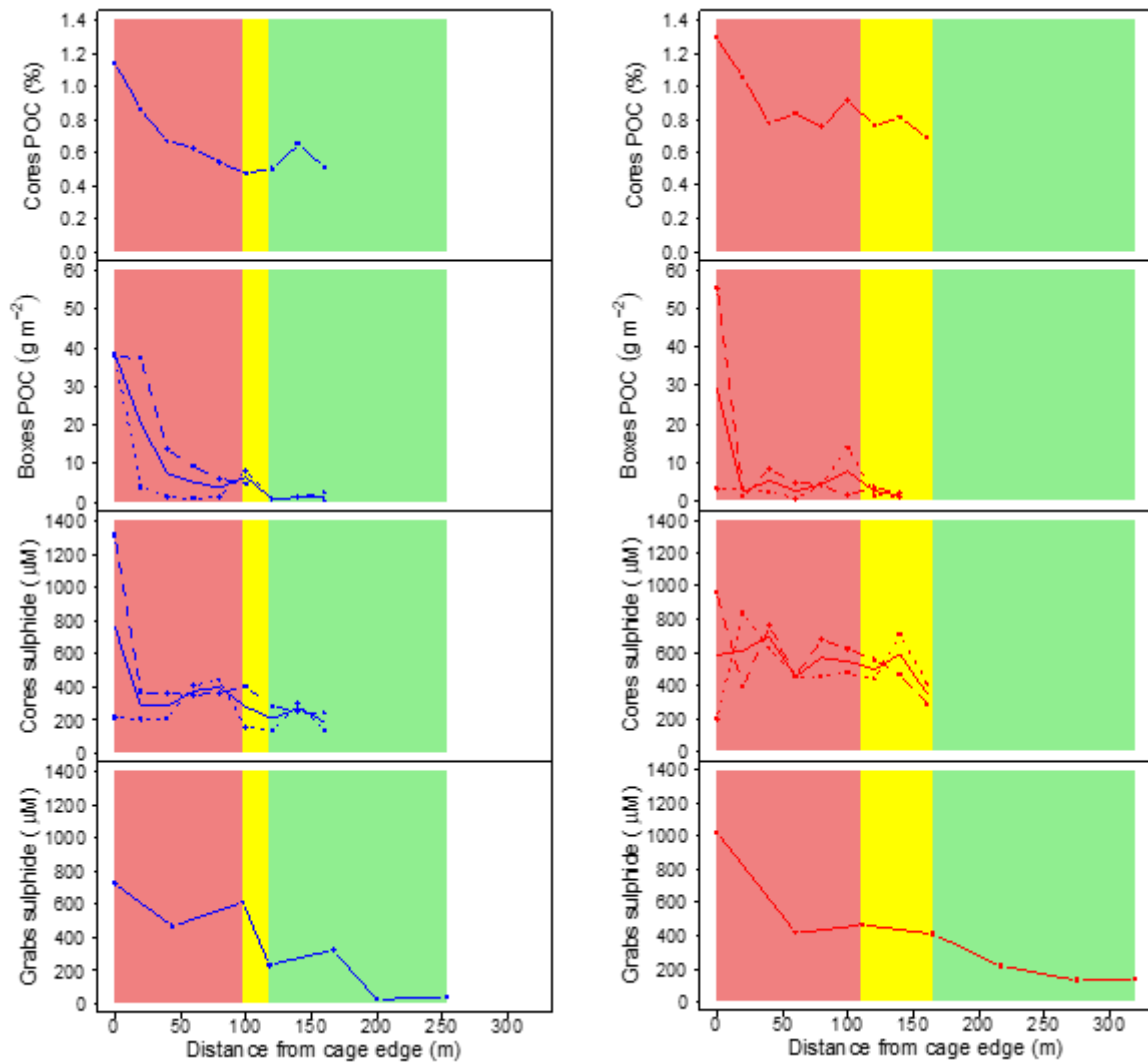


Figure 68: Comparison of measured parameters along the Blue easterly (left column) and Red south-easterly (right column) transects at Quanterness. Mean POC measured from syringe cores (top row); Estimated POC deposited into sediment boxes during the 7-day deployments (second row down); Mean sulphide measured in syringe cores (third row down); Mean sulphide measured from benthic grabs (bottom row). Where two deployments were made, dashed lines indicate deployment 'a' (neap tide) and dotted line deployment 'b' (spring tide), the solid line is the average of the results from deployment 'a' and deployment 'b'. The background shading indicates the IQI status of the benthic grab samples (red indicates 'Poor' or 'Bad', yellow indicates 'Moderate' and green indicates 'Good' or 'High' IQI status).

Despite the caveats regarding sample locations, the results confirm that the largest impacts occurred along the Blue (easterly) and Red (south-easterly) depositional axes with the impacts of enrichment as assessed by IQI extending a little further out along the south-easterly direction. Along these two axes, there seemed to be a good relationship between the IQI status as determined from the benthic grabs and the other measured parameters (Figure 68). Thus, sediment POC, estimated tidally averaged POC deposition into the sediment boxes and tidally

averaged sulphide levels measured in cores and grabs all declined with distance from the cage edge, and this appears to be reflected in the improving IQI status.

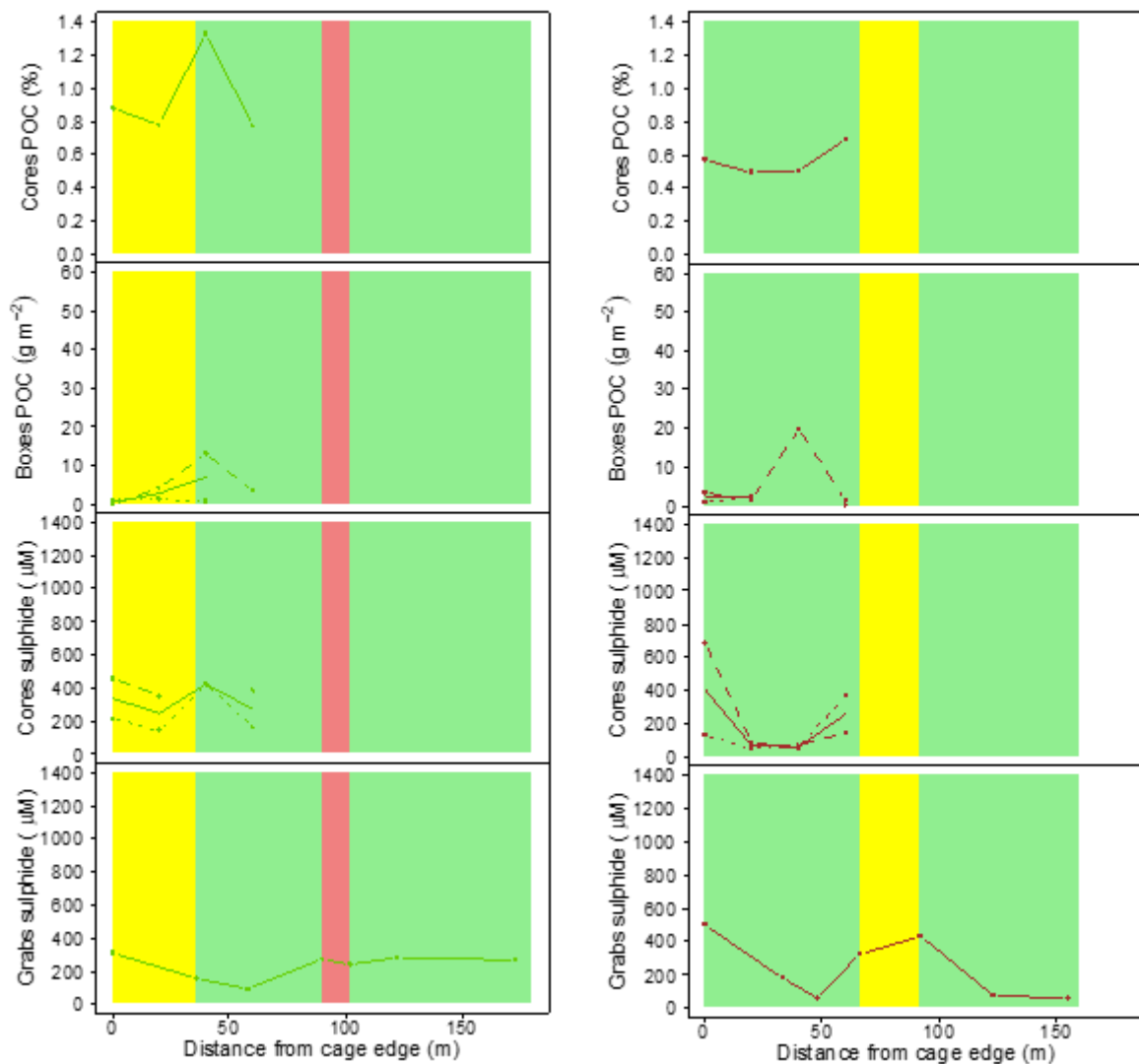


Figure 69: Comparison of measured parameters along the Green westerly (left column) and Brown northerly (right column) transects at Quanterness. Mean POC measured from syringe cores (top row); Estimated POC deposited into sediment boxes during the 7-day deployments (second row down); Mean sulphide measured in syringe cores (third row down); Mean sulphide measured from benthic grabs (bottom row). Where two deployments were made, dashed lines indicate deployment 'a' (neap tide) and dotted line deployment 'b' (spring tide), the solid line is the average of the results from deployment 'a' and deployment 'b'. The background shading indicates the IQI status of the benthic grab samples (red indicates 'Poor' or 'Bad', yellow indicates 'Moderate' and green indicates 'Good' or 'High' IQI status).

The relationship between IQI and other variables was less clear along the Green and Brown sampling transects, although this may have been affected by the lower number of syringe cores and sediment boxes in these directions. Compared with the Blue and Red transects, estimated organic carbon deposition rates close to the cage edge were lower, and sulphides less elevated.

This appears to be reflected in the IQI scores which indicated generally lower impacts along these two directions.

4.2.10. Modelling organic waste dispersal at *Quanterness* using *NewDEPOMOD*

Using the SEPA defaults, no RMSE could be computed because all the waste particles were moved completely out of the model domain during both 7-day periods corresponding to sediment box deployments. Likewise, removal of the tidal residual current resulted in a failure of the model to produce a depositional footprint. Consequently, no depositional footprint could be established using the recommended default settings, but these issues with more dispersive sites are known and possible approaches discussed in SEPA (2019a) and SRSL (2021).

To produce a depositional footprint, critical shear stress (*tauECrit*) had to be set to 2 or 20. Further adjustments of remaining parameters listed in Table 19 only led to marginal improvements in model fit as measured by the RMSE. The following combinations of parameter values yielded four models with the lowest RMSE using the full current meter data i.e., without the tidal residual current removed.

Table 19: Parameter values for four best fit NewDEPOMOD models at Quanterness using the full current meter data (that is without the tidal residual current removed). Parameter names in NewDEPOMOD: Resusp height (Transports.BedModel.releaseHeight.height); Hydraulic rough (Transports.bottomRoughnessLength.smooth); Crit stress (Transports.BedModel.tauECritMin); Layer mass (Transports.BedModel.dLayerMass); Horizontal bed dispersion (Transports.suspension.walker.dispersionCoefficient X and Y).

	Model			
	4	3	2	1
RMSE	9.1276	9.1536	9.1085	9.0552
Resusp height	2	1	0.44	2
Hydraulic rough	0.000001	0.001	0.001	0.000001
Crit stress	20	2	20	20
Layer mass	130	3375	3375	5
Dispersion	0.5	0.2	0.1	0.2

Because there were marginal differences between the fits of the four models, only results from the best-fit (model 1) are shown (Figure 70).

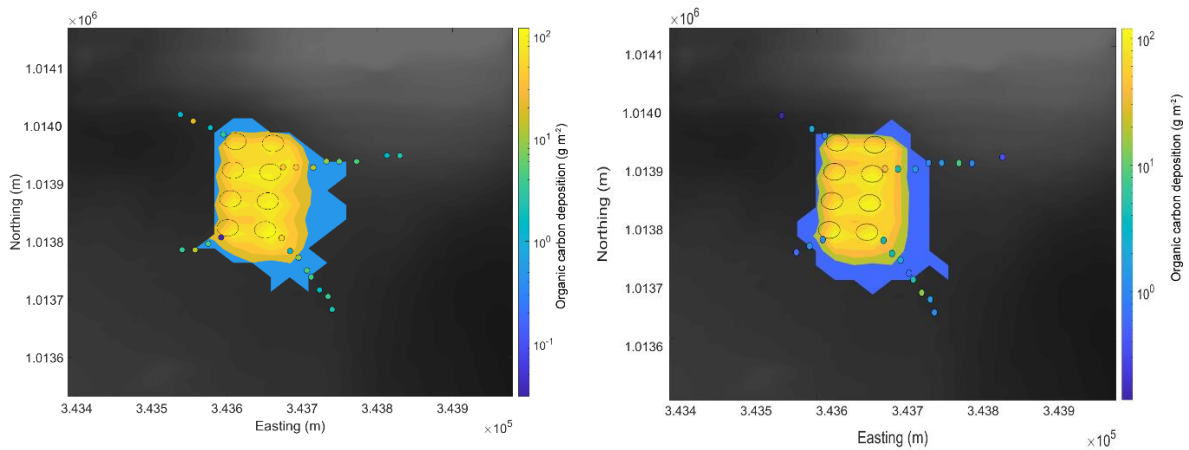
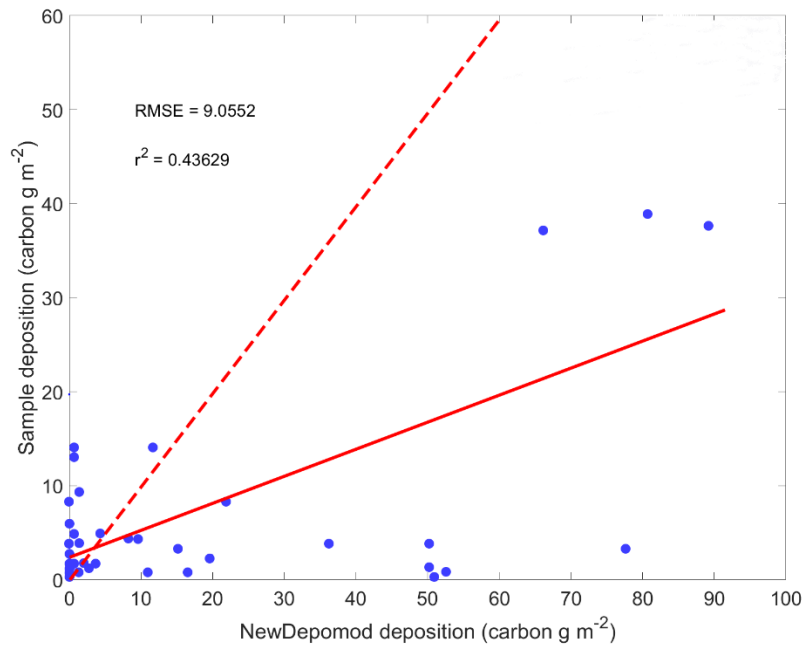


Figure 70: Best fit model results for *Quanterness*.

Top panel: Scatterplot of model predictions matched against estimated organic carbon deposition in the sediment boxes across both tidal state deployments. Dashed red line is a 1:1 relationship, solid red line is the RMSE fit.

Lower panels: NewDEPOMOD predicted footprint (model 1) as contours; Filled circles show the estimated carbon deposition in the sediment boxes plotted on the same colour scale. Lower left: Deployment 'a' (neap tide) Lower right: Deployment 'b' (spring tide). The organic carbon deposition scale is logarithmic to cover the 'exponential' decline in organic carbon deposition values with distance from the cages.

The contour plots show that adjusting critical shear stress (τ_{ECrit}) has constrained the particles to be under and close to the fish farm cages. The model footprint does now extend somewhat further to the east and southeast along the lines of maximum benthic impact as assessed by IQI and expected from consideration of the water current patterns. However, the extension of organic carbon deposition declines too rapidly with distance in the model predictions, particularly towards the east and south-east, suggesting that the resuspension and redistribution processes have not been fully captured in the model.

4.3. Bay of Meil field study results

4.3.1. Sediment particle size from syringe cores

The results from particle size analyses of sediment samples collected using syringe cores at Bay of Meil are given in Appendix 14. There was more variability in the seabed sediment at this site compared with Bay of Vady and Quanerness. Although the mean composition was still dominated by fine ($28.6\% \pm 10.8\%$, mean \pm std dev., $n = 28$) and very fine sands ($32.8\% \pm 13.5\%$, mean \pm std dev., $n = 28$) there was an increasing percentage of coarser sands moving south-easterly along the blue transect, which beyond 30 m from the cage perimeter became bare rock. In contrast, there was a decline in the percentage of coarser sands moving northerly (red transect) away from the cage perimeter. The maximum percentage of clay size particles was 2.6% and occurred 20 m out from the cages in the south-easterly direction (blue transect).

Visual inspection confirmed that the seabed surrounding the farm comprises sands with shell fragments and occasional macroalgae (Figure 71). There is also some evidence of bioturbation activity in the images.

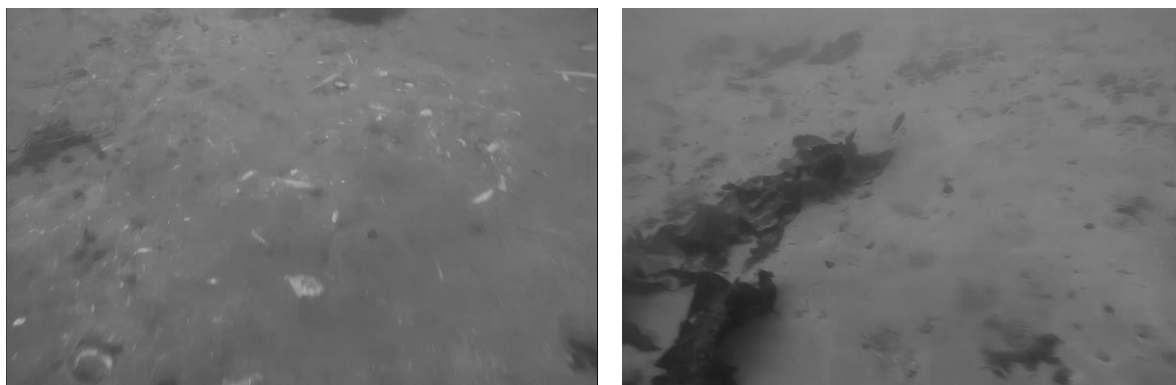


Figure 71: Images of the seabed at Bay of Meil farm site from video captured by diver on 14th Dec 2021, approximately 30 to 50 m south-south-west of the cages.

Sediment composition from syringe cores agreed with those from benthic grabs reported as part of SEPA compliance monitoring in 2021 (Pharmaq Analytiq, 2021). The only benthic grab with notably coarser material was collected at the southerly cage edge, where 5% gravel was noted. A higher percentage of coarse sands were also recorded in the syringe cores taken along the Red (south-easterly) transect out to 10 m from the cage edge.

4.3.2. Sediment POC from syringe cores collected at Bay of Meil

Results for the analysis of particulate organic carbon in the sediment core samples collected at Bay of Meil are given in Appendix 15. Levels of particulate organic carbon (POC) in sediment samples collected adjacent to the sediment boxes were generally low ($< 0.5\%$). POC levels along the Blue (easterly) and Red (southerly) transects were slightly elevated, reaching a maximum of 1.26 ± 0.28 (mean \pm std dev) at the cage edge on the Red transect (Figure 72).

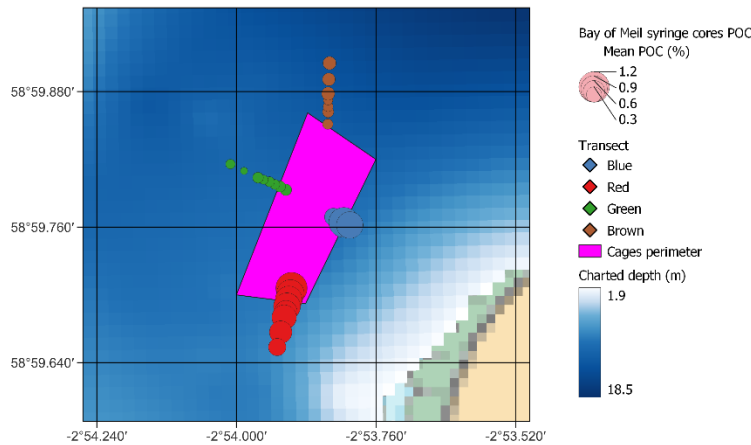


Figure 72: Sediment particulate organic carbon (POC) at Bay of Meil. The surface area of the circles is proportional to the mean POC as dry weight percentage based on analysis of duplicate syringe cores collected adjacent to each sediment sampling box.

4.3.3. Sulphides from syringe cores collected at Bay of Meil

Sulphides could not be measured on site from the syringe cores collected at the Bay of Meil because the SAMS chemist was not allowed on to the site at the time of sampling due to Covid-19 restrictions. Sulphides were therefore only measured in the benthic grab samples collected a little later in the year.

4.3.4. Sediment eDNA from syringe cores collected at Bay of Meil

The eDNA results are the subject of a separate PhD thesis and are not commented on further here.

4.3.5. Benthic grabs collected at Bay of Meil

The results of visual assessment of benthic grabs selected along the expected transect of maximum impact at Bay of Meil are given in Table 20.

Table 20: Visual appearance of surficial sediments collected at Bay of Meil by benthic grab

Grab	Transect	Distance from cage edge (m)	Grab content (%)	Consistency	Colour	H ₂ S	Beggiatoa	Faeces	Pellets
SS00	Red	0	70	Coarse sand	Grey	N	N	N	N
SS28	Red	28	70	Fine sand	Mid-brown	N	N	N	N
SS38	Red	39	70	Fine sand	Mid-brown	N	N	N	N
SS48	Red	50	70	Fine sand	Mid-brown	N	N	N	N
REF1	Yellow		70	Fine sand	Mid-brown	N	N	N	N
REF2	Yellow		70	Fine sand	Mid-brown	N	N	N	N

The visual assessments of sediment consistency are consistent with results from the sediment core particle size analyses (Section 4.3.1), being mainly fine sand but with a small proportion of gravel at the cage edge of the Red (southern) transect. There was no variability in visual colour between the samples, apart from SS00 which had a grey colour. No odour of hydrogen sulphide was noted in any of the samples.

Carbon loss on ignition (LOI) was extremely low on nearly all stations being between 0.97 – 1.81% on a dry weight basis but reached 2.64% in the SS00 sample.

The locations of the sediment boxes and benthic grabs were approximately coincident, so it seems reasonable to compare measurements made along the four transects (Figure 73). The outermost two planned grabs along the Blue transect failed to collect sediment but the attempted positions are shown in Figure 73.

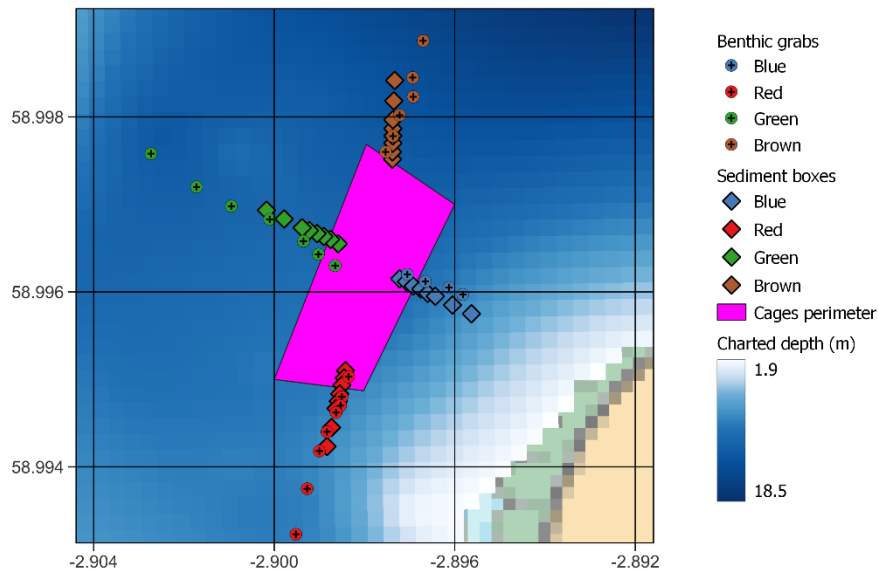


*Figure 73:
Comparison of the
locations of the
sediment boxes and
benthic grab
samples at Bay of
Meil.*

4.3.6. Sulphides from benthic grabs collected at Bay of Meil

The results of the sulphide measurements made on sub-samples collected from the benthic grabs collected at Bay of Meil are reported in Appendix 16.

Coefficients of variance were generally better than 40% but were poorer for low sulphide samples and one higher mean sulphide (Figure 74). This is not unexpected as the lowest levels were below the lower calibration point (100 μM). Because of time constraints the sulphide means were only based on duplicate, as opposed to triplicate analyses. Increasing the number of replicate analyses on each sample would likely reduce the CVs but additional measurements were not possible due to time constraints to analyse the samples within 48 h. Despite this the mean results were of acceptable quality because of the large range in the data.

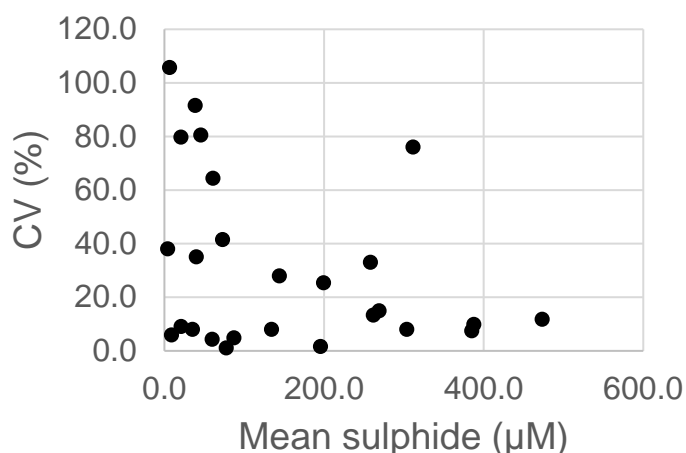


Figure 74: Relation between coefficient of variance (CV) and mean sulphide for replicated measurements on benthic grab samples collected at Bay of Meil.

At the reference sites (> 480 m from the nearest cage edge), mean sulphide levels were 35.3 ± 2.8 (mean \pm std dev) and 20.8 ± 16.6 μM .

The mean sulphide data around the farm are mapped in Figure 75. The highest levels were recorded close to the cages on the Green, Blue and Red transects respectively. Levels of sulphide generally declined moving away from the cages reaching levels of less than 150 μM in the furthest distant grabs, apart from along the Red transect where the furthest grab level was 196 ± 3.1 μM (mean \pm std dev).

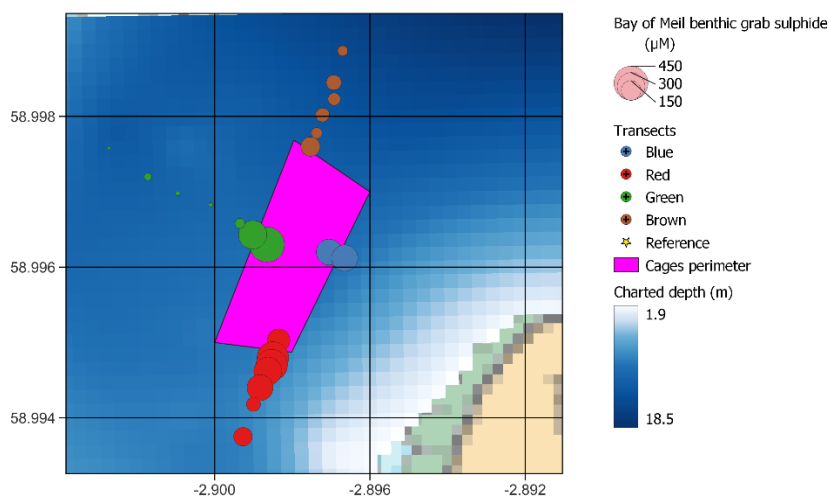


Figure 75: Mean sulphide levels as measured in benthic grabs collected at Bay of Meil. Reference site results not shown to allow zooming into the immediate farm results.

4.3.7. Faunal analyses from benthic grabs collected at Bay of Meil

A more complete discussion of the macrofaunal analyses, including more detail on the species recorded, can be found in the report prepared by Pharmaq Analytic and submitted to SEPA by Cooke Aquaculture. A summary of the infaunal results is shown in Table 21.

Only the first two planned stations along the Blue (easterly) transect could be sampled, further east the ground was reported to be rocky and could not be sampled using a benthic grab. Impact was evident at both stations with a dominance of enrichment tolerant nematodes.

Stations along the Red (southerly) transect showed signs of impact out to 76 m from the cage edge and patchy impact beyond that. Taxa diversity increased beyond 151 m although was still lower than recorded at the reference sites.

Apart from the first two stations, IQI ecological status was 'Good' or 'High' along the Green (westerly) transect. Taxa diversity and number of organisms was comparable to the reference sites although the density of enrichment polychaetes was higher, suggesting some organic deposition was still occurring along this transect.

In a northerly direction (Brown) transect, ecological condition at the cage edge was 'Bad' but was 'Good' or 'High' further out.

The infaunal data suggest benthic impacts are most marked at the cage edge with condition improving rapidly with distance apart from in the south-easterly direction where 'Moderate' conditions occur as far out as 151 m.

The consultants noted that it was difficult to fit a definitive mixing zone ellipse because of the lack of data along the eastern transect. SEPA acknowledge that monitoring organic deposition impacts over rocky areas is a problem and that the benthic grab approach is not suitable in such situations.

Table 21: Results of enhanced benthic monitoring at Bay of Meil, sampled on 30th August and 1st September 2021. S = Number of taxa, N = Abundance, d = Margalef's richness index, J' = Pielou's evenness index, $H' \log_2$ = Shannon-Wiener index, EP = Number of enrichment polychaete species (ITI taxa list); EP density = density of enrichment polychaete species (ITI taxa list); ITI = Infaunal Trophic Index; IQI = Infaunal Quality Index (ver 4); EP spp(IQI) = Number of enrichment polychaete species (IQI taxa list); EP density (IQI) = Density of enrichment polychaete species (IQI taxa list); Sulphide = Mean sulphide results from SAMS on-site analysis of benthic grab samples. Note that where stations were sampled in triplicate, the IQI reported below is based on the first two grabs as required by SEPA.

Station	Transect	Distance from cage edge (m)	S	N	d	J'	$H' \log_2$	EP spp (ITI)	EP density (ITI) (m ⁻²)	ITI	IQI	Eco status	Sulphide (μM)
EE0	Blue	0	27	2419	3.34	0.38	1.82	2	17021	4.34	0.409	Poor	258.2
EE25	Blue	25	57	911	8.22	0.52	3.01	2	22	17.02	0.509	Mod	269.2
EE50	Blue	55	Rock										
EE75	Blue	76	Rock										
SS0	Red	0	10	264	1.61	0.54	1.79	2	878	1.53	0.29	Poor	199.7
SS28	Red	28	33	186	6.12	0.79	3.98	1	378	54.77	0.592	Mod	388.0
SS38	Red	39	12	68	2.61	0.73	2.61	0	0	81.1	0.608	Mod	385.3
SS48	Red	50	20	67	4.52	0.77	3.34	1	11	74.75	0.637	Mod	303.8
SS75	Red	76	16	55	3.74	0.88	3.51	2	122	62.97	0.601	Mod	261.9
SS100	Red	102	18	65	4.07	0.73	3.03	2	33	82.54	0.65	Good	77.5
SS150	Red	151	42	408	6.82	0.66	3.54	1	100	61.93	0.595	Mod	134.3
SS200	Red	211	41	275	7.12	0.7	3.77	1	44	76.00	0.717	Good	195.7
WW0	Green	0	10	2455	1.15	0.15	0.49	3	26675	0.13	0.216	Bad	473.5
WW25	Green	26	48	718	7.15	0.59	3.28	2	389	62.21	0.615	Mod	311.6
WW50	Green	50	79	557	12.34	0.79	4.96	2	300	69.57	0.746	Good	38.7
WW100	Green	101	61	276	10.68	0.85	5.04	2	133	73.29	0.753	High	6.6
WW150	Green	152	67	398	11.02	0.84	5.12	1	56	77.67	0.839	High	9.0
WW200	Green	203	72	300	12.45	0.85	5.24	2	133	68.35	0.806	High	21.1
WW250	Green	274	47	193	8.74	0.85	4.74	1	78	73.48	0.749	Good	4.3

Table 21: Results of enhanced benthic monitoring at Bay of Meil, sampled on 30th August and 1st September 2021. *S* = Number of taxa, *N* = Abundance, *d* = Margalef's richness index, *J'* = Pielou's evenness index, *H' log2* = Shannon-Wiener index, *EP* = Number of enrichment polychaete species (ITI taxa list); *EP density* = density of enrichment polychaete species (ITI taxa list); *ITI* = Infaunal Trophic Index; *IQI* = Infaunal Quality Index (ver 4); *EP spp(IQI)* = Number of enrichment polychaete species (IQI taxa list); *EP density (IQI)* = Density of enrichment polychaete species (IQI taxa list); *Sulphide* = Mean sulphide results from SAMS on-site analysis of benthic grab samples. Note that where stations were sampled in triplicate, the *IQI* reported below is based on the first two grabs as required by SEPA.

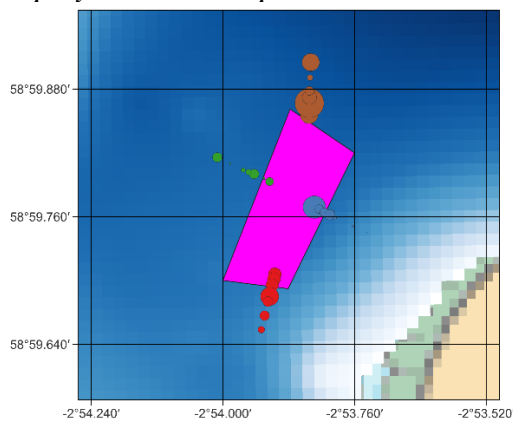
Station	Transect	Distance from cage edge (m)	S	N	d	J'	H' log2	EP spp (ITI)	EP density (ITI) (m ⁻²)	ITI	IQI	Eco status	Sulphide (µM)
NN0	Brown	0	10	2549	1.15	0.06	0.19	3	27753	0.68	0.228	Bad	144.2
NN25	Brown	23	52	214	9.5	0.88	5.02	1	44	65.73	0.733	Good	45.8
NN50	Brown	51	55	157	10.68	0.89	5.13	2	67	65.58	0.757	High	73.0
NN75	Brown	80	49	207	9	0.86	4.83	0	0	65.54	0.728	Good	60.0
NN100	Brown	102	49	199	9.07	0.87	4.88	0	0	66.5	0.784	High	87.2
NN150	Brown	151	75	363	12.55	0.85	5.28	1	56	63.48	0.814	High	40.1
NN200	Brown	208	41	156	7.92	0.84	4.49	1	44	57.9	0.719	Good	61.1
Ref 1	Yellow	480	38	214	6.9	0.79	4.14	0	0	66.67	0.722	Good	35.3
Ref 2	Yellow	495	92	513	14.58	0.80	5.22	1	11	69.23	0.838	High	20.8

4.3.8. Carbon flux from sediment boxes deployed at Bay of Meil

The results from the estimates of organic carbon deposited into the sediment boxes deployed at Bay of Meil are given in Appendix 17. Overall, there were fewer failures in recovery of sediment boxes compared with the Bay of Vady deployments although two boxes during the neap tide deployment were not recovered. Sediment boxes along the blue transect beyond 40 m from the cage edge were placed on rocky substrate i.e. they could not be sunk flush with the sediment surface.

Compared with Bay of Vady and Quanerness, the maximum estimated organic carbon deposition was higher at 96 g m^{-2} deposited over 7-days (Figure 76). Under neap tides the highest depositions were estimated to be occurring at the cage edge along the blue transect but elevated deposition was also observed at 30 m along the brown transect. There was also elevated deposition at 100 m along this transect although contamination of this sample with seaweed fragments which could not be removed before the sample was filtered cannot be ruled out. During deployment 'b' (spring tides) material appeared to be moved to the south leading to noticeable elevated deposition at the cage edge, and as far as 75 m out along the red transect.

Deployment a – Neap tides



Deployment b – Spring tides

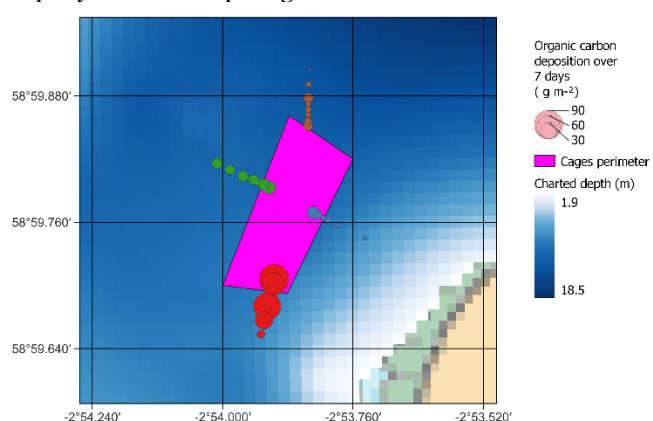


Figure 76: Mean deposition of organic carbon at Bay of Meil as estimated from seven-day deployments of sediment boxes. The surface area of the circles is proportional to the mean POC deposited based on triplicate analyses from the sediment boxes.

4.3.9. Comparison between measured variables at Bay of Meil

Relationships between the measured variables were compared along each transect with the IQI as determined from the benthic grabs (Figures 77 & 78). Note that the IQI colour band transitions are shown at the distance that a different IQI status occurred, because it is not known where the transition point would have been located between sampling points. The transition between states could thus occur closer to, but not further from the cage edge than indicated. It must also be borne in mind that the location of the measurements made on sediment cores, boxes and from benthic grabs were not completely aligned (Figure 73). Therefore, some of the differences between the patterns within and between the variables could be due to fine-scale spatial heterogeneity. Where results were determined from samples collected during neap and spring tides (sediment boxes), the results from each deployment were also averaged on the basis that this will likely represent the parameter over a whole tidal cycle.

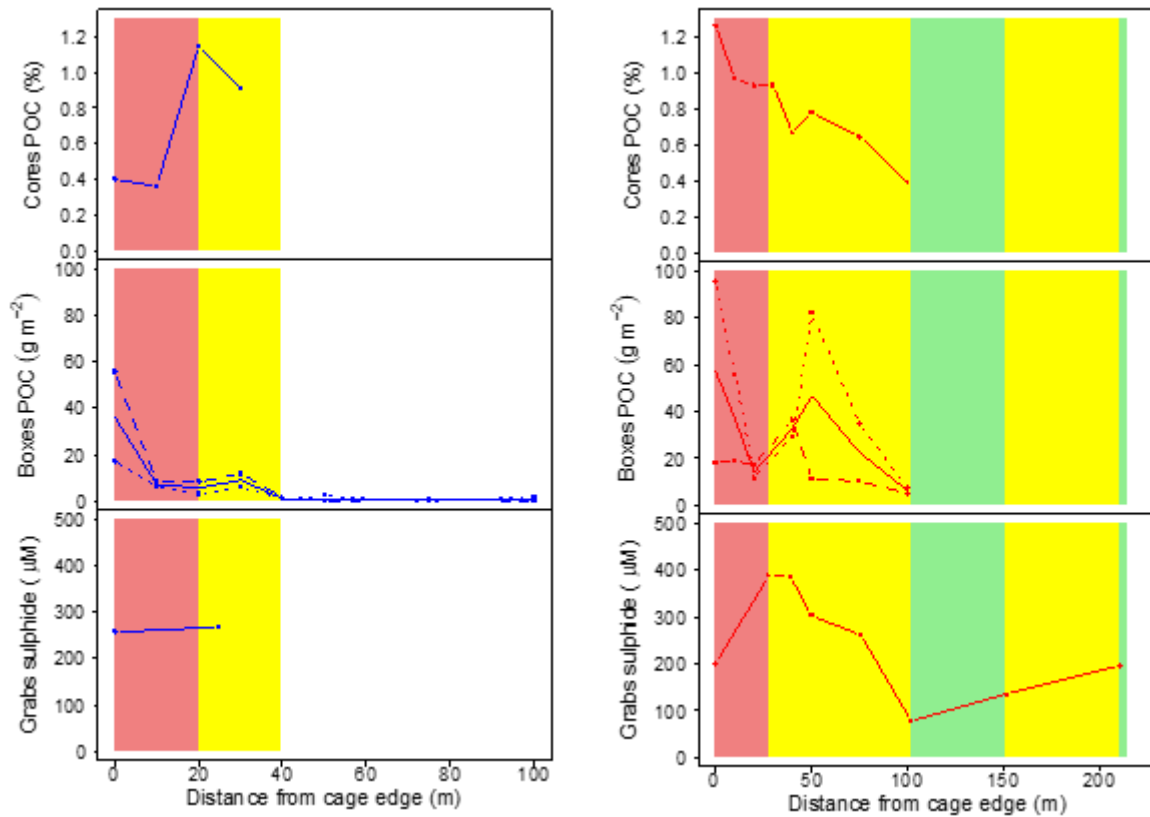


Figure 77: Comparison of measured parameters along the Blue easterly (left column) and Red southerly (right column) transects at Bay of Meil. Mean POC measured from syringe cores (top row); Estimated POC deposited into sediment boxes during the 7-day deployments (second row down); Mean sulphide measured from benthic grabs (bottom row). Where two deployments were made, dashed lines indicate deployment 'a' (neap tide) and dotted line deployment 'b' (spring tide), the solid line is the average of the results from deployment 'a' and deployment 'b'. The background shading indicates the IQI status of the benthic grab samples (red indicates 'Poor' or 'Bad', yellow indicates 'Moderate' and green indicates 'Good' or 'High' IQI status).

Despite the caveats regarding sample locations, the results confirm that the largest impacts occurred along the Blue (easterly) and Red (southerly) depositional axes. The estimated carbon deposition to the sediment boxes close to the cage edges were also higher on these transects compared with the westerly and northern axes. However, beyond about 40 m, the blue (easterly) transect ran into rocky substrate so the distance extent of most of the parameters is limited because grab samples could not be collected. Deposition to the sediment boxes may also have been affected by the fact that the boxes could not be sunk flush with the seabed. Along the Red (southerly) axis, there seemed to be reasonable agreement between the IQI status and the other measured parameters (Figure 77). Thus, sediment POC and estimated tidally averaged POC deposition into the sediment boxes declined with distance from the cage edge, and this appears to be reflected in the improving IQI status, although areas of 'Moderate' ecological status occurred as far out as 151 m in this direction. Despite the magnitude of carbon deposition to the sediment boxes being similar at the cage edge and around 50 m, this was not completely reflected in a 'Poor' IQI status at both locations. Comparing the neap and spring tide results suggests quite large variations in deposition over time along this transect and these varying patterns might influence the ecological status. The relationship with sulphide

concentration from the grab samples was less clear, although they seemed to be moderately elevated ($> 200 \mu\text{M}$) from the cage edge to around 75 m.

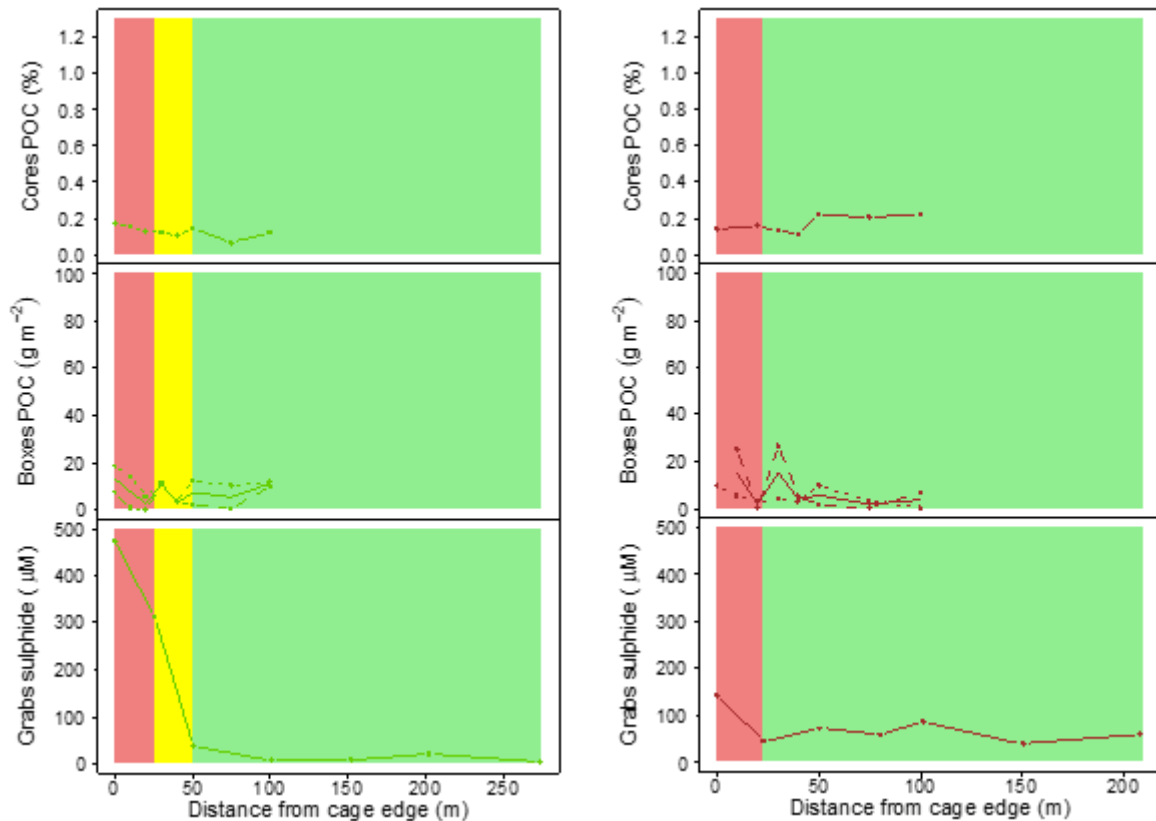


Figure 78: Comparison of measured parameters along the Green westerly (left column) and Brown northerly (right column) transects at Bay of Meil. Mean POC measured from syringe cores (top row); Estimated POC deposited into sediment boxes during the 7-day deployments (second row down); Mean sulphide measured from benthic grabs (bottom row). Where two deployments were made, dashed lines indicate deployment 'a' (neap tide) and dotted line deployment 'b' (spring tide), the solid line is the average of the results from deployment 'a' and deployment 'b'. The background shading indicates the IQI status of the benthic grab samples (red indicates 'poor' or 'bad', yellow indicates 'moderate' and green indicates 'good' or 'high' IQI status).

Compared with the Red transect, poorer IQI status extended to a smaller distance from the cage edge along the Green and Brown transects. The relationship between IQI and estimated carbon deposition to the sediment boxes was less clear along these transects, although this perception may be affected by the loss of the cage edge spring tide sampling box for the Brown transect. Along both transects, sediment sulphides were elevated close to the cage edge, although only marginally for the Brown transect.

4.3.10. Modelling organic waste dispersal at Bay of Meil using NewDEPOMOD

Using the SEPA defaults, no RMSE could be computed because all the waste particles were moved completely out of the model domain during both 7-day periods corresponding to sediment box deployments. These issues with more dispersive sites are known and possible approaches discussed in SEPA (2019a) and SRS (2021).

To produce a depositional footprint, critical shear stress (τ_{ECrit}) had to be set to 20. Further adjustments of remaining parameters listed in Table 22 only led to marginal improvements in model fit as measured by the RMSE. The following combinations of parameter values yielded four models with the lowest RMSE using the full current meter data.

Table 22: Parameter values for four best fit NewDEPOMOD models at Quanterness using the full current meter data (that is without the tidal residual current removed). Parameter names in NewDEPOMOD: Resusp height (Transports.BedModel.releaseHeight.height); Hydraulic rough (Transports.bottomRoughnessLength.smooth); Crit stress (Transports.BedModel.tauECritMin); Layer mass (Transports.BedModel.dLayerMass); Horizontal bed dispersion (Transports.suspension.walker.dispersionCoefficient X and Y).

	Model			
	4	3	2	1
RMSE	20.8728	20.8555	20.8447	20.8379
Resusp height	0.0555	0.0144	0.0555	0.0144
Hydraulic rough	0.1	0.1	0.01	0.001
Crit stress	20	20	20	20
Layer mass	5	3375	5	130
Dispersion	2	2	2	2

Because there were marginal differences between the fits of the four models, only results from the best-fit (model 1) are shown (Figure 79).

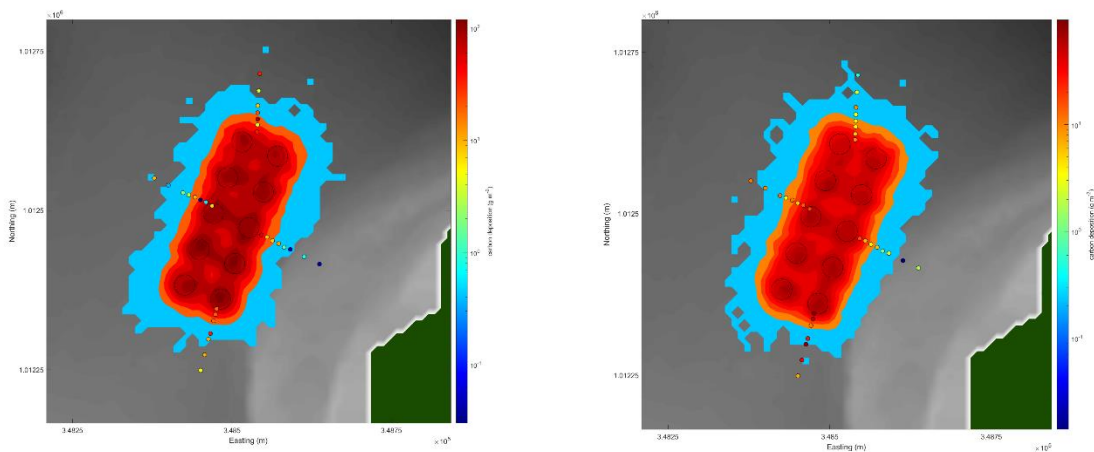
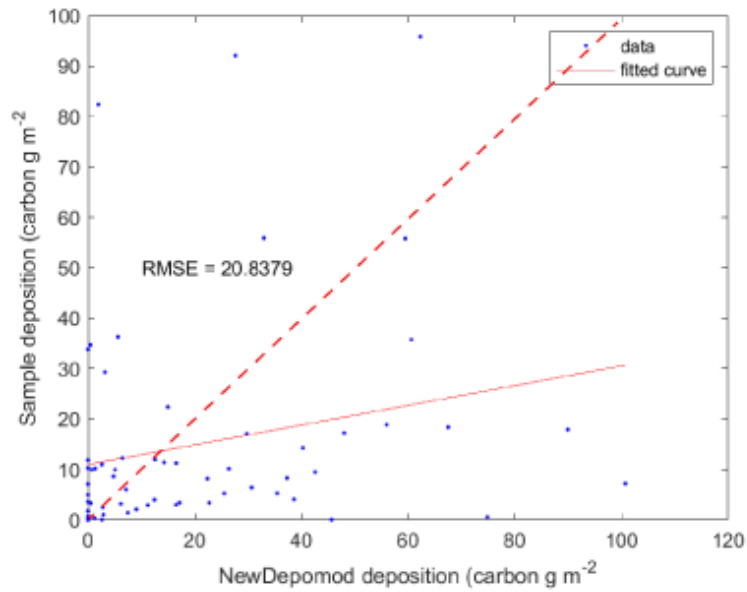


Figure 79: Best fit model results for Bay of Meil. Top panel: Scatterplot of model predictions matched against estimated organic carbon deposition in the sediment boxes across both tidal state deployments. Dashed red line is a 1:1 relationship, solid red line is the RMSE fit. Lower panels: NewDEPOMOD predicted footprint (model 1) as contours; Filled circles show the estimated carbon deposition in the sediment boxes plotted on the same colour scale. Lower left: Deployment 'a' (neap tide) Lower right: Deployment 'b' (spring tide). The organic carbon deposition scale is logarithmic to cover the 'exponential' decline in organic carbon deposition values with distance from the cages.

The contour plots show that adjusting critical shear stress (τ_{ECrit}) has constrained the particles to be under and close to the fish farm cages. However, the model footprint now does not extend far enough out, especially along the southerly transect where variables such as sediment box organic carbon deposition, sulphides and IQI suggest there are impacts out to at least 100 m distance from the cage edge (Figure 77). Furthermore, there is very little difference in the model footprint comparing the neap and spring tide periods. These results suggest that the resuspension and redistribution processes have not been fully captured in the model.

4.3.11. Comparison of sulphide data from Quanterness and Bay of Meil against the infaunal indices, ITI and IQI

The infaunal indices, ITI and IQI derived from benthic grabs were plotted against the sulphide measurements from Quanterness and from Bay of Meil (Figure 80) based on the data presented in Tables 18 & 21.

At Quanterness, both ITI and IQI gave similar patterns with a tendency for samples with 'Normal' ITI, or 'High' or 'Good' IQI to be associated with low sulphide levels ($< 200 \mu\text{M}$). However, there was considerable overlap for intermediate sulphide levels ($200 - 800 \mu\text{M}$) with several samples with sulphide levels in this range achieving poorer ecological status (< 60 ITI or < 0.64 IQI).

At Bay of Meil, there was a smaller range of sulphide concentrations with the maximum being just over $470 \mu\text{M}$. Benthic grab samples achieving 'Normal' ITI, or 'High' or 'Good' IQI again tended to be associated with low sulphide concentrations ($< 200 \mu\text{M}$). Above $200 \mu\text{M}$, samples had poorer ecological status and unlike Quanterness, there were no samples achieving 'High' or 'Good' IQI status when sulphide was elevated above this level.

In general, for a given sulphide level at the mid-to lower end of the values, IQI was represented in its full range. Sulphide values less than $\sim 600 \mu\text{M}$ are often indistinguishable in the sense that this range encompasses typical background levels of un-enriched sediments. Although there were few samples with sulphide levels greater than $600 \mu\text{M}$, they all had low IQI values. For this reason, the relationship between sulphide and faunal indices may be better represented by a nomogram (Hargrave *et al.*, 2008).

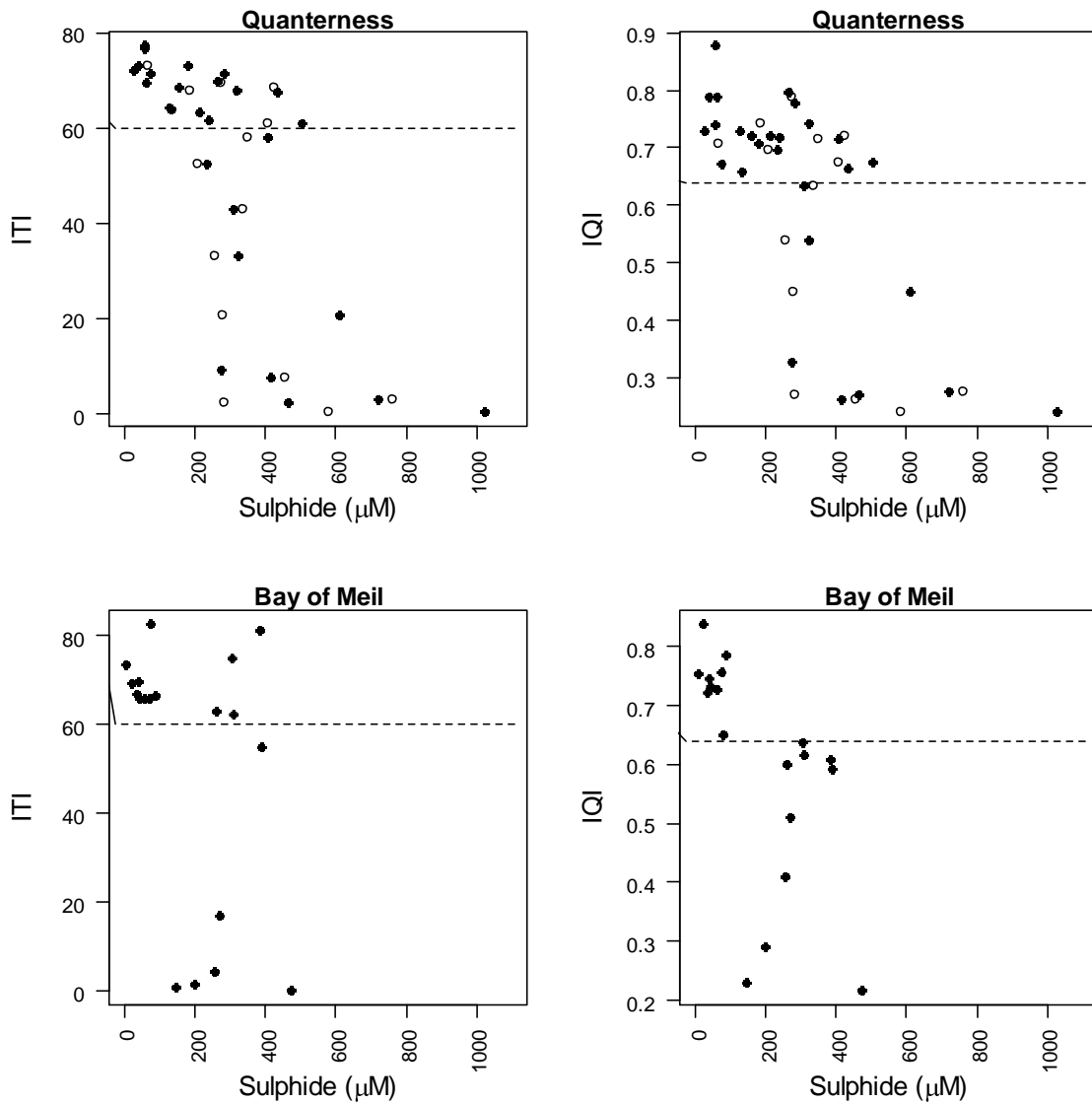


Figure 80: Scatterplots of the infaunal indices, ITI and IQI against sulphide measurements made at Quanterness and Bay of Meil. Open circles represent tidally averaged sulphide measurements made on syringe core samples which were matched to grab locations as closely as possible, and solid circles represent sulphides measured directly from grab samples. Note that distances from cage edges of syringe cores and benthic grabs were matched as closely as possible but did not always coincide exactly. Only benthic grab data was available from Bay of Meil as Covid-19 restrictions prevented sulphides being measured from sediment cores. Dashed horizontal lines for ITI represent the boundary between 'Normal' and 'Perturbed' status and for IQI the boundary between 'Good' and 'Moderate' status.

4.3.12. Comparison of sediment sulphides from Shelburne Bay and Port Mouton, Nova Scotia with IQI

The infaunal index IQI derived from benthic grabs and the sulphide measurements for Shelburne Bay and Port Mouton are shown in Table 23 and plotted in Figure 81.

Table 23: Surficial sediment sulphide concentrations and Infaunal Quality Index for Nova Scotian sites.

Site	Lat	Lon	Sulphide	IQI	Eco status
Port Mouton	43.91095	-64.81770	26	0.9106	High
Port Mouton	43.91335	-64.81410	279	0.9114	High
Port Mouton	43.91388	-64.81270	832	0.8489	High
Port Mouton	43.91474	-64.81118	546	0.8857	High
Port Mouton	43.91718	-64.80920	113	0.941	High
Port Mouton	43.91407	-64.81299	666	0.9527	High
Port Mouton	43.91479	-64.81114	1031	0.8769	High
Port Mouton	43.91805	-64.80822	36	0.8404	High
Port Mouton	43.91498	-64.81182	973	0.8175	High
Port Mouton	43.91487	-64.81188	3953	0.6244	Mod
Port Mouton	43.91582	-64.81100	759	0.8334	High
Port Mouton	43.91534	-64.81061	1447	0.8428	High
Shelburne Bay	43.71403	-65.32407	81	0.8571	High
Shelburne Bay	43.71483	-65.32345	263	0.9008	High
Shelburne Bay	43.71677	-65.32277	2920	0.8712	High
Shelburne Bay	43.71672	-65.32248	344	0.8974	High
Shelburne Bay	43.71790	-65.32257	1215	0.8627	High

The maximum sulphide concentrations observed at Port Mouton and Shelburne Bay were higher than for the Orkney sites, although most of the observations were less than 1000 μM . The Canadian sites are generally finer sediments and thus more depositional. There was a slight decline in IQI with increasing sulphide concentration but nearly all the IQIs would be assigned a ‘High’ ecological status. Like the Orkney sites, the highest sulphide showed the lowest IQI, although only represented by a single point in Port Mouton. Even without this sample there was a significant negative relationship between IQI and sulphide (Fig. 79). This suggests that over a wider and higher sulphide range, faunal indices and biogeochemical measures may be closely related. Despite this relationship, it is interesting that higher sulphides did not produce IQI values indicative of degraded conditions, in contrast to the results from Quanterness and Bay of Meil.

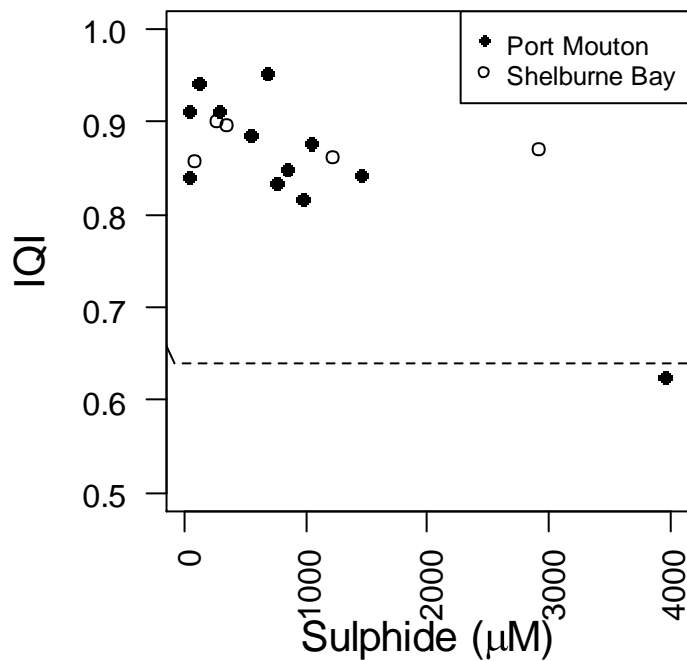


Figure 81: Scatterplot of the infaunal index IQI against sulphide measurements made at Port Mouton and Shelburne Bay, Nova Scotia, Canada. Dashed horizontal line represents the boundary between ‘Good’ and ‘Moderate’ IQI status.

At both Shelburne and Port Mouton, the sites studied had been followed for periods ranging from several months to years. Faunal recovery may have progressed despite lingering sulphides. The Shelburne Harbour, Sandy Point site was re-surveyed in 2013 and heralded as ‘still toxic’ in the popular press (<https://nsapes.ca/sea-bottom-still-toxic-shelburne-says-marine-scientist>), with reports of reduced faunal diversity (Milewski, 2014). Sulphide values up to 3,250 µM were recorded in 2013 but were as high as 12,000 µM in 2011 samples. Sediment organic carbon levels were elevated compared with reference sites and extensive bacterial mats (*Beggiatoa* sp.) were also recorded near the former fish farm. The Milewski report also pointed to elevated sediment copper and zinc levels which could be an added factor in interpreting biological recovery at that site.

5. Discussion of the INCREASE project results

5.1. Main conclusions from the INCREASE project

The main conclusion from the study was that it was necessary to tune-down the resuspension of particles from the default settings in NewDEPOMOD to realistically model the observed net carbon deposition rates at the three sites studied. This accords with previous studies undertaken at dispersive sites in New Zealand (Keeley *et al.*, 2013a) and Norway (Carvajalino-Fernández *et al.*, 2020b), general recommendations from SEPA for use of NewDEPOMOD (SEPA, 2019a) and our experience of using NewDEPOMOD to model several moderate to high flow fish farms in the Orkney Islands, Scotland (this report).

Although we could not confirm the underlying mechanism, the hypothesis advanced in Adams *et al.* seems credible. This hypothesis suggests that newly deposited organic material overlying previous accumulations is easily eroded, that is it has a low critical shear stress threshold and erodibility rates, as previously determined using tracers, and laboratory and benthic flume studies. However, because of local bed roughness once redistributed onto relatively clean sediment, the critical erosion threshold is increased, and the erodibility rate decreased. The effect appears particularly pronounced on sandy or coarser sediments which will have a higher bed roughness compared with mud.

Nevertheless, our results suggested that once resuspension was turned down, NewDEPOMOD was predicting deposition rates in the right order of magnitude compared with the observations and was broadly capturing the shape of deposition along the sampling transects. However, for future use, effectively turning off resuspension in NewDEPOMOD is not an entirely satisfactory approach. It is essentially an *ad hoc* fix to constrain the over-dispersal of resuspended material, but this in turn is likely to then over-estimate the settlement of organic waste close to the cages. Although modelling without resuspension is conservative, in the sense that it will tend to give a ‘worst case’ scenario, this is not very satisfactory from the industry viewpoint because it may un-necessarily limit the licenced biomass at a site, at least until sufficient benthic faunal monitoring data are collected to allow the model to be better tuned to the site. Furthermore, such an *ad hoc* approach is not addressing the possible mechanisms behind the observed dispersal patterns. Suggestions for future work and potential improvements to expand the options for modelling dispersal of organic waste from open cage fish farms using NewDEPOMOD at higher-energy sites are given in Section 7.1.

Near bed particle dynamics in sand or coarser sediments are complex and not easily captured in most resuspension models. Fine organic particles, including aquaculture waste, have a low erosion threshold when at the sediment surface, but depending on sediment grain size and form drag (due to shells, ripples etc.) may be incorporated into the interstices and subsequently partially protected from resuspension (Pilditch *et al.*, 1997). Bedload transport of the ambient grains may then be required to erode the fine material under these conditions. Moreover, organic particles may become part of the sediment surface biofilm which includes bacteria and under photic conditions benthic diatoms (Sutherland *et al.*, 2021). This biostabilisation greatly increases the erosion threshold of even sand beds and is particularly difficult to parameterise.

Recent developments in the sector may eventually mitigate seabed impacts from organic waste almost entirely. For example, sludge lift systems combined with impermeable collection funnels are being trialled in Norway and Scotland (Fish Farming Expert, 2021). However, such approaches will increase installation and operational costs and the collected sludge must still be disposed. Sludge from marine farms will also have a high salt content which may limit its

use for biodigestion. Open cage aquaculture is thus likely to remain significant for at least the foreseeable future, especially in the marine environment so that further research on improving organic waste dispersal and benthic impact modelling and monitoring is still justified.

5.2. Background data from the fieldwork sites

5.2.1. Water currents

Additional water current data were collected at three sites, Bay of Vady, Quanterness and Bay of Meil using an ADCP. The new data largely confirmed the current patterns originally submitted with the site licence applications to SEPA. However, there were some differences which illustrate how water currents can vary over quite small spatial scales as the new ADCP sites were at different locations to the original current meter positions. Also, for Quanterness and Bay of Meil there were large differences in the near surface water currents between the new and original data. This reflects local wind conditions at the time of data collection but illustrates the impact wind forcing can have. However, the near bed current patterns were similar suggesting that the wind impacts are largely confined to the upper part of the water column at these sites.

5.2.2. Sediment particle size

Sediment particle size can have a profound effect on the benthic impacts of organic enrichment. As well as potentially affecting particle resuspension, coarser-grained sediments may have a higher assimilative capacity for organic carbon because of increased diffusion and intrusion of oxygen from the overlying water (Brooks and Mahnken, 2003).

The natural sediment size profiles (PSA) from syringe cores were very similar to those reported to SEPA from grab samples collected for regulatory monitoring (Biotikos Ltd., 2016; Fish Vet Group, 2019). However, at Quanterness gravel was reported at up to 10% (by weight) in some grab samples collected along the northern and western transects (Fish Vet Group, 2019). Also, higher levels of silt were recorded in the laser granulometer results (up to 30%) compared with the grab samples (up to 12%). However, it is inadvisable to directly compare these data for several reasons. The different sample collection methods (syringe cores versus Van-Veen grabs), analytical techniques (laser granulometry versus dry sieving), and how the data are expressed (as percentage of particles by number versus percentage by fraction dry weight) can explain the differences. Although it is possible to interconvert results from laser analysis and dry sieving, this requires several assumptions or cross calibrations to be made (Shillabeer *et al.*, 1992). In the present study, the additional work required was not justified by the additional information which would result. It must also be borne in mind that syringe cores are likely to miss gravel, because its presence makes insertion of small coring tubes into the sediment more difficult. On the other hand, grab samples can underestimate the amount of fine material, especially when collecting from sandy sediments, as some of the finer material can be washed out of the grab during collection. Despite these caveats, the data all indicate that the sediments at all three study sites are largely dominated by fine and very fine sands.

Comparison of the grain sizes for the sand added to the sediment traps (300 – 600 μm) with the sediment profiles recorded from syringe cores taken at each site suggested that the material used in the traps was coarser than the natural sediment. The natural sediment profiles, based on syringe core samples, were dominated by grain sizes 63 – 250 μm . This difference between the sediment trap and surrounding sediments could have affected our results because there will be larger inter-grain spaces in coarser sediments which might therefore be better at trapping settling organic particles. Thus, in any future studies it is recommended to more closely match

the grain size of the material added to the sediment traps with the natural seabed sediment size profile based on previous sediment sampling at the study site. This could be accomplished by collecting sediment at the site for use in trays. However, collection and cleaning as well as transport back to the site is less feasible in remote locations like Orkney.

5.2.3. Sediment particulate organic carbon

The amounts of organic carbon stored in marine sediments can be substantial with important implications for global climate change (Luisetti *et al.*, 2019). Improving our understanding of how organic carbon is deposited, metabolised, and sequestered into marine sediments has thus received renewed interest.

For UK seas, there have been several studies aimed at improved mapping of organic carbon deposits with the ultimate aims of quantifying the stock of carbon stored in UK marine sediments and potentially protecting important depositional sites from anthropogenic disturbance.

Serpetti *et al.* (2012) showed a strong association between particulate organic carbon and the percentage of mud in the sediment (Figure 82). However, these data were collected across a relatively restricted area off Stonehaven, Scotland.

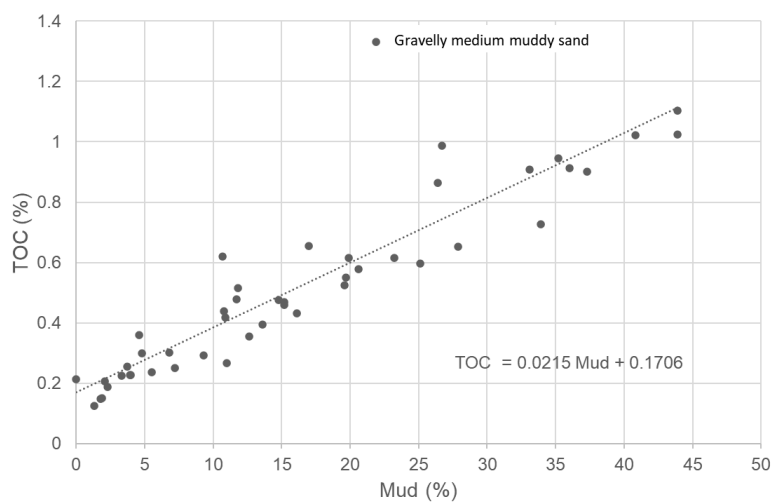


*Figure 82: The relationship between particulate organic carbon and percentage of mud (fractions smaller than 63 μm diameter) from samples collected off Stonehaven, Scotland. Redrawn from data in (Serpetti *et al.*, 2012).*

Diesing *et al.* (2017) used samples collected across much of the UK continental shelf and reached a similar conclusion, that the percentage of organic carbon can be related to the Folk class of the sediment (Table 24). Thus, with increasing coarseness, gravelly mud, mud and sandy mud have the highest POC concentrations and sand to gravel the lowest.

Table 24: Statistical summary of sample analyses presented in Diesing *et al.* (2017).

Folk class	POC		Dry bulk density	
	Mean (% dry wt.)	SD (% dry wt.)	Mean (kg m ⁻³)	SD (kg m ⁻³)
Gravelly mud	0.91	0.51	1011	102
Mud	0.88	0.20	580	29
Sandy mud	0.78	0.21	828	120
Slightly gravelly sandy mud	0.67	0.16	945	73
Muddy gravel	0.62	0.01	1314	125
Muddy sand	0.54	0.22	1323	99
Slightly gravelly muddy sand	0.54	0.22	1357	80
Gravelly muddy sand	0.49	0.23	1397	51
Muddy sandy gravel	0.29	0.10	1482	25
Sand	0.24	0.12	1511	25
Gravelly sand	0.23	0.10	1515	16
Slightly gravelly sand	0.22	0.11	1512	21
Sandy gravel	0.19	0.09	1521	13
Gravel	0.18	0.05	1529	8

These results seem intuitively reasonable as they reflect the depositional nature of muddier sediments and such relationships have been widely used to estimate the total carbon stocks stored in marine sediments. However, Diesing *et al.* (2017) cautioned that one must not naively assume that muddy sediments hold the largest carbon stocks in absolute terms. This is because of differences in dry bulk density i.e., the actual volume that each kilogram of substrate will occupy when hydrated and the much larger spatial area of the UK EEZ occupied by sandy sediments, compared with other types (Diesing *et al.*, 2017).

Naive extrapolation by area of these simple relationships to Irish and Scottish sea lochs is also unadvisable because presently available sediment maps are not at a fine enough spatial resolution to capture the real heterogeneity in sediment typology in many of these environments (Smeaton and Austin, 2019). However, despite this the basic relationship between Folk class and POC was seen to hold (Figure 83). From this we may expect POC in the sea lochs to be around 3% in mud and sandy mud sediments (but with a large range and outliers up to nearly 12%) whilst POC in fjordic sands is likely to be below 1%.

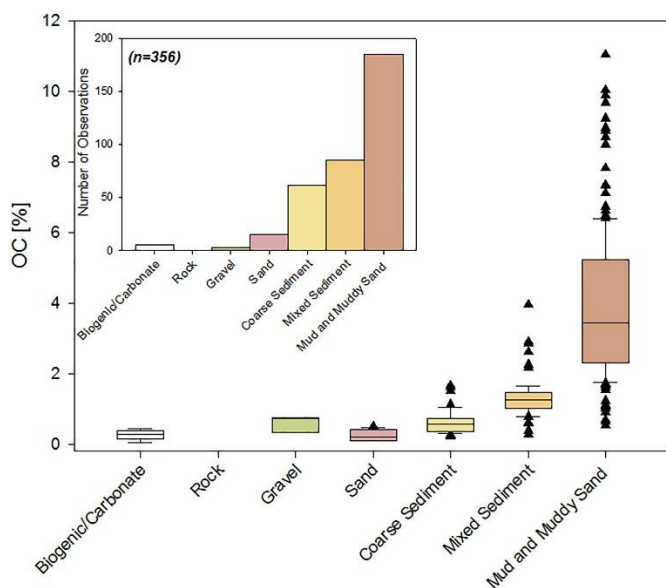


Figure 83: Organic carbon content of 356 sediment samples collected from 35 fjords around Scotland. Inset figure: Number of samples in each of the modified Folk classes. From (Smeaton and Austin, 2019).

The majority of POC levels recorded at the three study sites were less than 0.5 % (dry wt.). Slightly higher values (1– 2 %) were recorded at the start of some transects close to the cages. Nevertheless, overall levels of POC in the sediments surrounding the farms studied seem to be in-line with expected levels for unimpacted sandy or silty sand sediments and did not indicate any extreme problems with accumulation of organic carbon.

Caution in interpreting such data is advised however because small-scale variability in organic carbon enrichment related to fine spatial scale features is likely to occur, especially on an undulating seabed, such as at Bay of Vady (Figure 55). The sediment box results from this site also showed fine-scale variability, even comparing transects which were located quite close to each other (Figure 57). Material is more likely to accumulate at the bottom of ripple features and it is impossible to capture such fine-scale variability in models such as NewDEPOMOD. Moreover, these accumulations can easily be buried via ripple migration (Grant, 1988). Such small-scale patchiness could increase the variability in POC (and other related variables) because random variations in sampling position could easily lead one to miss, or to hit, small areas of relatively high organic waste deposition compared with average deposition in the surrounding seabed. Conversely, particle tracking models, such as NewDEPOMOD, can only ever be expected to reproduce the broad-scale average pattern of dispersal and deposition. Features such as undulations in the seabed (Figure 55), macroalgae (Figure 59) and burrows and shells (Figure 71) will all serve to trap waste particles potentially creating local areas of organic enrichment (Pilditch *et al.*, 1997). Therefore, comparing model predictions with observations, and tuning model parameters to better fit the observations, remains extremely challenging because of fine spatial and temporal scale features and processes which occur in the real world (Cromey *et al.*, 1998).

5.2.4. Use of sediment boxes to estimate organic carbon deposition

The need to monitor the footprint of open cage fish farms has received attention due to the global expansions of this form of aquaculture. Among the methods which have been suggested are measuring the sediment levels of carbon isotopes (Ye *et al.*, 1991), phospholipid isotopes (Mayor *et al.*, 2017), chemotherapeutics (Samuelson *et al.*, 2015) and astaxanthin (Sporsheim, 2017). Cromey *et al.* (1998). Cromey *et al.* (2002b) described studies where an artificial tracer was added to fish farm waste to measure re-suspension and dispersal. However, these authors

cautioned that the tracers probably did not mimic the properties of the waste very accurately. All the techniques mentioned use secondary indicators when what is really required are measurements of the actual net organic carbon deposition, since this is the source of the organic enrichment impacts on benthic communities. Measurements of carbon deposition would also allow direct comparison with carbon deposition rates as predicted by models such as DEPOMOD.

Sediment traps have often been used in several studies to try and directly measure carbon deposition rates around fish farms (Cromey *et al.*, 2002a; Stucchi *et al.*, 2005; Cromey *et al.*, 2012; Riera *et al.*, 2017). However, the problem with the classical cone or parallel sided cylindrical sediment trap is that it does not allow for resuspension of the settled material. Once trapped the material is protected from horizontal water flow and so in higher flow environments, classical traps measure the gross, rather than the net carbon accumulation.

Despite this caveat, some studies in higher energy environments have shown reasonable agreement between carbon deposition and modelled or expected deposition levels. Riera *et al.* (2017) for example showed very good agreement between observed and modelled organic matter deposition out to distances of 60 m from fish farms in Madeira and the Canaries, despite relatively high horizontal dispersion coefficients ($0.041\text{--}0.917\text{ m}^2\text{ s}^{-1}$).

In this study we strove to overcome this limitation by using boxes containing coarse sand, to mimic the surrounding seabed, which were sunk flush with the seabed surface. This follows work by Grant (Grant, 1985) where a similar approach was used to estimate carbon deposition at different states of the tide in a coastal environment.

The results obtained using this technique at two sites, Quanterness and Bay of Meil seemed to produce credible results. The scale of estimated carbon deposition rates were in line with expectations based on initial modelling and carbon deposition rates when plotted against distance from the cage boundary generally appeared to correlate with other measurements such as POC, sulphides and infaunal indices (see Sections 4.1.6, 4.2.8 & 4.3.8). Results from Bay of Vady seemed less convincing with high deposition out to 100 m on some transects. The sampling design also did not allow comparison with IQI as an enhanced benthic sampling was not undertaken at that site. The results may have reflected that this was the site where the technique was first tried and so dive teams were also learning how to deploy and recover the boxes. Results from Bay of Vady should thus be treated as a pilot study although the estimated deposition rates still seem reasonable.

Our sediment box results do come with several caveats. It is known that the characteristics of organic waste from fish farms may become altered quite rapidly due to flocculation and bacterial action (Stucchi *et al.*, 2005; Giles *et al.*, 2009). This could have led to a lower rate of resuspension for material deposited into the sediment boxes compared with the surrounding sediment, because the sediment boxes contained clean sand. At some point over the course of deployment, the sediment boxes will become equilibrated with the ambient sediment, and depending on the levels of bedload transport, the clean sediment completely replaced. It is important to retrieve the boxes prior to this state so that the particulate carbon dynamics are still detectable, but deployment also needs to be sufficiently long so that sufficient organic carbon accumulates above the detection threshold of the analytical method. Deployments of 7 days appeared to produce reproducible and credible results in the present study.

The main practical limitation of the approach developed here was diver time required for positioning and retrieving the traps. Commercial dive operations at Scottish fish farms generally use surface supplied compressed air rather than enriched mixtures so bottom time at depths much beyond 25 m are limited. The use of alternative gases (such as trimix) could

extend both depth and bottom time but would require specialist diving beyond that readily available at Scottish salmon farms. Nevertheless, this option might be worth considering at deeper sites which have proven particularly challenging to successfully model and where additional carbon deposition data would be valuable.

In terms of observation error, it would have been preferable to place replicate sediment boxes at each location to better capture the level of small-scale local variability in deposition rates at each site. However, this would have considerably increased the diver time needed for box placement and recovery beyond what was available in the present project. Nonetheless, in terms of spatial coverage, our data represent some of the most spatially detailed organic waste deposition measurements around fish farms ever collected.

Although we deployed boxes covering spring and neap periods, two 7-day deployments may be insufficient to fully capture variability in organic carbon deposition which could be affected by periods of strong wind or freshwater run-off. Such effects are assumed to impact waste dispersal particularly at shallow water sites (SEPA, 2019a). However, current meter measurements at Bay of Meil suggested that such effects may be largely confined to the near surface waters (Figures 35 and 37) and so have less effect once material has settled to the seabed. Nevertheless, sediment boxes were not deployed during periods of intense storms so one cannot exclude this as an important factor affecting waste dispersal at the sites studied.

Compared with classical design of benthic sediment traps, our sediment boxes did have several disadvantages. The main disadvantage is that sediment in the boxes could be quite easily disturbed during box recovery. In some cases, some of the clean sediment was lost as evidenced by the reduced amount in some of the sediment boxes when they were returned to the laboratory. This may have occurred through water current action exposing the box edges which could have further affected the local hydrodynamic flow over the test sediment. We also cannot rule out that some disturbance occurred when boxes were recovered by the divers.

The wash and filter technique also has the potential to add variability to the results. Direct quantification of POC in the test sediment would be preferable and given the higher sensitivity of the Skalar Primacs^{MCS} instrument in practice (when compared to the manufacturer recommendations), would be possible for at least some of the sediment boxes. If the technique were to be used again, we recommend performing an initial direct quantification to screen those sediment boxes where sufficient POC was deposited to be above the limit of detection. The remaining boxes could then be analysed using the wash and filtration technique. Such a two-step processing would save some analytical preparation time.

Our finding that resuspension needs to be tuned down substantially when modelling the sites studied in Orkney may imply that, apart from the most heavily impacted area, resuspension is less important than previously assumed, perhaps due to particles in low to moderate impacted areas being retained by bed roughness resulting in higher critical shear stress (Adams *et al.*, 2020). If this is the case then the classical design of sediment traps may perform adequately (within an acceptable margin of error) for directly validating waste dispersal models such as NewDEPOMOD, even at higher energy sites. However, comparisons between results obtained using the classical design and the open sediment box design could be informative.

We therefore recommend that in future studies traditional style sediment traps (Riera *et al.*, 2017) are deployed alongside the box style traps. A comparison of the results from both approaches would be beneficial in terms of evaluating the importance of resuspension and the degree to which this needs to be taken into account.

Accurately validating the deposition footprint at a farm is difficult with traps laid out in a transect design. Clearly if the actual maximum deposition occurs at a slightly different bearing to that predicted, then the sediment traps (and benthic monitoring grabs) may miss the areas of maximum impact. To comprehensively map organic waste deposition would require a grid design. However, deployment of sediment traps in such a grid would require use of acoustic positioning (for example see <https://www.teledynemarine.com/positioning-systems>), which was not available in the present study.

In the studies at Quanterness and Bay of Meil, sediment boxes were not placed at additional reference sites (although these were sampled using benthic grabs). We are unable therefore to estimate the natural background POC deposition rate at these sites but, over a 7-day period, it is likely to be low.

According to Hargrave (1994b) and annually averaged rates of background sedimentation are usually $< 1 \text{ g C m}^{-2} \text{ d}^{-1}$ and do not normally lead to anoxic conditions in sediments. The ultimate source for the natural carbon flux to the marine benthos is primary production. For offshore waters this is restricted to the euphotic zone so export rates can be used to provide an upper estimate for benthic carbon flux (ignoring losses due to grazing etc.). For example, for offshore Scottish waters, Heath and Beare (2008) estimated new production at between 140 and 260 $\text{mg C m}^{-2} \text{ d}^{-1}$. Other reports of measured natural carbon flux are of similar orders of magnitude: Kutti et al. (2007) reported the annually averaged background flux at approximately 200 m depth to be $110 \text{ mg C m}^{-2} \text{ d}^{-1}$ in an open Norwegian fjord; in the Fanafjorden, Wassmann (1984) estimated average flux at $300 \text{ mg C m}^{-2} \text{ d}^{-1}$; in an embayment near Austervoll, Aure and Ervik (1988) reported an annual averaged flux of $397 \text{ mg C m}^{-2} \text{ d}^{-1}$. However, such annually averaged fluxes do hide considerable seasonal variability (Overnell and Young, 1995). For example, in a Faroese fjord, average particulate organic carbon export from the euphotic zone was estimated to be $335 \text{ mg C m}^{-2} \text{ d}^{-1}$ but export rates of up to $1,080 \text{ mg C m}^{-2} \text{ d}^{-1}$ were recorded during the spring bloom (á Norði *et al.*, 2018). Single point or spatially averaged data can also obscure POC focussing where settling material becomes concentrated in certain areas of the seabed as also shown by á Norði *et al.* (2018). In inshore areas, organic carbon inputs can also include production by macroalgae and seagrasses, as well as terrestrial runoff, which can add to the POC of coastal waters.

There are relatively few direct measurements of background carbon flux for Scottish waters but Overnell and Young (1995) measured a benthic organic carbon flux of $240 \text{ mg C m}^{-2} \text{ d}^{-1}$ in Loch Linnhe whilst Brigolin *et al.* (2009) reported a background carbon flux of $38 \text{ mg C m}^{-2} \text{ d}^{-1}$ in Loch Creran, Scotland. Compared to reported typical average background carbon flux, the observed additional organic carbon from the fish farms investigated was generally much higher. The lowest level we measured was around $20 \text{ mg C m}^{-2} \text{ d}^{-1}$ (at Quanterness), suggesting that the method should be sensitive enough to detect organic carbon deposition rates down to typical background levels. However, in any future studies the use of additional sediment traps placed at one or two reference sites would be advisable to confirm the background particulate organic carbon flux.

5.2.5. Comparing modelled carbon deposition using NewDEPOMOD against estimated carbon deposition from the sediment boxes

The general agreement between the patterns of estimated carbon deposition and the infaunal impacts (assessed using IQI), sediment POC and sulphides data at three fish farms in Orkney suggest that the sediment boxes seemed to be capturing the general patterns in organic carbon deposition at these sites (albeit with some individual outlier results). It therefore seems reasonable to compare NewDEPOMOD modelling results with the sediment box estimates

treating the sediment box data as likely reflecting the ‘true’ levels of organic carbon deposition at these sites.

A key finding was that use of SEPA defaults resulted in complete failures to model realistic footprints. This is not an unexpected result and accords with previous modelling of more dispersive sites. What appears to happen is that particles become repeatedly resuspended and effectively bed-hop out of the model domain.

For each modelled site the best improvement in model fits came from increasing the critical shear stress (*Transports.BedModel.tauECritMin*) from its default value of 0.02 to 20. This is a very high value which in effect turns particle resuspension almost completely off (SRSL, 2021). Other adjustments to parameters such as hydraulic roughness (*Transports.bottomRoughnessLength.smooth*), particle resuspension release height (*Transports.BedModel.releaseHeight.height*), bed model dispersion (*Transports.suspension.walker.dispersionCoefficient*) and bed model layer mass (*Transports.BedModel.dLayerMass*) resulted in further small improvements in model fits.

Although increasing *tauECrit* to this level does constrain particles close to the cages, careful comparison of the modelled footprint with the sediment box results suggests that the footprints then fail to extend far enough away from the cages in the dominant directions of benthic impact. In effect, the model with this level of *tauECrit* is close to a simple settlement model with zero resuspension, a setup which appears to work reasonably well for very low-energy depositional environments but will underestimate dispersal in higher energy environments.

Taken overall, the results suggest that there is a key process which is incorrectly handled within NewDEPOMOD. The most likely explanation appears to be the use of spatially invariant *tauECrit* and possibly mass erosion (*Transports.BedModel.massErosionCoefficient*) coefficients, in the model. Published experimental and modelling evidence (sections 1.8.1, 1.8.2 and 1.8.4), along with the model fitting undertaken at three Orkney fish farms in the present project, suggests that these parameters should vary in relation to the amount of organic material deposited, and that the effect is very likely to be more important on sandy and coarser sediments, compared with mud. NewDEPOMOD simulates the bottom boundary layer using either a law-of-the-wall or Clauser chart method but does not resolve the viscous sublayer (Black et al, 2016; SRSL, 2021). Sediment accumulation between larger bed particles cannot, therefore, easily be reproduced, since increasing the bed roughness coefficient, z_0 , to account for larger bed particle sizes leads to greater resuspension (and therefore redistribution) of particles, rather than allowing accumulation in the larger pore spaces. This leads us to make several recommendations for future work and model testing in Section 7.1 of this report.

6. Discussion of the NAMAQI project results

6.1. Main conclusions from the NAMAQI Project

In Scotland most published research on benthic impacts of fish farms has been conducted in relatively low energy, depositional sites typically over muddy seabed. However, there are now many farms located in higher energy sites which are characterised by coarser seabed sediments. Sediment particle size is likely to have a profound effect on the benthic impacts of organic waste enrichment from farms meaning that conclusions drawn from depositional site studies may not be applicable. As well as potentially affecting particle resuspension, coarser-grained sediments may have a higher assimilative capacity for organic carbon because of increased diffusion and intrusion of oxygen from the overlying water (Brooks and Mahnken, 2003). This

should also tend to reduce the concentrations of sulphides associated with a certain level of carbon sedimentation through encouraging aerobic respiration.

Despite this, data collected in the NAMAQI project did show elevated sulphide levels close to fish farm cages, and elevated levels were also associated with the sampling transects where carbon sedimentation was greatest. The data indicated some increase in free sulphides even at locations where this was not recorded as an obvious smell in grab samples. It seems likely that local pockets of anoxia develop at these locations leading to increased anaerobic respiration, despite the sediment type being sand. Quantification of sulphide therefore appears to be a useful additional indicator of benthic habitat quality.

Data and experience from monitoring of fish farms in Canada also shows that measuring sediment sulphide levels can provide a useful indicator of the benthic community impacts of organic enrichment. Well away from fish farm cages sulphide levels were generally less than 750 μM but exceeded 1500 μM beneath the cages (Department of Fisheries and Oceans, 2012; Chang *et al.*, 2014). Similarly, when measured at two sites in Orkney, there were relationships between sulphide concentration and benthic community status, as assessed using the Infaunal Trophic Index (ITI) and Infaunal Quality Index (IQI) (Figure 84). Furthermore, the measurement of sediment sulphide levels is relatively rapid, and results can be provided within 48 h of sample collection. However, there remain some significant problems with recommending a wider adoption of sulphide measurements on Scottish fish farms.

Firstly, although there were relationships between measured sulphide levels and IQI ecological category (Figure 84), there was a lot of overlap between different levels. For example, at Quanterness, sulphide levels of 'Good' ecological status samples ranged from less than 100 to just over 500 μM with 'Moderate', 'Poor' and 'Bad' status samples having sulphide ranges of around 250 to over 1000 μM . At Bay of Meil there was perhaps better discrimination between 'Good' and 'Moderate' ecological status samples, but again little consistent discrimination between 'Moderate', 'Poor' and 'Bad' status samples based on sulphide concentration. There was also a smaller range of sulphide concentrations at Bay of Meil with none of the samples being above 500 μM , despite several grabs having 'Poor' or 'Bad' IQI scores. These conclusions, although based on sampling at only two farms, largely agree with Black and Nickell (2014) who found a similar large variability in ITI scores associated with intermediate (~200 – 1500 μM) levels of sulphide (Figure 19).

Secondly, there are concerns about the accuracy of the ISE method for quantifying sulphides in marine sediments (Brown *et al.*, 2011). Further research and practice is needed to explore the replacement analytical approach proposed by (Cranford *et al.*, 2017) for use in Scotland. All the analytical techniques available involve some wet chemistry using potentially toxic chemicals and the method proposed by Cranford (2017) requires a UV-spectrophotometer (approximate new cost around £4,000) and oxygen microprobes (indicative cost £8,000). In Canada, the problem of having trained chemists and analytical equipment available on site is overcome through the benthic monitoring being performed by a dedicated team of specialists, but in Scotland benthic sediment sample collection and initial processing are the responsibility of individual farms.

Thirdly, concentrations of sediment sulphides can change rapidly in the presence of oxygen. This means great care must be taken with the collection and handling of sediment samples (Cranford *et al.*, 2020).

Fourthly, except in totally anoxic conditions the levels of sulphides in the sediment can fluctuate quite rapidly. Sulphide measurements at Quanterness showed quite large differences between core samples collected in the same locations at neap versus spring tides, an effect

likely related to differences in near-bed water flow and thus degree of sediment oxygenation. Thus, to obtain representative measurements the collection of samples for sediment sulphides would require more careful consideration of timing when compared with sampling for infauna-based indices which fluctuate at longer timescales. Sampling at several different tidal states may thus be required to obtain a fuller picture for the true level of free sulphides in marine surficial sediments.

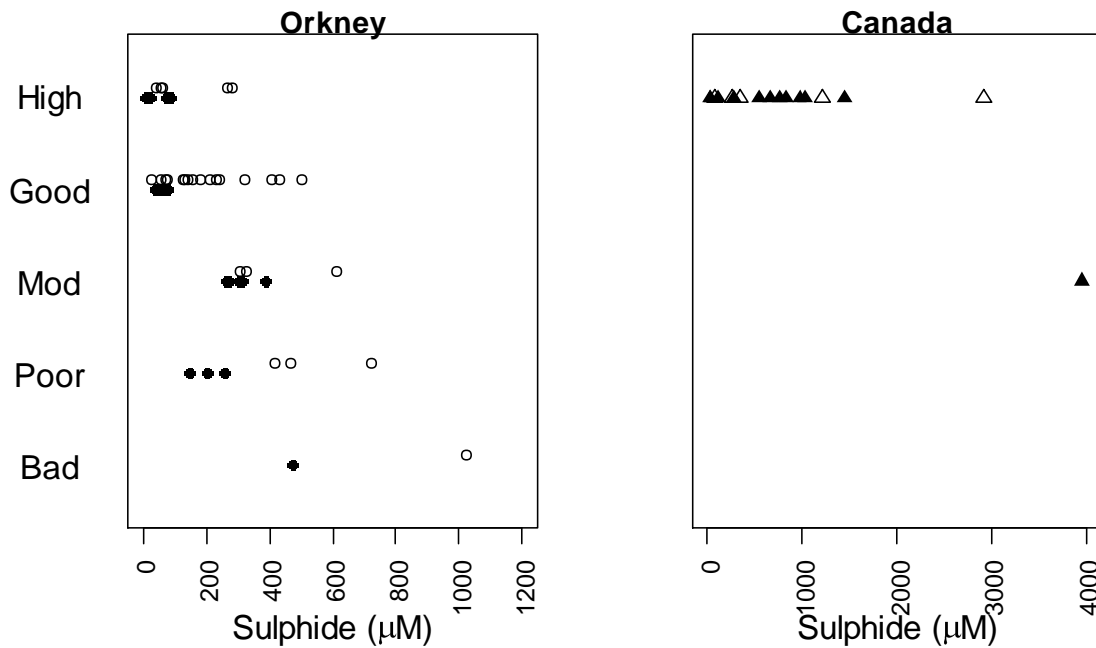


Figure 84: IQI ecological status from benthic grab samples plotted against sulphide levels measured at Orkney sites (Quanterness closed circles, and Bay of Meil open circles) and Nova Scotian sites (Shelburne Bay and open triangles, and Port Mouton closed triangles).

We conclude that whilst benthic infaunal impacts are undoubtedly related to sediment sulphide concentrations, based on data from the Orkney sites, it may be difficult to predict more finely resolved IQI levels with high confidence, particularly when sulphide concentrations are in the intermediate range (approximately 200 – 1500 µM). In contrast, acceptable IQIs seemed to occur up to very high sulphide concentrations at the Nova Scotian sites studied. The reasons for this difference are unclear but may merit further investigation. Some further research may also be justified using recent advances in sulphide analytical methods which could improve the precision of sulphide measurements (Cranford *et al.*, 2020). However, it should be noted that sulphides used for regulatory purposes in Canada are divided into broad categories (Nova Scotia Fisheries and Aquaculture 2021) which captures the imprecise nature of using sulphide as a basis for assessing biological impact.

Finally, we considered how a diagenetic module might be incorporated into NewDEPOMOD adding the ability to predict sediment sulphides. Such a development raises several technical issues, particularly regarding potential impacts on model run-times over larger spatial grids. We conclude that further software developments on a sulphide module are probably not justified at this time, given the uncertainties on the infaunal prediction skill from sulphide

measurements in the field, and whether SEPA would accept sulphide measurements as part of Scottish fish farm monitoring. However, if further research were to resolve these issues, then model development in relation to adding a diagenetic process module to NewDEPOMOD should be revisited. A diagenetic model is also being developed for a new Canadian depositional modelling framework based on Bravo and Grant (2018) and Cubillo et al. (2016).

6.2. Discussion on the practicalities of making sulphide measurements at Scottish fish farms

Although we were able to make sulphide measurements using facilities available at Cooke Aquaculture farms in Orkney, all the analytical methods available require wet chemistry. Some of the chemicals required are toxic meaning it may be difficult to handle them on typical farms unless a trained chemist is available. Preservation of pore water samples using zinc acetate with subsequent laboratory analysis using the methylene blue method may be another option which could be more practical in that much of the health and safety and need for specialised analytical equipment (UV spectrophotometer) would be removed from the farms themselves (Cranford *et al.*, 2020). However, the methylene blue method is not as sensitive as direct measurements on fresh samples which may raise further issues in relating sulphide measurements to IQI status.

Sulphide measurements made at Quanterness suggested large variability in results between samples collected at spring and neap tides. This is not surprising given that the balance between aerobic and anaerobic microbial activity will be related to oxygen availability, which in turn will be related to near-bed water current speeds and that the penetration depth of reoxygenation is likely to be greater in coarser, as opposed to fine-grained muddy, sediments. Determining the average sulphide status at a location, which might be expected to be related to biological community impacts, is thus likely to require sampling at different states of the tidal cycle.

Results from Quanterness and Bay of Meil showed quite variable relationships with infaunal ecological quality (IQI), especially at intermediate sulphide concentrations (200 – 1500 μM). Whilst some of this variability may derive from the use of the ion-selective electrode method for quantifying the sulphides, there is likely to be considerable inter-site variability in how biological communities react to sulphides (Cranford *et al.*, 2020). Published Canadian results (Figure 85) shows a similar S-shaped relationship between free sulphides when measured using the UV spectrophotometric method and macrofauna taxa richness (Cranford *et al.*, 2020). That paper did not calculate ITI or IQI but those metrics are strongly related to taxa richness in particular. This implies that the method will require testing across a wide range of sites and conditions if it were to be incorporated into Scottish fish farm monitoring.

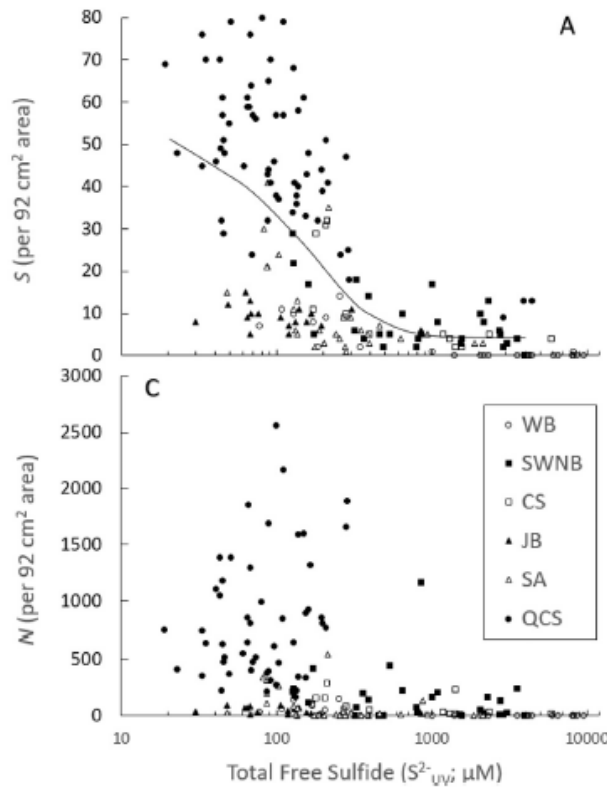
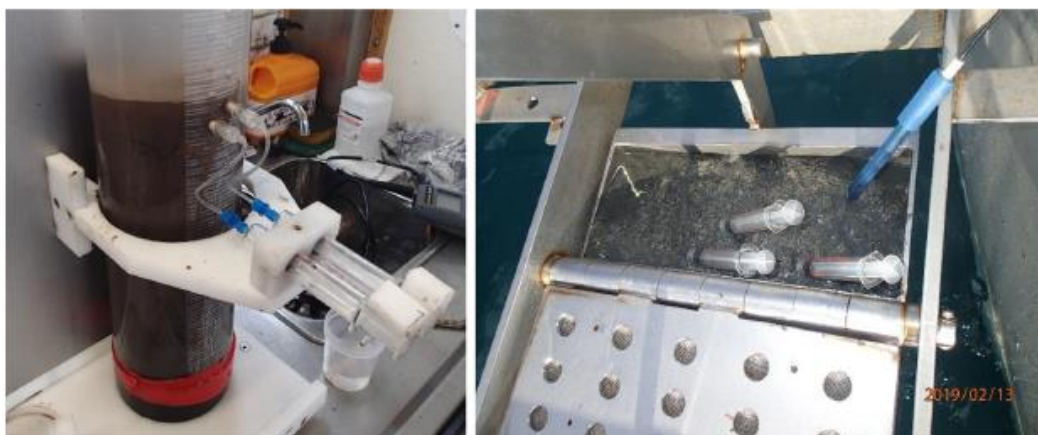


Figure 85: Relationship between total free sulphide and benthic macrofauna richness (S) and total organism abundance (N) as measured at coastal aquaculture sites. Note these included rainbow trout and mussel sites as well as salmon farms. From Cranford et al. (2020).

Quite a high proportion of the syringe cores collected in Orkney contained excessive seawater because of the coarse sediment which made it difficult for the divers to vertically insert the syringes. Collection of sediment for quantifying sulphides using a van-Veen grab was more reliable although grabs were not always full, a common issue when sampling coarser sediments using this equipment. For high quality sampling of coarser sediments for scientific research, material is usually collected using box corers. However, these are considerably heavier and more difficult to deploy and beyond the equipment available at most fish farms. Although the review by Narayanaswamy et al. (2016) is focussed on deep-water sampling, the discussion presented is also relevant to sampling sediments in shallower waters. Cranford et al. (2020) described a ‘Slo-corer’ which was used to obtain sediment cores without disturbing the sediment-water interface, but they also showed that acceptable data could be obtained from van Veen grabs (Figure 86).



*Figure 86: Extraction of pore-water for total free sulfide analysis from Slo-core samples (left; 1- and 2-cm depth) and grabs (right; 0 to 2 cm depth) by inserting RhizoCera into the sediment and applying a vacuum with a syringe. Pore-water for analysis was obtained from inside the RhizoCera as opposed to from inside the syringe to avoid atmospheric or metal (spring) contact. The ORP probe is visible in the grab sample at right. From Cranford *et al.* (2020).*

The approach could therefore be trialled as part of the standard benthic monitoring undertaken at Scottish fish farms but collecting pore water samples would increase the time required for conducting a benthic survey, perhaps by ten minutes per grab. Given that SEPA's enhanced benthic monitoring now requires many more stations to be sampled, any increase in time required to conduct a benthic survey might prove unattractive from the fish farm manager's perspective unless the additional measurements were proven and accepted to save time and money in the complete sample analysis cycle.

6.3. Discussion on including a diagenetic module in NewDEPOMOD

Several spatially resolved ecosystem models incorporating pelagic-benthic coupling have been developed. An example is the European Regional Shelf Seas model (Figure 87). However, although this model includes representation of aerobic and anaerobic microbial processes, it does not explicitly track sulphide species. Given the reasonably short time that fish faeces and feed pellets spend in the water column it is probably un-necessary to consider the water column processes, at least during the initial descent phase. Several more detailed models focussed on the benthic processes have been produced (Brigolin *et al.*, 2009; Bravo and Grant, 2018), and it is these which would likely form the basis for any incorporation of diagenesis into NewDEPOMOD.

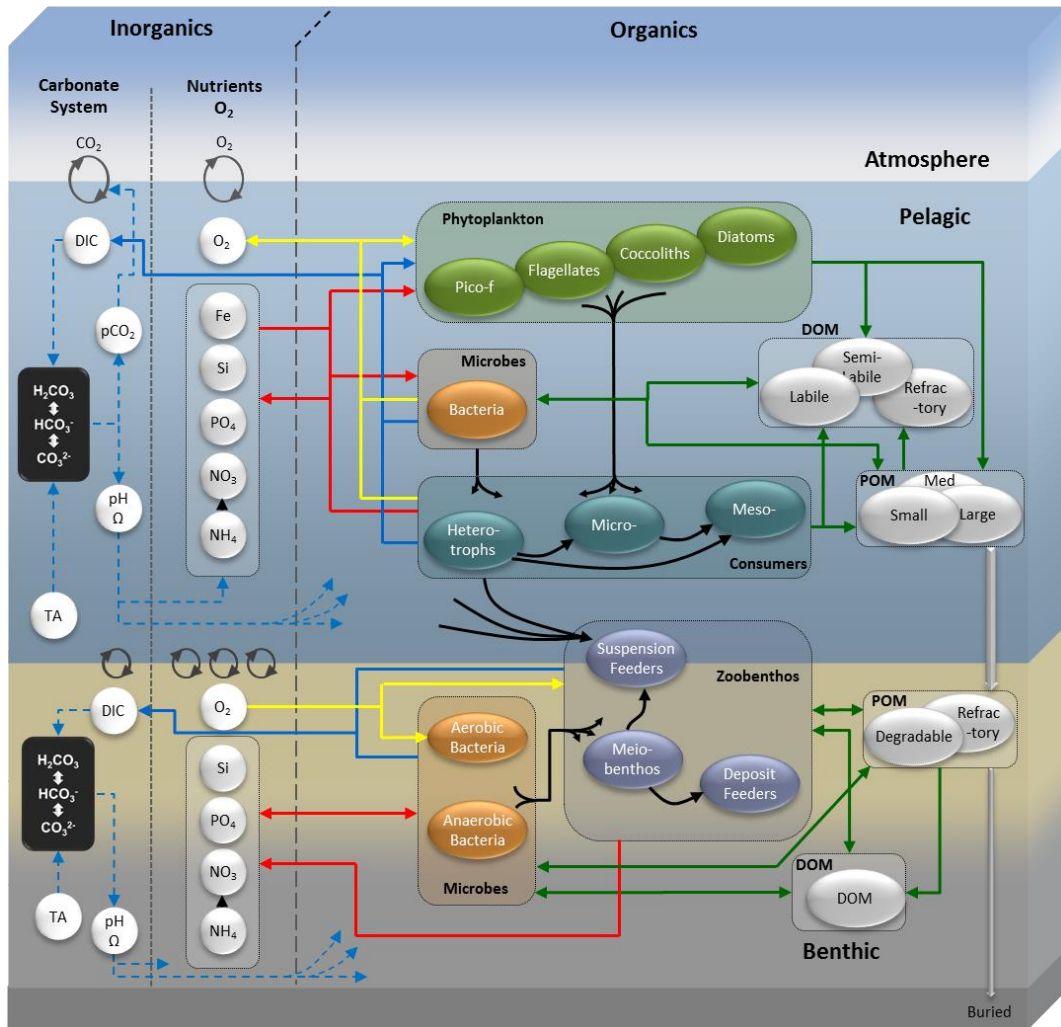


Figure 87: Graphical representation of the European Regional Shelf Ecosystem Model (ERSEM) from Plymouth Marine Laboratory.

NewDEPOMOD simulates the release of particles (feed and fish faeces) into the water column over time over a 2D horizontal grid. The grid is typically set up to be equivalent to 2 x 2 km with 25 m resolution. The particles are tracked as they settle and are affected by water flow and turbulence. Once settled they remain as particles for a period during which they may be moved by bottom currents, roll down slopes etc. Thereafter the particles become consolidated into the top layer of the bed. The particles contain a small number of different mass fractions - namely: total mass, un-degraded carbon, degraded and un-degraded treatment chemicals. These same mass fractions are also tracked after the particles are consolidated into the bed. The bed model consists of several sediment layers (typically 3 – 10). As more mass is added by deposition (to the top layer), the lower layers become compacted and are given a higher τ_c value (erosion threshold). The top layer can be eroded if the shear stress exceeds the current τ_c of that layer and sediment particles can then be transported to nearby cells (carrying the appropriate mass fractions with them). When these land, they are immediately consolidated into the top layer in the new cell. Once the top layer mass reaches a threshold it is pushed down, as are all lower layers and a new top layer is created with any remaining mass dumped into it. Each timestep (typically 1 minute) the layer mass fractions can be degraded, in effect some mass may move between un-degraded and degraded fractions using an exponential decay type relationship, currently this only occurs for treatment chemicals. At the end of the run, and on each timestep, the content of the top layer is available as a map of deposition of the different

mass fractions over the domain. The mass profile through the layers is also available but not generally output.

Diagenetic models typically simulate the relative quantities of the vertical movements through the sediment, and the chemical transitions of up to 14 – 17 chemical species via partial differential equations and reaction rates. For examples, see Bravo and Grant (2018), Brigolin et al. (2009) and Brigolin et al. (2009). The primary inputs are the time and space dependent fluxes of organic carbon from the fish farm and ambient quantities of primary reactants in both the water column and seabed. At present NewDEPOMOD does not simulate diagenetic processes in this manner but uses simple bulk decays as described above.

The first major point is that incorporating such a diagenetic model directly into NewDEPOMOD would slow model run-times to the point where the model would be for all practical purposes rendered useless. This is because of the number of additional computations which would be required at each timestep. The effect on runtime would be several orders of magnitude (typically: 4 x number of chemical species, 6 x timesteps, 6 x layers \approx 150 x). However, a separate standalone diagenetic module might be feasible, but this would depend on how much interaction is needed between the two models. Two potential schemes would be:-

1. Run NewDEPOMOD to completion and pass the quantities of carbon flux in each cell at each layer (perhaps split by timestamp) across to the diagenetic module to use, passing the results back to NewDEPOMOD to modify its final carbon amount(s). This is the approach taken in what is done in the Brigolin (2009) (though they did not feed results back to DEPOMOD).
2. Run NewDEPOMOD one timestep at a time. At each timestep, pass across the current flux of carbon (different carbon fractions?) onto the seabed per xy-cell/z-layer. Because of the chemical reactivities, the diagenetic module has to run using shorter timesteps and then passes the results back to NewDEPOMOD to modify its carbon amounts in each cell/layer. The erosion, resuspension and compaction process models are then run before looping to the next timestep.

During the bed-model processing, NewDEPOMOD has a slot for carrying out bioturbation – though this is an empty implementation at present, this might be a useful hook for launching this operation, alternatively extra slots could be added into the bed-model processing sequence.

Modifying NewDEPOMOD to include another 14 – 17 species to track the various chemicals would be a major structural change, so it might be better to let a separate diagenetic module handle this.

There are different sorts of carbon, labile and refractory so NewDEPOMOD would have to keep track of these, rather than just the single un-degraded carbon quantities as initially incorporated in the feed/faeces. One might need to distinguish between different forms of carbon in the feed/faeces particles as well as the bed layers.

It is unclear whether reactions would need handling while particles are settling or just when they are on the seabed. For shallower waters, settlement is likely sufficiently rapid that the latter is sufficient, for very deep sites the importance of in water column processes is largely unknown. If the latter, then the diagenetic module does not have to consider particles in flight and just needs the seabed info on carbon flux from NewDEPOMOD.

This consideration of coupling raises a number of issues if one assumes that the diagenetic module would be based on something like the Brigolin (2009) or Bravo and Grant (2018) models:-

1. Because of chemical reaction rates the diagenetic model would use a timestep of 10 s to capture the dynamics whereas NewDEPOMOD typically uses 60 s.
2. The diagenetic models would use 60 very thin layers (2.5 mm) at surface, NewDEPOMOD uses 3 – 10 layers of typically 2.0 to 5.0cm.
3. The diagenetic model tracks 14 or more species with reactions, NewDEPOMOD tracks (currently) 4 with no reactions.
4. The diagenetic model has feeding tied to tidal flow cycle, NewDEPOMOD has fixed periodic feeding.

There are several possible modifications which could be made to NewDEPOMOD to facilitate model coupling.

1. Change the release of fish feed to set times rather than as a continuous process. Faeces are also generated only at feed times.
2. Generate faeces at feed times and thereafter at some rate which is time dependent, increasing after feeding to max at T_p then decays at some rate λ , carbon deposition is therefore not continuous or limited to unrealistic very short bursts.
3. Such changes to the organic carbon release would also have to modify the initial quantities of in-feed chemicals with time.
4. Some additional chemical species may have to be transported in the feed and faeces. Consideration has to be given as to whether the chemical species just settle embedded within the feed/faeces particles or whether do they react with ambient chemical species in water column. In the simpler case the time dependent carbon deposition flux(x, y, t) from NewDEPOMOD and known fractions $frac_a$ of other species (a) is modified relatively simply.
5. In case that reactions in the water column must be included then $chem_{a_at_bed} = carbon_{released} * frac_a * (1 - \beta_a(T)*dt)$ where T : temperature; dt : fall time; $frac_a$: fraction of chemical species a in feed/faeces pellet; $chem_{a_at_bed}$: amount of chemical species a at the sea bed; $carbon_{released}$: amount of carbon released in feed faeces in cage; β_a : loss rate of species a as function of T (will vary through water column for deep sites and may depend on ambient quantities of reacting species).
6. Reactions in the consolidation / bed processes are where large changes in code would be required. The diagenetic models carry out chemical equation modelling for short timestep(s) mainly in the top sediment layers but over multiple thinner layers compared with NewDEPOMOD.
7. Ultimately the amount of carbon lost to respiration needs to be fed back to NewDEPOMOD to correct the settled pool for respiration. Because these more complex chemical processes also affect the carbon composition (balance of labile to refractory material) NewDEPOMOD would have to track at least one more carbon type than in the current version.
8. Lateral transport may be an issue if chemical species diffuse horizontally at very different rates. One may have to assume that grid cells are sufficiently large that horizontal diffusion is negligible compared to vertical processes.
9. The diagenetic model requires several additional environmental inputs compared with NewDEPOMOD. These include ambient O_2 itself dependent on current speed/turbulence,

ambient levels of the various reactants in the seabed, especially in the top layer; ambient temperature (and depth/time profile in water column) which affects chemical reaction rates; physical characteristics of seabed (some of which are already in NewDEPOMOD) but adding bioturbation and microbial parameters.

As previously mentioned, adding a diagenetic module would involve a large increase in the number of computations required at each timestep. It would therefore need to be developed using a fast compiled language such as C/C++ or FORTRAN. NewDEPOMOD is written in Java which has advantages for web-based delivery but would not be suitable for a diagenetic module due to its relatively slow speed. There are various communication mechanisms available to accomplish this. Operating across Java/C/C++ is common practice, but the situation regarding FORTRAN is less clear. There are numerous additional technicalities which would need to be explored before any software development work commenced.

Given all these issues, should the industry and regulators wish development of a diagenetic module for NewDEPOMOD to be progressed, this would require a well-structured and phased approach using modern software project management approaches. At this time, we cannot give a cost estimate for such a project, but it would be higher than for a moderate revision to NewDEPOMOD code.

7. Recommendations

7.1. Recommendations for future work from the INCREASE project

- a) The results from the INCREASE field studies have confirmed that particle resuspension as encoded in NewDEPOMOD remains problematic when modelling higher energy sites and the present configuration requires *ad hoc* fixes to reduce levels of particle dispersion. A possible cause of the problems is the use of a single value for bed shear-stress across the model domain (although other factors may also be important). Based on reported literature results, it seems likely that organic waste is more easily eroded from heavily enriched areas but becomes harder to resuspend when dispersed onto less enriched areas. The changes in critical shear stress are likely related to the increased bed roughness of less heavily impacted areas and this will have more impact when material is settled onto coarser sediments. This leads to a recommendation that NewDEPOMOD code should be reviewed to evaluate the feasibility of allowing critical bed shear stress to be related to the seabed type plus the degree of organic enrichment within each model cell. This will then require further testing to establish if this leads to improved model predictions of waste dispersal at more energetic sites.
- b) The use of sediment boxes to directly measure net (considering resuspension) organic carbon deposition appeared reasonably successful in that the results seem credible. The technique could be applied at additional farm sites to generate more measurements across a wider range of site conditions for direct comparison with predictions from NewDEPOMOD (or other particle dispersal modelling tools). However, the technique does have some serious limitations, especially regarding maximum deployment depth by divers using compressed air equipment. Furthermore, in any future studies, additional traditional design sediment traps should also be deployed for comparison, and one or two reference sites included to confirm background organic carbon deposition rates.

7.2. Recommendations for future work from the NAMAQI Project

- c) Sulphide measurements from two sites, Quanterness and Bay of Meil showed some relationships with benthic community impacts as assessed using the Infaunal Quality Index (IQI). However, there was considerable overlap of sulphide concentration ranges with IQI status suggesting that predicting status from sulphide concentration alone may be challenging. This conclusion agrees with previous published data from Black and Nickell (2014) who compared sulphide measurements with ITI at several Scottish fish farms and showed similar overlaps in biological response in the intermediate sulphide range (~200 – 1500 μM).
- d) Although sulphide does not appear to allow discrimination between ‘Moderate’, ‘Poor’ and ‘Bad’ IQI status at intermediate concentrations, sulphide measurements may nonetheless be useful to farm managers as a quick indication of stations which are highly likely to pass i.e. achieve ‘Good’ or ‘High’ ecological status (sulphide < 200 μM) or fail i.e. ‘Poor’ ecological status (sulphide > 1500 μM). This could potentially allow rapid screening of grab samples so that taxonomic or other forms of more costly analysis could be focussed on samples with intermediate sulphide status (which is the range within which the boundary of the permitted mixing zone is likely to lie). However, because of the lack of fine discriminatory power in relation to IQI states, sulphide measurements are unlikely to provide a realistic complete replacement for infaunal taxonomic analyses as required by SEPA. A further review of categorical approaches to sulphide as a monitoring tool as used in Nova Scotia is warranted.

- e) Whilst measurement of sulphides on farm sites was demonstrated to be achievable using the ion-specific electrode (ISE) approach, the method is not without problems. Achieving accurate results requires careful maintenance and calibration of the probes and a recent study claims the method is less accurate than direct quantification of sulphides by UV-absorption (Cranford *et al.*, 2020). We cannot therefore recommend the ISE approach as *an easy, rapid and reliable method* for evaluating benthic community status on Scottish fish farms although it continues to be used in monitoring benthic condition at Canadian fish farms. Within Canada, this analytical issue is being reviewed by the Department of Fisheries and Oceans (DFO) considering the large amount of sulphide data collected historically using the ISE method.
- f) Further field work at Scottish fish farms should thus explore the application of the recently published spectrophotometric methods described by Cranford *et al.* (2017, 2020 #11968). These methods may improve the accuracy of sulphide measurements compared with the ion-selective electrode (ISE) approach but would require additional equipment (UV-spectrophotometer) to be available at fish farm sites if analyses were to be performed on-site. Alternatively, samples may be preserved with zinc acetate and subsequently analysed using the methylene blue method, although this technique is not as sensitive as measuring UV-absorption on fresh samples. These approaches could potentially improve analytical precision and thus might improve discrimination between IQI status levels of benthic grab samples based on sulphide measurements. However, it must be cautioned that evidence to date suggests that biological responses to sediment sulphides appear to be quite variable and site specific (Chang *et al.*, 2013), especially when sulphide levels are in the intermediate range (~200 – 1500 μM). There also seemed to be large differences between IQI response to sulphides at Canadian sites when compared to the Orkney data suggesting that the ecological community response to sulphides may be quite variable. The method would thus require extensive calibration against IQI for use within the Scottish regulatory framework.
- g) Further work on sulphides could be piggybacked on existing SEPA compliance monitoring to reduce costs but the equidistant sampling designs used are not ideal as they tend to lead to an unbalanced number of samples at each IQI state. Additional sampling for sulphides (and using sediment traps if deployed) would therefore probably be required to fully investigate the relationships between sulphide concentrations, IQI, sediment type and other site-specific factors. Log-distance sampling designs (for example Figure 8) may be preferable to account for the usual exponential decline in organic waste deposition with distance from the cage edge.
- h) Development of a diagenesis sulphide module into NewDEPOMOD would be achievable but would require a dedicated software development project. We suggest that it may be more sensible to focus initially on recommendation (f), because we cannot yet say how useful fish farm sulphide measurements would be in the context of the Scottish regulatory framework.

8. Acknowledgements

The authors wish to thank:-

- Malakoff Diving Services who deployed and recovered the sediment boxes often under challenging conditions.
- Mr John Green (University of Essex) for running the carbon analyses.
- Prof. Mark Inall for kindly providing a Matlab script for extracting residual currents from ADCP timeseries. The approach uses tidal predictions produced by the Matlab Tidal Analysis Toolbox, Version 1.3b (Pawlowicz *et al.*, 2002).
- The management and administration team at SAIC for their support and understanding in relation to delays and difficulties experienced with the INCREASE and NAMAQI projects due to the Covid pandemic.
- Dr. Lin Lu for faunal analysis of Canadian benthic samples and Hart Keopke for his assistance in the field and laboratory work.
- J. Grant was supported via a Collaborative Research and Development Grant from the Canadian Natural Sciences and Engineering Research Council (partnership with Cooke Aquaculture, Canada).

Appendix 1: Expanded normative definitions of the different Ecological Quality Status levels for coastal waters (EUNIS Habitat A.4 sublittoral sediments). Reproduced from Phillips et al. (2014).

Quality status	Normative definition	Expanded interpretation
High	<p>Level of diversity and abundance of invertebrate taxa is within the range normally associated with undisturbed conditions.</p> <p>All disturbance-sensitive taxa associated with undisturbed conditions are present.</p>	<p>Invertebrate community shows no anthropogenic impact.</p> <ul style="list-style-type: none"> • Species richness and diversity high (for example, number of species, Shannon, Fisher, Margalef and Brillouin diversity indices) • Evenness high (Heip and Pielou indices); abundance ratio (abundance/number of taxa) low • Taxonomic range high (taxonomic diversity, distinctness, and breadth indices) • Community abundances (assessed by AMBI) – normal, unpolluted: <ul style="list-style-type: none"> • sensitive taxa (EGI) of dominant abundance • indifferent and tolerant taxa (EGII and EGIII) absent or of sub-dominant abundance • opportunistic taxa (EGIV) absent or of negligible abundance • indicator taxa (EGV) absent or of negligible abundance • Trophic structure (assessed by ITI) – normal: <ul style="list-style-type: none"> • dominated by water column and interface detritus feeders • Abundance of important characterising, structural or functional species unimpacted (for example, seapens or burrowing decapods, large bivalves)
Good	<p>Level of diversity and abundance of invertebrate taxa is slightly outside the range associated with the type-specific conditions.</p> <p>Most of the sensitive taxa of the type-specific conditions are present.</p>	<p>Invertebrate community shows slight anthropogenic impact.</p> <ul style="list-style-type: none"> • Species richness and diversity slightly reduced (for example, Shannon, Fisher, Margalef and Brillouin diversity indices) • Evenness slightly reduced (Heip and Pielou indices); abundance ratio slightly elevated • Taxonomic range slightly reduced (taxonomic diversity, distinctness, and breadth indices) • Community abundances (assessed by AMBI) – slightly unbalanced, slightly polluted: <ul style="list-style-type: none"> • sensitive taxa (EGI) abundance may range from high sub-dominant to absent • indifferent taxa (EGII) of low sub-dominant abundance • tolerant taxa (EGIII) of dominant abundance • opportunistic taxa (EGIV) and indicator taxa (EGV) abundance may range from negligible or low to equi-abundance with indifferent taxa • Trophic structure (assessed by ITI) – normal or slightly changed: <ul style="list-style-type: none"> • dominated by detritus and deposit feeders • Abundance of important characterising, structural, or functional species slightly reduced (for example, seapens or burrowing decapods, large bivalves)

Appendix 1: Expanded normative definitions of the different Ecological Quality Status levels for coastal waters (EUNIS Habitat A.4 sublittoral sediments). Reproduced from Phillips et al. (2014).

Quality status	Normative definition	Expanded interpretation
Moderate	<p>Level of diversity and abundance of invertebrate taxa is moderately outside the range associated with the type-specific conditions. Taxa indicative of pollution are present. Many of the sensitive taxa of the type-specific communities are absent.</p>	<p>Invertebrate community shows moderate anthropogenic impact.</p> <ul style="list-style-type: none"> • Species richness and diversity moderately reduced (for example, number of species, Shannon, Fisher, Margalef and Brillouin diversity indices) • Evenness moderately reduced (Heip and Pielou indices); abundance ratio moderately elevated • Taxonomic range moderate reduced. (taxonomic diversity, distinctness, and breadth indices) • Community abundances (assessed by AMBI) – transitional unbalanced to moderately polluted: • sensitive taxa (EGI) of negligible abundance or absent • indifferent taxa (EGII) of low sub-dominant abundance • tolerant taxa (EGIII), opportunistic taxa (EGIV) and indicator taxa (EGV) co- dominate the abundance • Trophic structure (assessed by ITI) – shows moderate change: • dominated by interface deposit feeders • Abundance of important characterising, structural or functional species moderately reduced. Some key species of negligible abundance or absent (for example, seapens or burrowing decapods, large bivalves)
Poor	<p>Waters showing evidence of major alterations to the values of the biological quality elements for the surface water body type and in which the relevant biological communities deviate substantially from those normally associated with the surface water body type under undisturbed conditions.</p>	<p>Invertebrate community shows major anthropogenic impact.</p> <ul style="list-style-type: none"> • Species richness and diversity shows major reduction (for example, number of species, Shannon, Fisher, Margalef and Brillouin diversity indices) • Evenness shows major reduction (Heip and Pielou indices); abundance ratio shows major elevation • Taxonomic range shows major reduction. (taxonomic diversity, distinctness, and breadth indices) • Community abundances (assessed by AMBI) – transitional moderately to heavily polluted: • sensitive and indifferent taxa (EGI and EGII) of negligible abundance or absent • tolerant taxa (EGIII) of sub-dominant abundance • opportunistic taxa (EGIV) and indicator taxa (EGV) co-dominate the abundance. • Trophic structure (assessed by ITI) – shows major change or degradation: • dominated by interface and subsurface deposit feeders • Abundance of important characterising, structural, or functional species shows major reduction. Many key species of negligible abundance or absent (for example, seapens or burrowing decapods, large bivalves)

Appendix 1: Expanded normative definitions of the different Ecological Quality Status levels for coastal waters (EUNIS Habitat A.4 sublittoral sediments). Reproduced from Phillips et al. (2014).

Quality status	Normative definition	Expanded interpretation
Bad	Waters showing evidence of severe alterations to the values of the biological quality elements for the surface water body type and in which large portions of the relevant biological communities normally associated with the surface water body type under undisturbed conditions are absent.	<p>Invertebrate community shows severe anthropogenic impact.</p> <ul style="list-style-type: none"> • Species richness and diversity shows severe reduction (for example, number of species, Shannon, Fisher, Margalef and Brillouin diversity indices) • Evenness shows severe reduction (Heip and Pielou indices); abundance ratio shows severe elevation • Taxonomic range severely reduced (Taxonomic diversity, distinctness, and breadth indices) • Community abundances (assessed by AMBI) – very heavily or extremely polluted: • azoic or if fauna present: <ul style="list-style-type: none"> – sensitive, indifferent and tolerant Taxa (EGI, EGII and EGIII) absent – opportunistic taxa (EGIV) of sub-dominant abundance – indicator taxa (EGV) of dominant abundance • Trophic structure (assessed by ITI) – shows severe degradation: • dominated by subsurface deposit feeders, or azoic • All important characterising, structural, or functional species of negligible abundance or absent (for example, seapens or burrowing decapods, large bivalves)

Appendix 2: Details of the sediment box layout and deployments at each study site.

Site	Deploy	Tides	Dates	Transect	Direction	Distance from cage edge (°)	Distance (m)	Lat (deg)	Lon (deg)
Bay of Vady	a	Neaps	07-14/05/2018	Red	287	0	59.13332	-2.93693	
	b	Springs	12-19/06/2018	Red	287	20	59.13337	-2.93727	
				Red	287	40	59.13342	-2.93760	
				Red	287	60	59.13347	-2.93793	
				Red	287	80	59.13350	-2.93827	
				Red	287	100	59.13355	-2.93860	
				Blue	301	0	59.13337	-2.93682	
				Blue	301	20	59.13347	-2.93712	
				Blue	301	40	59.13355	-2.93742	
				Blue	301	60	59.13365	-2.93772	
				Blue	301	80	59.13375	-2.93802	
				Blue	301	100	59.13383	-2.93832	
				White	321	0	59.13353	-2.93605	
				White	321	20	59.13368	-2.93627	
				White	321	40	59.13382	-2.93650	
				White	321	60	59.13397	-2.93672	
				White	321	80	59.13410	-2.93693	
				White	321	100	59.13423	-2.93715	
				Brown	356	0	59.13358	-2.93593	
				Brown	356	20	59.13377	-2.93597	
			Brown	356	40	59.13395	-2.93598		
			Brown	356	60	59.13413	-2.93602		
			Brown	356	80	59.13430	-2.93605		
			Brown	356	100	59.13448	-2.93608		
Quanterness	a	Neaps	31/05–07/06/2019	Blue	83	0	59.00868	-2.98353	
	b	Springs	10–17/06/2019	Blue	83	20	59.00870	-2.98320	
				Blue	83	40	59.00872	-2.98283	
				Blue	83	60	59.00877	-2.98250	
				Blue	83	80	59.00878	-2.98217	
				Blue	83	100	59.00880	-2.98182	
				Blue	83	120	59.00883	-2.98148	
				Blue	83	140	59.00885	-2.98113	
				Blue	83	160	59.00888	-2.98080	
				Red	152	0	59.00758	-2.98343	
				Red	152	20	59.00743	-2.98325	
				Red	152	40	59.00727	-2.98308	
				Red	152	60	59.00712	-2.98292	
				Red	152	80	59.00695	-2.98277	
				Red	152	100	59.00680	-2.98260	
				Red	152	120	59.00665	-2.98243	
				Red	152	140	59.00648	-2.98227	
				Red	152	160	59.00633	-2.98210	
				Green	242	0	59.00760	-2.98485	
				Green	242	20	59.00750	-2.98515	
			Green	242	40	59.00743	-2.98547		
			Green	242	60	59.00735	-2.98575		
			Brown	297	0	59.00920	-2.98492		
			Brown	297	20	59.00928	-2.98523		
			Brown	297	40	59.00937	-2.98555		
			Brown	297	60	59.00945	-2.98585		

Appendix 2: Details of the sediment box layout and deployments at each study site.

Site	Deploy	Tides	Dates	Transect	Direction	Distance from cage edge (°)	Distance (m)	Lat (deg)	Lon (deg)
Bay of Meil	a	Neaps	7–14/07/2021	Blue	116	0	58.99615	-2.89722	
				b	Springs	22–29/07/2021	Blue	116	10
	Blue	116	20	58.99607			-2.89692		
	Blue	116	30	58.99603	-2.89675				
	Blue	116	40	58.99598	-2.89660				
	Blue	116	50	58.99595	-2.89643				
	Blue	116	75	58.99585	-2.89605				
	Blue	116	100	58.99575	-2.89563				
	Red	193	0	58.99510	-2.89842				
	Red	193	10	58.99502	-2.89845				
	Red	193	20	58.99493	-2.89850				
	Red	193	30	58.99483	-2.89855				
	Red	193	40	58.99475	-2.89858				
	Red	193	50	58.99467	-2.89863				
	Red	193	75	58.99445	-2.89873				
	Red	193	100	58.99423	-2.89883				
	Green	295	0	58.99655	-2.89858				
	Green	295	10	58.99660	-2.89875				
	Green	295	20	58.99663	-2.89890				
	Green	295	30	58.99667	-2.89905				
	Green	295	40	58.99670	-2.89922				
	Green	295	50	58.99673	-2.89938				
	Green	295	75	58.99683	-2.89978				
	Green	295	100	58.99693	-2.90017				
	Brown	1	0	58.99752	-2.89738				
	Brown	1	10	58.99760	-2.89738				
	Brown	1	20	58.99770	-2.89737				
Brown	1	30	58.99778	-2.89737					
Brown	1	40	58.99787	-2.89737					
Brown	1	50	58.99797	-2.89737					
Brown	1	75	58.99818	-2.89735					
Brown	1	100	58.99842	-2.89733					

Appendix 3: Positions of benthic grabs collected at Bay of Vady. Note distances from cage edge are based on cages perimeter in 2018.

Grab code	Transect	Distance from cage edge (m)	Lat (deg)	Lon (deg)
WSW0	Green	10	59.13318	-2.93695
WSW25		40	59.13312	-2.93742
WSW50		65	59.13308	-2.93782
ENE25	Blue	50	59.13153	-2.93272
ENE50		77	59.13150	-2.93225
REF 1	Yellow	600	59.13813	-2.94228
REF 2		615	59.12672	-2.92650

*Appendix 4: Positions of benthic grabs collected at
Quanterness*

Grab code	Transect	Distance from cage edge (m)	Lat (deg)	Lon (deg)
T3 EE01	Blue	0	59.00867	-2.98342
T3 EE02		44	59.00847	-2.98277
T3 EE03		98	59.00833	-2.98185
T3 EE04		118	59.00837	-2.98145
T3 EE05		167	59.00830	-2.98062
T3 EE06		200	59.00840	-2.97997
T3 EE07		253	59.00832	-2.97907
T2 SE01	Red	0	59.00763	-2.98348
T2 SE02		60	59.00725	-2.98273
T2 SE03		111	59.00680	-2.98243
T2 SE04		165	59.00638	-2.98193
T2 SE05		217	59.00592	-2.98165
T2 SE06		275	59.00542	-2.98138
T2 SE07		319	59.00518	-2.98060
T4 WW01	Green	0	59.00820	-2.98485
T4 WW02		36	59.00803	-2.98538
T4 WW03		58	59.00805	-2.98582
T4 WW04		90	59.00807	-2.98640
T4 WW05		102	59.00798	-2.98657
T4 WW06		122	59.00792	-2.98690
T4 WW07		173	59.00798	-2.98783
T1 NN01	Brown	0	59.00925	-2.98457
T1 NN02		33	59.00948	-2.98425
T1 NN03		48	59.00965	-2.98437
T1 NN04		66	59.00982	-2.98432
T1 NN05		92	59.01003	-2.98423
T1 NN06		123	59.01033	-2.98430
T1 NN07		155	59.01063	-2.98427
Reference1	Yellow	509	59.01211	-2.99163
Reference2		503	59.00370	-2.98027

Appendix 5: Positions of benthic grabs collected at Bay of Meil.

Grab code	Transect	Distance from cage edge (m)	Lat (deg)	Lon (deg)
E0	Blue	0	58.99620	-2.89705
E25		25	58.99612	-2.89665
E50		55	58.99605	-2.89613
E75		76	58.99597	-2.89582
S0	Red	0	58.99503	-2.89835
S28		28	58.99480	-2.89850
S38		39	58.99470	-2.89853
S48		50	58.99462	-2.89863
S75		76	58.99440	-2.89883
S100		102	58.99418	-2.89900
S150		151	58.99375	-2.89927
S200		211	58.99323	-2.89952
W0		Green	0	58.99630
W25	26		58.99643	-2.89902
W50	50		58.99658	-2.89935
W100	101		58.99683	-2.90010
W150	152		58.99698	-2.90095
W200	203		58.99720	-2.90172
W250	274		58.99758	-2.90273
N0	Brown	0	58.99760	-2.89753
N25		23	58.99778	-2.89737
N50		51	58.99802	-2.89722
N75		80	58.99823	-2.89692
N100		102	58.99845	-2.89693
N150		151	58.99887	-2.89670
N200		208	58.99937	-2.89635
Ref 1	Yellow	480	58.99340	-2.90775
Ref 2		495	59.00212	-2.89815

Appendix 6: Results of PSA analysis of sediment core syringe samples collected at Bay of Vady. Mean percentage of particles by grain size based on duplicate syringe cores at each location. * indicates samples where the sediment name differed between the two duplicates, the differences being indicated by /.

Transect	Distance from cage edge (m)	Sediment	V Coarse sand	Coarse sand	Med sand	Fine sand	V Fine sand	V Coarse silt	Coarse silt	Med silt	Fine silt	V Fine silt	Clay
Red	0	Very coarse silty fine sand	0.0	0.0	5.9	54.7	23.1	5.1	4.6	3.2	2.1	0.6	1.0
Red	20	Moderately sorted fine sand	0.0	0.3	18.3	55.8	19.1	2.6	2.1	1.6	0.2	0.1	0.2
Red	40	Moderately sorted fine sand	2.0	4.2	20.2	51.4	16.9	1.9	1.4	1.1	0.4	0.3	0.4
Red	60	Poorly sorted fine sand	2.4	3.4	20.1	51.0	15.9	2.1	1.6	1.3	1.1	0.4	0.9
Red	80	Moderately sorted fine sand	2.2	1.9	22.7	52.1	15.4	2.0	1.6	1.2	0.4	0.2	0.4
Red	100	Moderately/Poorly sorted fine sand*	4.6	4.9	23.2	47.9	14.0	2.0	1.6	1.1	0.5	0.2	0.4
Blue	0	Very coarse silty fine sand	0.0	0.3	8.0	50.2	20.4	7.4	5.8	3.6	2.1	0.8	1.4
Blue	20	Very coarse silty fine sand	1.3	0.3	9.1	55.7	21.4	4.1	3.4	2.3	1.5	0.4	0.8
Blue	40	Moderately sorted fine sand	0.9	0.1	15.5	56.1	19.6	2.7	2.2	1.7	0.8	0.2	0.3
Blue	60	Very coarse/Moderately sorted fine sand*	0.6	3.7	14.0	51.5	18.8	2.8	2.5	2.3	2.2	0.7	1.0
Blue	80	Moderately sorted fine sand	0.0	0.0	18.3	55.5	19.6	2.5	1.9	1.5	0.9	0.1	0.0
Blue	100	Moderately/Poorly sorted fine sand	0.0	7.5	17.8	49.9	16.7	2.5	2.0	1.5	0.9	0.5	0.9
White	0	Very coarse silty fine sand	0.7	2.7	13.6	47.5	21.9	5.5	3.7	2.3	0.9	0.5	0.9
White	20	Very coarse silty fine sand	3.5	6.9	10.3	36.8	20.7	8.2	5.6	3.4	2.1	1.1	1.7
White	40	Very coarse silty fine sand	1.1	2.5	14.9	51.2	21.4	3.0	2.5	1.9	0.7	0.0	0.7
White	60	Poorly sorted fine sand	6.7	4.3	13.4	45.3	20.6	2.9	2.3	1.8	1.2	0.6	1.2
White	80	Moderately sorted fine sand	1.4	3.1	14.7	51.1	19.2	3.8	2.6	1.8	1.5	0.1	0.8
White	100	Moderately sorted fine sand	2.3	5.1	16.8	46.2	17.6	4.0	3.1	2.2	1.7	0.5	0.7

*Appendix 6: Results of PSA analysis of sediment core syringe samples collected at Bay of Vady. Mean percentage of particles by grain size based on duplicate syringe cores at each location. * indicates samples where the sediment name differed between the two duplicates, the differences being indicated by /.*

Transect	Distance from cage edge (m)	Sediment	V Coarse sand	Coarse sand	Med sand	Fine sand	V Fine sand	V Coarse silt	Coarse silt	Med silt	Fine silt	V Fine silt	Clay
Brown	0	Very coarse silty fine sand	1.1	4.8	8.5	36.7	19.6	11.1	7.6	4.5	3.0	1.1	2.3
Brown	20	Very coarse silty fine sand	2.7	3.6	18.0	47.1	18.0	3.1	2.6	2.1	1.6	0.6	0.9
Brown	40	Poorly sorted fine sand	1.8	6.8	23.8	43.9	16.0	2.4	2.1	1.8	1.5	0.1	0.0
Brown	60	Poorly sorted fine sand	1.4	21.6	18.5	36.9	14.1	1.8	1.5	1.4	1.2	0.6	1.2
Brown	80	Poorly sorted/Very coarse silty fine sand*	3.5	9.8	17.8	40.5	19.0	2.4	1.9	1.7	1.5	0.7	1.4
Brown	100	Very coarse/Moderately sorted fine sand*	1.4	4.1	16.7	42.7	22.2	3.9	3.2	2.6	1.7	0.6	1.0

Appendix 7: Results of POC analysis of sediment core syringe samples collected during the Bay of Vady fieldwork. Carbon results shown for each replicate syringe core and the mean and standard deviation of the duplicate measurements.

Transect	Distance from cage edge (m)	Syringe core 1 (% dry wt.)	Syringe core 2 (% dry wt.)	Mean (% dry wt.)	SD (% dry wt.)
Red	0	0.812	0.921	0.87	0.08
Red	20	0.437	0.549	0.49	0.08
Red	40	0.275	0.425	0.35	0.11
Red	60	0.545	0.349	0.45	0.14
Red	80	0.308	0.480	0.39	0.12
Red	100	0.311	0.687	0.50	0.27
Blue	0	1.299	1.190	1.24	0.08
Blue	20	0.976	0.708	0.84	0.19
Blue	40	0.508	0.526	0.52	0.01
Blue	60	0.501	0.436	0.47	0.05
Blue	80	0.414		0.41	
Blue	100	0.495	0.474	0.48	0.01
White	0	2.297	1.040	1.67	0.89
White	20	0.542	1.096	0.82	0.39
White	40	0.582	0.721	0.65	0.10
White	60	0.648	0.623	0.64	0.02
White	80	1.930	0.590	1.26	0.95
White	100	0.451	0.683	0.57	0.16
Brown	0	2.67	0.671	1.67	1.41
Brown	20	0.592	0.417	0.50	0.12
Brown	40	0.354	1.131	0.74	0.55
Brown	60	0.285	0.380	0.33	0.07
Brown	80	0.354	0.430	0.39	0.05
Brown	100	0.687	0.605	0.65	0.06

Appendix 8: Estimated organic carbon deposition rates (g m^{-2}) over the two, 7-day periods sediment boxes were deployed at Bay of Vady. Each box was analysed in triplicate (replicates 1 – 3).

Transect	Distance from cage edge (m)	Deployment a – Neap tides					Deployment b – Spring tides				
		Replicate			Mean	SD	Replicate			Mean	SD
		1 (g m^{-2})	2 (g m^{-2})	3 (g m^{-2})			1 (g m^{-2})	2 (g m^{-2})	3 (g m^{-2})		
Red	0	30.30	21.32	40.30	30.64	9.49	60.96	58.31	61.11	60.13	1.57
Red	20	39.53	47.30	51.16	46.00	5.92	53.87	47.19	60.47	53.84	6.64
Red	40	11.81	11.35	14.28	12.48	1.58	46.10	44.60	39.81	43.50	3.28
Red	60	4.30	3.90	3.29	3.83	0.51	Box not recovered				
Red	80	127.73	94.23	97.87	106.61	18.38	2.87	9.65	2.87	5.13	3.91
Red	100	0.00	0.00	0.00	0.00	0.00	3.08	2.69	3.20	2.99	0.26
Blue	0	170.43	185.27		177.85	10.49	22.91	26.45	21.39	23.58	2.59
Blue	20	35.35	30.85	38.89	35.03	4.03	13.45	11.26	12.61	12.44	1.11
Blue	40	9.45	10.37	12.95	10.92	1.81	15.13	13.84	21.09	16.68	3.87
Blue	60	9.53	4.92	4.32	6.26	2.85	Box not recovered				
Blue	80	Box not recovered					0.16	0.99	0.48	0.54	0.42
Blue	100	2.71	3.10	3.16	2.99	0.24	260.20	290.55	364.69	305.15	53.75
White	0	63.85	96.48	136.51	98.94	36.39	Box not recovered				
White	20	145.36	119.29	130.55	131.73	13.07	10.39	9.68	8.02	9.36	1.21
White	40	Box not recovered					28.85	20.12	22.91	23.96	4.46
White	60	7.03	11.82	7.76	8.87	2.58	3.81	4.66	4.27	4.24	0.43
White	80	3.83	2.17	1.08	2.36	1.38	Box not recovered				
White	100	4.43	3.46	2.01	3.30	1.21	3.82	2.55	2.37	2.91	0.79

Appendix 8: Estimated organic carbon deposition rates (g m^{-2}) over the two, 7-day periods sediment boxes were deployed at Bay of Vady. Each box was analysed in triplicate (replicates 1 – 3).

Transect	Distance from cage edge (m)	Deployment a – Neap tides					Deployment b – Spring tides				
		Replicate			Mean	SD	Replicate			Mean	SD
		1 (g m^{-2})	2 (g m^{-2})	3 (g m^{-2})			1 (g m^{-2})	2 (g m^{-2})	3 (g m^{-2})		
Brown	0	17.35	21.34	17.20	18.63	2.35	8.20	13.54		10.87	3.78
Brown	20	0.59	2.96	3.76	2.44	1.65	59.84	83.77	70.26	71.29	12.00
Brown	40	1.80	2.77	3.46	2.68	0.84	Box not recovered				
Brown	60	4.77	5.29	5.01	5.02	0.26	Box not recovered				
Brown	80	3.34	3.92	5.44	4.23	1.08	11.15	14.36	11.12	12.21	1.86
Brown	100	16.37	15.31	16.62	16.10	0.70	6.29	7.64	5.44	6.46	1.11

Appendix 9: Results of PSA analysis of sediment core syringe samples collected at Quanterness. Mean percentage of particles by grain size based on duplicate syringe cores at each location. * indicates samples where the sediment name differed between the two duplicates, the differences being indicated by /.

Transect	Distance from cage edge (m)	Sediment	V Coarse sand	Coarse sand	Med sand	Fine sand	V Fine sand	V Coarse silt	Coarse silt	Med silt	Fine silt	V Fine silt	Clay
Blue	0	Very coarse silty fine sand	1.3	3.3	16.1	50.2	15.1	5.5	3.6	2.1	1.5	0.6	0.9
Blue	20	Very coarse silty fine sand	3.3	7.7	15.8	45.2	15.2	3.9	3.3	2.3	1.5	0.8	1.4
Blue	40	Very coarse silty fine sand	0.9	3.4	8.8	46.1	19.6	6.0	5.4	3.7	2.9	1.1	2.3
Blue	60	Very coarse silty fine sand	1.1	3.6	14.1	51.5	17.0	3.7	3.1	2.4	2.0	0.6	1.2
Blue	80	Very coarse silty/Moderately sorted/ fine sand*	0.0	1.4	17.2	55.1	16.8	3.3	2.9	2.0	0.9	0.2	0.4
Blue	100	Very coarse silty fine sand	1.1	5.4	16.7	48.8	15.7	3.6	3.0	2.3	2.0	0.7	1.2
Blue	120	Poorly sorted fine sand	1.2	7.4	9.0	49.7	13.9	2.9	2.4	1.9	1.0	0.5	0.9
Blue	140	Very coarse silty fine sand	0.4	5.2	14.8	45.7	16.8	4.6	4.1	3.2	2.6	1.1	1.8
Blue	160	Very coarse/Fine/ silty fine sand*	0.0	4.5	13.7	42.6	15.5	5.0	5.2	4.9	4.3	1.8	2.9
Red	0	Very coarse silty fine sand	0.9	10.9	17.5	44.1	13.3	5.1	3.4	2.0	1.3	0.6	1.1
Red	20	Very coarse silty fine sand	0.0	2.6	13.1	51.9	18.9	5.6	3.6	2.0	1.2	0.4	0.8
Red	40	Very coarse silty fine sand	0.3	0.6	7.4	56.3	22.5	4.7	3.6	2.0	1.2	0.6	1.0
Red	60	Very coarse silty fine sand	0.9	1.8	9.0	50.5	20.9	5.5	4.2	2.7	2.1	0.9	1.7
Red	80	Very coarse silty fine sand	0.5	0.6	8.0	53.3	24.9	4.6	3.2	2.0	1.3	0.7	1.2
Red	100	Very coarse silty fine sand	2.3	2.7	5.9	47.4	24.4	6.8	4.6	2.8	2.1	0.5	0.8
Red	120	Very coarse silty fine sand	3.9	5.2	11.4	47.0	21.6	3.4	2.6	1.9	1.5	0.6	1.1
Red	140	Very coarse silty fine sand	0.4	4.4	11.2	42.0	23.8	6.1	4.4	3.1	2.3	0.9	1.6
Red	160	Very coarse silty fine sand	1.6	5.1	12.3	46.6	22.3	3.7	2.9	2.3	1.5	0.7	1.3

*Appendix 9: Results of PSA analysis of sediment core syringe samples collected at Quanterness. Mean percentage of particles by grain size based on duplicate syringe cores at each location. * indicates samples where the sediment name differed between the two duplicates, the differences being indicated by /.*

Transect	Distance from cage edge (m)	Sediment	V Coarse sand	Coarse sand	Med sand	Fine sand	V Fine sand	V Coarse silt	Coarse silt	Med silt	Fine silt	V Fine silt	Clay
Green	0	Very coarse silty fine sand	2.2	12.0	17.3	34.1	15.8	5.7	4.4	3.4	2.3	1.3	1.8
Green	20	Very coarse silty fine sand	1.7	11.3	19.9	37.3	12.9	5.2	4.2	3.1	2.1	1.1	1.6
Green	40	Coarse /Very coarse/ silty fine sand*	1.0	5.7	10.3	21.1	17.6	12.1	11.5	8.7	6.4	2.5	3.3
Green	60	Very coarse silty fine sand	0.3	7.0	16.4	33.0	16.3	6.8	6.2	5.4	4.6	1.5	2.7
Brown	0	Very coarse silty fine sand	2.9	9.6	15.7	43.4	14.2	3.7	3.3	2.7	2.1	0.9	1.5
Brown	20	Very coarse silty fine sand	1.4	6.9	16.3	47.4	15.1	3.1	2.9	2.5	2.0	1.0	1.7
Brown	40	Poorly sorted/ Very coarse silty/ fine sand*	1.9	7.5	17.0	47.4	15.3	2.9	2.4	2.0	1.5	0.9	1.4
Brown	60	Very coarse silty fine sand	2.4	7.6	15.3	46.2	15.2	3.5	3.0	2.5	1.8	1.0	1.5

Appendix 10: Results of POC analysis of sediment core syringe samples collected during the Quanterness fieldwork. Carbon results shown for each replicate syringe core and the mean and standard deviation of the duplicate measurements.

Transect	Distance from cage edge (m)	Syringe core 1 (% dry wt.)	Syringe core 2 (% dry wt.)	Mean (% dry wt.)	SD (% dry wt.)
Blue	0	1.386	0.898	1.14	0.35
Blue	20	0.713	1.011	0.86	0.21
Blue	40	0.609	0.734	0.67	0.09
Blue	60	0.577	0.674	0.63	0.07
Blue	80	0.525	0.567	0.55	0.03
Blue	100	0.444	0.503	0.47	0.04
Blue	120	0.484	0.519	0.50	0.02
Blue	140	0.547	0.754	0.65	0.15
Blue	160	0.524	0.497	0.51	0.02
Red	0	1.334	1.254	1.29	0.06
Red	20	1.114	0.991	1.05	0.09
Red	40	0.757	0.795	0.78	0.03
Red	60	0.819	0.846	0.83	0.02
Red	80	0.858	0.651	0.75	0.15
Red	100	1.040	0.794	0.92	0.17
Red	120	0.790	0.731	0.76	0.04
Red	140	0.846	0.782	0.81	0.05
Red	160	0.682	0.699	0.69	0.01
Green	0	0.878	0.880	0.88	0.00
Green	20	0.669	0.885	0.78	0.15
Green	40	1.304	1.357	1.33	0.04
Green	60	0.696	0.846	0.77	0.11
Brown	0	0.636	0.507	0.57	0.09
Brown	20	0.512	0.478	0.50	0.02
Brown	40	0.475	0.535	0.51	0.04
Brown	60	0.667	0.722	0.69	0.04

Appendix 11: Results of sulphide analysis of sediment core syringe samples collected at Quanterness. Sulphide as mean of triplicate measurements from single cores at each location. A 'N' in 'core OK' column indicates cores where the overlying seawater was visually assessed to comprise more than 10% of the syringe filled volume.

Transect	Distance from cage edge (m)	Core OK	Deployment a – Neap tides						Deployment b – Spring tides						
			Replicate			Mean	SD	CV	Core OK	Replicate			Mean	SD	CV
			1 (µM)	2 (µM)	3 (µM)	(µM)	(µM)	(%)		1 (µM)	2 (µM)	3 (µM)	(µM)	(µM)	(%)
Blue	0	N	1355.1	1256.7	1321.5	1311.1	50.0	3.8	Y	226.2	228.1	191.4	215.2	20.7	9.6
Blue	20	N	364.5	390.6	351.0	368.7	20.1	5.5	Y	191.4	208.9	207.3	202.5	9.7	4.8
Blue	40	N	415.9	311.5	346.7	358.0	53.1	14.8	Y	202.4	212.3	217.4	210.7	7.6	3.6
Blue	60	N	329.7	344.5	373.8	349.3	22.5	6.4	Y	379.7	452.4	382.7	404.9	41.1	10.2
Blue	80	Y	398.0	403.1	442.9	358.0	24.6	6.9	Y	445.2	438.2	434.7	439.4	5.4	1.2
Blue	100	N	437.4	410.7	360.0	402.7	39.3	9.8	Y	147.2	144.8	171.2	154.4	14.6	9.5
Blue	120	N	325.6	259.7	266.3	283.8	36.3	12.8	Y	135.9	132.7	134.8	134.5	1.6	1.2
Blue	140	N	246.9	248.5	253.2	249.5	3.3	1.3	Y	306.2	291.9	301.4	299.8	7.3	2.4
Blue	160	N	258.0	221.9		240.0	25.5	10.6	Y	119.6	137.0	147.2	134.6	13.9	10.3
Red	0	Y	947.2	1021.4	929.5	966.1	48.7	5.0	N	207.3	196.0	194.5	199.3	7.0	3.5
Red	20	Y	371.5	413.3		392.4	29.6	7.5	Y	911.8	842.0	747.2	833.6	82.6	9.9
Red	40	Y	809.5	760.3	727.5	765.8	41.3	5.4	Y	597.8	622.1	657.8	625.9	30.2	4.8
Red	60	Y	448.5	454.2	457.0	453.2	4.3	1.0	Y	448.8	456.0	467.0	457.3	9.2	2.0
Red	80	Y	718.5	633.6	683.2	678.4	42.6	6.3	N	448.8	441.7	470.8	453.7	15.2	3.3
Red	100	Y	683.2	573.0	606.4	620.9	56.5	9.1	Y	456.0	526.3	445.2	475.8	44.0	9.3
Red	120	Y	524.8	617.9	528.1	556.9	52.8	9.5	N	427.8	407.9	489.9	441.9	42.8	9.7
Red	140	Y	486.7	471.6	442.9	467.1	22.2	4.8	Y	701.0	729.5	690.0	706.8	20.4	2.9

Appendix 11: Results of sulphide analysis of sediment core syringe samples collected at Quanterness. Sulphide as mean of triplicate measurements from single cores at each location. A 'N' in 'core OK' column indicates cores where the overlying seawater was visually assessed to comprise more than 10% of the syringe filled volume.

Transect	Distance from cage edge (m)	Deployment a – Neap tides							Deployment b – Spring tides						
		Core OK	Replicate			Mean (µM)	SD (µM)	CV (%)	Core OK	Replicate			Mean (µM)	SD (µM)	CV (%)
			1 (µM)	2 (µM)	3 (µM)					1 (µM)	2 (µM)	3 (µM)			
Green	0	N	426.5	440.1	502.2	456.3	40.3	8.8	N	233.6	202.4	214.0	216.6	15.8	7.3
Green	20	N	307.7	385.7	357.7	350.4	39.6	11.3	N	143.7	155.6	129.6	142.9	13.0	9.1
Green	40	N							N	404.6	427.8	438.2	423.6	17.2	4.1
Green	60	N	338.1	431.9		385.0	66.4	17.2	N	161.9			161.9		
Brown	0	N	670.5	696.2		683.4	18.2	2.7	N	146.0	70.2	182.5	132.9	57.3	43.1
Brown	20	N	73.9	89.8	86.5	83.4	8.4	10.1	N	56.6	47.5	51.8	52.0	4.5	8.8
Brown	40	Y	51.3	85.9	72.1	69.8	17.4	25.0	N	47.9	58.9	51.4	52.7	5.6	10.7
Brown	60	N	142.1			142.1			N	373.7	370.7	367.8	370.7	3.0	0.8

Appendix 12: Results of sulphide analysis of benthic grab samples collected at Quanterness. Sulphide as mean of measurements from two grabs at each location.

Grab	Transect	Distance from cage edge (m)	Rep1 (μM)	Rep2 (μM)	Mean (μM)	SD (μM)	CV (%)
EE01	Blue	0	1043.9	399.9	721.9	455.4	63.1
EE02		44	349.1	583.5	466.3	165.7	35.5
EE03		98	819.7	403.0	611.4	294.7	48.2
EE04		118	180.9	284.7	232.8	73.4	31.5
EE05		167	376.5	266.0	321.2	78.1	24.3
EE06		200	24.4	25.4	24.9	0.7	2.7
EE07		253	11.9	66.2	39.1	38.4	98.3
SE01	Red	0	864.3	1187.0	1025.6	228.2	22.2
SE02		60	282.5	549.3	415.9	188.6	45.4
SE03		111	497.9	437.9	467.9	42.4	9.1
SE04		165	418.5	399.9	409.2	13.1	3.2
SE05		217	215.3	210.4	212.8	3.4	1.6
SE06		275	27.0	226.9	127.0	141.4	111.4
SE07		319	129.8	135.8	132.8	4.3	3.2
WW01	Green	0	250.4	368.0	309.2	83.2	26.9
WW02		36	144.2	170.3	157.3	18.4	11.7
WW03		58	89.6	97.4	61.0	5.5	5.9
WW04		90	278.3	268.0	273.1	7.3	2.7
WW05		102	213.6	268.0	240.8	38.4	16.0
WW06		122	282.5	282.5	282.5	0.0	0.0
WW07		173	362.5	172.9	267.7	134.1	50.1
NN01	Brown	0	379.3	629.3	504.3	176.7	35.0
NN02		33	180.9		180.9		
NN03		48	58.3	63.8	58.5	3.9	6.4
NN04		66	241.1	409.1	325.1	118.8	36.5
NN05		92	549.3	318.8	434.0	162.9	37.5
NN06		123	92.4	56.1	74.2	25.6	34.5
NN07		155	58.7	60.5	55.9	1.3	2.1
REF1	Yellow	509	55.7	81.8	68.8	18.5	26.9
REF2		503	152.1	131.7	141.9	14.4	10.1

Appendix 13: Estimated organic carbon deposition rates (g m^{-2}) over the two, 7-day periods sediment boxes were deployed at Quanterness. Each box was analysed in triplicate (replicates 1 – 3).

Transect	Distance from cage edge (m)	Deployment a – Neap tides					Deployment b – Spring tides				
		Replicate			Mean	SD	Replicate			Mean	SD
		1 (g m^{-2})	2 (g m^{-2})	3 (g m^{-2})	(g m^{-2})	(g m^{-2})	1 (g m^{-2})	2 (g m^{-2})	3 (g m^{-2})	(g m^{-2})	(g m^{-2})
Blue	0	32.96	30.04	50.51	37.84	11.07	49.25	33.06	33.59	38.63	9.20
Blue	20	32.96	40.53	38.66	37.38	3.94	2.39	2.35	6.67	3.80	2.48
Blue	40	12.79	15.81	12.73	13.78	1.77	2.45	0.76	1.28	1.50	0.87
Blue	60	11.65	6.40	10.13	9.39	2.70	0.93	1.10	1.22	1.08	0.15
Blue	80	4.87	3.77	9.75	6.13	3.18	1.22	1.39	1.70	1.44	0.24
Blue	100	5.40	5.14	3.97	4.84	0.76	10.21	7.43	7.41	8.35	1.61
Blue	120	Box not recovered					0.84	1.03	0.96	0.94	0.10
Blue	140	1.73	1.50	1.08	1.44	0.33	Box not recovered				
Blue	160	2.53	2.47	2.66	2.55	0.10	1.00	0.10	0.00	0.37	0.55
Red	0	57.98	53.20	55.10	55.43	2.40	3.40	3.79	3.28	3.49	0.27
Red	20	1.58	1.25	1.10	1.31	0.25	6.55	2.51	1.53	3.53	2.66
Red	40	8.38	10.46	6.56	8.47	1.95	2.18	2.18	3.43	2.60	0.72
Red	60	1.29	5.69	7.57	4.85	3.23	1.03	0.61	0.31	0.65	0.36
Red	80	5.15	4.99	2.15	4.10	1.69	4.85	4.44	4.10	4.46	0.38
Red	100	1.44	2.32	1.09	1.62	0.63	11.43	16.92	13.91	14.08	2.75
Red	120	2.52	3.64	5.10	3.75	1.29	1.66	2.08	1.14	1.63	0.47
Red	140	1.61	2.45	2.44	2.17	0.48	1.16	1.07	1.01	1.08	0.08
Red	160	Washed out – no sediment in box when recovered					Washed out – no sediment in box when recovered				

Appendix 13: Estimated organic carbon deposition rates (g m^{-2}) over the two, 7-day periods sediment boxes were deployed at Quanterness. Each box was analysed in triplicate (replicates 1 – 3).

Transect	Distance from cage edge (m)	Deployment a – Neap tides					Deployment b – Spring tides				
		Replicate			Mean	SD	Replicate			Mean	SD
		1 (g m^{-2})	2 (g m^{-2})	3 (g m^{-2})	(g m^{-2})	(g m^{-2})	1 (g m^{-2})	2 (g m^{-2})	3 (g m^{-2})	(g m^{-2})	(g m^{-2})
Green	0	0.00	0.00	0.00	0.00	0.00	1.03	1.04	0.91	0.99	0.07
Green	20	2.35	6.26	4.01	4.21	1.96	0.59	1.14	2.00	1.24	0.71
Green	40	10.25	15.39	13.23	12.95	2.58	0.63	0.40	0.87	0.63	0.23
Green	60	3.84	3.99	2.44	3.42	0.86	Box not recovered				
Brown	0	5.39	2.02	2.70	3.37	1.78	1.22	0.73	0.78	0.91	0.27
Brown	20	0.99	2.84	1.19	1.67	1.02	3.40	2.02	1.46	2.30	1.00
Brown	40	11.03	35.42	12.71	19.72	13.62	Box not recovered				
Brown	60	1.41	1.16	1.53	1.37	0.19	0.00	0.28		0.14	0.20

Appendix 14: Results of PSA analysis of sediment core syringe samples collected at Bay of Meil. Mean percentage of particles by grain size based on duplicate syringe cores at each location. * indicates samples where the sediment name differed between the two duplicates, the differences being indicated by /.

Transect	Distance from cage edge (m)	Sediment	Sand					Silt					Clay
			V Coarse sand	Coarse sand	Med sand	Fine sand	V Fine sand	V Coarse silt	Coarse silt	Med silt	Fine silt	V Fine silt	
Blue	0	Moderately sorted fine sand	0.6	0.7	2.9	28.0	43.3	17.2	2.8	1.9	1.4	0.3	0.7
Blue	10	Very coarse silty fine sand	4.4	8.2	5.6	23.5	31.6	14.5	2.7	2.2	1.6	0.8	1.5
Blue	20	Very coarse silty coarse sand	14.5	18.6	12.3	11.8	15.3	12.9	8.3	6.1	4.2	1.8	2.6
Blue	30	Coarse /Very coarse/ silty very coarse sand*	50.6	31.8	14.5	6.5	4.4	4.4	3.5	2.8	2.0	0.7	1.5
Blue	40	Rock											
Blue	50	Rock											
Blue	75	Rock											
Blue	100	Rock											
Red	0	Very coarse silty /Poorly sorted/ very coarse sand*	34.3	33.0	21.8	11.6	7.7	4.7	2.9	2.0	1.4	0.7	1.3
Red	10	Very coarse silty /Poorly sorted very/ coarse sand*	20.9	31.6	28.1	14.8	8.6	4.6	3.0	2.2	1.5	0.9	1.7
Red	20	Very coarse silty medium sand	5.3	13.5	25.0	22.7	17.7	10.5	3.9	2.3	1.7	0.8	1.3
Red	30	Very coarse silty fine sand	1.9	4.7	10.3	23.0	31.0	16.7	4.6	3.1	2.0	1.0	1.7
Red	40	Very coarse silty /Poorly sorted/ fine sand*	7.3	8.9	11.9	23.5	30.1	14.3	3.2	2.2	1.4	0.7	1.4
Red	50	Very coarse silty fine sand	2.6	3.8	6.6	23.1	33.7	18.9	4.8	3.0	1.8	0.9	1.7
Red	75	Very coarse silty fine sand	0.9	2.5	5.6	25.5	35.8	18.3	4.5	2.8	2.0	0.8	1.6
Red	100	Very coarse silty /Moderately sorted/ fine sand*	0.5	2.9	8.5	29.3	35.3	16.2	3.1	1.7	1.1	0.4	0.7

Appendix 14: Results of PSA analysis of sediment core syringe samples collected at Bay of Meil. Mean percentage of particles by grain size based on duplicate syringe cores at each location. * indicates samples where the sediment name differed between the two duplicates, the differences being indicated by /.

Transect	Distance from cage edge (m)	Sediment	Sand					Silt					Clay
			V Coarse sand	Coarse sand	Med sand	Fine sand	V Fine sand	V Coarse silt	Coarse silt	Med silt	Fine silt	V Fine silt	
Green	0	/Moderately/ Well sorted fine sand*	1.2	0.6	2.0	35.5	45.1	12.5	1.3	0.9	0.7	0.1	0.0
Green	10	Moderately well sorted fine sand	2.0	2.0	2.1	37.4	42.9	11.0	2.1	1.6	1.2	0.0	0.0
Green	20	Well sorted fine sand	0.0	0.0	3.0	38.7	45.3	10.2	1.3	0.9	0.7	0.0	0.0
Green	30	Well /Poorly/ sorted fine sand*	0.0	0.0	12.7	39.6	36.3	7.1	1.2	1.0	1.0	0.3	0.6
Green	40	Well sorted fine sand	0.4	0.4	2.5	38.2	45.5	10.7	1.1	0.7	0.7	0.0	0.0
Green	50	Very coarse silty /Well sorted/ fine sand*	0.0	0.0	0.0	38.2	45.3	10.9	1.7	1.1	1.1	0.3	1.3
Green	75	Well sorted fine sand	0.0	0.0	1.6	41.6	45.4	9.4	0.9	0.6	0.3	0.0	0.0
Green	100	Well sorted fine sand	0.2	0.2	2.3	42.7	45.0	7.6	0.9	0.6	0.4	0.1	0.3
Brown	0	Well /Moderately/ sorted fine sand*	0.0	0.0	1.6	41.1	45.0	7.8	1.3	1.0	0.9	0.2	0.8
Brown	10	Moderately well sorted fine sand	0.0	0.0	8.4	40.4	39.9	7.8	1.5	1.1	1.0	0.1	0.0
Brown	20	Well sorted fine sand	0.0	0.0	1.1	39.0	46.4	9.9	1.7	1.4	0.6	0.0	0.0
Brown	30	Well sorted fine sand	0.0	0.0	0.0	1.9	80.2	15.1	1.2	0.9	0.7	0.0	0.0
Brown	40	Moderately /Well/ sorted fine sand*	0.0	5.5	6.4	37.4	41.9	7.4	0.7	0.5	0.4	0.0	0.0
Brown	50	Moderately sorted fine sand	2.4	2.4	4.2	40.2	40.4	7.9	1.5	1.2	1.2	0.3	0.4
Brown	75	Moderately sorted fine sand	5.4	1.7	4.1	36.8	39.6	6.7	1.4	1.3	1.1	0.6	1.2
Brown	100	Moderately sorted fine sand	0.0	4.8	10.8	38.2	37.0	6.6	1.1	0.9	0.3	0.1	0.1

Appendix 15: Results of POC analysis of sediment core syringe samples collected during the Bay of Meil fieldwork. Carbon results shown for each replicate syringe core and the mean and standard deviation of the duplicate measurements.

Transect	Distance from cage edge (m)	Syringe core 1 (% dry wt.)	Syringe core 2 (% dry wt.)	Mean (% dry wt.)	SD (% dry wt.)
Blue	0	0.359	0.445	0.40	0.06
Blue	10	0.373	0.349	0.36	0.02
Blue	20	1.598	0.703	1.15	0.63
Blue	30	0.838	0.981	0.91	0.10
Blue	40	Rocky			
Blue	50	Rocky			
Blue	75	Rocky			
Blue	100	Rocky			
Red	0	1.461	1.064	1.26	0.28
Red	10	0.704	1.232	0.97	0.37
Red	20	1.081	0.781	0.93	0.21
Red	30	1.041	0.82	0.93	0.16
Red	40	0.771	0.556	0.66	0.15
Red	50	0.935	0.628	0.78	0.22
Red	75	0.667	0.624	0.65	0.03
Red	100	0.377	0.406	0.39	0.02
Green	0	0.252	0.096	0.17	0.11
Green	10	0.137	0.179	0.16	0.03
Green	20	0.111	0.147	0.13	0.03
Green	30	0.131	0.12	0.13	0.01
Green	40	0.081	0.137	0.11	0.04
Green	50	0.087	0.206	0.15	0.08
Green	75	0.056	0.085	0.07	0.02
Green	100	0.112	0.134	0.12	0.02
Brown	0	0.147	0.137	0.14	0.01
Brown	10	Missing			
Brown	20	0.133	0.182	0.16	0.03
Brown	30	0.123	0.141	0.13	0.01
Brown	40	0.11	0.115	0.11	0.00
Brown	50	0.15	0.293	0.22	0.10
Brown	75	0.151	0.262	0.21	0.08
Brown	100	0.141	0.306	0.22	0.12

Appendix 16: Results of sulphide analysis of benthic grab samples collected at Bay of Meil. Sulphide as mean of measurements from two grabs at each location.

Grab	Transect	Distance from cage edge (m)	Rep1 (μM)	Rep2 (μM)	Mean (μM)	SD (μM)	CV (%)
E1	Blue	0	318.5	197.9	258.2	85.3	33.0
E2	Blue	25	297.6	240.9	269.2	40.1	14.9
E3	Blue	55	Grab failed				
E4	Blue	76	Grab failed				
S1	Red	0	163.8	235.5	199.7	50.6	25.4
S2	Red	28	360.9	415.0	388.0	38.2	9.8
S3	Red	39	365.0	405.7	385.3	28.8	7.5
S4	Red	50	286.6	321.0	303.8	24.3	8.0
S5	Red	76	237.2	286.6	261.9	34.9	13.3
S6	Red	102	78.1	77.0	77.5	0.8	1.1
S7	Red	151	141.9	126.7	134.3	10.8	8.0
S8	Red	211	193.5	197.9	195.7	3.1	1.6
W00	Green	0	434.2	512.7	473.5	55.5	11.7
W25	Green	26	479.0	144.1	311.6	236.8	76.0
W50	Green	50	13.6	63.7	38.7	35.4	91.5
W100	Green	101	1.7	11.5	6.6	6.9	105.7
W150	Green	152	8.7	9.4	9.0	0.5	5.9
W200	Green	203	19.8	22.5	21.1	1.9	9.1
W250	Green	274	5.4	3.1	4.3	1.6	38.0
N00	Brown	0	115.7	172.7	144.2	40.3	27.9
N25	Brown	23	71.9	19.8	45.8	36.9	80.5
N50	Brown	51	94.4	51.6	73.0	30.3	41.5
N75	Brown	80	61.8	58.2	60.0	2.6	4.3
N100	Brown	102	84.3	90.2	87.2	4.2	4.8
N150	Brown	151	50.0	30.2	40.1	14.1	35.1
N200	Brown	208	88.8	33.3	61.1	39.3	64.4
REF1	Yellow	480	37.3	33.3	35.3	2.8	8.0
REF2	Yellow	495	32.5	9.1	20.8	16.6	79.7

Appendix 17: Estimated organic carbon deposition rates (g m^{-2}) over the two, 7-day periods sediment boxes were deployed at Bay of Meil. Each box was analysed in triplicate (replicates 1 – 3).

Transect	Distance from cage edge (m)	Deployment a – Neap tides					Deployment b – Spring tides				
		Replicate			Mean	SD	Replicate			Mean	SD
		1	2	3	(g m^{-2})	(g m^{-2})	1	2	3	(g m^{-2})	(g m^{-2})
Blue	0	41.22	75.90	50.27	55.80	17.99	14.81	20.07	16.78	17.22	2.66
Blue	10	6.25	10.10	8.64	8.33	1.95	5.42	7.42		6.42	1.42
Blue	20	5.44	9.81	9.39	8.21	2.41	2.21	3.17	3.57	2.98	0.70
Blue	30	11.98	10.04	13.91	11.98	1.94	6.29	5.06	6.78	6.04	0.89
Blue	40	1.93	1.60	0.75	1.43	0.61	0.90	0.94	1.36	1.07	0.26
Blue	50	0.02	0.05	0.05	0.04	0.02	2.97	2.25	2.21	2.48	0.42
Blue	75	1.00	0.55	0.59	0.71	0.25	0.00	0.00	0.00	0.00	0.00
Blue	100	0.12	0.00	0.00	0.04	0.07	1.55	1.59	2.19	1.77	0.36
Red	0	18.34	21.20	14.26	17.93	3.49	80.90	92.86	113.68	95.81	16.59
Red	10	21.28	19.68	15.68	18.88	2.88	63.79	47.99		55.89	11.17
Red	20	17.40	16.45	17.36	17.07	0.54	8.94	10.05	15.20	11.39	3.34
Red	30	Missing					Missing				
Red	40	32.98	40.00	35.94	36.31	3.52	24.34	33.41	30.21	29.32	4.60
Red	50	13.97	10.94	8.05	10.99	2.96	66.45	92.04	88.66	82.38	13.90
Red	75	8.73	9.53	12.66	10.31	2.08	26.39	28.63	49.10	34.71	12.51
Red	100	5.34	4.76	4.88	4.99	0.30	9.18	6.31	5.74	7.08	1.84

Appendix 17: Estimated organic carbon deposition rates (g m^{-2}) over the two, 7-day periods sediment boxes were deployed at Bay of Meil. Each box was analysed in triplicate (replicates 1 – 3).

Transect	Distance from cage edge (m)	Deployment a – Neap tides					Deployment b – Spring tides				
		Replicate			Mean	SD	Replicate			Mean	SD
		1 (g m^{-2})	2 (g m^{-2})	3 (g m^{-2})	(g m^{-2})	(g m^{-2})	1 (g m^{-2})	2 (g m^{-2})	3 (g m^{-2})	(g m^{-2})	(g m^{-2})
Green	0	8.39	9.17	3.98	7.18	2.80	16.09	19.27	19.80	18.39	2.00
Green	10	0.07	1.57	0.15	0.59	0.84	10.57	16.64	15.70	14.30	3.27
Green	20	0.03	0.00	0.05	0.03	0.03	4.76	5.22	5.83	5.27	0.54
Green	30	8.36	12.46	9.65	10.16	2.10	9.11	13.40		11.26	3.03
Green	40	3.82	3.02	3.47	3.43	0.40	3.43	2.89	2.43	2.92	0.50
Green	50	1.31	2.93	2.02	2.09	0.81	12.84	12.37	11.57	12.26	0.64
Green	75	0.07	0.29	0.70	0.35	0.32	10.50	9.91		10.20	0.41
Green	100	9.41	9.22	11.28	9.97	1.14	12.96	12.19	10.39	11.85	1.31
Brown	0	Missing					10.14	9.14	9.14	9.47	0.58
Brown	10	11.50	61.53	34.25	35.76	25.05	4.73	5.50	5.64	5.29	0.49
Brown	20	4.39	3.78		4.08	0.43	2.51	5.09	2.64	3.41	1.45
Brown	30	73.21	111.01		92.11	26.73	3.25	3.87	4.88	4.00	0.82
Brown	40	19.89	28.38	18.95	22.41	5.19	1.54	6.43	1.58	3.18	2.81
Brown	50	6.84	9.19	9.93	8.65	1.62	7.55	8.95	13.40	9.97	3.05
Brown	75	3.56	3.38	3.92	3.62	0.27	3.02	3.52	3.46	3.33	0.28
Brown	100	26.03	39.33	36.14	33.83	6.95	0.26	0.33	0.87	0.48	0.33

Appendix 18: Default NewDEPOMOD settings

#2021/04/26 11:09:14

#Mon Apr 26 11:09:14 BST 2021

Bathymetry.bufferZoneWidth=350.0

Bathymetry.minimumSurfaceDX=10.0

Bathymetry.minimumSurfaceDY=10.0

Bathymetry.surfaceDX=10.0

Bathymetry.surfaceDY=10.0

Eqs.Benthic.impactArea.contourLevel=4.0

Eqs.Benthic.impactArea.targetArea=500000

Eqs.Benthic.impactArea.targetAreaPercentageTolerance=1.0

Eqs.Benthic.minimumItiValue=10.0

Eqs.Benthic.minimumItiValuePercentageTolerance=1.0

Eqs.Benthic.samplingIti=30.0

Eqs.SEPA2019BenthicMixingZone.mixingZoneBoundaryTargetFlux=250.0

Eqs.SEPA2019BenthicMixingZone.mixingZoneBoundaryTargetFluxAbsoluteTolerance=1.0

Eqs.SEPA2019BenthicMixingZone.mixingZoneBoundaryTargetFluxSide=BELOW

Eqs.SEPA2019BenthicMixingZone.mixingZoneDistance=100

Eqs.SEPA2019BenthicMixingZone.mixingZoneExtentAdjustmentPercent=100.0

Eqs.SEPA2019BenthicMixingZone.mixingZoneExtentAreaTargetAbsoluteTolerance=625.0

Eqs.SEPA2019BenthicMixingZone.mixingZoneExtentFluxSide=BOTH

Eqs.SEPA2019BenthicMixingZone.mixingZoneIntensityFluxSide=BOTH

Eqs.SEPA2019BenthicMixingZone.mixingZoneIntensityTargetFlux=2000.0

Eqs.SEPA2019BenthicMixingZone.mixingZoneIntensityTargetFluxAbsoluteTolerance=100.0

Eqs.SEPA2019BenthicMixingZone.mixingZonePeakAverageTargetFlux=2000.0

Eqs.SEPA2019BenthicMixingZone.mixingZonePeakAverageTargetFluxAbsoluteTolerance=100.0

Eqs.SEPA2019BenthicMixingZone.mixingZonePeakAverageTargetFluxSide=BOTH

Eqs.SEPA2019ChemicalMixingZone.boundaryTarget=0.0235

Eqs.SEPA2019ChemicalMixingZone.boundaryTargetAbsoluteTolerance=0.0

Eqs.SEPA2019ChemicalMixingZone.boundaryTargetSide=BELOW

Eqs.SEPA2019ChemicalMixingZone.mixingZoneChemicalMaximum=0.235

Eqs.SEPA2019ChemicalMixingZone.mixingZoneChemicalMaximumAbsoluteTolerance=0.0

Eqs.SEPA2019ChemicalMixingZone.mixingZoneChemicalMaximumSide=BELOW

Eqs.SEPA2019ChemicalMixingZone.mixingZoneDistance=100.0

Eqs.benthic.defaultBenthicFarField.critical=true

Eqs.benthic.defaultBenthicFarField.enable=true

Eqs.benthic.defaultBenthicImpactedArea.critical=true

Eqs.benthic.defaultBenthicImpactedArea.enable=true

Eqs.benthic.defaultBenthicMixingZoneBoundary.critical=false

Eqs.benthic.defaultBenthicMixingZoneBoundary.enable=true

Eqs.benthic.defaultBenthicMixingZoneExtent.critical=true

Eqs.benthic.defaultBenthicMixingZoneExtent.enable=true

Eqs.benthic.defaultBenthicMixingZoneIntensity.critical=true

Eqs.benthic.defaultBenthicMixingZoneIntensity.enable=true

Eqs.benthic.defaultBenthicMixingZoneInternal.critical=false

Eqs.benthic.defaultBenthicMixingZoneInternal.enable=true

Eqs.benthic.defaultBenthicNearField.critical=false

Eqs.benthic.defaultBenthicNearField.enable=true

Eqs.benthic.defaultBiomassStep.enable=true

Eqs.benthic.defaultChemicalFarField.critical=false

Eqs.benthic.defaultChemicalFarField.enable=false

Eqs.benthic.defaultChemicalMixingZoneBoundary.critical=false

Eqs.benthic.defaultChemicalMixingZoneBoundary.enable=false

Eqs.benthic.defaultChemicalMixingZoneExtent.critical=false

Eqs.benthic.defaultChemicalMixingZoneExtent.enable=false

Eqs.benthic.defaultChemicalMixingZoneIntensity.critical=false

Eqs.benthic.defaultChemicalMixingZoneIntensity.enable=false

Eqs.benthic.defaultChemicalMixingZoneInternal.critical=false

Eqs.benthic.defaultChemicalMixingZoneInternal.enable=false
Eqs.benthic.defaultChemicalNearField.critical=false
Eqs.benthic.defaultChemicalNearField.enable=false
Eqs.benthic.defaultFauxFarField.enable=true
Eqs.benthic.defaultFauxImpactedArea.enable=true
Eqs.benthic.defaultFauxNearField.enable=true
Eqs.benthic.defaultOverTreatmentFactorStep.enable=false
Eqs.biomass.step=50.00
Eqs.cageAreaPercentageTolerance=1.0
Eqs.cageVolumeAdjustment=1.0
Eqs.calcide.farFieldContour=0.002
Eqs.calcide.nearFieldContour=10
Eqs.calcide.rhoBulk=1216.0
Eqs.chemical.defaultBenthicFarField.critical=false
Eqs.chemical.defaultBenthicFarField.enable=true
Eqs.chemical.defaultBenthicImpactedArea.critical=false
Eqs.chemical.defaultBenthicImpactedArea.enable=true
Eqs.chemical.defaultBenthicMixingZoneBoundary.critical=false
Eqs.chemical.defaultBenthicMixingZoneBoundary.enable=true
Eqs.chemical.defaultBenthicMixingZoneExtent.critical=false
Eqs.chemical.defaultBenthicMixingZoneExtent.enable=true
Eqs.chemical.defaultBenthicMixingZoneIntensity.critical=false
Eqs.chemical.defaultBenthicMixingZoneIntensity.enable=true
Eqs.chemical.defaultBenthicMixingZoneInternal.critical=false
Eqs.chemical.defaultBenthicMixingZoneInternal.enable=true
Eqs.chemical.defaultBenthicNearField.critical=false
Eqs.chemical.defaultBenthicNearField.enable=true
Eqs.chemical.defaultBiomassStep.enable=false
Eqs.chemical.defaultChemicalFarField.critical=true
Eqs.chemical.defaultChemicalFarField.enable=true
Eqs.chemical.defaultChemicalMixingZoneBoundary.critical=false
Eqs.chemical.defaultChemicalMixingZoneBoundary.enable=true
Eqs.chemical.defaultChemicalMixingZoneExtent.critical=true
Eqs.chemical.defaultChemicalMixingZoneExtent.enable=true
Eqs.chemical.defaultChemicalMixingZoneInternal.critical=true
Eqs.chemical.defaultChemicalMixingZoneInternal.enable=true
Eqs.chemical.defaultChemicalNearField.critical=false
Eqs.chemical.defaultChemicalNearField.enable=true
Eqs.chemical.defaultFauxFarField.enable=true
Eqs.chemical.defaultFauxNearField.enable=true
Eqs.chemical.defaultOverTreatmentFactorStep.enable=true
Eqs.farFieldAreaAdjust=0.0
Eqs.farFieldAreaDistance=100
Eqs.farFieldAreaPercentageTolerance=1.0
Eqs.fluxTrigger=10000.0
Eqs.massBalancePercentage=80.0
Eqs.massBalancePercentageTolerance=1.0
Eqs.nearFieldAreaDistance=25
Eqs.nearFieldAreaPercentageTolerance=1.0
Eqs.nearFieldContourPercentageTolerance=1.0
Eqs.none.carbon.farFieldContour=1.0
Eqs.none.carbon.nearFieldContour=3.0
Eqs.none.iti.farFieldContour=10.0
Eqs.none.iti.nearFieldContour=30.0
Eqs.none.solids.farFieldContour=192.75
Eqs.none.solids.nearFieldContour=1555.97
Eqs.overTreatmentFactor.step=0.01
Eqs.parameter.limit=true
Eqs.slice.defaultChemicalExport.critical=true
Eqs.slice.defaultChemicalExport.enable=true

Eqs.slice.defaultChemicalExport.exportLimit=0.922
Eqs.slice.defaultChemicalExport.exportTime=10195200
Eqs.slice.defaultFauxChemicalExport.enable=true
Eqs.slice.defaultRecordSurfaces=true
Eqs.slice.defaultRecordTimes=10195200,19612800
Eqs.slice.farFieldContour=0.763
Eqs.slice.nearFieldContour=7.63
Eqs.slice.rhoBulk=1400.0
Eqs.supervisor.enable=false
Eqs.supervisor.monitorOnly=true

FeedInputs.activeIngredientFormulationConcentrationEmbz=10.0
FeedInputs.activeIngredientFormulationConcentrationTfbz=2.0
FeedInputs.activeIngredientPresentationConcentrationEmbz=0.05
FeedInputs.activeIngredientPresentationConcentrationTfbz=10.0
FeedInputs.biomass=
FeedInputs.compoundName.embz=EMBZ
FeedInputs.compoundName.none=NONE
FeedInputs.compoundName.tfbz=TFBZ
FeedInputs.deltaT=3600.0
FeedInputs.faecesCarbonPercentage=30
FeedInputs.faecesCompoundConcentration=13.18681
FeedInputs.feedAbsorbedPercentage=85
FeedInputs.feedCarbonPercentage=49
FeedInputs.feedCompoundConcentration=2
FeedInputs.feedWastedPercentage=3
FeedInputs.feedWaterPercentage=9
FeedInputs.massUnitsSiConversionFactor=1.0
FeedInputs.nullInputId=badf00d0-0123-4567-badf-00d0badf00d0
FeedInputs.numberOfTimeSteps=3600
FeedInputs.plugLoadPeriod=
FeedInputs.timeUnitsSiConversionFactor=1

Flowmetry.deltaT=
Flowmetry.lengthUnitsSiConversionFactor=1.0
Flowmetry.meterDepth=
Flowmetry.meterDepths=
Flowmetry.neapSpringNeapStartSample=
Flowmetry.numberOfTimeSteps=
Flowmetry.siteDepth=
Flowmetry.siteTide=
Flowmetry.siteXCoordinate=
Flowmetry.siteYCoordinate=
Flowmetry.springNeapSpringStartSample=
Flowmetry.timeUnitsSiConversionFactor=1.0

Model.aggregateSurfaces.embz=true
Model.aggregateSurfaces.none=true
Model.aggregateSurfaces.outputNetcdf.embz=true
Model.aggregateSurfaces.outputNetcdf.none=true
Model.aggregateSurfaces.outputNetcdf.tfbz=true
Model.aggregateSurfaces.outputSurfile.embz=true
Model.aggregateSurfaces.outputSurfile.none=true
Model.aggregateSurfaces.outputSurfile.tfbz=true
Model.aggregateSurfaces.tfbz=true
Model.aggregateTimes.embz=18.0\;0.125\;20.0
Model.aggregateTimes.none=275.0\;0.125\;365.0
Model.aggregateTimes.tfbz=18.0\;0.125\;20.0

Model.biomassLimit=Infinity

Model.defaultCageVolumeAdjust=1.0
Model.defaultOverTreatmentFactor=1.0
Model.defaultSpecificFeedingRatePercent=0.7
Model.defaultStockingDensity=23

Model.iterationParameter.embz=OVERTREATMENTFACTOR
Model.iterationParameter.none=STOCKINGDENSITY
Model.iterationParameter.tfbz=OVERTREATMENTFACTOR

Model.maximumSpecificFeedingRatePercent=1.0
Model.maximumStockingDensity=30

Model.minimumSpecificFeedingRatePercent=0.1
Model.minimumStockingDensity=10

Model.run.number=-1
Model.run.numberOfParticles.embz=10
Model.run.numberOfParticles.none=1
Model.run.numberOfParticles.tfbz=10
Model.run.plugLoadPeriod.embz=5352
Model.run.plugLoadPeriod.none=0
Model.run.plugLoadPeriod.tfbz=168
Model.run.runType.embz=REFINING
Model.run.runType.none=SCOPING
Model.run.runType.tfbz=REFINING
Model.run.tide.embz=N
Model.run.tide.none=N
Model.run.tide.tfbz=N
Model.run.useNumber=true

Model.specificFeedingRatePercentUseMax=FALSE

Model.stockingDensityUseMax=TRUE

ModelTime.delta=60000
ModelTime.endTime.embz=19699200000
ModelTime.endTime.none=31989600000
ModelTime.endTime.tfbz=1728000000
ModelTime.releasePeriod.embz=19267200000
ModelTime.releasePeriod.none=31557600000
ModelTime.releasePeriod.tfbz=1296000000
ModelTime.startTime=0
ModelTime.timeUnitsSiConversionFactor=0.001

Particle.calcide.degradeT50Chemical=9936000

Particle.characteristicLengthOfFaeces.dispersion=0.0005
Particle.characteristicLengthOfFaeces.distribution=UNIFORM
Particle.characteristicLengthOfFaeces.location=0.005
Particle.characteristicLengthOfFeed.dispersion=0.0011
Particle.characteristicLengthOfFeed.distribution=UNIFORM
Particle.characteristicLengthOfFeed.location=0.011

Particle.consolidationTimeOfFaeces=345600
Particle.consolidationTimeOfFeed=345600

Particle.degradeT50Carbon=Infinity
Particle.degradeT50Chemical=Infinity

Particle.densityOfFaeces.dispersion=10.80

Particle.densityOfFaeces.distribution=UNIFORM
 Particle.densityOfFaeces.location=1080

Particle.densityOfFeed.dispersion=11.80
 Particle.densityOfFeed.distribution=UNIFORM
 Particle.densityOfFeed.location=1180.0

Particle.diameterOfFaeces.dispersion=0.0003
 Particle.diameterOfFaeces.distribution=UNIFORM
 Particle.diameterOfFaeces.location=0.003

Particle.diameterOfFeed.dispersion=0.0009
 Particle.diameterOfFeed.distribution=UNIFORM
 Particle.diameterOfFeed.location=0.009

Particle.lengthUnitsSiConversionFactor=1

Particle.massUnitsSiConversionFactor=1.0

Particle.none.degradeT50Chemical=Infinity

Particle.settlingVelocityOfFaeces.dispersion=0.0035
 Particle.settlingVelocityOfFaeces.distribution=UNIFORM
 Particle.settlingVelocityOfFaeces.location=-0.035

Particle.settlingVelocityOfFeed.dispersion=0.0095
 Particle.settlingVelocityOfFeed.distribution=UNIFORM
 Particle.settlingVelocityOfFeed.location=-0.095

Particle.slice.degradeT50Chemical=21600000

Particle.velocityUnitsSiConversionFactor=1

SeaWater.default.densityOfSeaWater=1027.0
 SeaWater.default.kinematicViscosity=0.000001212
 SeaWater.default.pressure=0.0
 SeaWater.default.salinity=35.0
 SeaWater.default.temperature=10.0

Transports.BedModel.bioTurbationMixingCoefficient=0.1
 Transports.BedModel.characteristicLengthOfSediment.dispersion=0.00011
 Transports.BedModel.characteristicLengthOfSediment.distribution=UNIFORM
 Transports.BedModel.characteristicLengthOfSediment.location=0.0011
 Transports.BedModel.contractionT50=900.0
 Transports.BedModel.dLayerMass=3375
 Transports.BedModel.densityOfFaeces.dispersion=10.0
 Transports.BedModel.densityOfFaeces.distribution=UNIFORM
 Transports.BedModel.densityOfFaeces.location=1080.0
 Transports.BedModel.densityOfFeed.dispersion=10.0
 Transports.BedModel.densityOfFeed.distribution=UNIFORM
 Transports.BedModel.densityOfFeed.location=1180.0
 Transports.BedModel.densityOfMud.dispersion=0.0
 Transports.BedModel.densityOfMud.distribution=DIRAC
 Transports.BedModel.densityOfMud.location=1400.0
 Transports.BedModel.expansionT50=14400.0
 Transports.BedModel.internalFrictionAngle=23
 Transports.BedModel.massErosionCoefficient=0.031
 Transports.BedModel.massErosionExponent=1
 Transports.BedModel.minimumSurfaceDX=10.0
 Transports.BedModel.minimumSurfaceDY=10.0

Transports.BedModel.mixingDepth=0.05
Transports.BedModel.numberOfLayers=3
Transports.BedModel.releaseHeight.height=0.12
Transports.BedModel.releaseHeight.instanceName=CARTESIANBEDRELEASEHEIGHTFIXED
Transports.BedModel.releaseParticles.particlesPerArea=0.0016
Transports.BedModel.releasePosition.instanceName=CARTESIANBEDRELEASEPOSITION
Transports.BedModel.releasePosition.position=CENTRE
Transports.BedModel.settlingVelocityOfSediment.dispersion=0.00057
Transports.BedModel.settlingVelocityOfSediment.distribution=UNIFORM
Transports.BedModel.settlingVelocityOfSediment.location=-0.0057
Transports.BedModel.surfaceDX=10.0
Transports.BedModel.surfaceDY=10.0
Transports.BedModel.tauECritMin=0.02

Transports.bed.instanceName=CARTESIANBEDNOTTRANSPORT
Transports.bed.walker.dispersionCoefficientX=0.1
Transports.bed.walker.dispersionCoefficientY=0.1
Transports.bed.walker.dispersionCoefficientZ=0.0
Transports.bed.walker.type=LATTICEWALKER
Transports.bedSlope.criticalAngle=30.0

Transports.bottomRoughnessLength.rough=0.054
Transports.bottomRoughnessLength.smooth=0.001273

Transports.consolidation.instanceName=DEFAULTCONSOLIDATION

Transports.degrader.instanceName=DEFAULTPPARTICLEDEGRADER

Transports.g=9.80665

Transports.intercept.type=ROOTFINDINGINTERCEPT

Transports.regime.frictionvelocity.type=LAWOFTHEWALL
Transports.regime.rough.constant=4.9
Transports.regime.rough.factor=5.6
Transports.regime.smooth.constant=0.0
Transports.regime.smooth.factor=0.65
Transports.regime.transitional.constant=0.0
Transports.regime.transitional.factor=8.18
Transports.release.instanceName=CARTESIANRELEASE
Transports.release.sampler.instanceName=RANDOMRELEASESAMPLER

Transports.resuspension.instanceName=CARTESIANRESUSPENSIONTRANSPORT
Transports.resuspension.settling.allowBuoyant=false
Transports.resuspension.settling.modifiedSettling=false
Transports.resuspension.walker.dispersionCoefficientX=0.1
Transports.resuspension.walker.dispersionCoefficientY=0.1
Transports.resuspension.walker.dispersionCoefficientZ=0.001456
Transports.resuspension.walker.type=LATTICEWALKER

Transports.settling.alpha=0.64
Transports.settling.intercept.absoluteAccuracy=0.1
Transports.settling.intercept.maxVal=100
Transports.settling.intercept.maximalOrder=5
Transports.shieldsParameterJames.coefficientOfDrag=1.100

Transports.shieldsParameterJames.k10=1.0
Transports.shieldsParameterJames.k4=0.0
Transports.shieldsParameterJames.k5=1.0
Transports.shieldsParameterJames.k7=1.0

Transports.shieldsParameterJames.lambda=1.0
Transports.shieldsParameterJames.mu=0.375
Transports.shieldsParameterJames.theoreticalBedHeight=0.001
Transports.shieldsParameterJames.velocityProfileFactor=1.0625

Transports.suspension.instanceName=CARTESIANSUSPENSIONTRANSPORT
Transports.suspension.settling.allowBuoyant=false
Transports.suspension.settling.modifiedSettling=false
Transports.suspension.walker.dispersionCoefficientX=0.1
Transports.suspension.walker.dispersionCoefficientY=0.1
Transports.suspension.walker.dispersionCoefficientZ=0.001
Transports.suspension.walker.type=LATTICEWALKER

Transports.vonKarmanConstant=0.41

endOfDataMarker=endOfDataMarker

startOfDataMarker=startOfDataMarker

Appendix 19: References

- á Norði, G., Glud, R. N., Simonsen, K., and Gaard, E. 2018. Deposition and benthic mineralization of organic carbon: A seasonal study from Faroe Islands. *Journal of Marine Systems*, 177: 53-61. <https://doi.org/10.1016/j.jmarsys.2016.09.005>.
- Adams, T. P., Black, K., Black, K., Carpenter, T., Hughes, A., Reinardy, H. C., and Weeks, R. J. 2020. Parameterising resuspension in aquaculture waste deposition modelling. *Aquaculture Environment Interactions*, 12: 401-415.
- Airoidi, L. 2003. The effects of sedimentation on rocky coast assemblages. *Oceanography and marine biology: an annual review*, 41: 161-236.
- Alfaro-Lucas, J. M., Shimabukuro, M., Ogata, I. V., Fujiwara, Y., and Sumida, P. Y. G. 2018. Trophic structure and chemosynthesis contributions to heterotrophic fauna inhabiting an abyssal whale carcass. *Marine Ecology Progress Series*, 596: 1-12.
- Ali, A., Thiem, Ø., and Berntsen, J. 2011. Numerical modelling of organic waste dispersion from fjord located fish farms. *Ocean Dynamics*, 61: 977-989. <https://doi.org/10.1007/s10236-011-0393-8>.
- Aure, J., and Ervik, A. S. 1988. The environmental effects of sea water fish farms [also incl. orthophosphate, silicate]. Rapport og Meldinger fra Fiskeridirektoratets Havforskningsinstitutt (Norway):
- Aurora, X. 2009a. Bay of Vady, Hydrographic and Site Survey Report, 23 pp.
- Aurora, X. 2009b. Quanterness, Hydrographic and Site Survey Report, 26 pp.
- Aurora, X. 2010. Bay of Meil, Hydrographic and Site Survey Report, 52 pp.
- Bagarinao, T. 1992. Sulfide as an environmental factor and toxicant: tolerance and adaptations in aquatic organisms. *Aquatic Toxicology*, 24: 21-62. [https://doi.org/10.1016/0166-445X\(92\)90015-F](https://doi.org/10.1016/0166-445X(92)90015-F).
- Baker, E. T., Milburn, H. B., and Tennant, D. A. 1988. Field assessment of sediment trap efficiency under varying flow conditions. *Journal of Marine Research*, 46: 573-592.
- Bannister, R. J., Johnsen, I. A., Hansen, P. K., Kutti, T., and Asplin, L. 2016. Near- and far-field dispersal modelling of organic waste from Atlantic salmon aquaculture in fjord systems. *ICES Journal of Marine Science*, 73: 2408-2419. <https://doi.org/10.1093/icesjms/fsw027>.
- Bannister, R. J., Valdemarsen, T., Hansen, P. K., Holmer, M., and Ervik, A. 2014. Changes in benthic sediment conditions under an Atlantic salmon farm at a deep, well-flushed coastal site. *Aquaculture Environment Interactions*, 5: 29-47.
- Belle, S. M., and Nash, C. E. 2008. Better management practices for net-pen aquaculture. *In Environmental Best Management Practices for Aquaculture*, pp. 261-330. Ed. by C. S. Tucker and J. A. Hargreaves. John Wiley & Sons Inc.

- Beulig, F., Røy, H., Glombitza, C., and Jørgensen, B. B. 2018. Control on rate and pathway of anaerobic organic carbon degradation in the seabed. *Proceedings of the National Academy of Sciences*, 115: 367. <https://doi.org/10.1073/pnas.1715789115>.
- Biggar Economics. 2020. Estimation of the wider economic impacts of the aquaculture sector in Scotland, 978-1-80004-031-1. 50 pp.
- Biotikos Ltd. 2016. Benthic survey for Bay of Vady, September 2016, 10 pp.
- Biotikos Ltd. 2019. Benthic survey report for Bay of Vady, 8 pp.
- Black, K., and Nickell, T. 2014. Sediment sulphide response to organic loading, Scottish Aquaculture Research Forum, 978-1-907266-63-8. 57 pp.
- Black, K. D., Carpenter, T., Berkely, A., Black, K., and Amos, C. 2016. Refining seabed processes for aquaculture. New DEPOMOD final report, SAM/004/12, 200 pp.
- Bloesch, J., and Burns, N. M. 1980. A critical review of sedimentation trap technique. *Schweizerische Zeitschrift für Hydrologie*, 42: 15-55. <https://doi.org/10.1007/BF02502505>.
- Gradistat: A grain size distribution and statistics package for the analysis of unconsolidated sediments by sieving or laser granulometer, Kenneth Pye Associates Ltd., Crowthorne, Berkshire, UK).
- Bravo, F., and Grant, J. 2018. Modelling sediment assimilative capacity and organic carbon degradation efficiency at marine fish farms. *Aquaculture Environment Interactions*, 10: 309-328.
- Brigolin, D., Pastres, R., Nickell, T. D., Cromey, C. J., Aguilera, D. R., and Regnier, P. 2009. Modelling the impact of aquaculture on early diagenetic processes in sea loch sediments. *Marine Ecology Progress Series*, 388: 63-80.
- Broch, O. J., Daae, R. L., Ellingsen, I. H., Nepstad, R., Bendiksen, E. Å., Reed, J. L., and Senneset, G. 2017. Spatiotemporal dispersal and deposition of fish farm wastes: A model study from central Norway. *Frontiers in Marine Science*, 4: <https://doi.org/10.3389/fmars.2017.00199>.
- Brooks, K. M., and Mahnken, C. V. W. 2003. Interactions of Atlantic salmon in the Pacific northwest environment: II. Organic wastes. *Fisheries Research*, 62: 255-293. [https://doi.org/10.1016/S0165-7836\(03\)00064-X](https://doi.org/10.1016/S0165-7836(03)00064-X).
- Brooks, K. M., Stierns, A. R., Mahnken, C. V. W., and Blackburn, D. B. 2003. Chemical and biological remediation of the benthos near Atlantic salmon farms. *Aquaculture*, 219: 355-377. [https://doi.org/10.1016/S0044-8486\(02\)00528-8](https://doi.org/10.1016/S0044-8486(02)00528-8).
- Brown, J. R., Gowen, R. J., and McLusky, D. S. 1987. The effect of salmon farming on the benthos of a Scottish sea loch. *Journal of Experimental Marine Biology and Ecology*, 109: 39-51. [https://doi.org/10.1016/0022-0981\(87\)90184-5](https://doi.org/10.1016/0022-0981(87)90184-5).

- Brown, K., McGreer, E., Taekema, B., and Cullen, J. 2011. Determination of total free sulphides in sediment porewater and artefacts related to the mobility of mineral sulphides. *Aquatic Geochemistry*, 17: 821-839. <https://doi/10.1007/s10498-011-9137-0>.
- Bull, D. C., and Williamson, R. B. 2001. Prediction of principal metal-binding solid phases in estuarine sediments from color image analysis. *Environmental Science & Technology*, 35: 1658-1662. <https://doi.org/10.1021/es0015646>.
- Burdige, D. J. 2007. Preservation of organic matter in marine sediments: controls, mechanisms, and an imbalance in sediment organic carbon budgets? *Chemical reviews*, 107 2: 467-85.
- Burke, M., Grant, J., Filgueira, R., and Stone, T. 2021. Oceanographic processes control dissolved oxygen variability at a commercial Atlantic salmon farm: Application of a real-time sensor network. *Aquaculture*, 533: 736143. <https://doi.org/10.1016/j.aquaculture.2020.736143>.
- Burrows, M. T., Kamenos, N. A., Hughes, D. J., Stahl, H., Howe, J. A., and Tett, P. 2014. Assessment of carbon budgets and potential blue carbon stores in Scotland's coastal and marine environment, Scottish Natural Heritage Commissioned Report, 761. 91 pp.
- Carvajalino-Fernández, M. A., Keeley, N. B., Fer, I., Law, B. A., and Bannister, R. J. 2020a. Effect of substrate type and pellet age on the resuspension of Atlantic salmon faecal material. *Aquaculture Environment Interactions*, 12: 117-129.
- Carvajalino-Fernández, M. A., Sævik, P. N., Johnsen, I. A., Albretsen, J., and Keeley, N. B. 2020b. Simulating particle organic matter dispersal beneath Atlantic salmon fish farms using different resuspension approaches. *Marine Pollution Bulletin*, 161: 111685. <https://doi.org/10.1016/j.marpolbul.2020.111685>.
- Cathalot, C., Lansard, B., Per Hall, O. J., Tenberg, A., Almroth-Rosell, E., Apler, A., Calder, L. *et al.* 2012. Spatial and temporal variability of benthic respiration in a Scottish sea loch impacted by fish farming: A combination of in situ techniques. *Aquatic Geochemistry*, 18: 515-541. <https://doi.org/10.1007/s10498-012-9181-4>.
- Chamberlain, J. 2002. Modelling the environmental impacts of suspended mussel (*Mytilus edulis* L.) farming. PhD, Napier University, Edinburgh.
- Chamberlain, J., and Stucchi, D. 2007. Simulating the effects of parameter uncertainty on waste model predictions of marine finfish aquaculture. *Aquaculture*, 272: 296-311. <https://doi.org/10.1016/j.aquaculture.2007.08.051>.
- Chamberlain, J., Stucchi, D., Lu, L., and Levings, C. 2005. The suitability of DEPOMOD for use in the management of finfish aquaculture sites, with particular reference to Pacific Region, Fisheries and Oceans Canada, Research document, 2005/035,
- Chang, B. D., Page, F. H., and Losier, R. J. 2013. Variables affecting sediment sulfide concentrations in regulatory monitoring at salmon farms in the Bay of Fundy, Canada. *Aquaculture Environment Interactions*, 4: 67-79.

Chang, B. D., Page, F. H., Losier, R. J., and McCurdy, E. P. 2014. Organic enrichment at salmon farms in the Bay of Fundy, Canada: DEPOMOD predictions versus observed sediment sulfide concentrations. *Aquaculture Environment Interactions*, 5: 185-208.

Chang, B. D., Page, F.H., Losier, R.J., and McCurdy, E.P. 2012. Predicting organic enrichment under marine finfish farms in southwestern New Brunswick, Bay of Fundy: Comparisons of model predictions with results from spatially-intensive sediment sulfide sampling, Fisheries and Oceans Canada, Canadian Science Advisory Secretariat Research Document 2012/078, 150 pp.

Chary, K., Callier, M. D., Covès, D., Aubin, J., Simon, J., and Fiandrino, A. 2021. Scenarios of fish waste deposition at the sub-lagoon scale: a modelling approach for aquaculture zoning and site selection. *ICES Journal of Marine Science*, 78: 922-939. <https://doi.org/10.1093/icesjms/fsaa238>.

Cranford, P., Brager, L., Elvines, D., Wong, D., and Law, B. 2020. A revised classification system describing the ecological quality status of organically enriched marine sediments based on total dissolved sulfides. *Marine Pollution Bulletin*, 154: 111088. <https://doi.org/10.1016/j.marpolbul.2020.111088>.

Cranford, P. J., Brager, L., and Wong, D. 2017. A dual indicator approach for monitoring benthic impacts from organic enrichment with test application near Atlantic salmon farms. *Marine Pollution Bulletin*, 124: 258-265. <https://doi.org/10.1016/j.marpolbul.2017.07.049>.

Cromey, C. J., Black, K. D., Edwards, A., and Jack, I. A. 1998. Modelling the deposition and biological effects of organic carbon from marine sewage discharges. *Estuarine, Coastal and Shelf Science*, 47: 295-308. <https://doi.org/10.1006/ecss.1998.0353>.

Cromey, C. J., Nickell, T. D., and Black, K. D. 2002a. DEPOMOD—modelling the deposition and biological effects of waste solids from marine cage farms. *Aquaculture*, 214: 211-239. [http://dx.doi.org/10.1016/S0044-8486\(02\)00368-X](http://dx.doi.org/10.1016/S0044-8486(02)00368-X).

Cromey, C. J., Nickell, T. D., Black, K. D., Provost, P. G., and Griffiths, C. R. 2002b. Validation of a fish farm waste resuspension model by use of a particulate tracer discharged from a point source in a coastal environment. *Estuaries*, 25: 916-929. <https://doi.org/10.1007/BF02691340>.

Cromey, C. J., Nickell, T. D., Treasurer, J., Black, K. D., and Inall, M. 2009. Modelling the impact of cod (*Gadus morhua* L.) farming in the marine environment—CODMOD. *Aquaculture*, 289: 42-53. <https://doi.org/10.1016/j.aquaculture.2008.12.020>.

Cromey, C. J., Thetmeyer, H., Lampadariou, N., Black, K. D., Kögeler, J., and Karakassis, I. 2012. MERAMOD: predicting the deposition and benthic impact of aquaculture in the eastern Mediterranean Sea. *Aquaculture Environment Interactions*, 2: 157-176. <https://doi.org/10.3354/aei00034>.

Cubillo, A. M., Ferriera, J. G., Robinson, S. M. C., Pearce, C. M., Corner, R. A., and Johansen, J. 2016. Role of deposit feeders in integrated multi-trophic aquaculture - A model analysis. *Aquaculture*, 453: 54-66. <https://doi.org/10.1016/j.aquaculture.2015.11.031>.

Deng, L., Bølsterli, D., Kristensen, E., Meile, C., Su, C.-C., Bernasconi, S. M., Seidenkrantz, M.-S. *et al.* 2020. Macrofaunal control of microbial community structure in continental margin sediments. *Proceedings of the National Academy of Sciences*, 117: 15911. <https://doi.org/10.1073/pnas.1917494117>.

Department of Fisheries and Oceans. 2012. Review of DEPOMOD predictions versus observations of sulfide concentrations around five salmon aquaculture sites in Southwest New Brunswick, Fisheries and Oceans Canada, DFO Canadian Science Advisory Secretariat Science Advisory Report 2012/042, 15 pp.

Diesing, M., Kröger, S., Parker, R., Jenkins, C., Mason, C., and Weston, K. 2017. Predicting the standing stock of organic carbon in surface sediments of the North–West European continental shelf. *Biogeochemistry*, 135: 183-200. <https://doi.org/10.1007/s10533-017-0310-4>.

Doglioli, A. M., Magaldi, M. G., Vezzulli, L., and Tucci, S. 2004. Development of a numerical model to study the dispersion of wastes coming from a marine fish farm in the Ligurian Sea (Western Mediterranean). *Aquaculture*, 231: 215-235. <https://doi.org/10.1016/j.aquaculture.2003.09.030>.

Droppo, I. G., Jaskot, C., Nelson, T., Milne, J., and Charlton, M. 2007. Aquaculture waste sediment stability: Implications for waste migration. *Water, Air, and Soil Pollution*, 183: 59-68. <https://doi.org/10.1007/s11270-007-9355-7>.

Dudley, R. W., Panchang, V. G., and Newell, C. R. 2000. Application of a comprehensive modeling strategy for the management of net-pen aquaculture waste transport. *Aquaculture*, 187: 319-349. [https://doi.org/10.1016/S0044-8486\(00\)00313-6](https://doi.org/10.1016/S0044-8486(00)00313-6).

Duplisea, D., Jennings, S., Malcolm, S. J., Parker, R., and Sivyer, D. 2001. Modelling the potential impacts of bottom trawl fisheries on carbon mineralisation and chemical concentrations in a soft sediment system. *Geochemical Transactions*, 14: 1-6.

Duplisea, D. E. 1998. Feedbacks between benthic carbon mineralisation and community structure: a simulation-model analysis. *Ecological Modelling*, 110: 19-43. [https://doi.org/10.1016/S0304-3800\(98\)00039-8](https://doi.org/10.1016/S0304-3800(98)00039-8).

Ervik, A. S., Hansen, P. K., Aure, J., Stigebrandt, A., Johannessen, P., and Jahnsen, T. 1997. Regulating the local environmental impact of intensive marine fish farming I. The concept of the MOM system (Modelling-Ongrowing fish farms-Monitoring). *Aquaculture*, 158: 85-94.

Ferry, J. G., and Lessner, D. J. 2008. Methanogenesis in marine sediments. *Annals of the New York Academy of Sciences*, 1125: 147-157.

Filgueira, R., Guyondet, T., Thupaki, P., Reid, G. K., Howarth, L. M., and Grant, J. 2021. Inferring the potential for nitrogen toxicity on seagrass in the vicinity of an aquaculture site using mathematical models. *Journal of Environmental Management*, 282: 111921. <https://doi.org/10.1016/j.jenvman.2020.111921>.

Findlay, R. H., and Watling, L. 1994. Toward a process level model to predict the effects of

salmon net-pen aquaculture on the benthos. Canadian Technical Report of Fisheries and Aquatic Sciences, 1949: 47-77.

Findlay, R. H., and Watling, L. 1997. Prediction of benthic impact for salmon net-pens based on the balance of benthic oxygen supply and demand. Marine Ecology Progress Series, 155: 147-157.

Findlay, R. H., Watling, L., and Mayer, L. M. 1995. Environmental impact of salmon net-pen culture on marine benthic communities in Maine: A case study. Estuaries, 18: 145. <https://doi.org/10.2307/1352289>.

Fish Vet Group. 2019. Quanterness benthic survey results, 21 pp.

Germano, J., Rhoads, D., Valente, R., Carey, D., and Solan, M. 2011. The use of sediment profile imaging (SPI) for environmental impact assessments and monitoring studies. Oceanography and marine biology, 49: 235-298. <https://doi.org/10.1201/b11009-7>.

Ghanawi, J., and McAdam, B. J. 2020. Using fatty acid markers to distinguish between effects of salmon (*Salmo salar*) and halibut (*Hippoglossus hippoglossus*) farming on mackerel (*Scomber scombrus*) and whiting (*Merlangius merlangus*). Aquaculture Research, 51: 2229-2242. <https://doi.org/10.1111/are.14568>.

Giles, H., Broekhuizen, N., Bryan, K. R., and Pilditch, C. A. 2009. Modelling the dispersal of biodeposits from mussel farms: The importance of simulating biodeposit erosion and decay. Aquaculture, 291: 168-178. <https://doi.org/10.1016/j.aquaculture.2009.03.010>.

Gillibrand, P. A., and Turrell, W. R. 1997. Simulating the dispersion and settling of particulate material and associated substances from salmon farms, Aberdeen Marine Laboratory, 97, 3, 21 pp.

Gillibrand, P. A., Turrell, W. R., Moore, D. C., and Adams, R. D. 1996. Bottom water stagnation and oxygen depletion in a Scottish sea loch. Estuarine, Coastal and Shelf Science, 43: 217-235. <https://doi.org/10.1006/ecss.1996.0066>.

Glud, R. N. 2008. Oxygen dynamics of marine sediments. Marine Biology Research, 4: 243-289. <https://doi.org/10.1080/17451000801888726>.

Gowen, R. J., Bradbury, N. B., and Brown, J. R. 1989. The use of simple models in assessing two of the interactions between fish farming and the marine environment. *In* Aquaculture - A Technology in Progress, pp. 189–199. Ed. by R. Billard and N. de Pauw. European Aquaculture Society, Bredene, Belgium.

Gowen, R. J., Smyth, D., and Silvert, W. 1994. Modelling the spatial distribution and loading of organic fish farm waste to the seabed. Canadian Technical Report of Fisheries and Aquatic Sciences, 1949: 19-30.

Grant, J. 1985. A method for measuring horizontal transport of organic carbon over sediments.

Canadian Journal of Fisheries and Aquatic Sciences, 42: 595-602. <https://doi.org/10.1139/f85-077>.

Grant, J. 1988. Intertidal bedforms, sediment transport, and stabilization by benthic microalgae. *In* Tide-influenced sedimentary environments and facies, pp. 499-510. Ed. by P. J. DeBoer, A. Van Gelder and S. D. Nio. Reidel, Dordrecht, Holland.

Grant, J., and Hargrave, B. T. 1987. Benthic metabolism and the quality of sediment organic carbon. *Biological Oceanography*, 4: 243-264. <https://doi.org/10.1080/01965581.1987.10749493>.

Grieshaber, M. K., and Völkel, S. 1998. Animal adaptations for tolerance and exploitation of poisonous sulfide. *Annual Review of Physiology*, 60: 33-63.

Hall-Spencer, J., and Bamber, R. 2007. Effects of salmon farming on benthic crustacea. *Ciencias Marinas*, 33: 353-366.

Hall-Spencer, J., White, N., Gillespie, E., Gillham, K., and Foggo, A. 2006. Impact of fish farms on maerl beds in strongly tidal areas. *Marine Ecology Progress Series*, 326: 1-9.

Hall, P. O. J., Anderson, L. G., Holby, O., JKollberg, S., and Samuelsson, M.-O. 1990. Chemical fluxes and mass balances in a marine fish cage farm. I. Carbon. *Marine Ecology Progress Series*, 61: 61-73.

Hamoutene, D. 2014. Sediment sulphides and redox potential associated with spatial coverage of *Beggiatoa* spp. at finfish aquaculture sites in Newfoundland, Canada. *ICES Journal of Marine Science*, 71: 1153-1157. <https://doi.org/10.1093/icesjms/fst223>.

Hargrave, B. 1994a. A benthic enrichment index, Canadian Technical Reports Fisheries Aquatic Science, 1949, 79-91 pp.

Hargrave, B. T. 1994b. Modelling benthic impacts of organic enrichment from marine aquaculture. Canadian technical report of fisheries and aquatic sciences/Rapport technique canadien des sciences halieutiques et aquatiques, 1949: 16.

Hargrave, B. T. 2003. Far-field environmental effects of marine finfish aquaculture. Canadian technical report of fisheries and aquatic sciences/Rapport technique canadien des sciences halieutiques et aquatiques, 2450: 1-35.

Hargrave, B. T. 2010. Empirical relationships describing benthic impacts of salmon aquaculture. *Aquaculture Environment Interactions*, 1: 33-46.

Hargrave, B. T., Duplisea, D. E., Pfeiffer, E., and Wildish, D. J. 1993. Seasonal changes in benthic fluxes of dissolved oxygen and ammonium associated with marine cultured Atlantic salmon. *Marine Ecology Progress Series*, 96: 249-257.

Hargrave, B. T., Holmer, M., and Newcombe, C. P. 2008. Towards a classification of organic enrichment in marine sediments based on biogeochemical indicators. *Marine Pollution Bulletin*, 56: 810-824. <https://doi.org/10.1016/j.marpolbul.2008.02.006>.

- Hartstein, N. D., and Stevens, C. L. 2005. Deposition beneath long-line mussel farms. *Aquacultural engineering*, 33: 192-213. <https://doi.org/10.1016/j.aquaeng.2005.01.002>.
- Heath, M. R., and Beare, D. J. 2008. New primary production in northwest European shelf seas, 1960-2003. *Marine Ecology Progress Series*, 363: 183-203. <https://doi.org/10.3354/meps07460>.
- Heilskov, A. C., and Holmer, M. 2001. Effects of benthic fauna on organic matter mineralization in fish-farm sediments: importance of size and abundance. *ICES Journal of Marine Science*, 58: 427-434.
- Hevia, M., Rosenthal, H., and Gowen, R. J. 1996. Modelling benthic deposition under fish cages. *Journal of Applied Ichthyology*, 12: 71-74. <https://doi.org/10.1111/j.1439-0426.1996.tb00065.x>.
- Holmer, M., Wildish, D. J., and Hargrave, B. 2005. Organic enrichment from marine finfish aquaculture and effects on sediment biogeochemical processes. *Handbook of Environmental Chemistry*, 5: 1-x. <https://doi.org/10.1007/b136010>.
- Johannessen, P. J., Botnen, H. B., and Tvedten, O. F. 1994. Macrobenthos: before, during and after a fish farm. *Aquaculture Research*, 25: 55-66. <https://doi.org/10.1111/j.1365-2109.1994.tb00666.x>.
- Jørgensen, B. B., Findlay, A. J., and Pellerin, A. 2019. The biogeochemical sulfur cycle of marine sediments. *Frontiers in Microbiology*, 10: Jørgensen10.3389/fmicb.2019.00849.
- Jusup, M., Geček, S., and Legović, T. 2007. Impact of aquacultures on the marine ecosystem: Modelling benthic carbon loading over variable depth. *Ecological Modelling*, 200: 459-466. <https://doi.org/10.1016/j.ecolmodel.2006.08.007>.
- Kalantzi, I., and Karakassis, I. 2006. Benthic impacts of fish farming: Meta-analysis of community and geochemical data. *Marine Pollution Bulletin*, 52: 484-493. <https://doi.org/10.1016/j.marpolbul.2005.09.034>.
- Karakassis, I., Hatziyanni, E., Tsapakis, M., and Plaiti, W. 1999. Benthic recovery following cessation of fish farming: a series of successes and catastrophes. *Marine Ecology Progress Series*, 184: 205-218.
- Karakassis, I., Pitta, P., and Krom, M. D. 2005. Contribution of fish farming to the nutrient loading of the Mediterranean. *Scientia Marina*, 69: 313-321.
- Keeley, N., Valdemarsen, T., Woodcock, S., Holmer, M., Husa, V., and Bannister, R. 2019. Resilience of dynamic coastal benthic ecosystems in response to large-scale finfish farming. *Aquaculture Environment Interactions*, 11: 161-179.
- Keeley, N. B., Cromey, C. J., Goodwin, E. O., Gibbs, M. T., and Macleod, C. M. 2013a. Predictive depositional modelling (DEPOMOD) of the interactive effect of current flow and resuspension on ecological impacts beneath salmon farms. *Aquaculture Environment Interactions*, 3: 275-291.

- Keeley, N. B., Forrest, B. M., and Macleod, C. K. 2013b. Novel observations of benthic enrichment in contrasting flow regimes with implications for marine farm monitoring and management. *Marine Pollution Bulletin*, 66: 105-116. <https://doi.org/10.1016/j.marpolbul.2012.10.024>.
- Kristensen, E. 2000. Organic matter diagenesis at the oxic/anoxic interface in coastal marine sediments, with emphasis on the role of burrowing animals. *Hydrobiologia*, 426: 1-24. <https://doi.org/10.1023/A:1003980226194>.
- Kutti, T., Ervik, A., and Hansen, P. K. 2007. Effects of organic effluents from a salmon farm on a fjord system. I. Vertical export and dispersal processes. *Aquaculture*, 262: 367-381. <https://doi.org/10.1016/j.aquaculture.2006.10.010>.
- Law, B. A., Hill, P. S., Milligan, T. G., and Zions, V. 2016. Erodibility of aquaculture waste from different bottom substrates. *Aquaculture Environment Interactions*, 8: 575-584. <https://doi.org/10.3354/aei00199>.
- Luisetti, T., Turner, R. K., Andrews, J. E., Jickells, T. D., Kröger, S., Diesing, M., Paltriguera, L. *et al.* 2019. Quantifying and valuing carbon flows and stores in coastal and shelf ecosystems in the UK. *Ecosystem Services*, 35: 67-76. <https://doi.org/10.1016/j.ecoser.2018.10.013>.
- Lumb, C. M. 1989. Self-pollution by Scottish salmon farms? *Marine Pollution Bulletin*, 20: 375-379. [https://doi.org/10.1016/0025-326X\(89\)90314-7](https://doi.org/10.1016/0025-326X(89)90314-7).
- Macleod, C. K., Moltschaniwsky, N. A., Crawford, C. M., and Forbes, S. E. 2007. Biological recovery from organic enrichment: some systems cope better than others. *Marine Ecology Progress Series*, 342: 41-53.
- Macleod, C. K., Moltschaniwskyj, N. A., and Crawford, C. M. 2006. Evaluation of short-term fallowing as a strategy for the management of recurring organic enrichment under salmon cages. *Marine Pollution Bulletin*, 52: 1458-1466. <https://doi.org/10.1016/j.marpolbul.2006.05.007>.
- Magill, S. H., Thetmeyer, H., and Cromey, C. J. 2006. Settling velocity of faecal pellets of gilthead sea bream (*Sparus aurata* L.) and sea bass (*Dicentrarchus labrax* L.) and sensitivity analysis using measured data in a deposition model. *Aquaculture*, 251: 295-305. <https://doi.org/10.1016/j.aquaculture.2005.06.005>.
- Mayor, D. J., Gray, N. B., Hattich, G. S. I., and Thornton, B. 2017. Detecting the presence of fish farm-derived organic matter at the seafloor using stable isotope analysis of phospholipid fatty acids. *Scientific Reports*, 7: 5146. <https://doi.org/10.1038/s41598-017-05252-w>.
- Mayor, D. J., Zuur, A. F., Solan, M., Paton, G. I., and Killham, K. 2010. Factors affecting benthic impacts at Scottish fish farms. *Environmental Science & Technology*, 44: 2079-2084.
- McGhie, T. K., Crawford, C. M., Mitchell, I. M., and O'Brien, D. 2000. The degradation of fish-cage waste in sediments during fallowing. *Aquaculture*, 187: 351-366. [https://doi.org/10.1016/S0044-8486\(00\)00317-3](https://doi.org/10.1016/S0044-8486(00)00317-3).

Mente, E., Pierce, G. J., Spencer, N. J., Martin, J. C., Karapanagiotidis, I. T., Santos, M. B., Wang, J. *et al.* 2008. Diet of demersal fish species in relation to aquaculture development in Scottish sea lochs. *Aquaculture*, 277: 263-274. <https://doi.org/10.1016/j.aquaculture.2008.02.022>.

Milewski, I. 2014. Aquaculture survey and macro-invertebrate analysis report: Shelburne Harbour - Former Sandy Point lease site, Conservation Council of New Brunswick, 29 pp.

Narayanaswamy, B., Bett, B., Lamont, P., Rowden, A., Bell, E. M., & Menot, L. . 2016. Corers and grabs. *In* Biological Sampling in the deep-sea pp. 207-227. Ed. by lackwell Publishing (Oxford).

Nilsson, H. C., and Rosenberg, R. 2000. Succession in marine benthic habitats and fauna in response to oxygen deficiency: analysed by sediment profile-imaging and by grab samples. *Marine Ecology Progress Series*, 197: 139-149.

Okubo, A. 1971. Oceanic diffusion diagrams. *Deep-sea Research*, 18: 789-802.

Overnell, J., and Young, S. 1995. Sedimentation and carbon flux in a Scottish Sea Loch, Loch Linnhe. *Estuarine, Coastal and Shelf Science*, 41: 361-376. <https://doi.org/10.1006/ecss.1995.0068>.

Panchang, V., Cheng, G., and Newell, C. 1997. Modeling hydrodynamics and aquaculture waste transport in coastal Maine. *Estuaries*, 20: 14-41. <https://doi.org/10.2307/1352717>.

Pawlowicz, R., Beardsley, B., and Lentz, S. 2002. Classical tidal harmonic analysis including error estimates in MATLAB using T_TIDE. *Computers and Geosciences*, 28: 929-937.

Pearson, T. H., and Rosenberg, R. 1976. A comparative study of the effects on the marine environment of wastes from cellulose industries in Scotland and Sweden. *Ambio*, 5: 77-79.

Pereira, P. M. F., Black, K. D., McLusky, D. S., and Nickell, T. D. 2004. Recovery of sediments after cessation of marine fish farm production. *Aquaculture*, 235: 315-330. <https://doi.org/10.1016/j.aquaculture.2003.12.023>.

Pharmaq Analytiq. 2021. Benthic survey report - Bay of Meil, Orkney Islands, 12 pp.

Phillips, G. R., Anwar, A., Brooks, L., Martina, L. J., Prior, A., and Miles, A. C. 2014. Infaunal quality index: WFD classification scheme for marine benthic invertebrates., Environment Agency, SC080016, 193 pp.

Pilditch, C. A., Emerson, C. W., and Grant, J. 1997. Effect of scallop shells and sediment grain size on phytoplankton flux to the bed. *Continental Shelf Research*, 17: 1869-1885. [https://doi.org/10.1016/S0278-4343\(97\)00050-2](https://doi.org/10.1016/S0278-4343(97)00050-2).

Pohle, G., Frost, B., and Findlay, R. 2001. Assessment of regional benthic impact of salmon mariculture within the Letang Inlet, Bay of Fundy. *ICES Journal of Marine Science*, 58: 417-426. <https://doi.org/10.1006/jmsc.2000.1039>.

Price, C., Black, K. D., Hargrave, B. T., and Morris, J. A. J. 2015. Marine cage culture and the environment: effects on water quality and primary production. *Aquaculture Environment Interactions*, 6: 151-174. [10.3354/aei00122](https://doi.org/10.3354/aei00122).

Reid, G. K., Liutkus, M., Robinson, S. M. C., Chopin, T. R., Blair, T., Lander, T., Mullen, J. *et al.* 2009. A review of the biophysical properties of salmonid faeces: implications for aquaculture waste dispersal models and integrated multi-trophic aquaculture. *Aquaculture Research*, 40: 257-273. <https://doi.org/10.1111/j.1365-2109.2008.02065.x>.

Riera, R., Becerro, M. A., Ramos, E., Monterroso, Ó., and Rodríguez, M. 2015. Response of different benthic habitats to off-shore fish cages. *Aquaculture Research*, 46: 1490-1500. <https://doi.org/10.1111/are.12306>.

Riera, R., Pérez, Ó., Cromey, C., Rodríguez, M., Ramos, E., Álvarez, O., Domínguez, J. *et al.* 2017. MACAROMOD: A tool to model particulate waste dispersion and benthic impact from offshore sea-cage aquaculture in the Macaronesian region. *Ecological Modelling*, 361: 122-134. <https://doi.org/10.1016/j.ecolmodel.2017.08.006>.

Ritz, D. A., Lewis, M. E., and Shen, M. 1989. Response to organic enrichment of infaunal macrobenthic communities under salmonid seacages. *Marine Biology*, 103: 211-214. <https://doi.org/10.1007/BF00543349>.

Samuelsen, O. B., Lunestad, B. T., Hannisdal, R., Bannister, R., Olsen, S., Tjensvoll, T., Farestveit, E. *et al.* 2015. Distribution and persistence of the anti sea-lice drug teflubenzuron in wild fauna and sediments around a salmon farm, following a standard treatment. *Science of the Total Environment*, 508: 115-121. <https://doi.org/10.1016/j.scitotenv.2014.11.082>.

Sardenne, F., Simard, M., Robinson, S. M. C., and McKindsey, C. W. 2020. Consumption of organic wastes from coastal salmon aquaculture by wild decapods. *Science of the Total Environment*, 711: 134863. <https://doi.org/10.1016/j.scitotenv.2019.134863>.

Schaanning, M., and Hansen, P. K. 2005. The suitability of electrode measurements for assessment of benthic organic impact and their use in a management system for marine fish farms. *In The Handbook of Environmental Chemistry*, 5.M: pp. 381-408. Ed. by B. T. Hargrave. Springer Verlag.

Scottish Government. 2020. Scottish Fish Farm Production Survey 2019, Marine Scotland Science, 1363-5867. 62 pp.

Seeberg-Elverfeldt, J., Schlüter, M., Feseker, T., and Kölling, M. 2005. Rhizon sampling of porewaters near the sediment-water interface of aquatic systems. *Limnology and Oceanography: Methods*, 3: 361-371.

SEPA. 2019a. Aquaculture modelling: Regulatory guidance for the aquaculture sector: Version 1.0, Scottish Environment Protection Agency, 74 pp.

SEPA. 2019b. Protection of the marine environment: Discharges from marine pen fish farms: A strengthened regulatory framework, Scottish Environment Protection Agency, 7 pp.

SEPA. 2021. NewDeopomod draft guidance - 09/02/2021,

Serpetti, N., Heath, M., Rose, M., and Witte, U. 2012. High resolution mapping of sediment organic matter from acoustic reflectance data. *Hydrobiologia*, 680: 265-284. <https://doi.org/10.1007/s10750-011-0937-4>.

Shillabeer, N., Hart, B., and Riddle, A. M. 1992. The use of a mathematical model to compare particle size data derived by dry-sieving and laser analysis. *Estuarine, Coastal and Shelf Science*, 35: 105-111. [https://doi.org/10.1016/S0272-7714\(05\)80059-9](https://doi.org/10.1016/S0272-7714(05)80059-9).

Silvert, W. 1994. Modelling benthic deposition and impacts of organic loading. Canadian Technical Report of Fisheries and Aquatic Sciences, 1949: 1-18.

Silvert, W. 2005. Modelling the environmental impacts of marine aquaculture. *In Strategic Management of Marine Ecosystems*, pp. 109-125. Ed. by E. Levner, I. Linkov and J.-M. Proth. Springer, Netherlands.

Smeaton, C., and Austin, W. E. N. 2019. Where's the Carbon: Exploring the Spatial Heterogeneity of Sedimentary Carbon in Mid-Latitude Fjords. *Frontiers in Earth Science*, 7: 269.

Sowles, J. W., Chruchill, L., and Silvert, W. 1994. The effect of benthic carbon loading on the degradation of bottom conditions under farm sites. Canadian Technical Report of Fisheries and Aquatic Sciences, 1949: 31-46.

Sporsheim, K. 2017. Astaxanthin as a biomarker for fish feed loading in the marine ecosystem, Department of Biology, Norwegian University of Science and Technology.

SRSL. 2021. NewDEPOMOD user guide, SAMS Research Services Limited, 143 pp.

Stigebrandt, A. 2011. Carrying capacity: general principles of model construction. *Aquaculture Research*, 42: 41-50. <https://doi.org/10.1111/j.1365-2109.2010.02674.x>.

Stucchi, D., Sutherland, T.-A., Levings, C., and Higgs, D. 2005. Near-field depositional model for salmon aquaculture waste. *In Environmental Effects of Marine Finfish Aquaculture*, pp. 157-179. Ed. by B. T. Hargrave. Springer Berlin Heidelberg, Berlin, Heidelberg.

Sutherland, T. F., Amos, C. L., and Grant, J. 2021. The resuspension and deposition of biomediated sediments in Upper South Cove, Nova Scotia, Canada. *Journal of Coastal Research*, 38: 19-34. <https://doi.org/10.2112/JCOASTRES-D-20-00104.1>.

Sweetman, A. K., and Chapman, A. 2015. First assessment of flux rates of jellyfish carcasses (jelly-falls) to the benthos reveals the importance of gelatinous material for biological C-cycling in jellyfish-dominated ecosystems. *Frontiers in Marine Science*, 2: <https://doi.org/10.3389/fmars.2015.00047>.

Talbot, J. W., and Talbot, G. A. 1974. Diffusion in shallow seas and in English coastal and estuarine waters. *Rapports et Procès-Verbaux des Réunions du Conseil International pour l'Exploration de la Mer*, 167: 93-110.

Tomassetti, P., and Porrello, S. 2005. Polychaetes as indicators of marine fish farm organic enrichment. *Aquaculture International*, 13: 109-128. <https://doi.org/10.1007/s10499-004-9026-2>.

Uglem, I., Toledo-Guedes, K., Sanchez-Jerez, P., Ulvan, E. M., Evensen, T., and Sæther, B. S. 2020. Does waste feed from salmon farming affect the quality of saithe (*Pollachius virens* L.) attracted to fish farms? *Aquaculture Research*, 51: 1720-1730. <https://doi.org/10.1111/are.14519>.

Verardo, D. J., P.N., F., and McIntyre, A. 1990. Determination of organic carbon and nitrogen in marine sediments using the Carlo Erba NA-1500 analyzer. *Deep Sea Research Part A. Oceanographic Research Papers*, 37: 157-165. [https://doi.org/10.1016/0198-0149\(90\)90034-S](https://doi.org/10.1016/0198-0149(90)90034-S).

Weise, A. M., Cromey, C. J., Callier, M. D., Archambault, P., Chamberlain, J., and McKindsey, C. W. 2009. Shellfish-DEPOMOD: Modelling the biodeposition from suspended shellfish aquaculture and assessing benthic effects. *Aquaculture*, 288: 239-253. <https://doi.org/10.1016/j.aquaculture.2008.12.001>.

Wentworth, C. K. 1922. A scale of grade and class terms for clastic sediments. *The Journal of Geology*, 30: 377-392. <https://doi.org/10.1086/622910>.

Weston, D. P. 1990. Quantitative examination of macrobenthic community changes along an organic enrichment gradient. *Marine Ecology Progress Series*, 61: 233-244.

Westrich, J. T., and Berner, R. A. 1984. The role of sedimentary organic matter in bacterial sulfate reduction: The G model tested. *Limnology and Oceanography*, 29: 236-249.

White, C. A., Nichols, P. D., Ross, D. J., and Dempster, T. 2017. Dispersal and assimilation of an aquaculture waste subsidy in a low productivity coastal environment. *Marine Pollution Bulletin*, 120: 309-321. <https://doi.org/10.1016/j.marpolbul.2017.05.042>.

White, J. 1990. The use of sediment traps in high-energy environments. *Marine Geophysical Researches*, 12: 145-152. 10.1007/BF00310569.

Whitmarsh, D., and Wattage, P. 2006. Public attitudes towards the environmental impact of salmon aquaculture in Scotland. *European Environment*, 16: 108-121. <https://doi.org/10.1002/eet.406>.

Wilding, T. A., Cromey, C. J., Nickell, T. D., and Hughes, D. J. 2012. Salmon farm impacts on muddy-sediment megabenthic assemblages on the west coast of Scotland. *Aquaculture Environment Interactions*, 2: 145-156.

Wildish, D. J., Akagi, H. M., Hargrave, B. T., and Strain, P. M. 2004. Inter-laboratory calibration of redox potential and total sulfide measurements in interfacial marine sediments and the implications for organic enrichment assessment. Canadian technical report of fisheries and aquatic sciences/Rapport technique canadien des sciences halieutiques et aquatiques, 2546: 29.

Wildish, D. J., Hargrave, B. T., MacLeod, C., and Crawford, C. 2003. Detection of organic

enrichment near finfish net-pens by sediment profile imaging at SCUBA-accessible depths. *Journal of Experimental Marine Biology and Ecology*, 285-286: 403-413. [https://doi.org/10.1016/S0022-0981\(02\)00540-3](https://doi.org/10.1016/S0022-0981(02)00540-3).

Wilson, P. S., and Vopel, K. 2015. Assessing the sulfide footprint of mussel farms with sediment profile imagery: A New Zealand trial. *PLoS ONE*, 10: e0129894. <https://doi.org/10.1371/journal.pone.0129894>.

Word, J. Q. 1979. The infaunal trophic index, Annual Report 1978 Southern California Coastal Water Research Project, 19-41 pp.

Ye, L.-X., Ritz, D. A., Fenton, G. E., and Lewis, M. E. 1991. Tracing the influence on sediments of organic waste from a salmonid farm using stable isotope analysis. *Journal of Experimental Marine Biology and Ecology*, 145: 161-174. [https://doi.org/10.1016/0022-0981\(91\)90173-T](https://doi.org/10.1016/0022-0981(91)90173-T).